University of Alberta

Development of Liquid Chromatography Mass Spectrometry Methods for the Identification and Quantification of Acylcarnitines in Biological Samples

by

Azeret Zuniga

A thesis submitted to the Faculty of Graduate Studies and Research
in partial fulfillment of the requirements for the degree of

Doctor of Philosophy

Department of Chemistry

Fall 2012
Edmonton, Alberta

Abstract

The field of metabolomics follows the Greek premise where metabolic changes are believed to be indicative of disease. Acylcarnitines, for example, can be dysregulated in the presence of various diseases including genetic metabolic disorders and multiple sclerosis. Liquid chromatography mass spectrometry-based quantitative metabolomics using stable isotope-labeled internal standards has proved to be one of the most accurate and reliable approaches for biomarker discovery.

The main objective of this work was to develop, validate and apply both qualitative and quantitative ultra-high performance liquid chromatography tandem mass spectrometry (UHPLC-MS/MS) platforms for the detection, identification and quantification of acylcarnitines in various biological samples.

Comprehensive acylcarnitine profiling was performed in urine, plasma, dried blood spots and red blood cell pellets. Compounds were putatively identified based on mass, relative retention times and fragmentation pattern. Only by analyzing various sample types can a truly comprehensive acylcarnitine profile be obtained.

In an effort to improve metabolite identification strategies a web-based tool called MyCompoundID was developed. It is an expansion of the Human Metabolome Database and makes use of the fragmentation tools of the software

package ChemDraw. Using this tool, the identification rate of metabolites in urine and plasma were greatly increased.

Another major area of this work focused on the quantification of acylcarnitines in urine and plasma. A simple and robust esterification reaction was employed to introduce a $^{12}C_2$ or $^{13}C_2$ labeled ethyl group to acylcarnitines in order to produce a series of reference and internal standards. Calibration curves were prepared in unesterified urine and plasma to overcome the lack of analyte-free matrices. Method validation was performed to assess accuracy, precision, limits of detection and quantification as well as linear dynamic range. The results obtained correlated well with previously published values.

Future work could focus on the application of these methods to clinical samples to search for biomarkers for various diseases. Additionally, analysis of acylcarnitines in dried biofluid spots would be an interesting application. Sample preparation times could be reduced by combining analyte extraction and derivatization into a single step using microwave technology. The use of this technology could be useful for many applications.

Acknowledgements

The successful completion of this research project would not have been possible without the support of many people**.** It is my pleasure to express my appreciation to all those who have, in one way or another, made this thesis possible.

My utmost gratitude goes to my supervisor, Dr. Liang Li, for giving me the invaluable opportunity to join his laboratory. His guidance, advice and trust throughout the course of my graduate program have been instrumental in my becoming a thriving researcher. I would also like to thank the members of my supervisory committee, for the very constructive discussions I had with Professors James Harynuk and Jed Harrison. Professors Fiona Bamforth and John Vederas both had very insightful comments during my candidacy examination and thesis defense, and for that I would like to thank them. I would also like to thank Professor Alan Doucette for agreeing to participate in my thesis defense and for his very valuable suggestions and comments.

I would like to thank all the members of Dr. Li's research group, especially Avalyn Stanislaus for her friendship, her continuous advice and support, as well as for being so encouraging and helpful every step of the way. This experience would not have been the same without her. I would also like to thank Mingguo Xu, for his friendship, his help with multiple computer-related issues and for making the past few years of my life much more enjoyable. My appreciation also goes to Melisa Brown for her professional training and Dr. Bryce Young for his wise words about tackling a PhD program one day at a time.

I would like to gratefully acknowledge Dr. David Wishart and the HMDB team for the opportunity of being part of the Human Metabolome Project.

My gratitude also goes to Raymond Lemieux, Dr. Eric Flaim, Jonathan Clark and Dr. Nancy Zhang of the INRF for allowing us the use of their instrumentation and for always lending us a helping hand.

Our collaborators from the Department of Computer Science, Dr. Guohui Lin and his group, Dr. Jianjun Zhou, Ronghong Li and Yi Shi played a crucial role in the development of the web-based tool, MyCompoundID, described in Chapter 6. My sincere gratitude goes to them for their hard work and numerous discussions.

In the Chemistry Department, I would like to thank Dr. Sandra Marcus and Dr. Gareth Lambkin for allowing us to make use of the cell culture lab. Special thanks go to Dr. Randy Whittal and the rest of the Mass Spectrometry lab for their help throughout the course of my research. I would also like to thank Randy Benson, Paul Crothers and the rest of the Machine Shop team for their constant help with our instrument pumps and for always being a pleasure to chat with. From the Electronics Shop, I would like to thank Al Chilton for bringing the UPLC system back to life when it was most needed. I would also like to recognize the Chemistry supporting staff (general office, purchasing, mailroom and shipping/receiving) for all their kind help. I would especially like to thank Anita Weiler for her time and patience and Ryan Lewis for always being "a breath of fresh air" as well as for always making sure we got all the supplies we needed.

My sincere gratitude goes to Drs. David and Chris Herold of The Association for Mass Spectrometry: Applications to the Clinical Laboratory, Inc. for believing in my work and for allowing me the opportunity to disseminate my research at their annual conference on three separate occasions.

Cambridge Isotopes generously donated the 1,2-$^{13}C_2$ ethanol used for my quantification experiments described in Chapters 4 and 5. For that I would like to express my appreciation.

I feel very fortunate to have life-long friends who have been an immense support throughout the years, Ana Paola Ruiz, Olga Cornejo, Darlene Asayo-Gooch, Erin Miller, Amy Danko and Tracey Dennis, I am grateful to know that neither time nor distance will ever change our friendship. I have also met wonderful people in Edmonton who I wish to thank for their friendship, especially Vicki Cooper, Steve Kibbe and all the members of both my soccer teams.

My deepest appreciation goes to Cara Jones and Ian Clark as well as the rest of the Clark family for their warmth, encouragement and such wonderful moments.

I would also like to express my deepest gratitude to both of my “Canadian families”, the Asayo’s and the Dennis’, thank you for making Canada my home away from home especially during those first few difficult years.

I have no words to express my love and gratitude for Rhett Clark. Thank you for being an endless source of love, support, confidence and inspiration in my life.

Despite the geographical distance, my family has always been very close to me. I would like to thank my parents, Irma Morales and Fernando Zuniga as well as my brother Leonardo, for their love, encouragement and words of wisdom throughout the years, which have shaped me into the person I am today.

Table of Contents

List of Tables

List of Figures

List of Abbreviations

^{o}C	degree Celsius
%	percent
2MBC	2-methylbutyrylcarnitine
A	multi-path term in the van Deemter equation
Å	Angstrom
AC	alternating current
ACN	acetonitrile
amu	atomic mass units
ATP	adenosine triphosphate
B	longitudinal diffusion term in the van Deemter equation
BMI	body mass index
BSA	bovine serum albumin
C	mass transfer term in the van Deemter equation
CACT	carnitine acylcarnitine translocase
CAT	carnitine acetyltransferase
CDEA	cocodiethanolamide
CE	collision energy
CE-MS	capillary electrophoresis mass spectrometry
CID	collision-induced dissociation
CV	coefficient of variation
CoA	coenzyme A

CPT	carnitine palmitoyltransferase
CV	coefficient of variation
C*X*	acylcarnitine with *X* number of carbons along its fatty acid chain
C*X*-I	branched acylcarnitine
C*X*:*Y*	acylcarnitine with *Y* degrees of unsaturation
C*X*:DC	dicarboxylic acid carnitine conjugate
C*X*+=O	acylcarnitine containing a carbonyl group
C*X*+OH	acylcarnitine containing a hydroxyl group
CYP	cytochrome P450 enzyme
d	distance
Da	dalton
DBS	dried blood spot
DC	direct current
DNA	deoxyribonucleic acid
DPS	dried plasma spot
DUS	dried urine spot
EDTA	ethylenediaminetetraacetic acid
EML	evidence-based metabolome library
EPI	enhanced product ion
ESI	electrospray ionization
EtOH	ethanol
FA	formic acid
FAD	flavin adenine dinucleotide

$FADH_2$	reduced form of flavin adenine dinucleotide
FAO	fatty acid oxidation disorder
FDA	Food and Drug Administration
FT	Fourier transform
g	gram
g	relative centrifugal force
GC	gas chromatography
GC-MS	gas chromatography mass spectrometry
H	height equivalent to a theoretical plate
h	hour
H_2SO_4	sulfuric acid
HCl	hydrochloric acid
HLB	hydrophilic-lipophilic balance
HLM	human liver microsomes
HMDB	Human Metabolome Database
HPLC	high performance liquid chromatography
IBD	isobutyryl-CoA dehydrogenase
IDA	information dependent acquisition
IEM	inborn error of metabolism
IMM	inner mitochondrial membrane
k	retention factor
L	litre
LC	liquid chromatography

LC-MS	liquid chromatography-mass spectrometry
LCAD	long-chain acyl-CoA dehydrogenase
LIT	linear ion trap
m	mass
m/z	mass-to-charge
M	molar
MCAD	medium-chain acyl-CoA dehydrogenase
MCX	mixed-mode cation-exchange
min	minute
MRM	multiple reaction monitoring
MS	mass spectrometry
MS/MS	tandem mass spectrometry
MS + MS/MS	MS followed by tandem MS
MS^3	multiple-stage mass spectrometry
NAD^+	nicotinamide adenine dinucleotide
NADH	reduced form of nicotinamide adenine dinucleotide
NADPH	nicotinamide adenine dinucleotide phosphate
NMR	nuclear magnetic resonance
PBS	phosphate-buffered saline
PEG	polyethylene glycol
pH	potential of hydrogen
ppm	parts per million
Q	quadrupole

QQQ	triple quadrupole
q	charge
QIT	quadrupole ion trap
r	radius
R^2	square of the correlation coefficient
RBC	red blood cell
RE	relative error
RF	radiofrequency
RNA	ribonucleic acid
RP	reversed-phase
rpm	revolutions per minute
s	seconds
S/N	signal-to-noise ratio
SCAD	short-chain acyl-CoA dehydrogenase
SCX	strong cation exchange
SIL	stable isotope-labeled
SPE	solid-phase extraction
SRM	selected reaction monitoring
t	time
TOF	time-of-flight
TIC	total ion chromatogram
U	DC voltage
u	linear velocity

UHPLC	ultra high performance liquid chromatography
UPLC	ultra performance liquid chromatography
V	voltage
VLCAD	very long chain acyl-CoA dehydrogenase
v/v	volume/volume
XIC	extracted ion chromatogram
α	selectivity factor (in liquid chromatography)
m	milli- (10^{-3})
μ	micro- (10^{-6})

Chapter 1

Introduction to Liquid Chromatography Mass Spectrometry and Metabolome Analysis

1.1 Metabolomics

The notion that changes in tissues and biological fluids are indicative of disease goes back at least as far as ancient Greece. For example, Hippocrates used his senses as instruments to diagnose his patients. The field of metabolomics follows this notion and aims to test this theory by applying modern analytical techniques to analyze complex biological samples.[1] Metabolomics is commonly defined as the detection, identification and quantification of all small molecules or metabolites (any molecule excluding genetic material, proteins and large peptides) in a biological system.[2] This comprehensive approach is distinct from metabolite profiling, which is a targeted approach where pre-defined metabolites usually related to specific metabolic pathways are identified and quantified. Small molecule research recently developed into a combination of the two.[3] In many cases, there is interest in detecting and quantifying as many biologically related metabolites as possible. Metabolic analyses have become very useful for disease diagnosis, since alterations in the proteome are typically intensified at the metabolic level. In fact, researchers claim that metabolomics is more tightly linked to phenotype than any other of the "omics" sciences.[2]

1.1.1 Metabolomics and Systems Biology

Systems Biology aims to find a direct connection between genotype and phenotype by studying gene expression as well as protein and metabolite profiles in order to obtain a deeper understanding of a biological system.[4,5] This concept

was developed since it has become clear that a complete understanding of the condition of genes and proteins in a biological system does not reveal its phenotype.[6] It has led to the analysis of metabolites which, being the downstream products of gene and protein expression, are thought to be more closely related to phenotype.[5, 7] Figure 1.1 is a depiction of the Omics cascade.

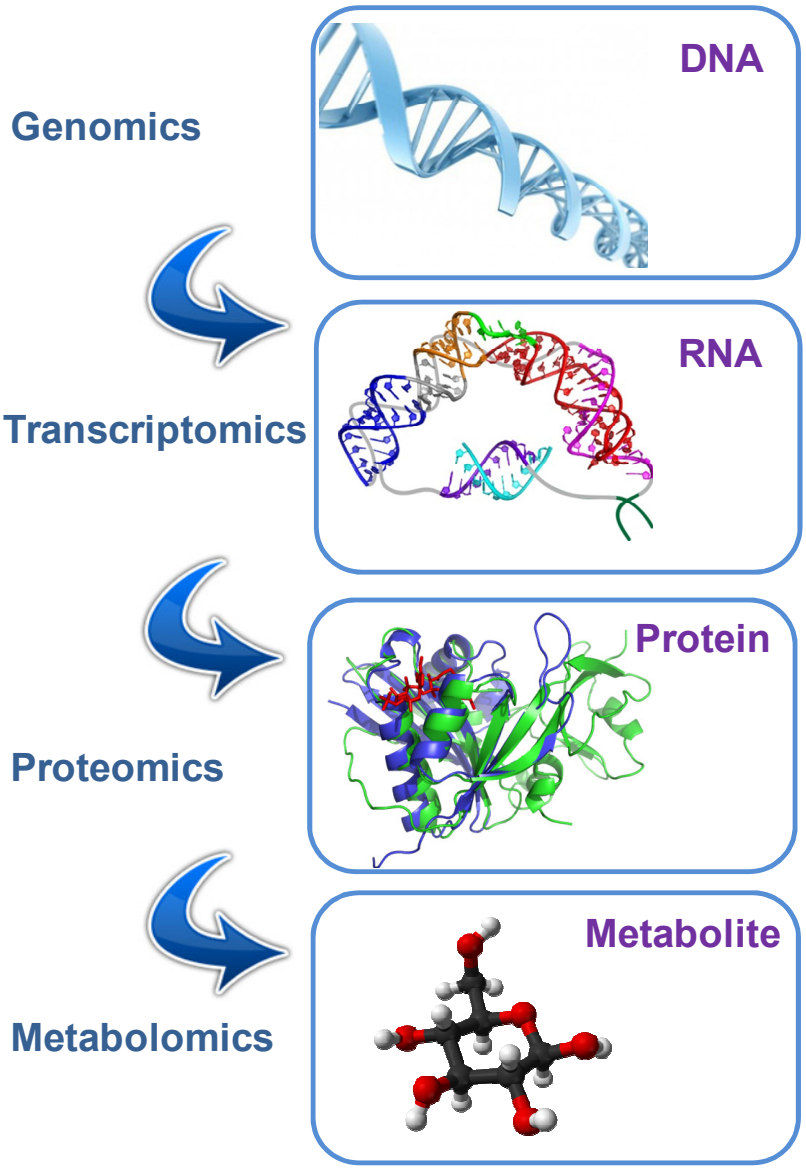

Figure 1.1 Omics cascade. Relationship of metabolomics to other Omics approaches.

Theoretically, the relationships between genes, proteins and metabolites can be discovered, and the cause of disorders and illnesses can be elucidated. Unfortunately, these links are time displaced, making it extremely challenging to find these connections.[8] Moreover, exogenous material introduced into a particular biological system, as well as other environmental factors such as temperature and stress complicate matters even further.[1] As a result, researchers tend to focus on a single discipline. Figure 1.2 is a depiction of these time-displaced connections between gene expression and phenotype.

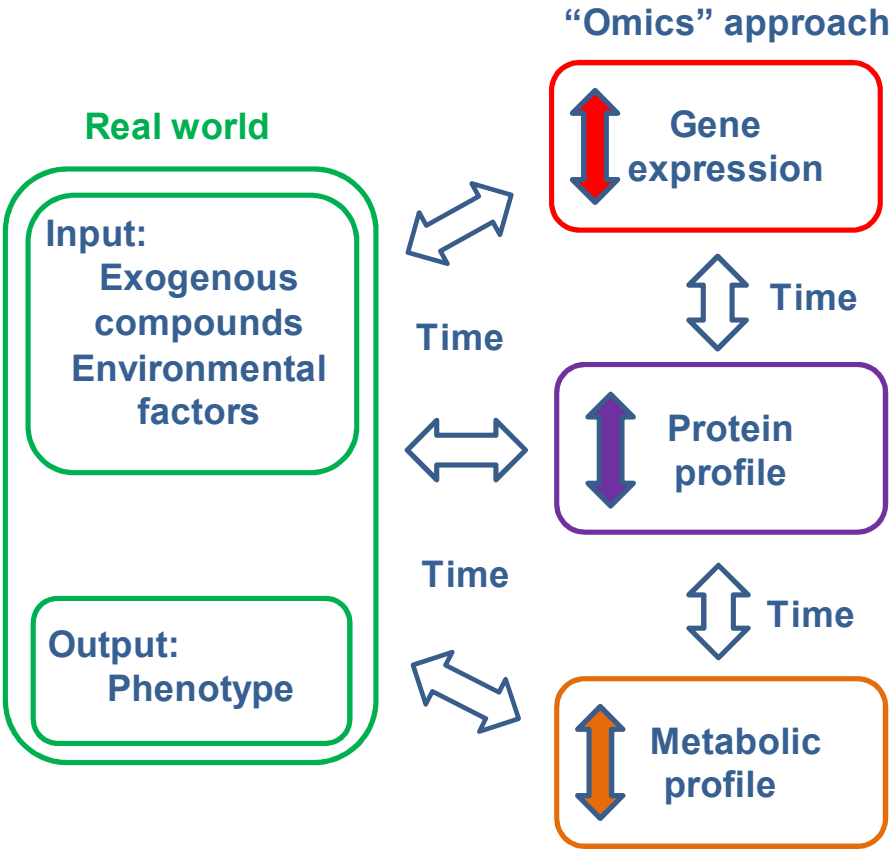

Figure 1.2 Relationship between Omics approach and the real world. Time-displaced connections are shown between actual phenotype and measured Omics responses. Adapted from Nicholson *et al*.[8]

1.1.2 Challenges associated with metabolome analysis

The main challenges associated with this area of research are well known. The size of the metabolome, which still remains unknown, poses one of the major challenges of this field. In any given biological sample there could be tens of thousands of different metabolites present, making their detection a hurdle. The large concentration dynamic range for these metabolites easily exceeds nine orders of magnitude, further complicating their simultaneous detection.[9] A third, and also very important challenge, is the chemical diversity of metabolites, making it necessary in some cases to utilize more than one analytical platform to obtain an accurate depiction of the metabolic profile of a particular sample. To this end, many analytical techniques have been developed and are continuously being improved. The most widely used techniques for metabolomic analyses are liquid chromatography-mass spectrometry (LC-MS), gas chromatography/ mass spectrometry (GC-MS), capillary electrophoresis-mass spectrometry (CE-MS) and nuclear magnetic resonance (NMR).

1.1.3 Metabolite identification

The aforementioned challenges have been but minor hurdles compared to the challenge that is, up to this day, the bottleneck of metabolomics: compound identification. Using LC/MS approaches it is difficult to obtain a definitive identification of all the features (molecular entities with a unique *m/z* and a particular retention time)[10] found in a sample. By definition, features could be metabolite fragments, metabolite-solvent adducts or the same metabolite containing different isotopic abundances. It is therefore advantageous to filter out these redundancies before attempting to identify a particular metabolite.[11] There are different levels of identification that have been previously described.[12] In this work, *de-novo* MS/MS spectral interpretation was utilized to putatively identify detected metabolites. Microsome incubates of synthetic standards were also used to produce phase I metabolites of the available synthetic standards. Human liver microsomes are vesicles from the rough endoplasmic reticulum containing

enzymes which produce phase I metabolites. Phase I reactions include oxidation, reduction and hydrolysis among others. Data obtained from these incubates were used to putatively identify phase I metabolites. In order to obtain definitive metabolite identification, LC-MS data was directly compared to that of synthetic standards. Figure 1.1 depicts the two workflows employed in this work for metabolite identification.

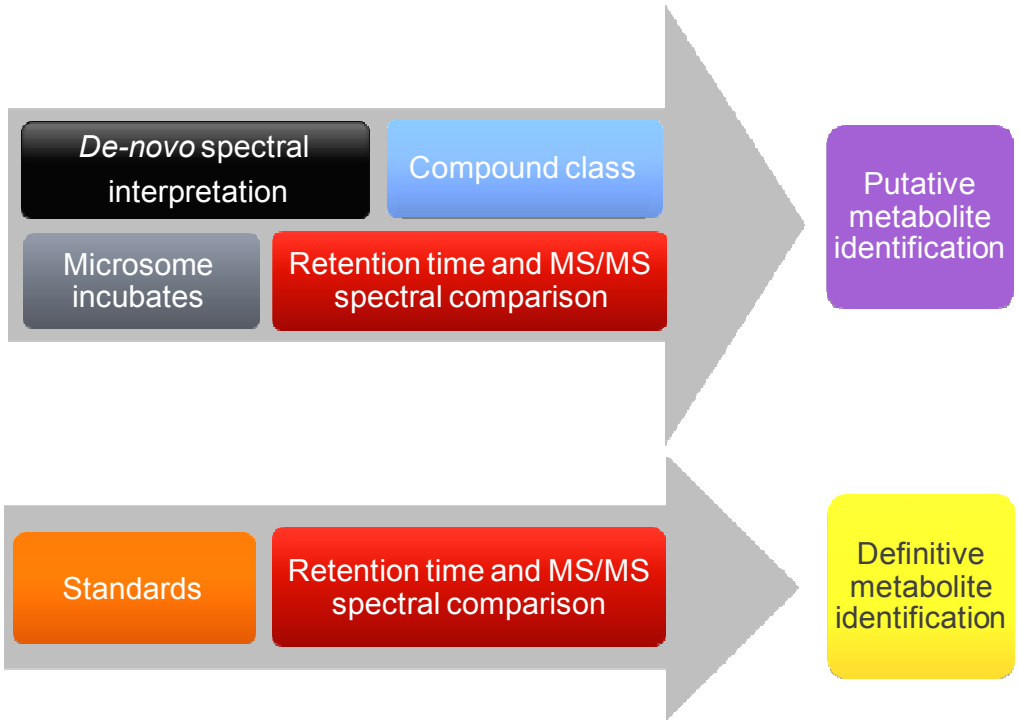

Figure 1.3 Metabolite identification approaches. Standards and microsome incubates were used as references for structure elucidation leading to putative and definitive metabolite identification, respectively. Manual MS/MS spectral interpretation only lead to putative metabolite identification.

MS-based metabolite databases have become more common and widely used to further aid the identification process. Some databases provide reference MS/MS spectra from synthetic standards, whereas others provide either raw or annotated MS and MS/MS data obtained from biofluids or tissue extracts. Some examples of these databases are the Human Metabolome Database (HMDB),[13] the

Metlin database[14] and Massbank.[15] In this work, a web-based tool called MyCompoundID which is based on the HMDB, but focused on facilitating MS/MS spectral interpretation to obtain more confident metabolite identification is described.

1.2 Liquid Chromatography

1.2.1 Ultra-high pressure systems (sub-two micron particles)

Ultra-high pressure LC systems utilizing sub two-micron particle size columns provide rapid, high-resolution separations and have thus been widely used for metabolomics analyses. High flow rates may be utilized without sacrificing chromatographic resolution. Moreover, these systems provide the high efficiency to separate species that are difficult to resolve on regular high performance liquid chromatography (HPLC) systems, such as structural or stereo-isomers.

Efficiency in liquid chromatography can be described in terms of the van Deemter equation (Equation 1.1). H is equal to the height of a theoretical plate, u is the linear velocity of the mobile phase and A, B and C are constants. The A term (also known as the multi-path term) is related to eddy diffusion through the column; the B term is proportional to longitudinal diffusion and C is dependent on the mass transfer of the analyte between the mobile and the stationary phase. The column efficiency is maximized when H is at its minimum. Smaller particles have an effect on both the A and C terms. Smaller particles cause an averaging effect on the multiple-path term, thus reducing the A term. Analytes can also more easily partition between the mobile and stationary phases when smaller particles are used, thus also reducing the C term.[16] Figure 1.4 is an overlay of three theoretical van Deemter curves for three columns with different particle sizes. It can be observed that for the sub-2 μm column, there is very little increase in

theoretical plate height with increasing linear velocity as compared to columns with 5 or 10 µm particles.

$$H = A + \frac{B}{u} + Cu \tag{1.1}$$

Equation 1.2 demonstrates the inverse relationship between particle size (d_p) and efficiency (N), with L being the length of the column. The relationship between resolution (R_s) and efficiency is shown in Equation 1.3, where α is the selectivity factor, and k'_2 is the retention factor. From these two equations one can recognize that as particle size decreases, the efficiency of the separation increases, which in turn also increases resolution.[16]

$$N = 3500L/d_p \tag{1.2}$$

$$R_S = \frac{\sqrt{N}}{4} \cdot \frac{\alpha - 1}{\alpha} \cdot \frac{k'_2}{(k'_2 + 1)} \tag{1.3}$$

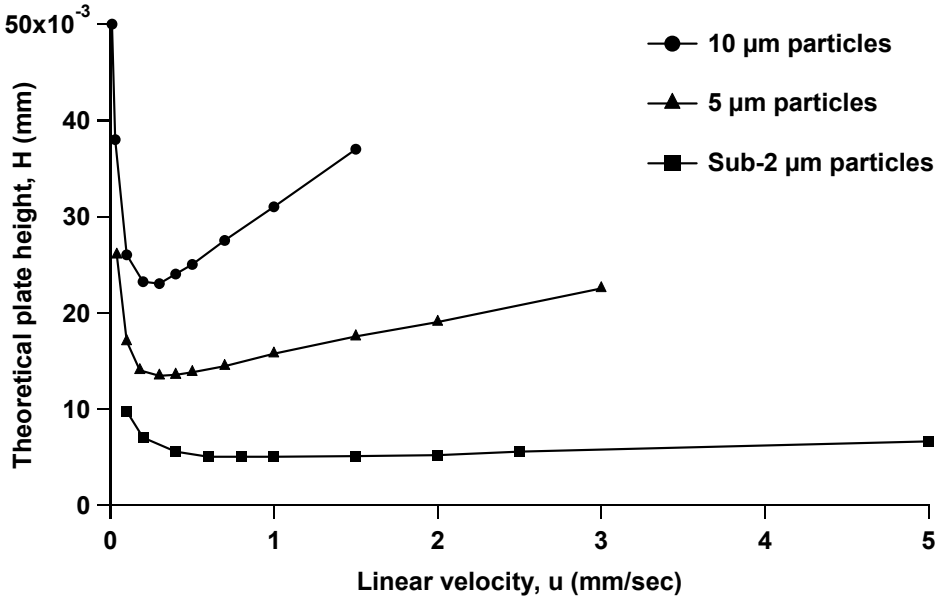

Figure 1.4 Theoretical van Deemter plots displaying the effect of column particle size on theoretical plate height (H). It can be observed that at high linear velocities, the value of H is much lower for a smaller particle size. Adapted from Hitachi High Technologies America, Inc.

While ultra-high pressure systems have become commonplace due to their improved characteristics compared to HPLC systems, an area of concern is the frictional heating produced when pumping mobile phase through a column at very high flow rates and pressures. Equation 1.4 describes this frictional heating, where F represents volume flow rate (in m^3/s) and p is the pressure drop in the column (in N/m^2). The generated temperature gradients (both radial and longitudinal) have detrimental effects on efficiency. In order to minimize this effect, smaller diameter columns (1 to 2.1 mm) are typically used.

$$\text{Power} = F \times p \tag{1.4}$$

1.2.2 Waters ACQUITY UPLC™ system

Ultra-high pressure systems have to be specially designed to be able to withstand the high pressures produced by small particle columns (up to 15,000 psi).[17] Stainless steel tubing and fittings are necessary to accomplish this task. Pumps capable of delivering solvent reproducibly at these high pressures are also needed, together with injection systems that prevent the column from undergoing large pressure fluctuations. In 2004, Waters introduced the ACQUITY UPLC™ system capable of performing separations using shorter columns, and/or higher flow rates for increased speed, with superior resolution and sensitivity.[18] This system was employed to develop the qualitative methods used for the detection and identification of acylcarnitines in various biological fluids described in Chapters 2 and 3.

1.2.3 Agilent 1290 Infinity UHPLC system

For the purposes of our studies, it was found that the Agilent UHPLC system offered the same capabilities as the Waters ACQUITY UPLC™ system, with the advantage of containing two identical binary high pressure pumps that allow for the usage of a two-column system controlled by a switching valve. This system was utilized for all quantitative studies. Pump 1 (or elution pump) can carry out the analytical separation through column 1 while pump 2 (or regeneration pump) washes and re-equilibrates the second column. This

alternating process allows for higher throughput analyses since the time needed for column flushing and re-equilibration (more than 40% of the total run time in our experiments) can be eliminated. Figure 1.5 shows how a 10-port switching valve can be used to alternate analyses from one column to another.

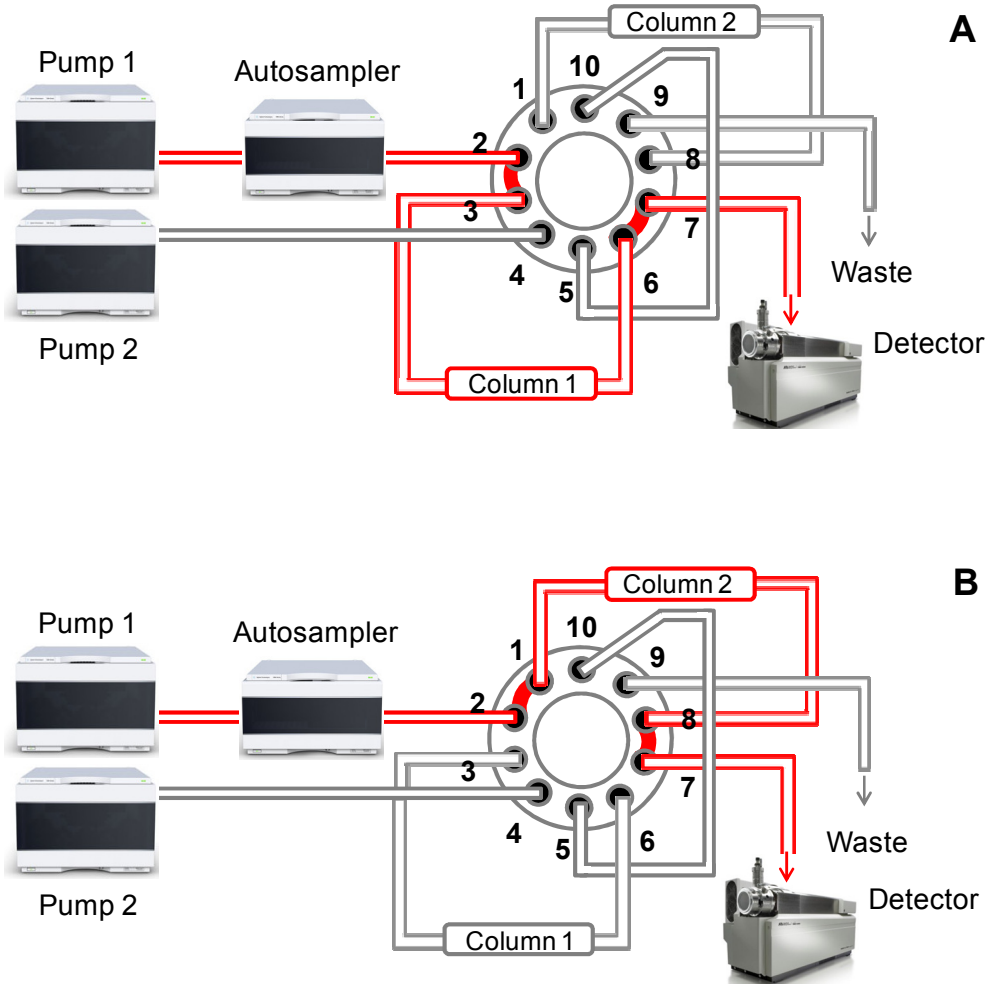

Figure 1.5 UHPLC alternating column regeneration system. In position A, the eluent from pump 1 goes through column 1 carrying out the analytical separation, while the eluent from pump 2 goes through the second column and into waste. In position B, the eluent from pump 1 goes through column 2 and into the detector while that of pump 2 goes through the first column for flushing and regeneration. The valve allows switching from one position to the other. Adapted from Agilent 1290 Infinity UHPLC user manual.

1.3 Electrospray Ionization

Electrospray ionization (ESI) has revolutionized many areas of research since it allows the coupling of two of the most powerful analytical techniques known to date: liquid chromatography and mass spectrometry. Together, LC-MS has allowed the development of research areas such as toxicology, drug and biomarker discovery, among others.[19, 20] Interestingly, ESI which has been so instrumental in LC-MS analysis, also poses its main limitation, especially for quantitative analyses. It is susceptible to matrix effects which are described as the enhancement or suppression of the ionization efficiency on an analyte by the presence of co-eluting substances.[21] This phenomenon is described further in Section 1.5.1. Another limitation is that ESI response is only linear up to total electrolyte concentrations of about 10^{-5} M which may also limit quantitative assays.

Albeit having these limitations, ESI has become one of the most widely used ionization techniques since the advantages that it offers outweigh its limitations. Its main advantage for small molecule analysis is that it works well for non-volatile and thermally-labile compounds due to the fact that it is a relatively soft ionization technique operating at atmospheric pressure and moderate temperatures.

1.3.1 Mode of operation

In the positive ion mode, a high voltage (2-5 kV) is applied to a capillary carrying the LC eluent. The exit of this capillary is strategically placed near the inlet of the mass spectrometer which acts as a counter electrode. Positive ions will accumulate at the liquid surface which is drawn out of the capillary, while negative ones will be drawn towards the inside of the capillary. The repulsion of the positive ions at the surface and the pull of the electric field on these ions overcome the surface tension of the solvent, forming a Taylor cone. The cone extends into a filament and subsequently into a fine mist.[22] An axial flow of

nebulizing gas can be utilized in order to pneumatically assist the solvent evaporation process. Figure 1.6 is a schematic of the electrospray process.

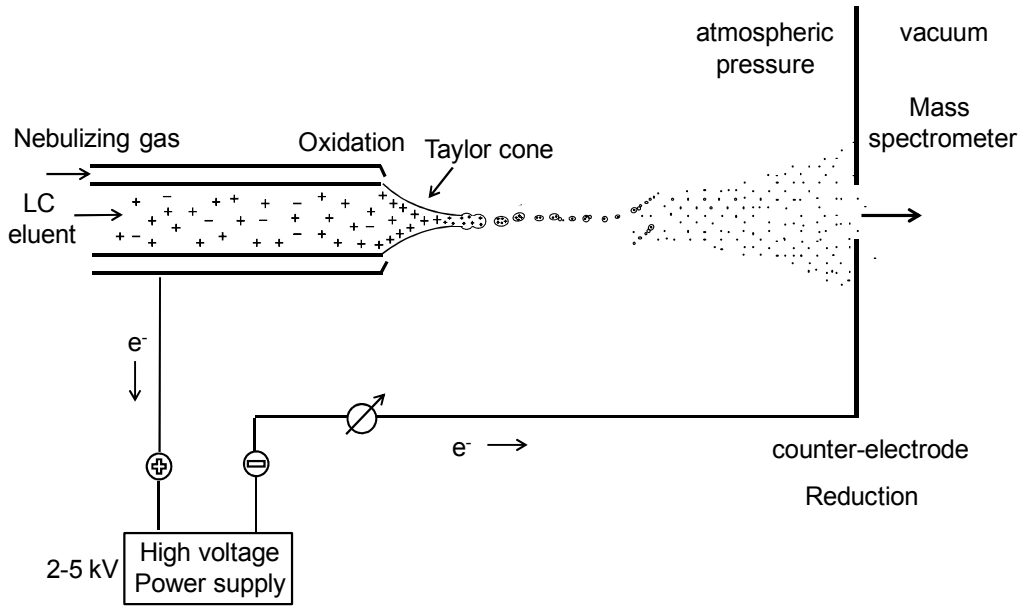

Figure 1.6 Schematic of the electrospray process. Adapted from Kebarle *et al*.[23]

1.3.2 Mechanism of the electrospray ionization process

Kebarle and Tang[23] describe four major processes involved in ESI which are described as follows; production of charged droplets at the capillary tip, shrinkage of charged droplets, repeated droplet disintegrations and finally generation of gas phase ions.

1.3.2.1 Production of charged droplets

The electric field at the tip of the capillary can be described using Equation 1.5, where V_c is the potential difference between the capillary and the counter electrode, r_c is the radius of the capillary and d is the distance between the capillary tip and the counter electrode. It is this potential which causes the electrophoretic movement of ions inside the capillary (towards the liquid surface in the case of positive ions). This is the main mechanism responsible for droplet

charging.[23, 24] Polar analytes lacking basic or acidic groups may form adducts (with sodium, ammonium or other solvent molecules) in solution before the charge separation process takes place.

$$E_c = \frac{2V_c}{r_c \ln\left(\frac{4d}{r_c}\right)} \quad (1.5)$$

Another mechanism responsible for droplet charging is electrochemical oxidation. This process, occurring at the metal-solvent interface, introduces positive ions into the solution by converting metal atoms into cations and electrons or, more importantly, by neutralizing negative ions in solution and producing electrons.[22] The metal ions produced by this reaction don't typically interfere with conventional mass spectrometric analyses.

Finally, analytes can also become charged upon undergoing gas-phase proton-transfer reactions. Once in the gas phase, protonated molecules may transfer their proton(s) to solvent or analyte molecules with higher gas-phase basicity. Noteworthy is that solution-phase basicity and gas-phase proton affinities are not necessarily related. It is therefore in some cases difficult to predict the gas-phase basicity of an ion.

1.3.2.2 Shrinkage of charged droplets

During their flight towards the mass spectrometer's focusing devices, shrinkage of charged droplets is accomplished by flowing of dry gas at moderate temperatures. AB Sciex instruments utilize a flow of nitrogen gas called "curtain gas" that runs perpendicular to the ion path which not only aids solvent evaporation, but also removes any droplets that might enter the mass spectrometer.

1.3.2.3 Repeated droplet disintegrations

As E_c increases (Equation 1.5), the tip of the Taylor cone, being the least stable, elongates into a thin liquid filament which breaks into individual charged droplets. This occurs when the cone reaches its Rayleigh limit, the point where

the surface tension (K) of the solution is equal to the coulombic repulsion of the charges accumulated along the liquid surface (Q). That is, droplet disintegrations will occur when Q^2 is greater than KR^3, where R is the droplet radius. Droplet fission is asymmetrical, where offspring droplets carry about 2% of the parent droplet mass and about 15% of its charge, meaning that with each fission, their charge density dramatically increases. Figure 1.7 is a schematic of the fate of an ESI droplet showing three subsequent fissions which occur at progressively shorter times. About 20 droplets are produced from each fission; eventually droplets become small enough to be able to produce gas phase ions.

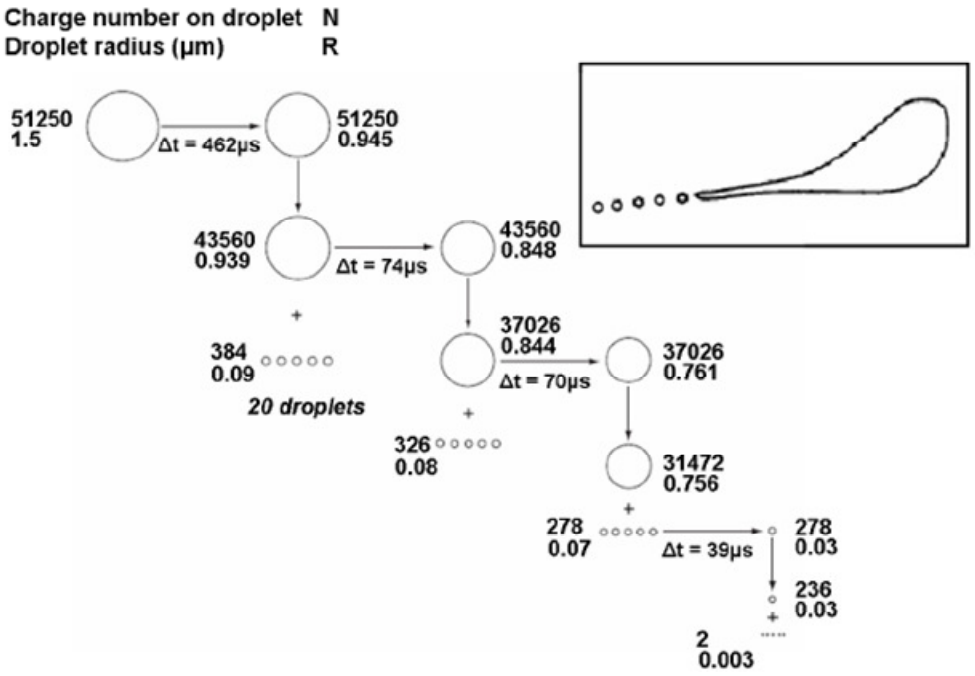

Figure 1.7 Schematic representation of the time history of an initial ESI droplet. Δt corresponds to the time required for evaporative droplet shrinkage to a size where fission occurs. Only the first three successive fissions of the initial droplet are shown. Reprinted with permission from (Kebarle, P.; Tang, L. *Analytical Chemistry* 1993, *65*, 972A-986A). Copyright (1993) American Chemical Society.

1.3.2.4 Generation of gas phase ions

Two different mechanisms aiming to explain the formation of gas phase ions in ESI have been proposed, one is the charge residue (or single ion in droplet) model while the other is the ion evaporation model. There has been no definitive evidence as to which model more accurately describes the mechanism of gas phase ion generation.

1.3.2.4.1 Charge residue model

Dole *et al.*[25] proposed a simple model stating that as charge density increases due to solvent evaporation, droplets continuously divide into smaller and smaller droplets (with radii of about 1 nm) until single gas phase ions are produced.

1.3.2.4.2 Ion evaporation theory

This model, proposed by Iribarne and Thompson[26] and based on transition state theory, assumes that solvent evaporation increases the charge density along the droplet surface until coulombic repulsion overcomes the solvent's surface tension. The droplet undergoes elastic deformation, and once the charge overcomes the activation barrier, repulsion will force solvated ions to escape from the surface of the droplets. Subsequent solvent evaporation leads to the formation of gas phase ions. Figure 1.8 shows a schematic of the ejection of a solvated ion from a large solvent droplet.

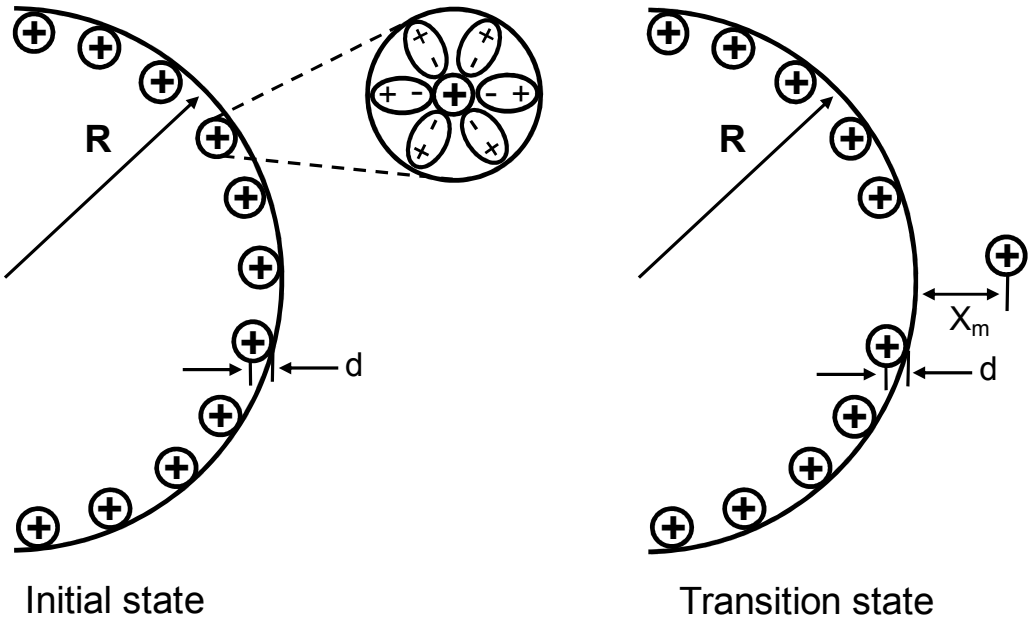

Figure 1.8 Iribarne and Thompson's model for ion evaporation. Initial and transition states show droplet radius R. D is the radius of an ion plus solvent shell. In the transition state, a solvated ion was expelled and is at a distance X_m from the outside of the droplet. Adapted with permission from (Kebarle, P.; Tang, L. *Analytical Chemistry* 1993, *65*, 972A-986A). Copyright (1993) American Chemical Society.

1.4 Mass Spectrometry

The vast majority of the work described herein was performed on a QTRAP® system which is a triple quadrupole-linear ion trap hybrid. However, in order to obtain high mass accuracy measurements for assessing the validity of the web-based tool MyCompoundID described in Chapter 6, a time-of-flight (TOF) instrument was employed. The 4000 QTRAP® will be described in detail in the following sections followed by a more succinct description of the TOF mass analyzer.

1.4.1 Quadrupole theory

Quadrupole-based mass spectrometers are readily used in many research areas including clinical screening and diagnostics, as well as environmental,

toxicologic and drug discovery studies. The development of the triple quadrupole (QQQ) mass spectrometer by Yost and Enke[27] has allowed for more sensitive and selective analyses by monitoring compounds based on their characteristic fragmentation patterns, as opposed to a single precursor mass.

Quadrupoles are true mass analyzers in the sense that they resolve ions based on their mass-to-charge ratio (*m/z*) as opposed to kinetic energy or momentum, as in the case of magnetic sector instruments. Their resolving power results directly from the stability of ions in the electric field within the instrument and thus ion velocity distributions have no effect on resolution.[28]

This mass analyzer consists of four cylindrical metal rods aligned in such a way to create a hyperbolic field upon applying ac and dc potentials. The ac voltage applied is in the radio-frequency range so it is in some cases referred to as RF voltage. Figure 1.9 shows a simplified schematic of a quadrupole mass filter. The blue trace corresponds to an ion that has a stable trajectory and is able to reach the detector. The red trace corresponds to an unstable ion which collides with the rods along the way and is therefore not detected.

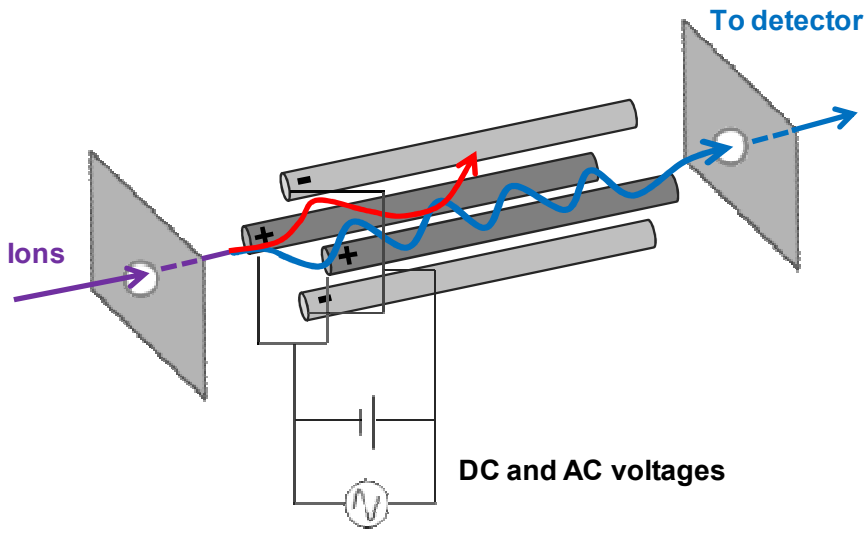

Figure 1.9 Schematic of a quadrupole mass filter. The red trace shows the trajectory of an unstable ion while the blue one shows the trajectory of a stable ion that reaches the detector. Adapted from the University of Bristol website. URL: http://www.chm.bris.ac.uk/ms/theory/quad-massspec.html (Accessed March 2012).

The same overall potential is applied to the rods along the x-axis, whereas the rods along the y-axis receive the same potential but of opposite sign. An ac voltage of alternating polarity is also applied to both pairs of rods. Ions with a small range of *m/z* values will have stable paths along the electric field defined by U + V Cos (ωt), where U is the magnitude of the DC potential, V is the magnitude of the ac or RF waveform and ω is its angular frequency which is defined by 2πf where f is frequency. A nearly ideal hyperbolic field is created when r =1.148 r_o, where r is the rod radius and r_o is the field radius. Figure 1.10 shows the voltages applied to the rods along the x and y-axes.

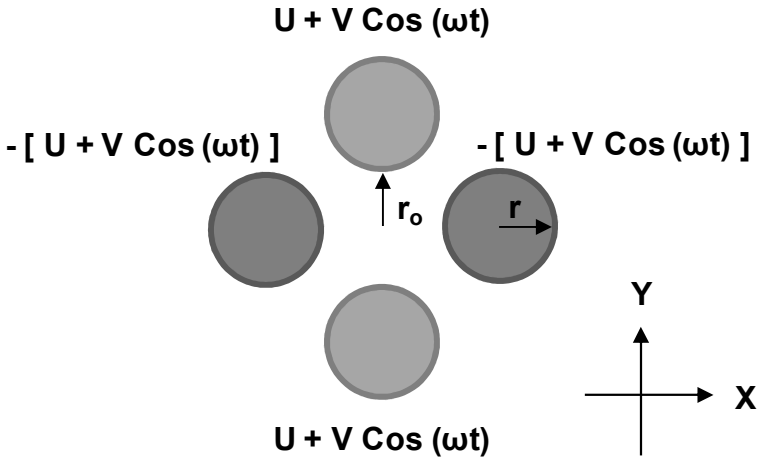

Figure 1.10 Schematic of a set of quadrupoles showing the voltages applied along both the x and y-axes. The z-axis goes into the page and is the direction that ions have to follow to reach the detector. R_o is the radius of the field and r is the radius of the rods.

1.4.1.1 Equations describing ion trajectories

The potential (ϕ) at any point in the hyperbolic field at time (t) can be defined by Equation 1.6 where x and y are distances along the corresponding coordinate axes, all other terms are described above.

$$\boldsymbol{\Phi = [\, U + V\, Cos\, (\omega t)\,] \frac{x^2 - y^2}{2r_o^2}} \tag{1.6}$$

The magnitude of the electric field can be obtained by taking the partial derivative of the potential equation as a function of the distance along any of the coordinate axes. Equations 1.7, 1.8 and 1.9 describe the electric field along the x, y and z-axes respectively.

$$\boldsymbol{E_x = -\frac{\delta \Phi}{\delta x} = -[\, U + V\, Cos\, (\omega t)\,] \frac{x}{r_o^2}} \tag{1.7}$$

$$\boldsymbol{E_y = -\frac{\delta \Phi}{\delta y} = [\, U + V\, Cos\, (\omega t)\,] \frac{y}{r_o^2}} \tag{1.8}$$

$$\boldsymbol{E_z = -\frac{\delta \Phi}{\delta z} = 0} \tag{1.9}$$

From Equations 1.7 and 1.8 it can be observed that the ion trajectory is independent along both coordinate axes. It can also be observed from Equation 1.9 that the applied potentials don't have an effect on the position and velocity of an ion along the z-axis. The a and q parameters are used to more succinctly describe the displacement of an ion within the device and can be defined as follows, with e in this case being the charge of the ion instead of z, and m being its mass.

$$\boldsymbol{a = \frac{4eU}{\omega^2 r_o^2 m}} \tag{1.10}$$

$$\boldsymbol{q = \frac{2eV}{\omega^2 r_o^2 m}} \tag{1.11}$$

F is defined as the force applied on a particular ion and is given by the magnitude of the electric field multiplied by the charge of the particle, and by Newton's law, F = ma. Using this information, equations 1.7 and 1.8 can be written in terms of the force applied to the ions. The a and q parameters can be substituted into these equations, with u representing either x or y and $\xi = t/2$.

Rearranging and applying the chain and product rules, the canonical form of Mathieu's differential equation can be obtained (Equation 1.12).[28]

$$\frac{d^2u}{d\xi^2} + [\, a_u + 2q_u Cos\, 2\xi \,]u = 0 \qquad (1.12)$$

1.4.1.2 The stability diagram

A bounded solution to the Mathieu equation (1.12) corresponds to a situation where the movement of an ion along either the x or y-axis remains finite; i.e the ion has a stable trajectory. In the case of an unbound solution, an ion would not have a stable trajectory and would therefore collide with the rods before reaching the detector. It can be observed from Equation 1.12 that ion trajectories depend only on the a and q parameters. A stability region can be defined as a collection of points in a-q space that corresponds to stable solutions of the Mathieu equation. Figure 1.11 depicts this region which is known as an a-q stability diagram, showing the mass scan line where only ions with mass m+1 are stable. Note that the mass (m) of an ion is inversely proportional to parameters a and q, so heavier ions require higher voltages to pass through the tip of the a-q diagram. This way, the tip of the diagram serves as a narrow band pass filter.

If the dc voltage is maintained as a fraction of the ac potential, the U/V ratio will remain constant. By doing so, the operating points of the mass filter will lie along a straight line which is called the mass scan line, with slope equal to 2U/V. The simplest way of operating a quadrupole as a mass analyzer, that is; to obtain a mass spectrum, is to increase both the dc and ac potentials applied to the rods while maintaining their ratio constant. As the voltages are increased, ions of increasing *m/z* ratio will pass through the tip of the a-q diagram and will reach the detector. The mass range of a quadrupole is typically 5 – 4000 amu and is dependent on the frequency of the RF voltage which is several hundred kilohertz.

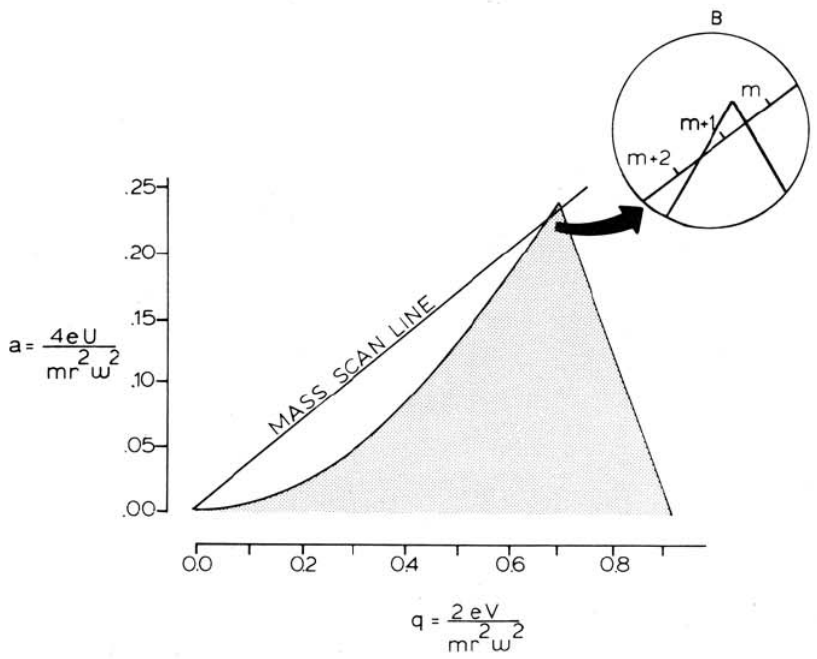

Figure 1.11 The a-q stability diagram. The shaded area represents stable areas in a-q space with bounded solutions to the Mathieu's differential equation. Reprinted with permission from (Miller, P.E.; Denton, M.B. *J. Chem. Educ.*, **1986**, 63 (7), 617-622). Copyright (1986) American Chemical Society.

Most modern mass spectrometers contain ion focusing devices at the front end, whether they are focusing lenses and/or RF-only rod systems (quadrupoles, hexapoles or octopoles). In the case of the rod systems, no dc potential is applied. This is equivalent to setting the a parameter equal to zero, making the slope of the mass scan line zero as well. Ions with a large range of *m/z* values will be stable within the instrument and can be detected. However, these systems do not provide total ion transmission; they are actually high pass mass filters. Ions with higher masses and thus lower q values travel more easily through the device. These systems are nonetheless very effective ion guides and have thus been employed for this purpose.

1.4.2 Triple quadrupole-linear ion trap hybrid (QTRAP®)

Recent advancements in mass spectrometry technology have allowed for more reliable quantification and characterization of small molecules due to its

accuracy, sensitivity, robustness and speed. There is still, however, no single mass spectrometer with all these desirable characteristics. [29, 30] Researchers have very frequently utilized two complementary MS platforms to obtain qualitative data such as accurate mass and quantitative information in MS/MS mode.[31] Hybrid instruments have been developed in an attempt to combine the advantages of two complementary mass spectrometers in a single system. The AB Sciex QTRAP® mass spectrometer is a triple quadrupole-linear ion trap hybrid. The third quadrupole can be utilized as a regular quadrupole or as a linear ion trap (LIT) with mass-selective axial ion ejection. The system has the ability to perform triple quadrupole-type scans, namely, neutral loss scan, precursor ion scan and multiple reaction monitoring, while having the sensitivity of a linear ion trap. Figure 1.12 is a schematic of the instrument's ion path including ion focusing lenses (IQ) and quadrupoles (stubbies), the RF/DC quadrupoles (Q1 and Q3), the collision cell (Q2) and the channeltron detector. The detector is an electron multiplier made of a semi-conducting material and curved in order to prevent positive ion feedback. Its signal amplification is inversely proportional to *m/z* ratio. Negative ions must first interact with a dynode converter that converts them into positive ions which can then be detected by the channeltron.

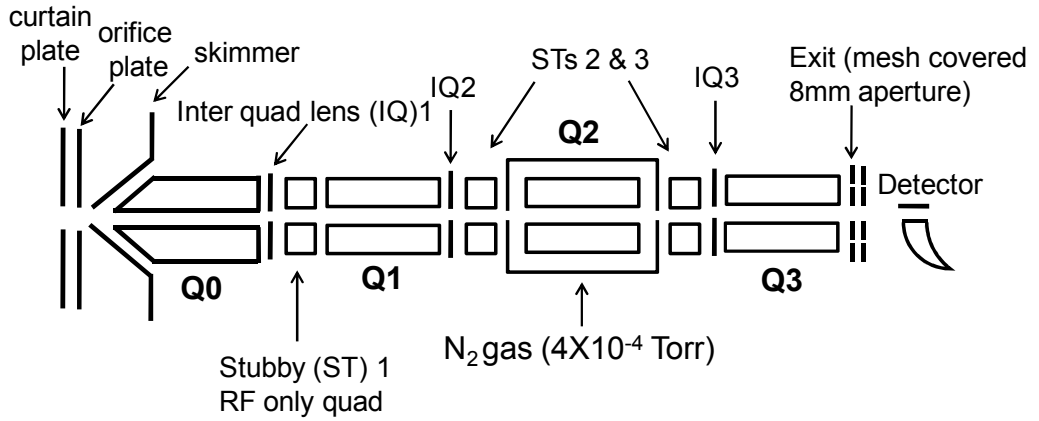

Figure 1.12 QTRAP® 4000 mass spectrometer schematic. Q, quadrupole rod set. Adapted from AB Sciex website URL:
http://www.absciex.com/Documents/Downloads/Literature/mass-spectrometry-cms_040200.pdf

1.4.2.1 Scan modes

This instrument platform can perform all of the triple quadrupole-type scan modes as well as linear ion trap mode scans. In this work, only triple quadrupole-type scans were utilized, with the exception of the product ion scan, this section will therefore mainly focus on these scan types. All QQQ scans are based on collision-induced dissociation which is comprised of two steps; collisional activation followed by ion dissociation. Collisional activation occurs when a small fraction of an ion's translational energy is converted into internal energy. Enough vibrational energy in a molecule will initiate bond ruptures. The location of the charge on the ion and the stability of the products play a major role in which fragments are the most abundant. The 4000 QTRAP® offers various other capabilities such as polarity switching and MS^3 which were not required for the work described in this thesis and will therefore not be discussed further.

1.4.2.1.1 Neutral loss scan

In a neutral loss scan, the first quadrupole or Q1 will scan all ions within a specified mass range, these ions will undergo collision-induced dissociation (CID) in the pressurized collision cell or Q2. During CID, ions will be accelerated through the collision cell and will undergo a number of collisions with a dry gas (N_2 in this case). The internal energy produced from this process will cause an energized ion to dissociate into fragments. The third quadrupole or Q3 will then scan all ions within a specific mass range but will do so at an offset relative to Q1, corresponding to a neutral loss that is specified by the user. Under these conditions, only precursor ions which upon fragmentation give rise to a specific neutral loss will be detected.

1.4.2.1.2 Precursor ion scan

In a precursor ion scan, Q1 will scan all ions within a specific mass range, these ions will then fragment in Q2 (same as in a neutral loss scan) except that in this case, Q3 is set to only allow fragment ions of a particular *m/z* ratio to travel

through and be detected. By doing so, only precursor ions which upon CID produce a fragment ion of a particular *m/z* will be detected.

1.4.2.1.3 Selected reaction monitoring scan

In a selected reaction monitoring scan, Q1 will select precursor ions of a particular *m/z* ratio. These ions will fragment in Q2, accelerate into Q3 where only fragment ions of a particular *m/z* ratio will be allowed to pass through and reach the detector. This type of scan offers the highest sensitivity, since selecting and monitoring a single reaction pair (precursor and fragment) at a time will considerably minimize the background signal.[32] When more than one reaction pair is being monitored in a single injection, this type of scan becomes multiple reaction monitoring or MRM. While this is a very sensitive scan, it has the disadvantage that previous knowledge of the fragmentation patterns of the metabolites of interest is necessary. Moreover, the fragment ions to be monitored have to be carefully chosen in order to maximize sensitivity and specificity. The most intense fragment ions will provide the highest sensitivity. However, it is also important to choose fragments that are characteristic of the compounds being studied, rather than monitoring the loss of a water molecule, for example, which is much less specific. Another consideration with this type of scan is the optimization of the dwell time (amount of time for which each reaction is monitored). High dwell times (≈50 ms) offer high signal to noise (S/N) ratios but increase the total cycle time, lowering the frequency of data collection. Optimization is therefore necessary in order to obtain acceptable S/N ratios while gathering enough data points to adequately define sharp UHPLC peaks.[31]

1.4.2.1.4 Product ion scan

The 4000 QTRAP® offers the capability of performing "tandem-in-space" fragmentation with the high sensitivity of a linear ion trap (LIT). The instrument manufacturer's full name for this scan is enhanced product ion scan or EPI since the third quadrupole is utilized as a linear ion trap, which enhances the sensitivity of the scan. In a product ion scan or MS/MS scan, the isolation of the precursor

ion takes place in Q1, the fragmentation process takes place in Q2, and Q3 in this case can act as a linear ion trap. Fragment ions emerging from the collision cell will be trapped in Q3 (allowing for ion accumulation) and scanned out according to their *m/z* ratio. Trapping of ions has been shown to dramatically increase the sensitivity of the scan. This instrument offers three different scan speeds in LIT mode; 250, 1000 and 4000 amu/s. Higher scan speeds result in more data points collected but at the expense of lower resolution.[33] It is advantageous to perform CID in the collision cell of the device rather than in the LIT since the MS/MS spectra obtained are more informative. This is due to the multiple collisions with the auxiliary gas that an ion may undergo in a collision cell as compared to an ion trap. Moreover, trapping systems, especially 3-D ion traps suffer from a low mass cut-off, meaning that fragment ions with a *m/z* less than 1/3 of that of the precursor will not be stable in the trap and will therefore be lost. This effect is not as prominent in a linear ion trap since RF/DC trapping is more efficient. In a LIT, ions are trapped radially by the RF voltage applied to the rods and axially by DC biased plates.

Another advantage of a LIT as compared to a 3-D ion trap is the reduced space-charge effects due to overfilling of the trap which affect both accuracy and resolution. The 4000 QTRAP® system allows the user to either determine the trapping time in the LIT or chose the dynamic fill time option were the instrument will perform a 30 ms pre-scan which will automatically determine the fill time.[29] Figure 1.13 shows a schematic of how each of these scan modes described above work.

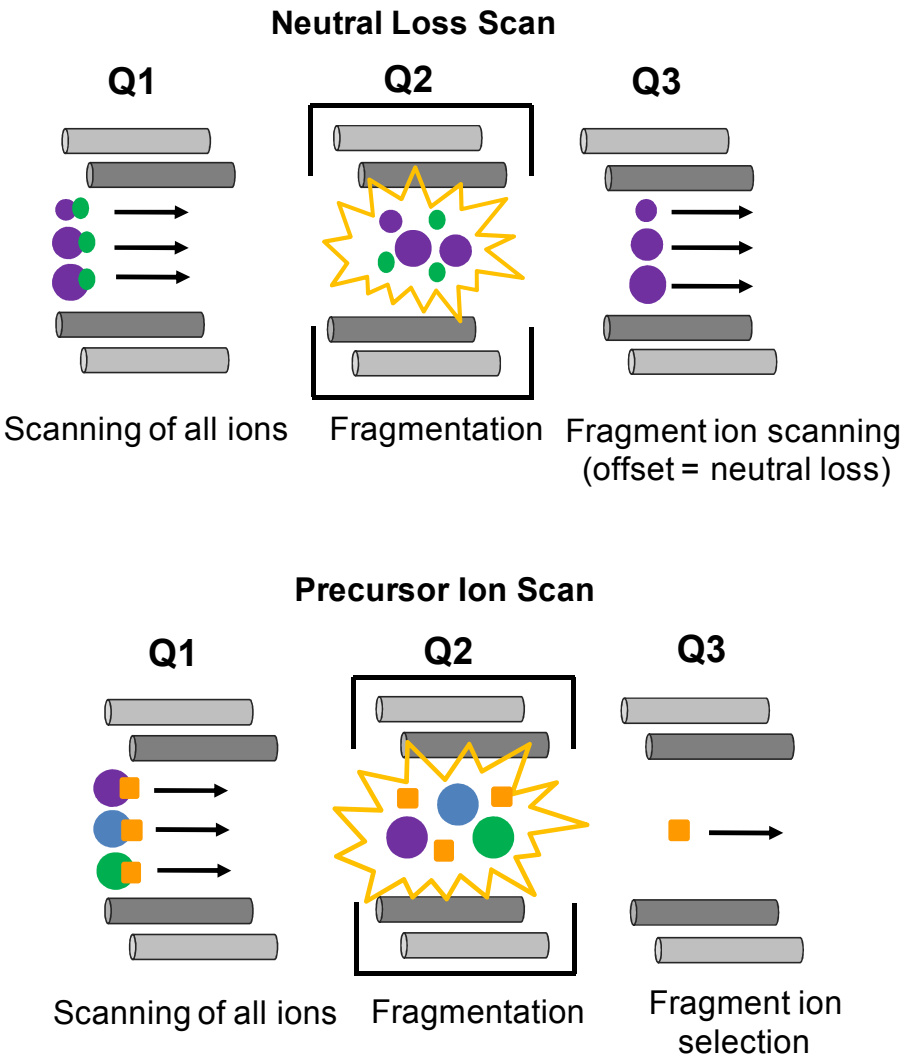

Figure 1.13 QTRAP® scan modes. In neutral loss mode, all ions that upon collision-induced dissociation (CID) have a characteristic neutral loss will be detected. In precursor ion mode, only ions that upon CID produce a specific fragment ion will be detected.

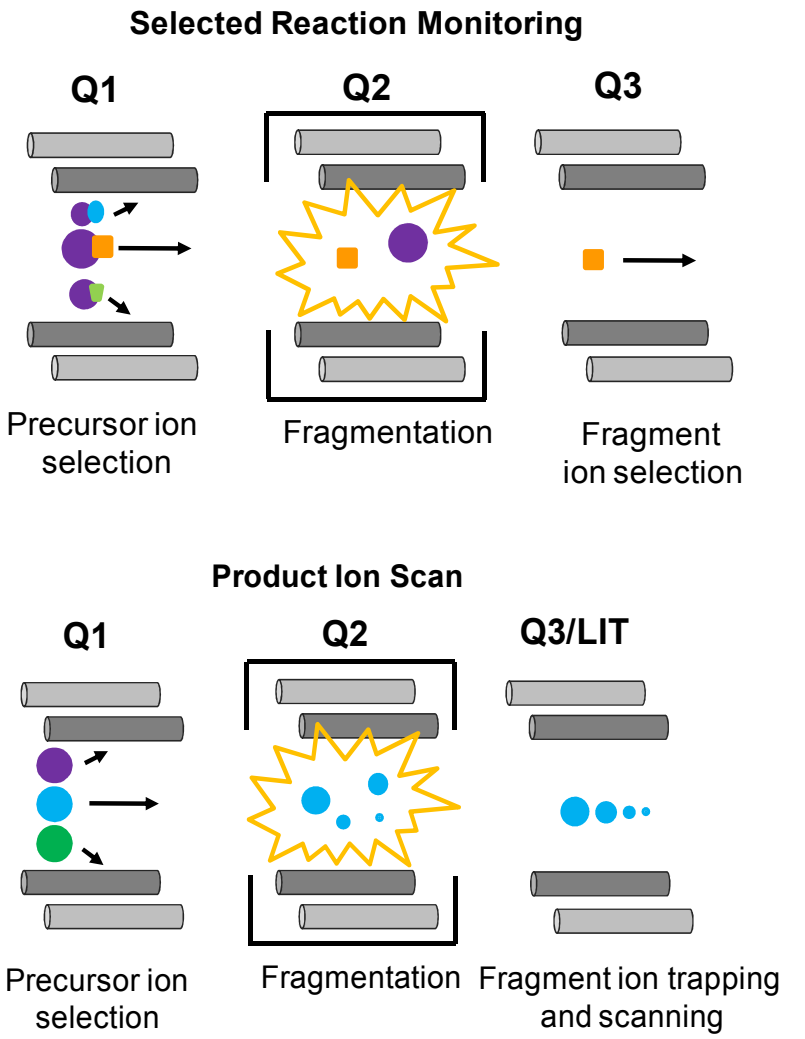

Figure 1.14 QTRAP® scan modes (continued). In selected reaction monitoring mode, a specific precursor ion is selected in Q1 and a specific fragment ion is selected in Q3. During a product ion scan all fragments from a specific precursor ion are trapped, scanned and detected.

1.4.2.2 Information-dependent acquisitions

A very useful feature of this mass spectrometer is its ability to perform "on-the-fly" information-dependent acquisitions. This feature allows the combination of two or more scan types in a single LC-MS run, thereby significantly increasing sample throughput. The most common combination is having a survey scan (neutral loss, precursor ion or selected reaction monitoring) followed by a product

ion scan. This allows for collection of fragmentation information on the compounds of interest during the same LC-MS run. The user can select the conditions under which a specific ion will be chosen to do subsequent MS/MS analysis, such as ion abundances, selected *m/z* values or mass ranges. The second scan (dependent scan) is then performed on the candidates using the selection criteria. As soon as ions are detected, the instrument automatically switches to product ion mode, as soon as it is performed, the instrument switches back to the survey scan. Figure 1.14 illustrates an IDA experiment works.

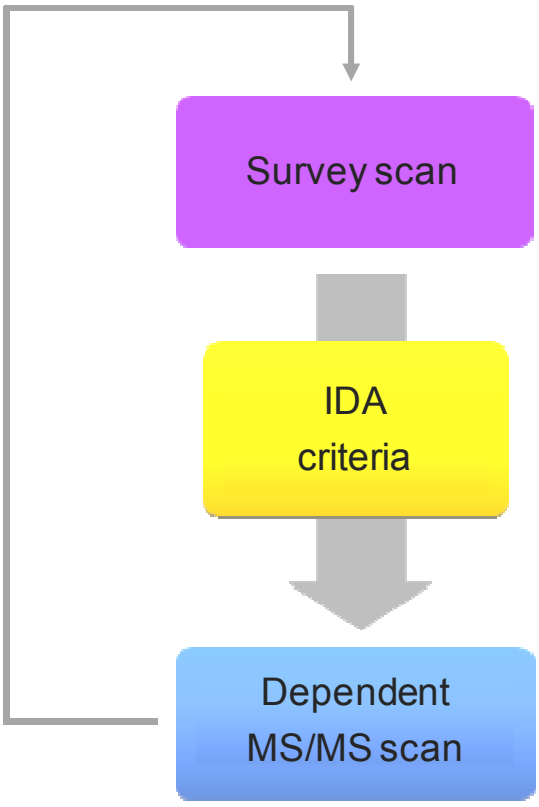

Figure 1.15 Schematic of an information-dependent acquisition (IDA) experiment.

1.4.2.3 Limitations of this mass spectrometer system

The biggest limitation of the 4000 QTRAP® in terms of its use for metabolite identification is its inherent low mass accuracy; neither quadrupoles nor linear ion traps can provide the high mass accuracy and resolution that a time-of-flight (TOF) or a Fourier transform (FT) mass spectrometer can offer. For this reason, in order to obtain reliable compound identification, it is still common for researchers to combine data from a TOF and a QTRAP® system.[31]

1.4.3 Time-of-flight mass analyzer

The TOF mass analyzer provides the mass accuracy that the QTRAP® cannot. It is comprised of three main components, a sample introduction and ion focusing region, a drift region and a detector. The heated glass capillary, skimmer, octopoles, quadruple and beam slicer, all form part of the Agilent orthogonal 6220 TOF sample introduction and ion focusing region. The quadrupole and beam slicer together normalize the starting positions of ions before they are pulsed into the flight tube. The drift region is a field-free flight tube where ions are separated according to their flight time. Finally, the detector is comprised of a microchannel plate.

Focused ions are accelerated into the flight tube by an ion pulser which is strategically placed orthogonal to the initial ion path in order to compensate for the ions' initial spatial and temporal distribution. The ions travel with velocities that are inversely proportional to their masses and thus lighter ions will reach the detector before heavier ones. More specifically, the force applied to the ions is equal to their kinetic energy. That is, $V \cdot e = 1/2m\nu^2$, where V is the voltage applied, e is the charge of an ion, m is its mass and ν is velocity. Since velocity is equal to distance (D) over time (t), these variables can be substituted into the previous equation and upon rearranging, an expression relating an ion's flight time (t) to its mass (m) can be obtained (Equation 1.13).[34]

$$t = \sqrt{\frac{mD^2}{2V \cdot e}} \tag{1.13}$$

Even with an orthogonal ion pulser, the resolution of a simple, linear TOF is often limited. The introduction of the reflectron system by Mamyrin *et al*.[35] in 1973 provided a significant improvement in this area. The reflectron is a series of metal meshes with increasing potentials. It increases the focal length of the instrument, allowing for better peak separation. Moreover, it compensates for the initial energy distribution of ions with the same *m/z* ratio. Faster ions will travel deeper into the reflectron allowing for slower ions to "catch up". The electric mirrors which initially slow ions down will accelerate them back into the flight tube at the end of which ions will be focused as they reach the detector.[34] Figure 1.15 is a schematic of the Agilent oa 6220 TOF mass analyzer.

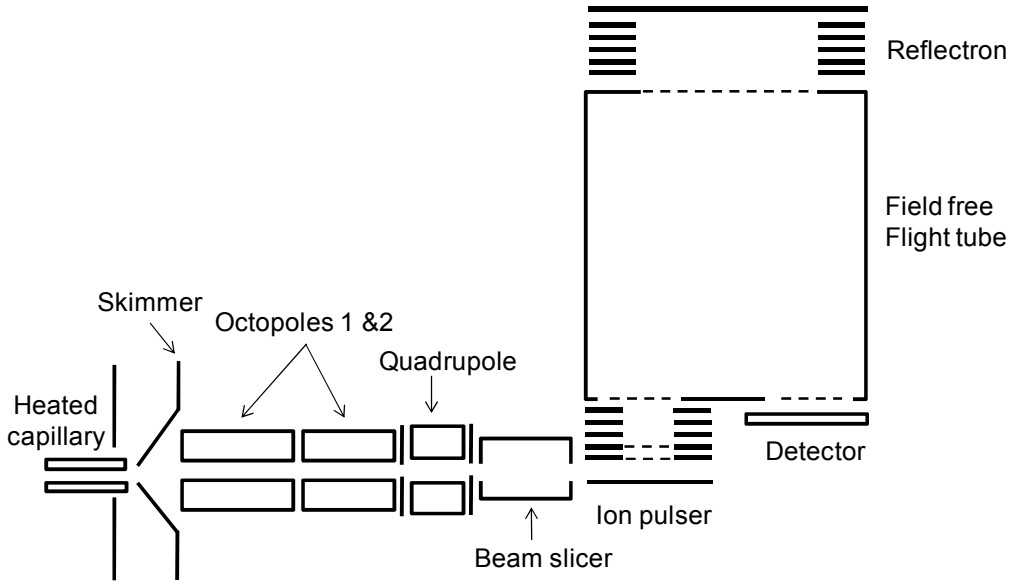

Figure 1.16 Schematic of the Agilent 6220 oa TOF mass spectrometer. Adapted from University of Duisburg-Essen's website URL: http://www.uni-due.de/imperia/md/content/waterscience/ss09/4121_01z_ss09_agilent_024_qtof_performanceoverview_animation.swf.

1.5 Quantification

The accuracy and precision of metabolite quantification strategies have improved dramatically with recent advancements in LC-MS instrumentation. However, there are a few areas of concern when complex biological samples are being studied, the most important being matrix effects. This phenomenon, as well as various approaches to try to minimize its effects will be discussed in the next sections.

1.5.1 Matrix effects

The effect of co-eluting species on the ionization efficiency of analytes in a complex matrix was first described by Kebarle and Tang.[23] It is known that nonpolar, surface-active analytes have a higher ESI response, since they reside at the solvent-air interface and enter the gas phase more readily. However, researchers have tried to explain what happens when there are many other species present in the sample. One theory explains matrix effects as being caused by a change in the properties of the ESI droplets caused by less volatile species present in the droplet which interfere with droplet formation and evaporation. This ultimately decreases the number of gas phase ions that are introduced into the mass spectrometer.[36] Matrix effects are also described as the limited amount of excess charge available on the surface of ESI droplets, causing competition for these charges, limiting an analyte's ionization efficiency. Additionally, the charge on the surface of the droplet inhibits ejection of ions trapped inside.[37]

Regardless of the cause of this phenomenon, it is important to identify and correct matrix effects as much as possible when developing ESI-MS methods. It is especially difficult to identify matrix effects when developing assays with very high specificities such as MRM-based methods where only specific ions are detected. In these cases no interferences at the chromatographic level are observed, although interfering species at high concentrations may actually be

present.[38] For this reason sample clean up, efficient chromatographic separations and adequate method validation strategies are necessary.

There are various methods of identifying matrix effects, including post-column infusion, where a standard solution containing the compound of interest is infused at a constant rate through a t-splitter in between the LC column effluent (containing the sample of interest) and the mass spectrometer. The two solutions will mix before reaching the ionization source and changes in the analyte signal due to sample components can be identified as matrix effects.[39] This strategy however, does not work with endogenous compounds since they are already present in the sample. In these instances, different methods have to be employed. Comparison of calibration curve slopes prepared in neat solvents and in the matrix of interest has been used for this purpose.[40] Another way to overcome matrix effects in the analysis of endogenous metabolites is the standard addition approach which is described in the next section. In this work, comparison of slopes in solvent and the matrix of interest was employed and the results obtained were compared to a classic standard addition approach.

1.5.2 Standard addition

The standard addition approach is very effective for the accurate quantification of compounds in a complex matrix. Known amounts of analyte are added to a sample (containing an unknown amount of analyte). The instrument response is recorded upon each addition. Assuming the instrument response increases linearly with each addition, a linear relationship between concentration of added analyte and analytical response can be established. This line can then be extrapolated back to the x-axis (Y = 0) which corresponds to the concentration of analyte originally present in the sample. A major limitation of this technique is that it is very labour intensive since a standard addition curve has to be constructed for each individual sample. Figure 1.16 shows how a standard addition curve can be used to calculate the concentration of an unknown.

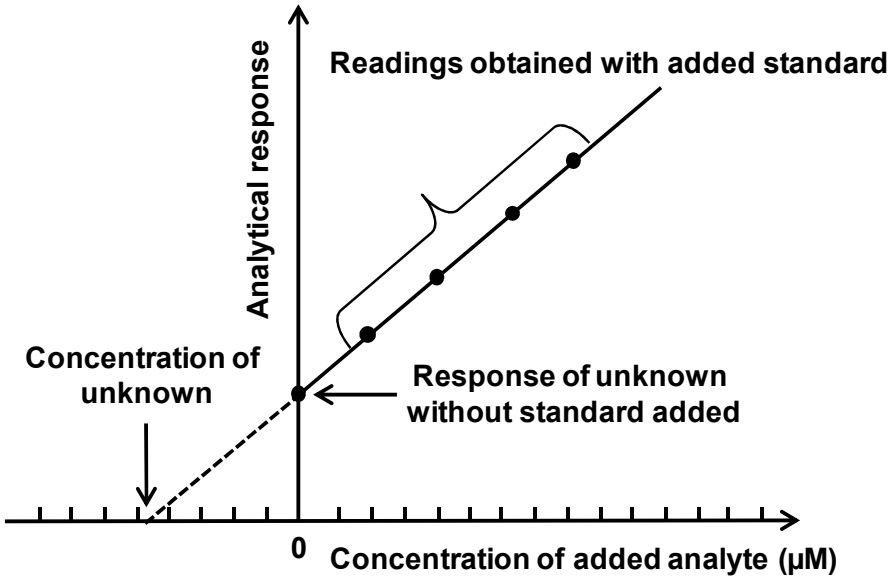

Figure 1.17 Theoretical standard addition curve showing how to obtain the concentration of the unknown present in the sample.

1.5.3 Stable isotope dilution approach

The stable isotope dilution approach where each compound of interest has its own stable isotope-labeled internal standard has been proven to be the most accurate for metabolite quantification. However, selecting an appropriate internal standard is extremely important to be able to account for sample preparation losses, instrument drift and matrix effects. Structural analogs and stable isotope-labeled (SIL) internal standards are the most common. SIL internal standards are generally preferred since they have the same physico-chemical properties as the compounds of interest; they co-elute and have very similar ionization efficiencies. Deuterated and ^{13}C-labeled standards are the most common, with ^{13}C-labeled standards being generally preferred, due to the isotope effect observed at the chromatographic level with deuterated standards which may compromise the precision of the assay.[41] A major disadvantage of this type of standards is that they are not always commercially available and they can be quite costly. There are also other areas of concern that need to be carefully addressed when using SIL internal standards such as the isotopic purity of the standards, cross-contamination

and cross-talk between MS/MS channels.[42] In a triple quadrupole system, cross-talk occurs when there is no time for the collision cell to empty completely before the next MRM transition is initiated. It is especially prominent when the same fragment ion is monitored in Q3 for subsequent transitions and it may cause false positive results.[43] Cross-talk therefore needs to be identified and troubleshot as part of method validation.

1.5.4 Chemical derivatization

Certain polar analytes such as free carnitine may exhibit poor retention in a reversed phase separation, making them more susceptible to ion suppression. In order to improve their ionization efficiency and chromatographic behaviour, chemical derivatization can be employed.[44] The ESI response of these compounds can be improved by increasing their chargeability and/or by increasing their hydrophobicity and hence their surface activity.[45]

Acylcarnitines have chemical properties that set them apart from most endogenous metabolites. First, they have a wide range of hydrophobicities, so their ESI responses depend directly on the length of their acyl moiety. Secondly, although they contain a quaternary amine group (rendering them a permanent positive charge) they also contain a carboxylic acid group, making them zwitterionic. It is therefore necessary to protonate the acid group in order to successfully analyze them by LC-MS. In the case of the very short-chain species, they are more easily detected upon derivatization.

Esterification has been the derivatization reaction of choice for increasing the ESI response of acylcarnitines. There have been reports on butyl[46] as well as 4'-bromophenacyl esters.[47, 48] The added group increases their hydrophobicity and blocks the potential negative charge from the carboxylic acid group. In the work described herein, acylcarnitine ethyl esters were synthesized. The derivatization reaction served a double purpose; it improved their ESI response and allowed for the introduction of a $^{12}C_2$ or $^{13}C_2$ label. The heavy labeled acylcarnitine ethyl esters formed were used as an internal standard without the

need to acquire a separate set of isotopically labeled standards. An added advantage of this approach is that the fragmentation of acylcarnitine ethyl esters is not governed by the added group. All the fragments present in the MS/MS spectrum of an unlabeled acylcarnitine are present in that of a labeled one. Additionally, an extra fragment ion at *m/z* 113 can be observed characteristic of acylcarnitine ethyl esters. This fragment can be utilized as further confirmation of the identity of detected metabolites as such.

Due to the lack of analyte-free matrices when analyzing endogenous compounds, the use of surrogate matrices for building calibration curves has been explored.[49, 50] In this work, all acylcarnitines were derivatized, underivatized urine and plasma were therefore used as matrices for all quantification experiments. This stable isotope dilution/surrogate matrix approach was compared to standard addition experiments to assess its accuracy.

1.6 Method validation

Method validation for quantitative LC-MS/MS assays is intended to demonstrate that a particular assay is adequate and reliable for a particular research application. The process includes analysis of quality control samples, determination of linear dynamic range, precision, accuracy, matrix effects, limits of detection and quantification as well as stability.[51] However, there is no true consensus for what the acceptable limits for these determinations are. Moreover, different laboratories require different levels of validation. For example, a more rigorous method validation is required for laboratories in the pharmaceutical industry which have to abide by federal regulatory agencies such as the Food and Drug Administration (FDA). Academic-based research laboratories on the other hand often apply a "fit- for- purpose" approach, where the intended use of the data is what determines the depth of the validation process.[52] This approach was utilized for the work described in this thesis. As part of the method validation process, the suitability of underivatized matrices for construction of calibration

curves was assessed. This was carried out by comparing the slope in of the calibration curves prepared in authentic and surrogate matrices using a specialized Student's t-test (process described in Chapters 4 and 5).

1.7 Model system: carnitine and its acyl derivatives

Carnitine (3-hydroxy-4-N-trimethylammonium butyrate) is an endogenous metabolite synthesized in the body from lysine and methionine, with the l-isomer being the biologically active form. There are also various dietary sources of this compound, mainly red meat, grains and dairy products.[53, 54] The esterified forms of carnitine, the acylcarnitines, are formed by acyltransferases which have organic acid chain length specificities.[55] Figure 1.17 shows the structure of free carnitine and describes the esterification of carnitine which produces acylcarnitines. These compounds have important biological functions such as shuttling acyl groups into mitochondria for β-oxidation. They have therefore become biomarkers for various disorders.[56] Due to their biological relevance, acylcarnitines were utilized in this work as a model system to apply LC-MS- based qualitative and quantitative methods to.

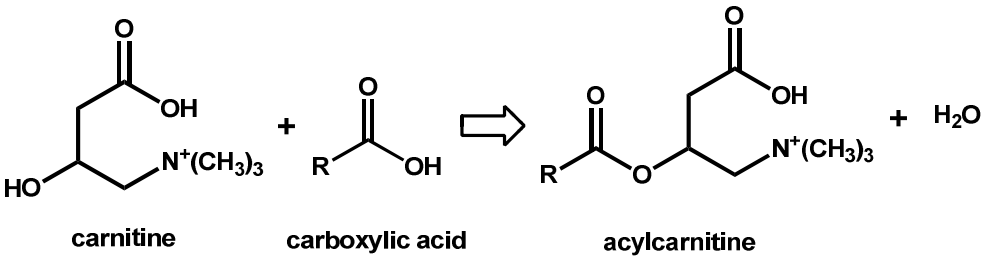

Figure 1.18 Acylcarnitine biosynthesis. An ester linkage is formed between the OH group of carnitine and a carboxylic acid producing a specific acylcarnitine and water. In biological systems this reaction is catalyzed by acyltransferases.

1.7.1 β-oxidation of fatty acids

β-oxidation is a four-step process by which activated fatty acids are shortened by two carbon units which are released in the form of acetyl-CoA. The

first step of this process is the dehydrogenation of an acyl-CoA group into a trans-2-enoyl-CoA molecule controlled by an acyl-CoA dehydrogenase enzyme. This step is followed by the addition of a hydroxyl group across the double bond of trans-2-enoyl-CoA by enoyl-CoA hydratase producing 3-hydroxyacyl-CoA. The third step is carried out by hydroxyacyl-CoA dehydrogenase which turns the 3-hydroxyacyl-CoA into a 3-ketoacyl-CoA. The fourth and last step of the cycle is the cleavage of the 3-hydroxyacyl-CoA by the thiol group of a CoA molecule to produce a shortened acyl-CoA group and an acetyl-CoA molecule. The resulting acyl-CoA can undergo another β-oxidation cycle while the acetyl-CoA formed can enter the citric acid cycle to produce energy in the form of ATP.[57] Figure 1.18 depicts all four reactions involved in the β-oxidation process including all cofactors required.

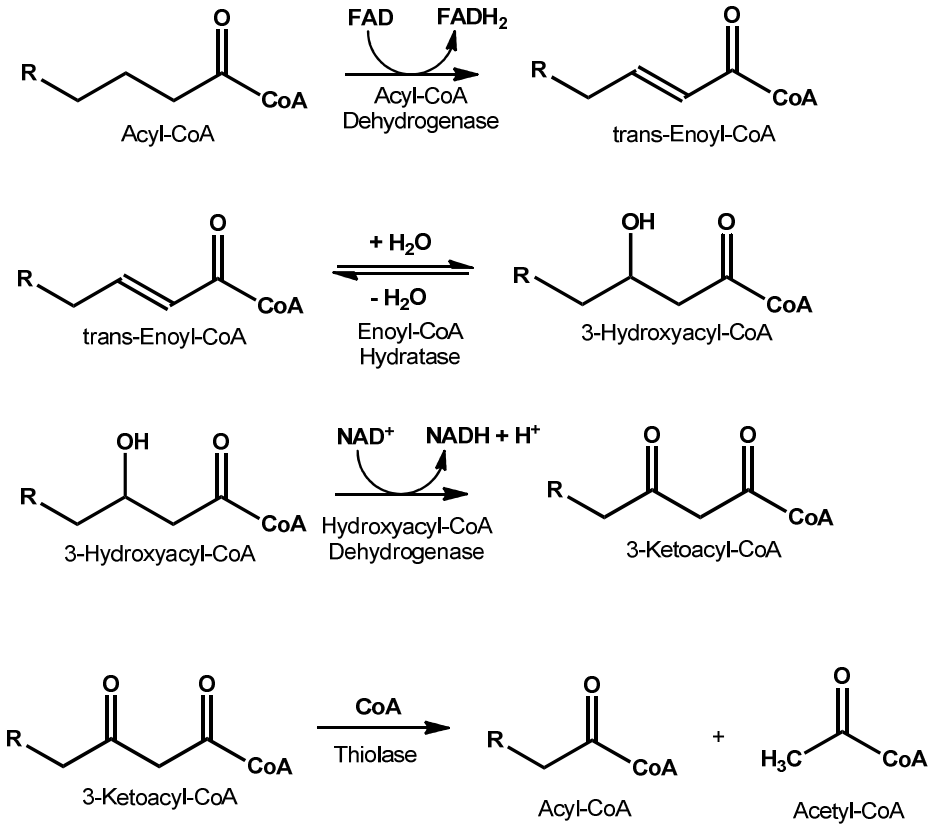

Figure 1.19 The four reactions involved in fatty acid β-oxidation. FAD, flavin adenine dinucleotide; $FADH_2$, reduced form of FAD; NAD^+, Nicotinamide adenine dinucleotide; NADH, reduced form of NAD^+.

1.7.2 Biological functions

1.7.2.1 Transport of fatty acids into the mitochondria

Carnitine plays a pivotal role in mitochondrial fatty acid oxidation. It conjugates to activated organic acids aiding their transfer into the inner mitochondrial membrane where β-oxidation takes place.[58] This conjugation takes place by transferring an acyl group from acyl-CoAs to free carnitine, producing acylcarnitines and free CoAs. This enzymatic reaction, controlled by carnitine palmitoyltransferase 1 or CPT 1, is important for homeostasis since it controls the acyl-CoA/ free CoA ratio.

Figure 1.19 depicts the group of enzymes involved in acylcarnitine metabolism. CPT 1 controls the formation of acylcarnitines from acyl-CoA and carnitine. This process is of great importance since acyl-CoA species themselves are unable to cross the inner mitochondrial membrane. Once medium and long-chain acylcarnitines are produced, they can then cross this membrane with the help of carnitine acylcarnitine translocase (CACT). CPT 2 controls the transfer of the acyl group from acylcarnitines back to CoA. The acyl-CoA species produced can then undergo β-oxidation in the mitochondrial matrix, producing acetyl-CoA which is then converted to acetylcarnitine by carnitine acetyltransferase. These enzymatic reactions describe the pivotal role that carnitine plays in fatty acid β-oxidation since in its absence, fatty acids would not be able to enter the mitochondrial matrix where β-oxidation takes place.

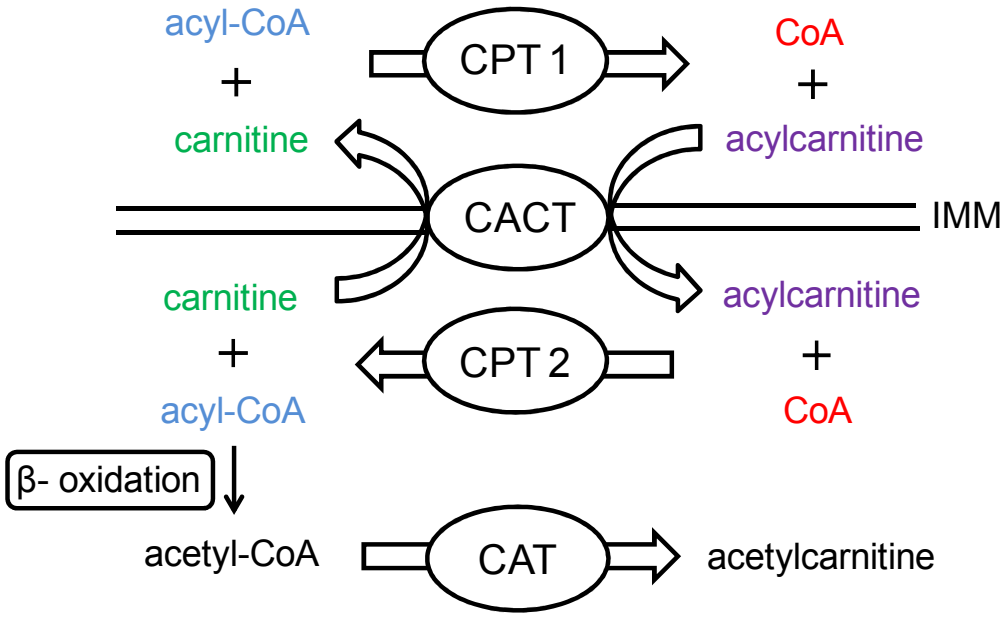

Figure 1.20 Schematic of acylcarnitine metabolism. CPT 1, carnitine palmitoyl transferase 1; CACT, carnitine acylcarnitine translocase; CPT 2, carnitine palmitoyltransferase 2; CAT, carnitine acetyltransferase; IMM, inner mitochondrial membrane. Adapted from Houten.[59]

1.7.2.2 Maintaining the acyl-CoA/ CoA ratio

It has been recognized that carnitine acts as a cofactor in the transfer of acyl groups out of mitochondria as well. Particularly important is the transfer of acetyl groups from acetyl-CoA produced inside the mitochondria out into the cytoplasm. Through this process, the ratio of acyl-CoA to CoA inside the mitochondria can be modulated. In any case where acyl-CoA species increase, the ratio of acyl-CoA/CoA increases dramatically since not only are acyl-CoA species increasing, but the concentration of free CoA as a result decreases. Carnitine can conjugate to these acyl groups with the help of carnitine acyltransferases, thereby increasing the free CoA concentration and restoring the ratio. The acylcarnitines formed can leave the mitochondria and be excreted. [60]

1.7.2.3 Elimination of potentially toxic compounds

The acyl-CoA species that accumulate in the presence of certain metabolic disorders such as propionyl-CoA (in the case of methylmalonic aciduria and propionic academia) are potentially very toxic due to their effects on other metabolic pathways.[60] Carnitine can conjugate with excess acyl groups which can be excreted in the urine, lowering the potential of these groups reaching toxic levels.

1.7.3 Acylcarnitines in various biofluids

The total carnitine pool in humans is found mostly in the cardiac and skeletal muscles. Plasma only contains about 1% of the total body carnitine pool. It is however, routinely analyzed for disease diagnosis and biomarker discovery studies.[61] Urine on the other hand, contains a variety of acylcarnitine species (mainly structural analogs) since urinary excretion is the main mechanism of acylcarnitine elimination. Not all acylcarnitine species are found in all biofluids, it is therefore necessary to analyze as many biofluids as possible in order to obtain a truly comprehensive acylcarnitine profile.

1.7.4 Acylcarnitine nomenclature

Acylcarnitine nomenclature is adapted from that of fatty acids, where the number following the letter C corresponds to the number of carbon atoms in the fatty acid chain conjugated to carnitine. The denomination +OH corresponds to a hydroxyl group added to the fatty acid chain conjugated to carnitine. A carbonyl group added to the fatty acid chain conjugated to carnitine is denoted by +=O. Similarly, a dicarboxylic acid conjugated to carnitine is denoted by: DC. Finally, a colon followed by a number corresponds to the degrees of unsaturation along the fatty acid chain (for example :1 corresponds one degree of unsaturation).

1.7.5 Acylcarnitine structure and fragmentation

Acylcarnitines contain a permanent positive charge which makes amenable for ESI-MS. Their ionization efficiency also depends on the chain-length of the organic acid conjugated to carnitine. Their fragmentation patterns upon collision-induced dissociation have been previously studied.[62-64] Acylcarnitines can be identified as such by confirmation of the presence of two neutral losses and three characteristic fragment ions, all of which come from the carnitine side of the molecule. The neutral losses of 59 and 161 Da correspond to the loss of the trimethylamine moiety and the loss of the carnitine backbone, respectively. The peak at *m/z* 60 corresponds to $HN^+(CH_3)_3$. The peak at *m/z* 85 ($^+CH_2$-CH=CHCOOH) corresponds to a McLafferty rearrangement of the butyric acid chain with the loss of the trimethylamine moiety. The peak at *m/z* 144 [$(CH_3)_3N^+CH_2CH$=CHCOOH] corresponds to the product of sole McLafferty rearrangement. Mass spectrometry methods were developed and optimized for this work by monitoring these neutral losses and characteristic fragment ions.

1.7.6 Acylcarnitine isomers

Acylcarnitines are found in various isomeric forms; namely, structural, optical or geometric. Distinguishing between different isomeric forms is extremely challenging when using ESI as the ionization source and performing low-energy collision-induced dissociation. This is because carbon chains are not easily cleaved, leaving the position of a double bond or a hydroxyl group unknown. It is, however, very useful for accurate disease diagnosis to differentiate between isomers, since in some cases only a particular isomer is elevated in the presence of a certain disease. For example, butyrylcarnitine (straight chain) is elevated in patients with short-chain acyl-CoA dehydrogenase (SCAD) deficiency. Isobutyrylcarnitine (branched chain) on the other hand, is elevated in patients with isobutyryl-CoA dehydrogenase (IBD) deficiency.[65] In this work, a significant amount of effort was employed to attempt to separate as many isomeric species as possible.

1.7.7 Dysregulation in the presence of various disorders

The onset of many disorders poses a metabolic stress on the human body which causes alterations in the fatty acid oxidation processes. These alterations may result in changes in the acylcarnitine profile. This explains why acylcarnitines have been found to be dysregulated in very diverse disorders, from diabetes to multiple sclerosis to sepsis. It is believed that certain cells under stress have an increased carnitine demand resulting in carnitine being down-regulated in the presence of these disorders.[66, 67] Moreover, carnitine deficiency has been implicated with endotoxin-mediated multiple organ failure. While acylcarnitines can be dysregulated in the presence of many disorders, they have only been clinically validated as biomarkers for certain inborn errors of metabolism.

1.7.7.1 Inborn errors of metabolism

Inborn errors of metabolism (IEM) are a group of disorders characterized by a single gene mutation which causes a decrease or loss of activity of an enzyme involved in an important metabolic pathway. The two most common types are fatty acid oxidation disorders (FAOs) and organic acidemias. These disorders present severe symptoms and while they are not curable, they are for the most part treatable if diagnosed early. There are more than 500 different types of IEMs and although they are rare, when combined, they account for a significant amount of morbidity and mortality in children and newborns.[68] This has prompted many countries to screen newborns for these disorders by analyzing acylcarnitines and amino acids using ESI-MS/MS.

The acyl-CoA dehydrogenases are a family of enzymes involved in the first step of β-oxidation. They have different chain length specificities, ranging from short to medium to long and very long-chain species. Deficiencies in these enzymes are common, with medium chain acyl-CoA dehydrogenase (MCAD) deficiency being the most common. It has an incidence rate of 1 in 10,000 - 15,000 in most populations.[69, 70] Most MCAD deficient patients are homozygous for the A985G missense mutation and are of Northern European ancestry. This

mutation results in a lysine to glutamic acid substitution. These patients are unable to metabolize medium-chain fatty acids (see figure 1.20). Some of the most common symptoms include, but are not limited to, hypoglycemia, lethargy, vomiting and seizures.[71] Treatment can be quite simple and includes avoidance of fasting, a low-fat diet as well as carnitine supplementation. In terms of their prognosis, although acute episodes can be life-threatening, many patients can be managed by avoidance of fasting. These patients therefore have an excellent long-term prognosis.

MCAD deficiency may cause increased medium-chain fatty acids, acylcarnitines, acylgylcines and dicarboxylic acids in urine and plasma.[72] Screening of dried blood spots by ESI-MS/MS has shown that the most clinically relevant metabolite for this disease is octanoylcarnitine (>0.3 μM) and/or an elevated C8/C10 ratio (>5). However, second-tier testing is always necessary to reach a confident diagnosis and may include molecular genetic analyses for known mutations as well as enzyme and cell culture studies.[73]

Since acylcarnitines have been found to be diagnostically relevant in a wide range of diseases, the analytical methods developed and described in this thesis focused on detecting, identifying and quantifying as many acylcarnitines as possible in various biological samples. The rationale behind these efforts is that, by analyzing more acylcarnitines, new and more specific biomarkers for these disorders can potentially be found.

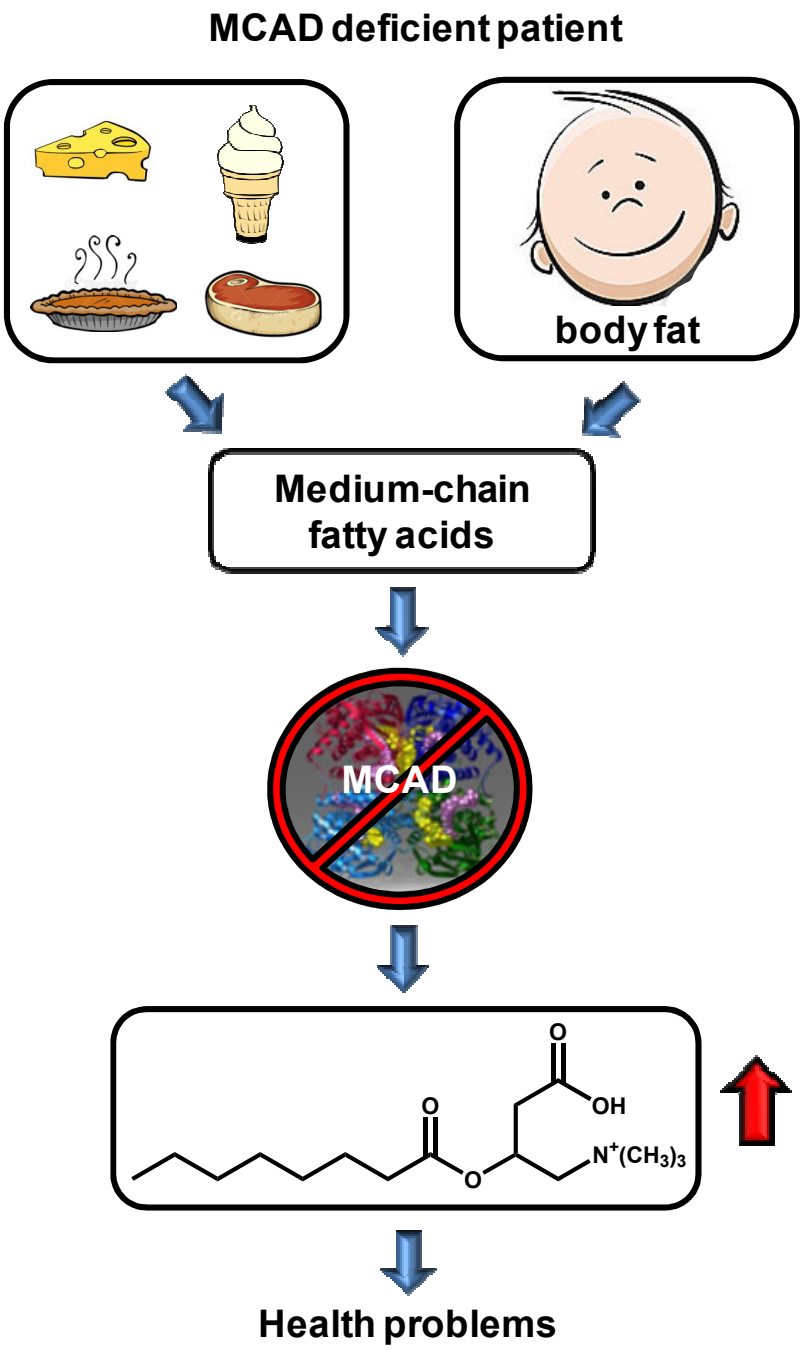

Figure 1.21 Medium-chain acyl-CoA dehydrogenase (MCAD) deficient patient. Low or lack of activity of the MCAD enzyme results in elevated levels of octanoylcarnitine and severe health problems. Adapted from the Screening, Technology and Research in Genetics website. URL: http://www.newbornscreening.info/index.html (accessed March 2012).

1.7.8 Previous published work on acylcarnitine analysis

Acylcarnitines have previously been analyzed by CE, CE-MS, LC-MS and GC-MS.[62, 74-77] Due to the fact that the work described herein was performed by LC-MS, only recently reported LC-MS methods will be discussed in this section. Minkler and colleagues[47, 49] proposed a derivatization reaction to increase the ionization efficiency of acylcarnitines. They synthesized the pentaflourophenacyl ester derivatives of these compounds. They claim the reaction to be mild enough not to cause hydrolysis of the ester linkage present in acylcarnitines. They also found that the fragmentation patterns of acylcarnitines change upon addition of this large pentaflourophenacyl group. For quantification studies, they utilized deuterated internal standards and used phosphate-buffered bovine serum albumin solution as a matrix to create calibration curves. Using this approach, Minkler *et al*. quantified 43 acylcarnitines in various types of biological samples including urine, plasma and skeletal muscle. They applied their methodology to samples from patients suffering from inborn errors of metabolism. They also provided cut-off values for normal acylcarnitine concentrations based on large sample cohorts.

Maeda and colleagues[78] developed an LC-MS method which involved solid-phase extraction for sample preparation with no derivatization step. Their LC-MS method focused on the chromatographic separation of short- and medium-chain acylcarnitine structural isomers. Their quantification strategy included the use of deuterated internal standards. Calibration curves were prepared in water since they found only a 3% difference in the slope of calibration curves prepared in serum, urine and water. They attributed the similarity in slopes to their solid-phase extraction protocol. Using this strategy they quantified 13 acylcarnitines in urine and 10 in plasma samples from five healthy volunteers.

Ghoshal *et al*.[79] developed a quantitative LC-MS method and used deuterated internal standards to quantify ten acylcarnitines in plasma without derivatization. Their method accurately identified patients with a variety of inborn errors of metabolism.

The work described in this thesis is based on the development and application of qualitative and quantitative LC-MS methods for the identification and quantification of acylcarnitines in various biofluids. Strong emphasis was placed on the chromatographic separation of as many acylcarnitine isomers as possible in order to obtain a comprehensive acylcarnitine profile in healthy individuals. Quantification was performed using $^{13}C_2$ labeled internal standards which were prepared in-house. Using these internal standards is advantageous since ^{13}C-labeled analytes do not exhibit the isotope effect that deuterated standards do. Acylcarnitines were quantified as their ethyl ester derivatives. It was found that addition of a small label does not change the fragmentation pattern of acylcarnitine ethyl esters as compared to regular acylcarnitines, allowing for their easy identification. Calibration curves were prepared in actual human urine and plasma (unesterified) as opposed to synthetic matrices. Using these methods, 32 acylcarnitines were quantified in plasma. Additionally, a total of 76 species were quantified in urine which is the most comprehensive quantitative urinary acylcarnitine profile reported to date.

1.8 Scope of Thesis

The main objective of this work was to develop and validate qualitative as well as quantitative UHPLC-MS/MS methods for the identification and quantification of endogenous acylcarnitines in complex biological samples. Acylcarnitines were chosen as a model system to apply these methods on since they are of high biological relevance. Chapter 2 describes a UPLC-MS/MS method for the comprehensive profiling of urinary acylcarnitines in healthy individuals. Chapter 3 describes the application of this analytical approach to plasma, dried blood spots and red blood cell pellets. Chapter 4 describes the development and validation of a method for the accurate and precise quantification of acylcarnitines in the urine of 20 healthy volunteers. Optimization of a UHPLC-MS/MS method for plasma acylcarnitines was carried out and was utilized to quantify these compounds in ten healthy volunteers; the results are

described in Chapter 5. The bottleneck of metabolomics studies has been compound identification, so in an attempt to ease this process, a web-based tool called MyCompoundID was developed. Chapter 6 describes the development and application of this tool for faster and more confident metabolite identification. Finally, conclusions and future work involving dried biofluid spots and microwave technology are described in Chapter 7.

1.9 Literature cited

(1) Nicholson, J. K.; Lindon, J. C. *Nature* **2008**, *455*, 1054-1056.

(2) Ryan, D.; Robards, K. *Analytical Chemistry* **2006**, *78*, 7954-7958.

(3) Weckwerth, W.; Morgenthal, K. *Drug Discovery Today* **2005**, *10*, 1551-1558.

(4) Snoep, J.; Westerhoff, H.; Alberghina, L.; Westerhoff, H. V.; Springer Berlin / Heidelberg, 2005; Vol. 13, pp 13-30.

(5) Fiehn, O. *Plant Molecular Biology* **2002**, *48*, 155-171.

(6) Villas-Bôas, S. G.; Mas, S.; Åkesson, M.; Smedsgaard, J.; Nielsen, J. *Mass Spectrometry Reviews* **2005**, *24*, 613-646.

(7) Dettmer, K.; Aronov, P. A.; Hammock, B. D. *Mass Spectrometry Reviews* **2007**, *26*, 51-78.

(8) Nicholson, J. K.; Connelly, J.; Lindon, J. C.; Holmes, E. *Nature Reviews Drug Discovery* **2002**, *1*, 153-161.

(9) Want, E. J.; Cravatt, B. F.; Siuzdak, G. *ChemBioChem* **2005**, *6*, 1941-1951.

(10) Lee, D. Y.; Bowen, B. P.; Northen, T. R. *BioTechniques* **2010**, *49*, 557-565.

(11) Brown, M.; Dunn, W. B.; Dobson, P.; Patel, Y.; Winder, C. L.; Francis-McIntyre, S.; Begley, P.; Carroll, K.; Broadhurst, D.; Tseng, A.; Swainston, N.; Spasic, I.; Goodacre, R.; Kell, D. B. *Analyst* **2009**, *134*.

(12) Sumner, L.; Amberg, A.; Barrett, D.; Beale, M.; Beger, R.; Daykin, C.; Fan, T.; Fiehn, O.; Goodacre, R.; Griffin, J.; Hankemeier, T.; Hardy, N.;

Harnly, J.; Higashi, R.; Kopka, J.; Lane, A.; Lindon, J.; Marriott, P.; Nicholls, A.; Reily, M.; Thaden, J.; Viant, M. *Metabolomics* **2007**, *3*, 211-221.

(13) Wishart, D. S.; Knox, C.; Guo, A. C.; Eisner, R.; Young, N.; Gautam, B.; Hau, D. D.; Psychogios, N.; Dong, E.; Bouatra, S.; Mandal, R.; Sinelnikov, I.; Xia, J.; Jia, L.; Cruz, J. A.; Lim, E.; Sobsey, C. A.; Shrivastava, S.; Huang, P.; Liu, P.; Fang, L.; Peng, J.; Fradette, R.; Cheng, D.; Tzur, D.; Clements, M.; Lewis, A.; De Souza, A.; Zuniga, A.; Dawe, M.; Xiong, Y.; Clive, D.; Greiner, R.; Nazyrova, A.; Shaykhutdinov, R.; Li, L.; Vogel, H. J.; Forsythe, I. *Nucleic Acids Research* **2009**, *37*, D603-D610.

(14) Smith, C. A.; Maille, G. O.; Want, E. J.; Qin, C.; Trauger, S. A.; Brandon, T. R.; Custodio, D. E.; Abagyan, R.; Siuzdak, G. *Therapeutic Drug Monitoring* **2005**, *27*, 747-751.

(15) Horai, H.; Arita, M.; Kanaya, S.; Nihei, Y.; Ikeda, T.; Suwa, K.; Ojima, Y.; Tanaka, K.; Tanaka, S.; Aoshima, K.; Oda, Y.; Kakazu, Y.; Kusano, M.; Tohge, T.; Matsuda, F.; Sawada, Y.; Hirai, M. Y.; Nakanishi, H.; Ikeda, K.; Akimoto, N.; Maoka, T.; Takahashi, H.; Ara, T.; Sakurai, N.; Suzuki, H.; Shibata, D.; Neumann, S.; Iida, T.; Tanaka, K.; Funatsu, K.; Matsuura, F.; Soga, T.; Taguchi, R.; Saito, K.; Nishioka, T. *Journal of Mass Spectrometry* **2010**, *45*, 703-714.

(16) Miller, J. M. *Chromatography: Concepts and Contrasts*, 2nd ed.; John Wiley and Sons, Inc.: New Jersey, 2005.

(17) Nováková, L.; Solichová, D.; Solich, P. *Journal of Separation Science* **2006**, *29*, 2433-2443.

(18) Swartz, M. E. *Journal of Liquid Chromatography & Related Technologies* **2005**, *28*, 1253-1263.

(19) Thevis, M.; Schänzer, W. *Analytical and Bioanalytical Chemistry* **2007**, *388*, 1351-1358.

(20) Van Eeckhaut, A.; Lanckmans, K.; Sarre, S.; Smolders, I.; Michotte, Y. *Journal of Chromatography B* **2009**, *877*, 2198-2207.

(21) Paul J, T. *Clinical Biochemistry* **2005**, *38*, 328-334.

(22) Andries P, B. *Journal of Chromatography A* **1998**, *794*, 345-357.

(23) Kebarle, P.; Tang, L. *Analytical Chemistry* **1993**, *65*, 972A-986A.

(24) Cech, N. B.; Enke, C. G. *Mass Spectrometry Reviews* **2001**, *20*, 362-387.

(25) Dole, M.; Mack, L. L.; Hines, R. L.; Mobley, R. C.; Ferguson, L. D.; Alice, M. B. *The Journal of Chemical Physics* **1968**, *49*, 2240-2249.

(26) Iribarne, J. V.; Thomson, B. A. *The Journal of Chemical Physics* **1976**, *64*, 2287-2294.

(27) Yost, R. A.; Enke, C. G. *Analytical Chemistry* **1979**, *51*, 1251-1264.

(28) Miller, P. E.; Denton, M. B. *Journal of Chemical Education* **1986**, *63*, 617.

(29) Hopfgartner, G.; Zell, M. In *Using Mass Spectrometry for Drug Metabolism Studies*; Korfmacher, W., A. , Ed.; CRC Press: Boca Raton, 2010, pp 277-304.

(30) Le Blanc, J. C. Y.; Hager, J. W.; Ilisiu, A. M. P.; Hunter, C.; Zhong, F.; Chu, I. *PROTEOMICS* **2003**, *3*, 859-869.

(31) Martínez Bueno, M. J.; Agüera, A.; Gómez, M. J.; Hernando, M. D.; García-Reyes, J. F.; Fernández-Alba, A. R. *Analytical Chemistry* **2007**, *79*, 9372-9384.

(32) Xia, Y.-Q.; Miller, J. D.; Bakhtiar, R.; Franklin, R. B.; Liu, D. Q. *Rapid Communications in Mass Spectrometry* **2003**, *17*, 1137-1145.

(33) Hager, J. W. *Rapid Communications in Mass Spectrometry* **2002**, *16*, 512-526.

(34) Chu, C., S.; Lebrilla, C., B In *Biomedical Applications of Biophysics*; Hue, T., Ed.; Humana Press: New York, 2010, pp 137-154.

(35) Mamyrin, B. A.; Karataev, V. I.; Shmikk, D. V.; Zagulin, V. A. *Journal of Experimental and Theoretical Physics* **1973** *64,* 82-89.

(36) King, R.; Bonfiglio, R.; Fernandez-Metzler, C.; Miller-Stein, C.; Olah, T. *Journal of the American Society for Mass Spectrometry* **2000**, *11*, 942-950.

(37) Andries P, B. *Journal of Chromatography A* **1998**, *794*, 345-357.

(38) Hernández, F.; Sancho, J. V.; Pozo, O. J. *Analytical and Bioanalytical Chemistry* **2005**, *382*, 934-946.

(39) Bonfiglio, R.; King, R. C.; Olah, T. V.; Merkle, K. *Rapid Communications in Mass Spectrometry* **1999**, *13*, 1175-1185.

(40) Karnes, H. T.; Shiu, G.; Shah, V. P. *Pharmaceutical Research* **1991**, *8*, 421-426.

(41) Wang, S.; Cyronak, M.; Yang, E. *Journal of Pharmaceutical and Biomedical Analysis* **2007**, *43*, 701-707.

(42) Matuszewski, B. K.; Constanzer, M. L.; Chavez-Eng, C. M. *Analytical Chemistry* **2003**, *75*, 3019-3030.

(43) Hughes, N.; Wong, E.; Fan, J.; Bajaj, N. *The AAPS Journal* **2007**, *9*, E353-E360.

(44) Al-Dirbashi, O. Y.; Santa, T.; Al-Qahtani, K.; Al-Amoudi, M.; Rashed, M. S. *Rapid Communications in Mass Spectrometry* **2007**, *21*, 1984-1990.

(45) Santa, T.; Al-Dirbashi, O. Y.; Yoshikado, T.; Fukushima, T.; Imai, K. *Biomedical Chromatography* **2009**, *23*, 443-446.

(46) Millington, D. S.; Kodo, N.; Terada, N.; Roe, D.; Chace, D. H. *International Journal of Mass Spectrometry and Ion Processes* **1991**, *111*, 211-228.

(47) Minkler, P. E.; Ingalls, S. T.; Hoppel, C. L. *Analytical Chemistry* **2005**, *77*, 1448-1457.

(48) Poorthuis, B. J. H. M.; Jille-Vlcková, T.; Onkenhout, W. *Clinica Chimica Acta* **1993**, *216*, 53-61.

(49) Minkler, P. E.; Stoll, M. S. K.; Ingalls, S. T.; Yang, S.; Kerner, J.; Hoppel, C. L. *Clinical Chemistry* **2008**, *54*, 1451-1462.

(50) Li, H.; Rose, M. J.; Tran, L.; Zhang, J.; Miranda, L. P.; James, C. A.; Sasu, B. J. *Journal of Pharmacological and Toxicological Methods* **2009**, *59*, 171-180.

(51) Shah, V.; Midha, K.; Findlay, J.; Hill, H.; Hulse, J.; McGilveray, I.; McKay, G.; Miller, K.; Patnaik, R.; Powell, M.; Tonelli, A.; Viswanathan, C. T.; Yacobi, A. *Pharmaceutical Research* **2000**, *17*, 1551-1557.

(52) Lee, J.; Devanarayan, V.; Barrett, Y.; Weiner, R.; Allinson, J.; Fountain, S.; Keller, S.; Weinryb, I.; Green, M.; Duan, L.; Rogers, J.; Millham, R.; O'Brien, P.; Sailstad, J.; Khan, M.; Ray, C.; Wagner, J. *Pharmaceutical Research* **2006**, *23*, 312-328.

(53) Steiber, A.; Kerner, J.; Hoppel, C. L. *Molecular Aspects of Medicine* **2004**, *25*, 455-473.

(54) Bieber, L. L. *Annual Reviews of Biochemistry* **1988**, *57*, 261-283.

(55) Bremer, J. *Physiological Reviews* **1983**, *63*, 1420-1480.

(56) Pitt, J. J.; Eggington, M.; Kahler, S. G. *Clinical Chemistry* **2002**, *48*, 1970-1980.

(57) Houten, S.; Wanders, R. *Journal of Inherited Metabolic Disease* **2010**, *33*, 469-477.

(58) Hirche, F.; Fischer, M.; Keller, J.; Eder, K. *Journal of Chromatography B* **2009**, *877*, 2158-2162.

(59) Houten, S. M. *Annals of Medicine* **2009**, *41*, 402-407.

(60) Chalmers, R. A.; Roe, C. R.; Stacey, T. E.; Hoppel, C. L. *Pediatric research* **1984**, *18*, 1325-1328.

(61) Reuter, S. E.; Evans, A. M.; Chace, D. H.; Fornasini, G. *Annals of Clinical Biochemistry* **2008**, *45*, 585-592.

(62) Heinig, K.; Henion, J. *Journal of Chromatography B* **1999**, *735*, 171-188.

(63) Vernez, L.; Hopfgartner, G. r.; Wenk, M.; Krähenbühl, S. *Journal of Chromatography A* **2003**, *984*, 203-213.

(64) Tallarico, C.; Pace, S.; Longo, A. *Rapid Communications in Mass Spectrometry* **1998**, *12*, 403-409.

(65) Ferrer, I.; Ruiz-Sala, P.; Vicente, Y.; Merinero, B.; Pérez-Cerdá, C.; Ugarte, M. *Journal of Chromatography B* **2007**, *860*, 121-126.

(66) Famularo, G.; de Simone, C.; Trinchieri, V.; Mosca, L. *Annals of the New York Academy of Sciences* **2004**, *1033*, 132-138.

(67) Möder, M.; Kießling, A.; Löster, H.; Brüggemann, L. *Analytical and Bioanalytical Chemistry* **2003**, *375*, 200-210.

(68) Wilcken, B.; Wiley, V.; Hammond, J.; Carpenter, K. *New England Journal of Medicine* **2003**, *348*, 2304-2312.

(69) Gregersen, N.; Blakemore, A. I. F.; Winter, V.; Andresen, B.; Kølvraa, S.; Bolund, L.; Curtis, D.; Engel, P. C. *Clinica Chimica Acta* **1991**, *203*, 23-34.

(70) Rhead, W. *Journal of Inherited Metabolic Disease* **2006**, *29*, 370-377.

(71) Raghuveer, T. S.; Garg, U.; Graf, W. D. *American family physician* **2006**, *73*, 1981-1990.

(72) Chace, D. H.; Hillman, S. L.; Van Hove, J. L. K.; Naylor, E. W. *Clinical Chemistry* **1997**, *43*, 2106-2113.

(73) Chace, D. H.; DiPerna, J. C.; Mitchell, B. L.; Sgroi, B.; Hofman, L. F.; Naylor, E. W. *Clinical Chemistry* **2001**, *47*, 1166-1182.

(74) Pormsila, W.; Morand, R.; Krähenbühl, S.; Hauser, P. C. *Journal of Chromatography B* **2011**, *879*, 921-926.

(75) Chalcraft, K. R.; Britz-McKibbin, P. *Analytical Chemistry* **2008**, *81*, 307-314.

(76) Lowes, S.; Rose, M. E. *Analyst* **1990**, *115*, 511-516.

(77) Fu, X.-w.; Iga, M.; Kimura, M.; Yamaguchi, S. *Early Human Development* **2000**, *58*, 41-55.

(78) Maeda, Y.; Ito, T.; Suzuki, A.; Kurono, Y.; Ueta, A.; Yokoi, K.; Sumi, S.; Togari, H.; Sugiyama, N. *Rapid Communications in Mass Spectrometry* **2007**, *21*, 799-806.

(79) Ghoshal, A. K.; Guo, T.; Soukhova, N.; Soldin, S. J. *Clinica Chimica Acta* **2005**, *358*, 104-112.

Chapter 2

Ultra-high performance liquid chromatography tandem mass spectrometry for the comprehensive analysis of urinary acylcarnitines*

2.1 Introduction

Metabolomics involves the study of the metabolome, which is broadly defined as all low molecular mass compounds found in a biological system. One sub-metabolome is the lipid metabolome, i.e., the lipid metabolites produced from enzymatic action on parent lipids or their precursors.[1-5] Although lipid metabolites are only a fraction of the total lipid mass in cells, they are involved in many biological processes and some of them have been implicated in diseases.[2, 5-8] Due to the large number of possible structures of lipids as well as many types of enzymatic processes involved in lipid metabolism, the chemical composition of the lipid metabolome is expected to be highly complex. The focus of this work is the analysis of a sub-class of the lipid metabolome, namely acylcarnitines.[9, 10] Although most acylcarnitines are fatty acid derivatives, some of these species are produced from the products of amino acid catabolism.

* A form of this chapter was published as: Zuniga, A., and Li, L., 2011, "Ultra-high performance liquid chromatography tandem mass spectrometry for the comprehensive analysis of urinary acylcarnitines" *Analytica Chimica Acta*, 689, 77-84.

Carnitine (3-hydroxy-4-N-trimethyl-ammonium butyrate) plays a key role in fatty acid oxidation.[9] It can be conjugated to fatty acids to form acylcarnitines, which facilitates fatty acid transport into the mitochondrial matrix where oxidation takes place. Acylcarnitines have become important biomarkers for various types of diseases including inborn errors of metabolism, renal tubular diseases, and diabetes mellitus type II.[9-13] For example, current newborn screening methods for the diagnosis of inborn errors of metabolism include the analysis of carnitine and acylcarnitines in dried blood spots by electrospray ionization tandem mass spectrometry (ESI-MS/MS).[13-17] It has been found, however, that occasional ambiguities arise due to the genetic severity of the disease or the condition of the patient at the time of sample collection; in such cases, other diagnostic tools are needed. [18-20] Urinary acylcarnitine analysis can also be useful since the distribution pattern of these species or the excretion of particular acylcarnitines provides some information about metabolic disease.[12, 21-23] To separate and identify isomeric acylcarnitine species which are indistinguishable by direct infusion ESI-MS/MS methods, chromatographic or capillary electrophoresis techniques have been combined with MS.[23-26] In general, these targeted studies only analyzed a small number of acylcarnitines.[27-29]

In this work, an LC-MS/MS method was designed for identifying as many acylcarnitines as possible from biofluids, such as human urine. The main objective was to better define the chemical diversity of acylcarnitines and to generate MS/MS spectra of these compounds that can be used for future unknown metabolite identification experiments. This method is based on the use of ultra-high performance liquid chromatography (UPLC) combined with triple quadrupole-linear ion trap hybrid mass spectrometry.[30] This method can be used to detect a total of 76 distinct masses and, by performing a high-resolution chromatographic separation at the front-end, more than 300 species can be detected within an 85-min elution time. This allows us to generate an MS/MS spectral library of 355 different acylcarnitines; only 43 of them have been previously reported.[12, 22, 23, 25, 28, 31-35] These spectra will be deposited into the

Human Metabolome Database (HMDB)[36] as a resource for potential identification of unknown metabolites in targeted or untargeted metabolome profiling work. The current HMDB spectral library consists of MS/MS spectra of only ~900 metabolite standards. Due to the limited number of standards available, expansion of this library is a challenging task. Thus, generation of MS/MS spectra of metabolites from biological samples with tentative structural assignment is one way to expand the library. Deposition of 355 MS/MS spectra of different acylcarnitines should increase the utility of the HMDB library for unknown metabolite identification. This is particularly true, considering that acylcarnitines seem to be present in large numbers in biofluids, such as urine, which are commonly used for disease biomarker discovery.

2.2 Experimental

2.2.1 Chemicals and reagents

Except otherwise noted, all chemicals and reagents were purchased from Sigma-Aldrich Canada (Oakville, Ontario). The 15 acylcarnitine standards used in this work for method development were acetylcarnitine (C2), propionylcarnitine (C3), isobutyrylcarnitine (C4-I), butyrylcarnitine (C4), pivaloylcarnitine (C5, branched), 2-methylbutyrylcarnitine (2MBC), isovalerylcarnitine (C5-I), valerylcarnitine (C5, straight chain), hexanoylcarnitine (C6), octanoylcarnitine (C8), decanoylcarnitine (C10), dodecanoylcarnitine (C12), tetradecanoylcarnitine (C14), palmitoylcarnitine (C16), and stearoylcarnitine (C18). These standards were purchased from Dr. Herman Ten Brink, VU Medical Centre, Amsterdam, the Netherlands.

2.2.2 Microsomal incubations

Microsome incubations were performed using pooled human liver microsomes and a NADPH regenerating system (NRS) (Becton Dickinson, Franklin Lakes, NJ), consisting of Solutions A and B. Solution A contained 26.1

mM NADP+, 66 mM glucose-6-phosphate and 66 mM $MgCl_2$ in H_2O and Solution B comprised of 40 U/mL glucose-6-phosphate dehydrogenase in 5 mM sodium citrate.

In order to generate phase I metabolites of the available acylcarnitine standards, individual standards were incubated with pooled human liver microsomes and NADPH regenerating system in the presence of phosphate buffer at a pH of 7.40. For each incubation of an acylcarnitine standard, an NRS solution was prepared by adding 25 µL of Solution A and 5 µL of solution B to 70 µL of phosphate buffer. Microsomes were rapidly thawed and put on ice until needed. Twenty-five micro-litres of pooled human liver microsomes (total protein content of 2 mg/mL) were diluted with 100 µL of phosphate buffer and 100 µL of NRS solution and placed in a water bath at 37 °C for 5 minutes. Twenty-five microlitres of 0.5 mM test compound (acylcarnitine standard) in H_2O was also pre-warmed to 37 °C and added to the microsome dilution. Controls were prepared in the same manner except human liver microsomes were replaced by 25 µL of phosphate buffer. Incubates and controls were immediately placed in an incubator/rotor set at 37 °C and oscillating at 150 rpm for 6 hrs, which was found to be the optimal incubation time. The reaction was terminated by adding 100 µL of 5% acetic acid in ACN. The solution was vortexed, centrifuged for 5 min at 16,000 g and the supernatant was stored at -20 °C pending analysis.

2.2.3 Urine samples

Urine was collected from six healthy volunteers (two males and four females) who were not on any special diet or taking any nutritional supplements. An informed consent was obtained from each volunteer and ethics approval for this work was obtained from the University of Alberta in compliance with the Arts, Science and Law Research Ethics Board policy. The volunteers were all adults, ranging from 24 to 38 years of age. The urine samples were collected as first morning void samples for all six volunteers. Urine samples were centrifuged for 10 min at 16,000 g to remove any solids. The resulting supernatants were then

decanted and subjected to sample clean-up by solid-phase extraction (SPE) as described in Section 2.2.4.

2.2.4 Solid-phase extraction

SPE was used as a means of analyte extraction and sample clean-up. SPE was performed on a 16-port vacuum manifold (Alltec, Nicholasville, KY) using Oasis® 3 cc/60 mg, 60 µm, mixed-mode cation exchange (MCX) SPE cartridges (Waters Corporation, Milford, MA). It has been previously reported that methanol can convert approximately 40% of dicarboxylic acylcarnitines to the mono-methyl esters, as the sulfo group on the cartridge can actually catalyze the methylation. [23] Thus acetonitrile (ACN) was used as an eluent in this work. The cartridges were first conditioned with 1 mL of ACN, followed by equilibration with 1 mL of H_2O. The same volume of urine was then loaded onto the cartridges. The sample flow-through was discarded since early trials showed that there were no acylcarnitines in detectable amounts in this fraction. The washing step involved the addition of 1 mL of 2% formic acid (FA) in H_2O. Analyte elution was performed with 1 mL of 5% NH_4OH in 60% ACN, followed by another elution using the same volume of 5% NH_4OH in 100% ACN. The individual solutions from the washing step and subsequent two elutions were collected and evaporated to dryness in a Savant SpeedVac concentrator system (Global Medical Instrumentation or GMI, Ramsey, Minnesota) and reconstituted in 100 µL of mobile phase A (see below). In the case of the microsome incubates, the same protocol was followed except that 350 µL of sample and working solutions were used.

2.2.5 UPLC

Chromatographic separation was performed on an ACQUITY UPLC® system (Waters Corporation, Milford, MA) consisting of a binary solvent manger, a sample manager and a column compartment. The column used was a BEH (Ethylene Bridged Hybrid) C_{18} 1.0 mm i.d. × 150 mm with 1.7 µm particle size. A 5 µL sample aliquot was injected onto the column with the column temperature

maintained at 25 ˚C and eluted at a flow rate of 50 µL/min. A gradient elution program with two mobile phases was used: 0.1% FA, 4% ACN in H_2O (eluent A) and 0.1% FA in ACN (eluent B). The gradient started by holding 0% B for 11 min, followed by an increase to 50% B in 90 min. The gradient was subsequently increased to 100% B over a period of 5 min and held for 10 min. At 105.10 min after injection, the system was returned to 100% A for 25 min at a flow rate of 75 µL/min to re-equilibrate the column. Finally, the flow rate was brought back down to 50 µL/min and held for 5 min in order to allow the pressure in the system to stabilize.

2.2.6 ESI-MS

The MS system used was a 4000 QTRAP® MS/MS System (Applied Biosystems, Foster City, CA) equipped with a Turbo V™ ion source. Information dependent acquisitions (IDAs) were performed using precursor ion of 85 and neutral loss of 59 as survey scans. Based on the acylcarnitines found, an IDA method was developed using multiple reaction monitoring (MRM) as a survey scan to obtain better sensitivity. The method contained 76 MRM transitions, which can be summarized as acylcarnitine $m/z \rightarrow 85$, each having a dwell time of 10 ms. During the survey scan, for every data point acquired, the 4 most intense peaks were selected for subsequent enhanced product ion scan (i.e., MS/MS).

The ESI source was set to positive ion mode with the following settings: the curtain gas, 10 psi; the collision-activated dissociation (CAD) gas, high; the ion source voltage, 5000 V; the source temperature, 350 °C; and gases 1 and 2 set to 20 and 15 psi, respectively. The declustering potential (DP) was set to 40 V. The collision energy (CE) was 40 V and the entrance potential (EP) was set to 8 V, while the collision cell exit potential (CXP) was set to 15 V. The resolution for both Q1 and Q3 was set to high. The enhanced product ion parameters in the linear ion trap were the followings: the CE, 35 V with a collision energy spread

(CES) of 5 V; the Q3 entry barrier, 6 V; and the scan rate, 4000 Da/s for a scan range of 50 to 550 Da. Dynamic fill time was selected.

2.3 Results and Discussion

2.3.1 MS method optimization

The UPLC-MS/MS method was developed with the objective of detecting as many acylcarnitines as possible and thus a considerable effort was devoted to optimizing the selectivity and sensitivity of the method. The high selectivity of this method can be attributed to the use of SPE as a means of analyte extraction (see below) as well as the use of selective mass spectrometric scan modes (precursor ion, neutral loss and MRM) which effectively reduce the presence of possible isobaric interferences, i.e. compounds with the same mass. Mass spectral acquisition was based on IDA methods with survey scans linked to information-dependent enhanced product ion scans. For each chromatographic data point, the four most intense ions were selected for subsequent enhanced product ion scans. This particular method is advantageous since both MS and MS/MS information can be obtained from a single injection. Moreover, utilizing a QTRAP® mass spectrometer instead of a triple quadrupole has the added advantage of using a sensitive linear ion trap to scan fragment ions out, producing better quality MS/MS spectra.[30]

The fragmentation pattern of fifteen acylcarnitine standards (ranging from C2 to C18) was studied in order to develop MS/MS-based selective scan modes. IDA methods with neutral loss of 59 Da and precursor ion of *m/z* 85 as survey scans were developed. The optimal collision energy for the dependent product ion scan was found to vary according to the acylcarnitine chain length. Since a wide range of acylcarnitine chain lengths were found in urine, a CE of 32 V and a collision energy spread (CES) of 5 V were used. In this way, product ion spectra collected at 27, 32 and 37 V could be added and displayed as one spectrum. This provided information-rich MS/MS spectra of all acylcarnitines containing peaks

from a number of fragment ions across a wide mass range in a single run. A comprehensive list of all potential acylcarnitines found using both scan types was then created and used to develop a list of transitions to be employed in a more sensitive MRM method. These transitions consisted of a particular acylcarnitine $m/z \rightarrow 85$, since all acylcarnitines upon collision-induced dissociation produce a fragment ion at *m/z* 85 which at a high enough collision energy, is the base peak in the spectra. A CE of 40 V was found to be optimal for this survey scan. The MRM method developed was the one utilized for all further analyses.

2.3.2 Sample clean-up and chromatographic separation

SPE was utilized as a means of analyte extraction as well as sample fractionation and concentration. Lipophilic-cation exchange mixed-mode cartridges were found to be efficient in extracting acylcarnitines. Sample fractionation was carried out to further reduce the complexity of urine samples. As an example, Figure 2.1 shows the ion chromatograms obtained from three SPE fractions of the urine sample of a healthy individual, illustrating different types of acylcarnitines detected in different fractions. It is worth noting however, that many acylcarnitine species were found in more than one SPE fraction.

The use of a UPLC system was found to provide the chromatographic separation needed to resolve structural isomers of particular acylcarnitines. For the 15-cm column used, both the flow rate and gradient conditions were optimized. All acylcarnitines eluted in less than 85 min. Figure 2.2 A shows a representative total ion chromatogram (TIC) with MRM used as a survey scan. Peaks are distributed across the gradient elution time window, indicating that acylcarnitines with a wide range of hydrophobicity can be found in human urine. One known and two unknown acylcarnitine species are labeled on the chromatogram. Panels B-D in Figure 2.2 show the product ion spectra of hexanoylcarnitine (C6) and unknown species 1 and 2, respectively. For all three spectra, characteristic fragment ions bearing the signature of acylcarnitines (e.g., *m/z* 60, 85, 144 and others; see below) can be found.

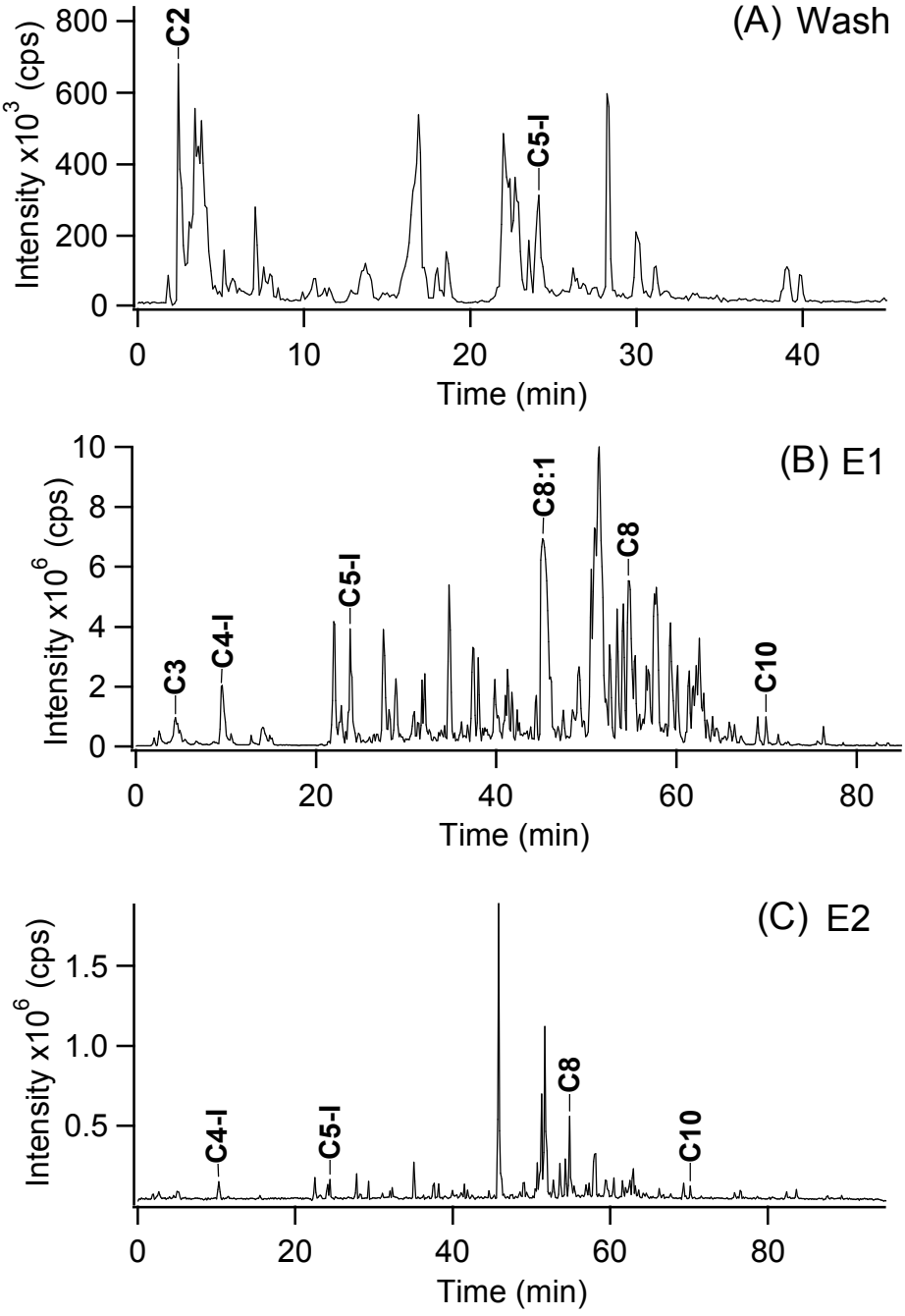

Figure 2.1. Total Ion Chromatogram (TIC) of three SPE fractions collected from the urine of individual A. (A) washing fraction, (B) first elution fraction, E1 (C) second elution fraction, E2. Some species such as C5-I were found in all three fractions.

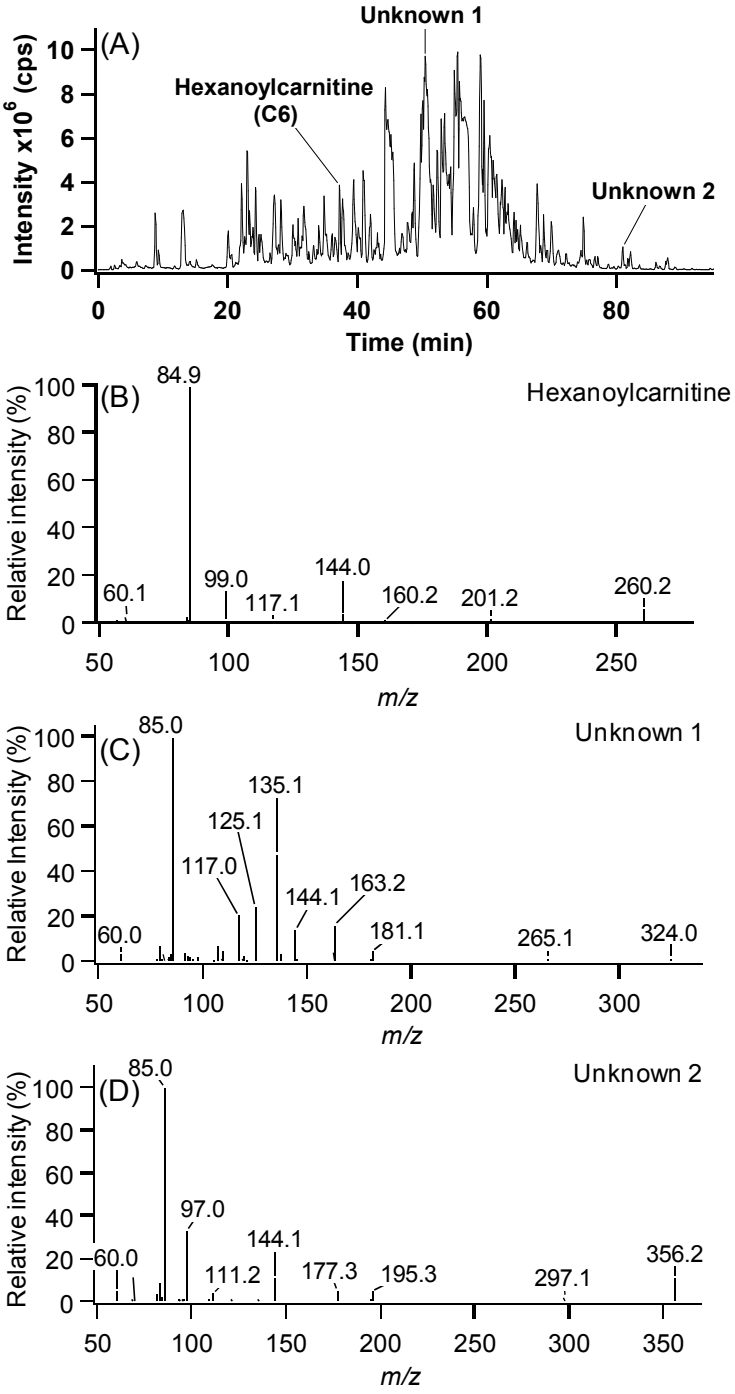

Figure 2.2. (A) TIC of the urinary acylcarnitine profile of a healthy individual obtained using MRM as a survey scan. Two compounds that were identified as acylcarnitines, but had unconfirmed structures are labeled on the chromatogram, along with hexanoylcarnitine which was confirmed by comparison to a standard. The product ion spectra of these species are shown in (B) - (D), depicting the characteristic acylcarnitine fragment ions of *m/z* 60, 85 and 144, as well as the neutral losses of 59 and 161 Da.

The presence of isobaric species and isomers of acylcarnitines in urine is evident in the extracted ion chromatogram (XIC) of almost any MRM transition. Figure 2.3A shows an XIC of MRM transition 354 → 85. Only twelve out of a total of 29 peaks found were identified as acylcarnitines. This example shows that performing a chromatographic separation at the front-end, the number of false positive results can be greatly reduced. The inset is an enlarged area of the XIC (from 40 to 45 min) showing five baseline-resolved isomeric peaks. Five product ion spectra corresponding to acylcarnitine isomers with *m/z* 354 shown in the inset of Figure 2.3A are shown in Panels B-F. Again, these spectra display several fragment ion peaks that are characteristic of acylcarnitines.

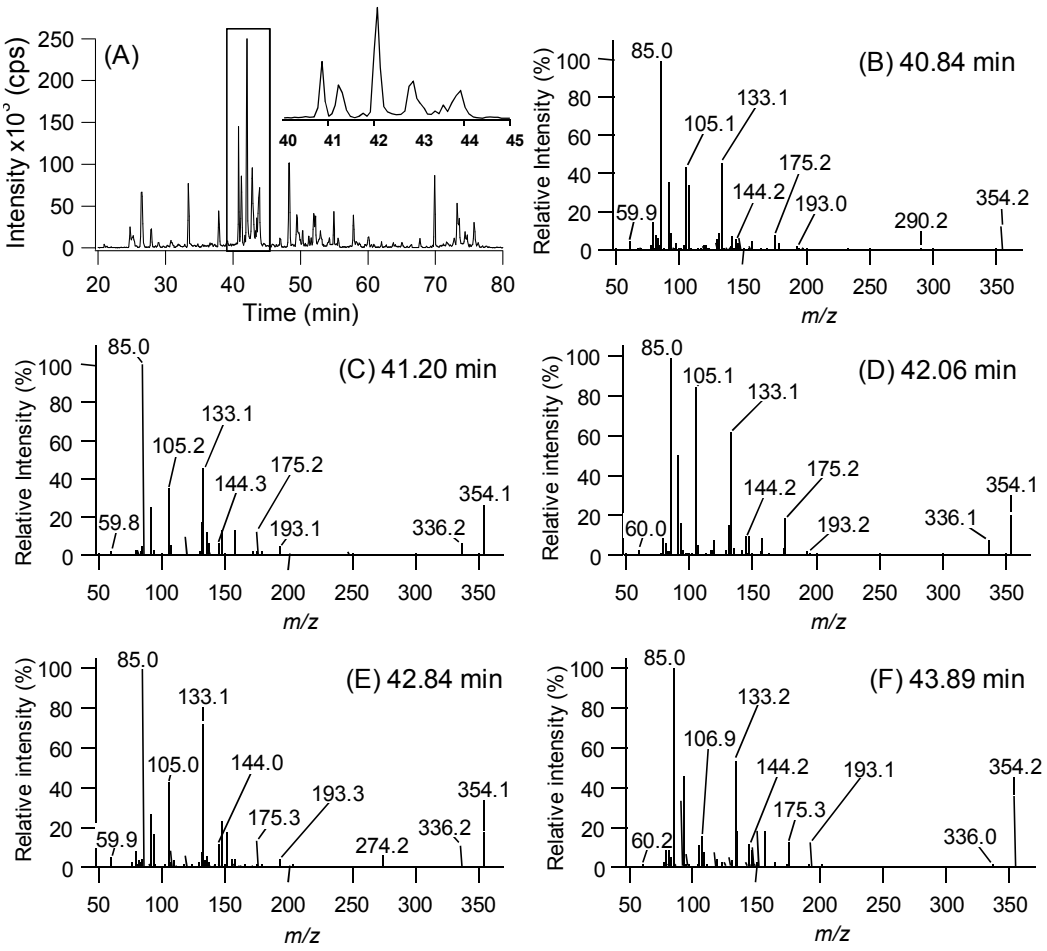

Figure 2.3(A) Extracted ion chromatogram (XIC) of MRM transition 354 → 85 with the inset of an expanded region between 40 to 45 min displaying five baseline-resolved isomeric species. The product ion spectra of the five species are shown in (B)- (F).

2.3.3 Acylcarnitine identification

In general, metabolites were identified as acylcarnitines based on the presence of five characteristic fragment ions, which have been previously reported.[11, 27, 37] In addition, other characteristic fragments and neutral losses determined from this work were used as further confirmation of the identity of these metabolites. As an example, the MS/MS spectrum of pimeloylcarnitine (C7:DC) and its proposed fragmentation pattern are shown in Figure 2.4. Displayed in the figure are the five main characteristic peaks including the neutral losses of 59 and 161 Da corresponding to the loss of the trimethylamine moiety and the loss of the carnitine backbone, respectively, as well as the peaks at *m/z* 60, 85 and 144. The peak at *m/z* 60 corresponds to $HN^+(CH_3)_3$. The peak at *m/z* 85 ($^+CH_2$-CH=CHCOOH) corresponds to a McLafferty rearrangement of the butyric acid chain with the loss of the trimethylamine moiety. The peak at *m/z* 144 [$(CH_3)_3N^+CH_2CH$=CHCOOH] corresponds to the product of sole McLafferty rearrangement. In addition to those five common fragment ions, there is another fragment ion that is common to the acylcarnitine family, which is the neutral loss of 77 Da. It corresponds to the loss of trimethylamine in addition to a loss of H_2O from the carboxylic acid group in the carnitine backbone. Another neutral loss commonly observed is the loss of 143 Da which gives rise to the positively charged fatty acid group. [25] The loss of 189 Da which corresponds to the loss of the carnitine backbone in addition to the loss of CO is another prominent neutral loss. There are guidelines that recommend using 3 or more specific ions (may or may not include the precursor ion) to confirm the identity of a known compound in a sample. [38, 39] In this work, the presence of at least 3 of the characteristic peaks in the product ion spectra was considered as sufficient evidence to identify compounds as acylcarnitines.

Further structure elucidation was performed as extensively as possible by MS/MS spectral interpretation. Hydroxy-acylcarnitines were identified by the loss of 179 Da which corresponds to the loss of the carnitine backbone in addition to the loss of H_2O from the OH group along the fatty acid chain. Additionally, 3-

hydroxy acylcarnitines can be distinguished from other isomeric species (those having the OH group on a different position along the chain) by a characteristic peak at *m/z* 145 ($HOC{=}CH_2OCHCH_2CH_2OHC{=}O^+$).[40] Carnitine conjugates of dicarboxylic acids (DCs), such as pimeloylcarnitine, were identified by the loss of 179 and 207 Da which correspond to the loss of the carnitine backbone in addition to H_2O or the carboxylic acid group, respectively.

Due to the limited availability of acylcarnitine standards, definitive identification of the detected acylcarnitines in urine is difficult. To assist in compound identification, human liver microsomes were utilized to produce phase I metabolites of individual acylcarnitine standards. Because these metabolites share a similar core structure to the parent acylcarnitine, their MS/MS spectra can be easily assigned to particular chemical structures. Comparison of the MS/MS spectra and retention time information of the microsome-produced metabolites with those found in urine samples provides a means of putative identification of unknown acylcarnitines. Figure 2.5 illustrates how microsomal incubates were used to aid the identification of these compounds in urine, using hydroxyoctanoylcarnitine with *m/z* 304 as an example. The structure of this metabolite is shown in Figure 2.5A. Figure 2.5B is an overlay of XICs of transition 304 → 85 from a 6-h microsome incubation of octanoylcarnitine, a commercially available standard, and a urine sample. Knowing the structure of octanoylcarnitine and its MS/MS spectrum as well as the mass shift of the metabolite from the parent compound, the presence of metabolites of octanoylcarnitine can be easily determined (i.e., different structural isomers of hydroxyoctanoylcarnitine).

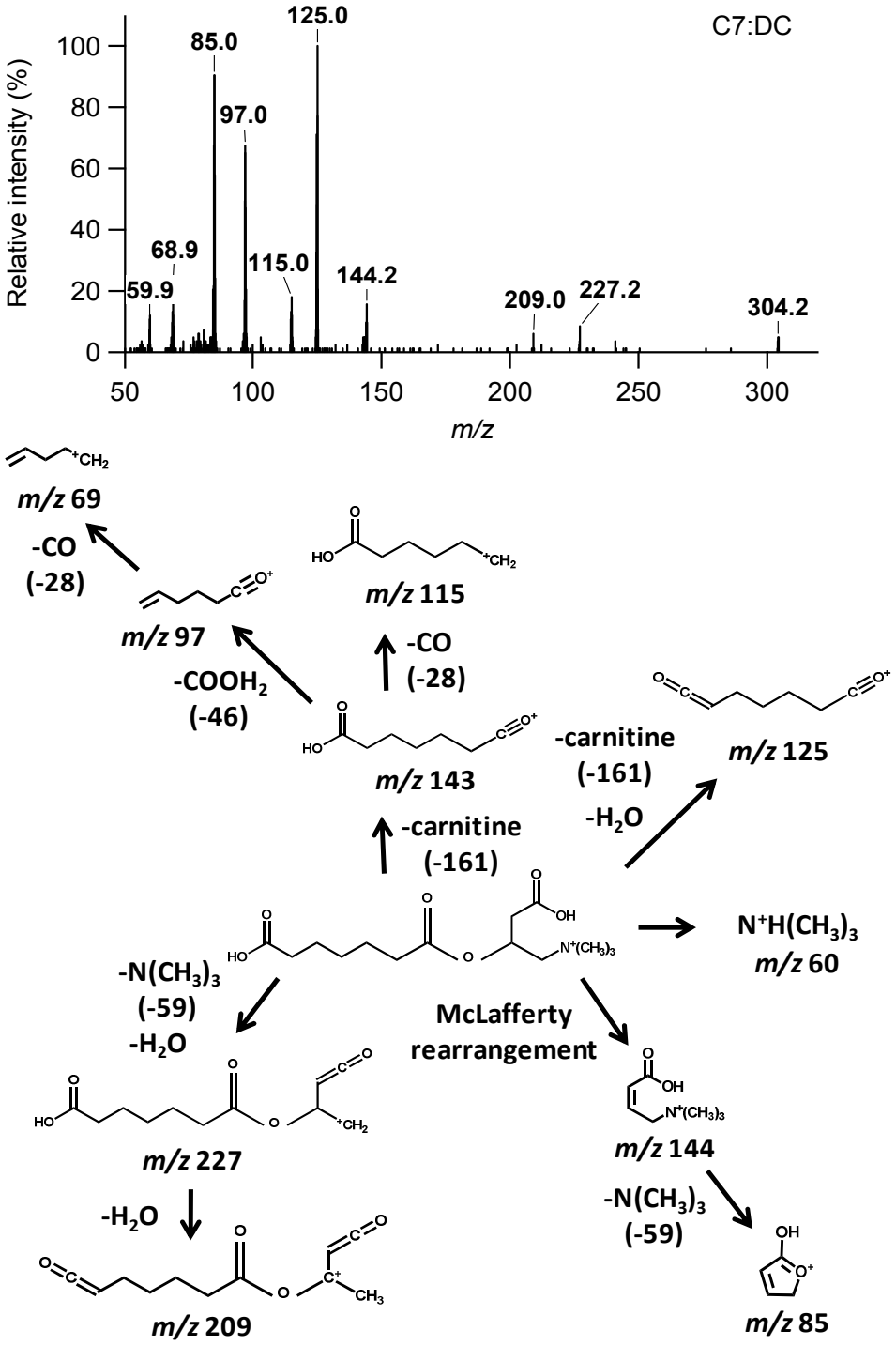

Figure 2.4. Top: MS/MS spectrum of C7:DC (pimeloylcarnitine) obtained on a 4000 QTRAP® mass spectrometer with a CE of 32 V and a collision energy spread (CES) of 5 V. Bottom: Fragmentation schematic of C7:DC (pimeloylcarnitine) showing the neutral losses and common fragment ions observed upon collision-induced dissociation.

The XICs shown in Figure 2.5B illustrate the high-resolution chromatographic separation of the structural isomers of hydroxyoctanoylcarnitine. Each species has the OH group located at a different position along the fatty acid chain. Panels C and D in Figure 2.5 show the product ion spectra corresponding to the peaks marked with a star in the XIC of the microsome incubation and the urine sample, respectively. Similar retention times and MS/MS spectra suggest that the urine sample contains isomers of hydroxyoctanoylcarnitine. However, in this particular case, the exact location of the OH group on the fatty acid chain for a particular chromatographic peak could not be determined. The presence of the 3-hydroxy species is expected since it is a fatty acid oxidation intermediate. It is possible that the other isomers found are product of ω-oxidation. Figure 2.6 shows the proposed fragmentation pathways used to explain the fragment ions observed in the MS/MS spectra.

Appendix Section 2.1 contains a partial list of the 355 acylcarnitines found in the urine of healthy individuals, including all isomeric species. The full version of this list can be found in the electronic Appendix which can be obtained by contacting Dr. Liang Li (liang.li@ualberta.ca). Tentative structural assignments were carried out by direct comparison with available standards, *de-novo* MS/MS spectral interpretation, retention time or relative retention time (when standards were not available) and microsome incubations of the available standards. Confirmed structures, either by straight comparison with standards or by microsomal incubations were marked with a "C". It should be noted that, when using low-energy collision-induced dissociation of the protonated molecule, the fatty acid chain conjugated to carnitine cannot be fragmented and thus it is not possible to pinpoint the location of a double bond, a hydroxyl group or a carbonyl group. Similarly, structural isomers cannot be distinguished.

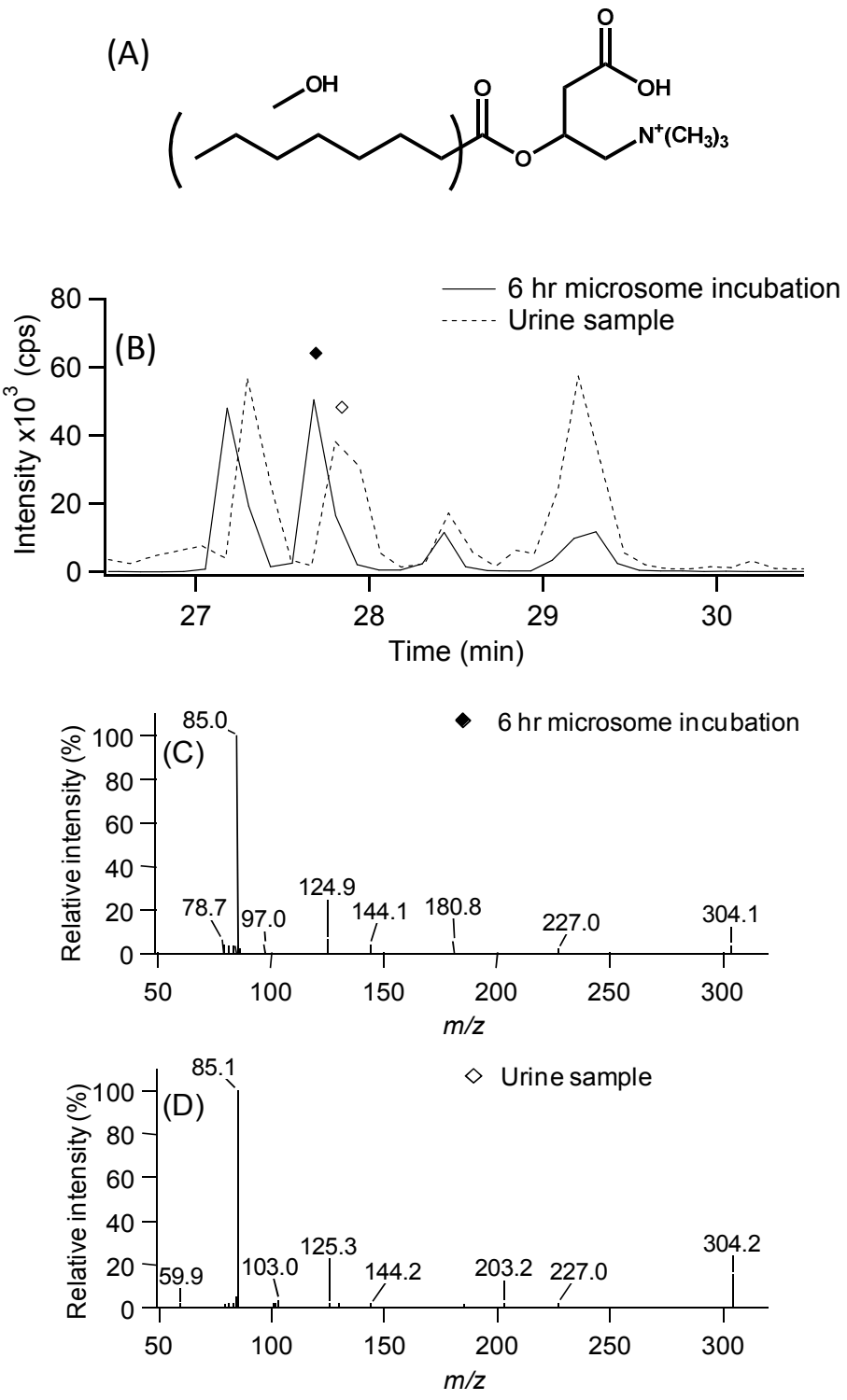

Figure 2.5. (A) Structure of hydroxyoctanoylcarnitine where the OH group is located on the fatty acid chain. (B) Extracted ion chromatograms (XICs) of m/z 304 of urine sample and 6 hour microsome incubation of octanoylcarnitine. The product ion spectra corresponding to the marked peaks on the XICs of a microsome incubation and urine are shown in (C) and (D), respectively.

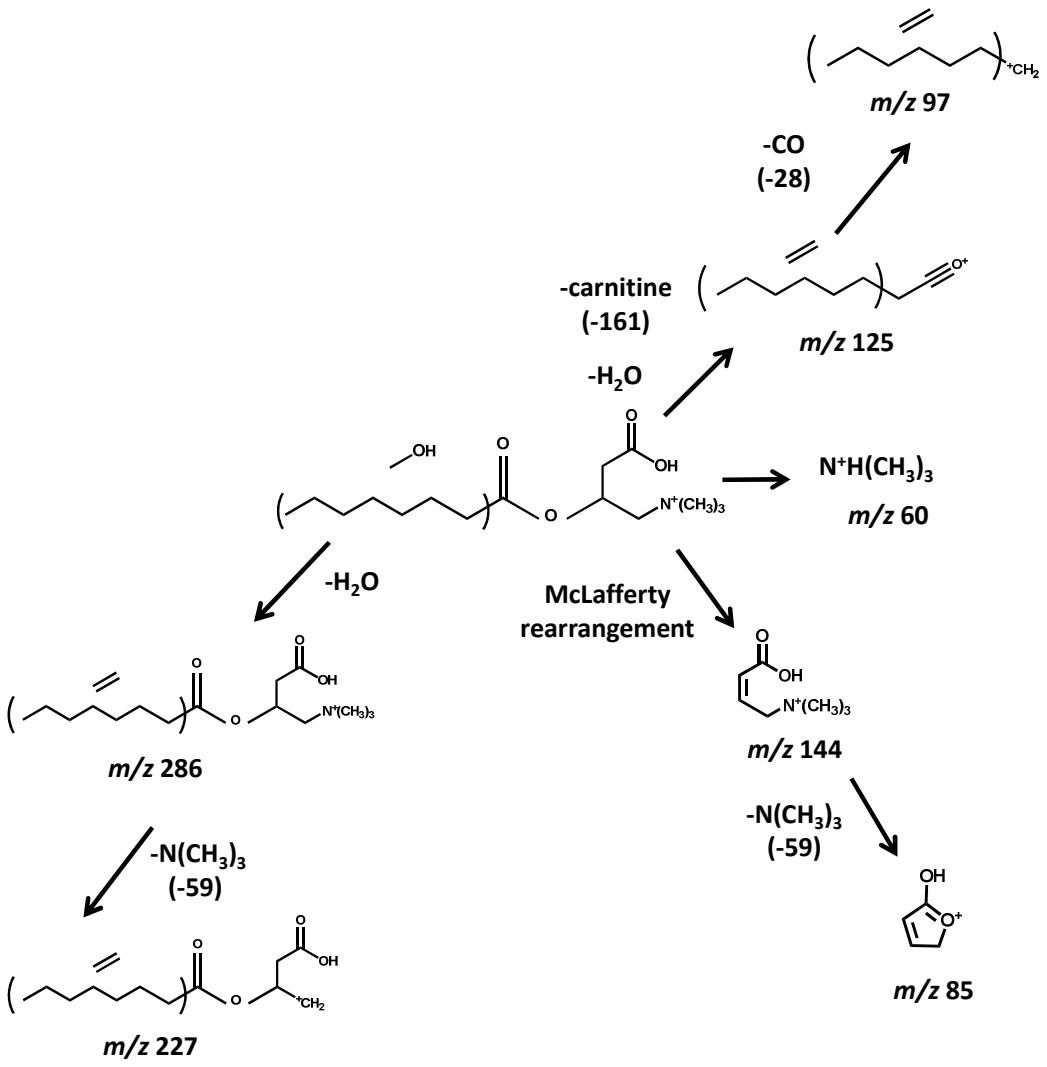

Figure 2.6. Fragmentation schematic of one of the structural isomers of C8+OH (hydroxyoctanoylcarnitine) showing the neutral losses and common fragment ions observed upon collision-induced dissociation. The position of OH and of the double bond on the fatty acid chain is undetermined.

An MS/MS spectral library containing the product ion spectra of all individual 355 species found in human urine is provided in the electronic Appendix. Four representative MS/MS spectra can be found in Appendix Section 2.2. In spectra where the compound structure is known or proposed, the structures of the compound and its major fragment ions are shown. In the case where a compound structure cannot be deduced, the proposed structures of some fragment ions are also given whenever possible.

In the absence of authentic standards, this method assigns tentative structures to the detected acylcarnitines. The MS/MS spectra with tentative structural assignments should still be useful in metabolomic profiling work. For example, if a researcher who is interested in biomarker discovery of a disease is able to match for the molecular ion mass and the MS/MS spectrum of an unknown metabolite with one of the library acylcarnitines showing a proposed structure, he or she may synthesize a compound based on the proposed structure to confirm the identity of the unknown. If this unknown is a potential biomarker of a disease, synthesis of an authentic standard is well justified. Even if the unknown happens to match a library acylcarnitine with no proposed structure, knowing that it is a member of the acylcarnitine family can still be useful. One might be able to determine if the unknown is a product of a metabolic reaction of a known acylcarnitine. Future development in sample handling (e.g., better fractionation of acylcarnitines from biofluids to improve sample clean-up) and MS/MS methods (e.g., MS^3 or alternative activation scheme[41]) may allow for the elucidation of chemical structures for most of the acylcarnitines detected.

Appendix Section 2.1 contains a partial table of all detected acylcarnitines. Note that, when more than one compound was found for a specific *m/z* value, each compound in the table containing all detected species was labeled with its *m/z* and a letter in brackets that matches the letter used for the spectra in the MS/MS library. Retention time information is also provided in the table. Although the chromatographic retention time of a particular compound is likely to be different for different column chemistry and separation conditions, the order of

elution should still be a valuable tool for identification of unknowns in other studies, particularly when similar column and separation conditions are used. A search tool was developed to facilitate unknown metabolite identification and is described in Chapter 6.

2.3.4 Reproducibility and acylcarnitine profiling of human urine

To assess the reproducibility of this method, three aliquots of the same urine sample were subjected to SPE and UPLC-MS/MS analysis in three parallel experiments. Figure 2.7 shows an overlay of three TICs corresponding to each one of the experimental replicates analyzed. Both retention times and peak intensities show good reproducibility; the retention time difference between runs varies from compound to compound but is generally within 12 s.

This UPLC-MS/MS method was applied to examine the urinary acylcarnitine profiles of a healthy individual over a consecutive five-day period.

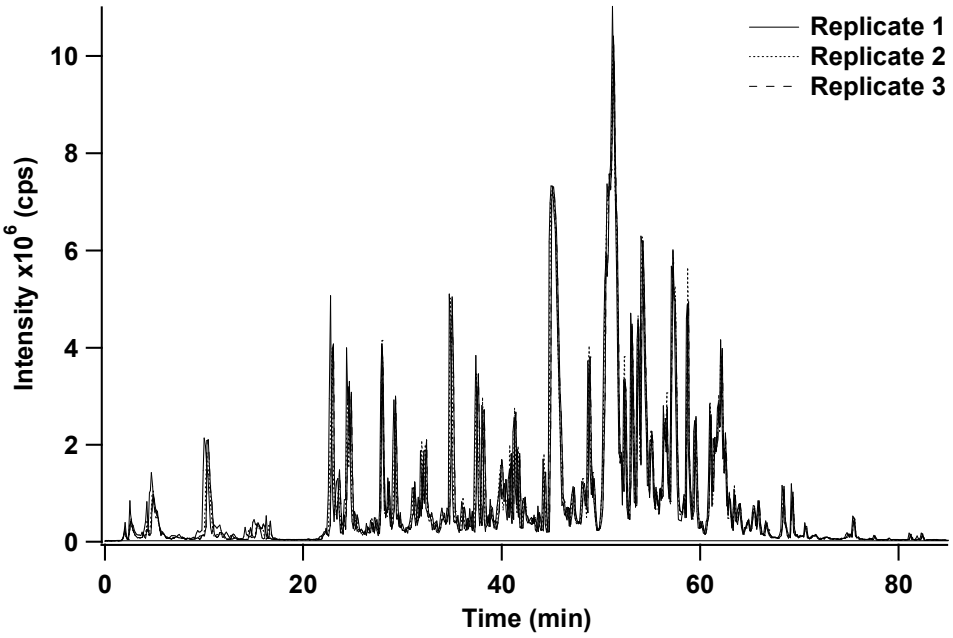

Figure 2.7. Total ion chromatograms of three replicate runs of urine sample from individual A.

Figure 2.8 shows the total ion chromatograms using 76 MRM transitions obtained from first morning urine collections over five consecutive days along with a pooled urine sample. Six confirmed species are labeled on the chromatogram. As the figure shows, the overall profiles are quite similar. However, some peak intensities, particularly those corresponding to isobutyrylcarnitine (C4-I) and octanoylcarnitine (C8) are found to fluctuate relative to the rest of the peaks in the chromatograms.

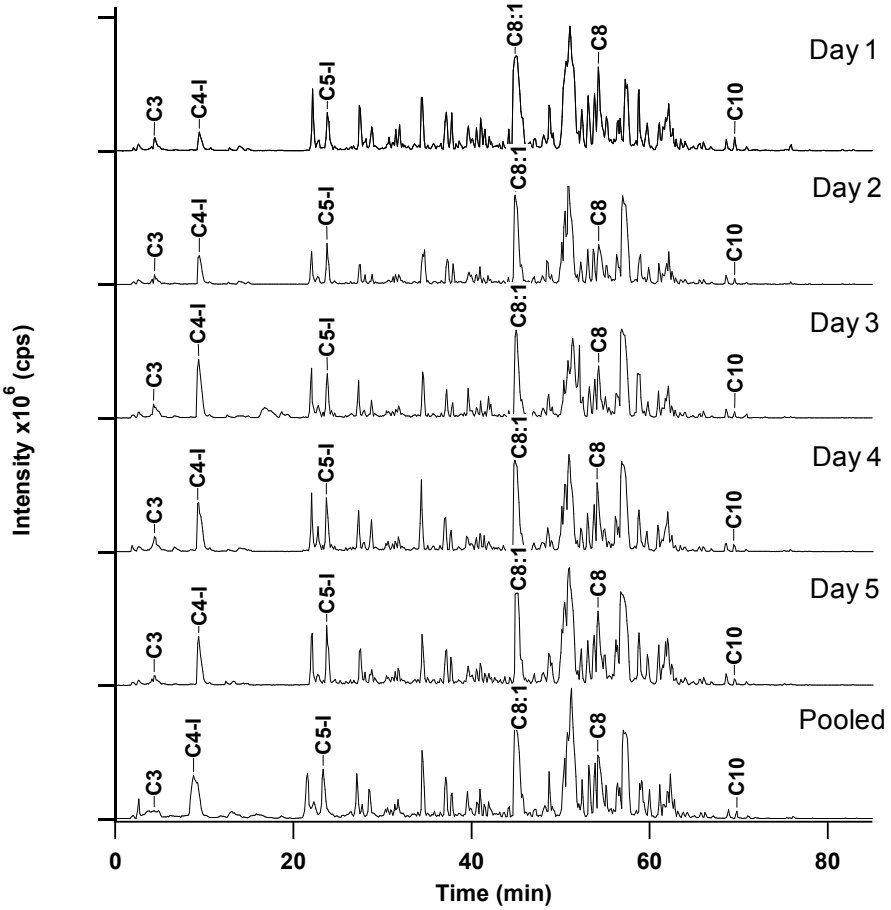

Figure 2.8. Day-to-day variability in the urinary acylcarnitine profile of a healthy individual. Urine from a healthy individual was collected at the same time for five consecutive days. Six total ion chromatograms of SPE-processed samples corresponding to days 1 to 5 and a pooled sample are shown. Several identified peaks are labeled.

A preliminary study was performed to examine the acylcarnitine profiles of urine collected from different individuals. Urine specimens from 4 female and 2 male healthy volunteers were subjected to SPE and analyzed using this UPLC-MS/MS method. Figure 2.9 displays the TICs of the individual urine samples. The chromatographic traces are generally quite similar. However, they show subtle differences in the relative intensities of some peaks, especially propionyl (C3) and isobutyrylcarnitine (C4-I). Interestingly, the chromatogram shown in Figure 2.5F seems to have peaks with lower intensities compared to the other five individuals in the region from 25 to 40 min (corresponding to middle-chain acylcarnitines). It is worth noting that the differences in relative intensities observed may be partially due to differences in the matrices themselves and thus a quantitative analysis should be performed in order to confirm that these differences are solely due to differences in acylcarnitine concentrations.

The urine specimen from individual A was found to contain the highest number of acylcarnitines, with a total of 277, while individuals B-F had 235, 269, 245, 258 and 209 different species, respectively. In total, 355 different acylcarnitines were found (see full table in electronic Appendix and partial table in Appendix Section 2.1). The frequency of detection for a given acylcarnitine is shown in the table, column 2 (e.g., n=6 means this compound was detected in all 6 individuals). Out of the 355 acylcarnitines, 130 species were common to all 6 individuals and only 31 acylcarnitines were found to be present in only one individual. Three species were exclusive to a pooled sample from the 5 consecutive day urine collection performed by individual A.

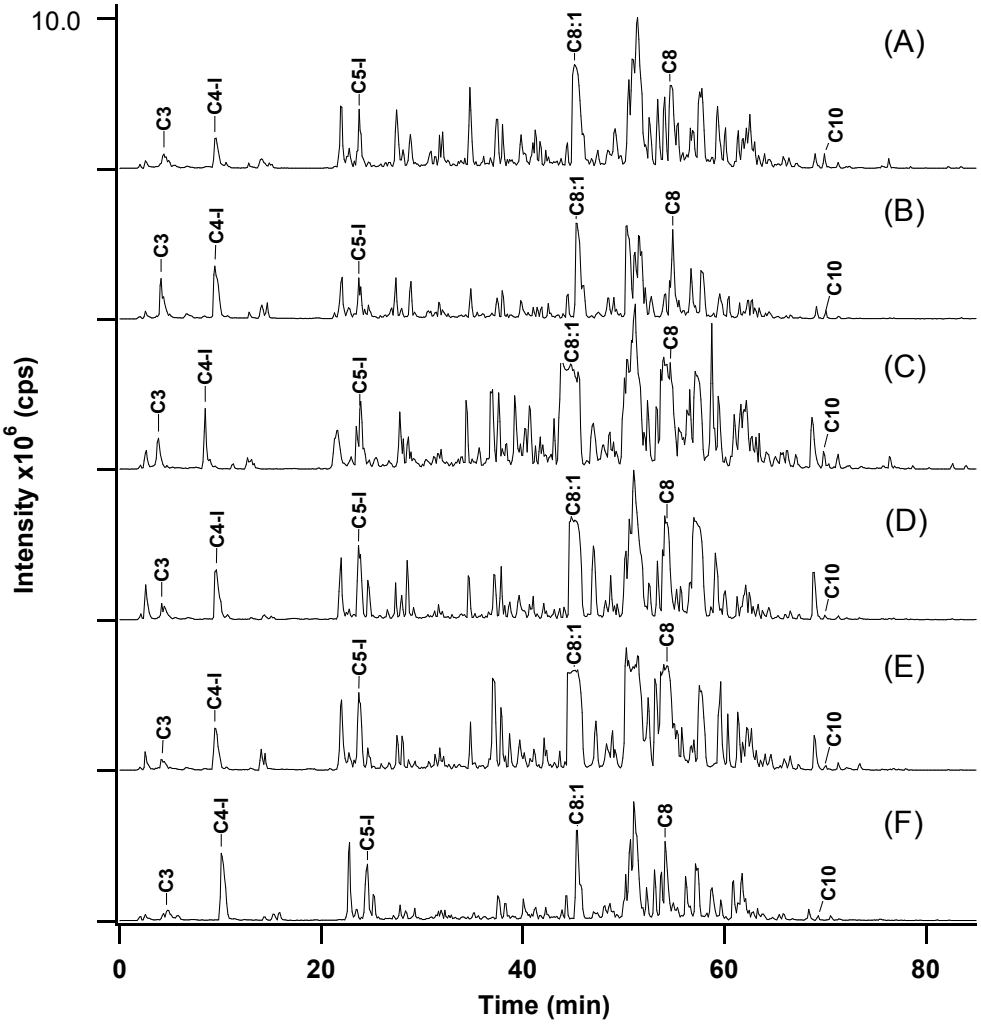

Figure 2.9. Urinary acylcarnitine profiles from SPE-processed samples of six healthy individuals. Six TICs corresponding to individuals A to F are shown. Several peaks are labeled with their corresponding assigned structures.

The above results indicate that a large number of acylcarnitines can be detected from urine of different individuals or a single individual with samples being collected at different times. Only 43 of the 355 acylcarnitines detected in this work have been previously reported in the urine of healthy individuals. [12, 22, 23, 25, 28, 31-35] However, there are several species that have been reported in the urine of healthy individuals which were not detected using the method described herein.[28, 32] These are mainly long-chain acylcarnitines and their phase I

metabolites. This is most likely due to the limitation of the use of SPE for analyte extraction, the ESI conditions used as well as the low abundance of these species in urine. Different extraction techniques tailored to long-chain species such as liquid-liquid extraction could aid in the detection of these more hydrophobic species. Other species that were not detected by this method were different isomers of C5+OH and C5:1 (see the footnotes in Appendix Section 2.1 for the nomenclature). These species have been shown to preferentially form glycine conjugates. [22, 42] The analysis of dicarboxylic acids conjugated to carnitine has been shown to be challenging due both to their lower abundance in biological fluids as well as their lower ionization efficiencies. [43] Using the current method, C3:DC was not detected and only one isomer of C4:DC and C5:DC were observed. It is likely that these species were present in very low abundance in the urine of individuals involved in this study.

2.4 Conclusions

A selective and reproducible UPLC-MS/MS method with the ability to resolve acylcarnitine isomers and provide a comprehensive acylcarnitine profile in urine has been developed. A total of 355 species were detected in the urine of six healthy individuals. This represents the most comprehensive list of urinary acylcarnitines reported to date. Future work will be focused on the development of a quantitative UPLC-MS/MS method that can be applied for accurate quantification of acylcarnitines in various types of biological samples. Similar methods could be developed for detecting other types of lipid metabolites with the ultimate goal of defining the chemical identities of the entire lipid metabolome while expanding the MS/MS spectral library to include a large number of metabolites.

2.5 Literature cited

(1) Gross, R. W.; Han, X. L. *American Journal of Physiology- Endocrinology and Metabolism* **2009**, *297*, E297-E303.

(2) Wenk, M. R. *Nature Reviews Drug Discovery* **2005**, *4*, 594-610.

(3) Zehethofer, N.; Pinto, D. M. *Analytica Chimica Acta* **2008**, *627*, 62-70.

(4) Han, X. L.; Gross, R. W. *Mass Spectrometry Reviews* **2005**, *24*, 367-412.

(5) German, J. B.; Gillies, L. A.; Smilowitz, J. T.; Zivkovic, A. M.; Watkins, S. M. *Current Opinion in Lipidology* **2007**, *18*, 66-71.

(6) Piomelli, D.; Astarita, G.; Rapaka, R. *Nature Reviews Neuroscience* **2007**, *8*, 743-754.

(7) Glatz, J. F. C.; Luiken, J.; Bonen, A. *Physiological Reviews* **2010**, *90*, 367-417.

(8) Catala, A. *Chemistry and Physics of Lipids* **2009**, *157*, 1-11.

(9) Evans, A. M.; Fornasini, G. *Clinical Pharmacokinetics* **2003**, *42*, 941-967.

(10) Jones, L. L.; McDonald, D. A.; Borum, P. R. *Progress in Lipid Research* **2010**, *49*, 61-75.

(11) Heinig, K.; Henion, J. *Journal of Chromatography B* **1999**, *735*, 171-188.

(12) Moder, M.; Kiessling, A.; Loster, H.; Bruggemann, L. *Analytical and Bioanalytical Chemistry* **2003**, *375*, 200-210.

(13) Rashed, M. S.; Ozand, P. T.; Bucknall, M. P.; Little, D. *Pediatric Research* **1995**, *38*, 324-331.

(14) Chace, D. H.; Kalas, T. A. *Clinical Biochemistry* **2005**, *38*, 296-309.

(15) Nagaraja, D.; Mamatha, S. N.; De, T.; Christopher, R. *Clinical Biochemistry* **2010**, *43*, 581-588.

(16) Thevis, M.; Schänzer, W. *Analytical and Bioanalytical Chemistry* **2007**, *388*, 1351-1358.

(17) Fingerhut, R.; Ensenauer, R.; Rochinger, W.; Arnecke, R.; Olgemoller, B.; Roscher, A. A. *Analytical Chemistry* **2009**, *81*, 3571-3575.

(18) Kobayashi, H.; Hasegawa, Y.; Endo, M.; Purevsuren, J.; Yamaguchi, S. *Journal of Chromatography B* **2007**, *855*, 80-87.

(19) Abdenur, J. E.; Chamoles, N. A.; Guinle, A. E.; Schenone, A. B.; Fuertes, A. N. J. *Journal of Inherited Metabolic Disease.* **1998**, *21*, 624-630.

(20) Matern, D.; Tortorelli, S.; Oglesbee, D.; Gavrilov, D.; Rinaldo, P. *Journal of Inherited Metabolic Disease* **2007**, *30*, 585-592.

(21) Smith, E. H.; Thomas, C.; McHugh, D.; Gavrilov, D.; Raymond, K.; Rinaldo, P.; Tortorelli, S.; Matern, D.; Highsmith, W. E.; Oglesbee, D. *Molecular Genetics and Metabolism* **2010**, *100*, 241-250.

(22) Maeda, Y.; Ito, T.; Ohmi, H.; Yokoi, K.; Nakajima, Y.; Ueta, A.; Kurono, Y.; Togari, H.; Sugiyama, N. *Journal of Chromatography B* **2008**, *870*, 154-159.

(23) Maeda, Y.; Ito, T.; Suzuki, A.; Kurono, Y.; Ueta, A.; Yokoi, K.; Sumi, S.; Togari, H.; Sugiyama, N. *Rapid Communications in Mass Spectrometry* **2007**, *21*, 799-806.

(24) Ferrer, I.; Ruiz-Sala, P.; Vicente, Y.; Merinero, B.; Perez-Cerda, C.; Ugarte, M. *Journal of Chromatography B* **2007**, *860*, 121-126.

(25) Yang, S. M.; Minkler, P.; Hoppel, C. *Journal of Chromatography B* **2007**, *857*, 251-258.

(26) Chalcraft, K. R.; Britz-McKibbin, P. *Analytical Chemistry* **2009**, *81*, 307-314.

(27) Vernez, L.; Hopfgartner, G.; Wenk, M.; Krahenbuhl, S. *Journal of Chromatography A* **2003**, *984*, 203-213.

(28) Minkler, P. E.; Stoll, M. S. K.; Ingalls, S. T.; Yang, S. M.; Kerner, J.; Hoppel, C. L. *Clinical Chemistry* **2008**, *54*, 1451-1462.

(29) Horvath, T. D.; Stratton, S. L.; Bogusiewicz, A.; Pack, L.; Moran, J.; Mock, D. M. *Analytical Chemistry* **2010**, *82*, 4140-4144.

(30) Hager, J. W.; Le Blanc, J. C. Y. *Journal of Chromatography A* **2003**, *1020*, 3-9.

(31) Moder, M.; Loster, H.; Herzschuh, R.; Popp, P. *Journal of Mass Spectrometry* **1997**, *32*, 1195-1204.

(32) Mueller, P.; Schulze, A.; Schindler, I.; Ethofer, T.; Buehrdel, P.; Ceglarek, U. *Clinica Chimica Acta* **2003**, *327*, 47-57.

(33) Libert, R.; VanHoof, F.; Thillaye, M.; Vincent, M. F.; Nassogne, M. C.; Stroobant, V.; deHoffmann, E.; Schanck, A. *Analytical Biochemistry* **1997**, *251*, 196-205.

(34) Libert, R.; Van Hoof, F.; Laus, G.; De Nayer, P.; Jiwan, J. L. H.; de Hoffmann, E.; Schanck, A. *Clinica Chimica Acta* **2005**, *355*, 145-151.

(35) Minkler, P. E.; Ingalls, S. T.; Hoppel, C. L. *Analytical Chemistry* **2005**, *77*, 1448-1457.

(36) Wishart, D. S.; Knox, C.; Guo, A. C.; Eisner, R.; Young, N.; Gautam, B.; Hau, D. D.; Psychogios, N.; Dong, E.; Bouatra, S.; Mandal, R.; Sinelnikov, I.; Xia, J. G.; Jia, L.; Cruz, J. A.; Lim, E.; Sobsey, C. A.; Shrivastava, S.; Huang, P.; Liu, P.; Fang, L.; Peng, J.; Fradette, R.; Cheng, D.; Tzur, D.; Clements, M.; Lewis, A.; De Souza, A.; Zuniga, A.; Dawe, M.; Xiong, Y. P.; Clive, D.; Greiner, R.; Nazyrova, A.; Shaykhutdinov, R.; Li, L.; Vogel, H. J.; Forsythe, I. *Nucleic Acids Research* **2009**, *37*, D603-D610.

(37) Tallarico, C.; Pace, S.; Longo, A. *Rapid Communications in Mass Spectrometry* **1998**, *12*, 403-409.

(38) *Food and Drug Administration, Guidance for Industry Guidance: Bioanalytical Method Validation, US Department of Health and Human Services, FDA, Centre for Drug Evaluation and Research, Rockville, MD*, 2001.

(39) *Food and Drug Administration, Guidance for Industry, Mass Spectrometry for Confirmation of the Identity of Animal Drug Residues (Guidance 118), U.S. Department of Health and Human Services, FDA, Center for Veterinary Medicine, Rockville, MD* 2003.

(40) Su, X.; Han, X. L.; Mancuso, D. J.; Abendschein, D. R.; Gross, R. W. *Biochemistry* **2005**, *44*, 5234-5245.

(41) Yoo, H. J.; Liu, H. C.; Hakansson, K. *Analytical Chemistry* **2007**, *79*, 7858-7866.

(42) Rashed, M. S. *Journal of Chromatography B: Biomedical Sciences and Applications* **2001**, *758*, 27-48.

(43) Chace, D. H.; Kalas, T. A.; Naylor, E. W. *Clinical Chemistry* **2003**, *49*, 1797-1817.

Chapter 3

Comprehensive profiling of acylcarnitines in plasma, dried blood spots and red blood cell pellets by Ultra performance liquid chromatography tandem mass spectrometry*

3.1 Introduction

The total acylcarnitine pool in the human body has been found to be highly compartmentalized. Approximately 98% of the total is located in cardiac and skeletal muscles. Although plasma only constitutes about 1%, it plays a vital role in transporting carnitine and its esters to different parts of the body for usage and storage. It is thus still commonly used as an indicator of overall carnitine status.[1, 2] Acylcarnitines that do not undergo tubular reabsorption in the kidneys are excreted in the urine, making urine another very useful biofluid for acylcarnitine analysis.[3-5] Moreover, it has been found that acylation of carnitine may also take place in the renal tubule. Thus the kidneys themselves also contribute to acylcarnitine production. These compounds can also be found in other biological fluids such as bile, further expanding the possibilities of available sample types.

* A form of this chapter is in preparation for publication as: Zuniga, A., Li, L. "Comprehensive profiling of acylcarnitines in plasma, dried blood spots and red blood cell pellets by Ultra performance liquid chromatography tandem mass spectrometry."

As a result, acylcarnitines have been profiled in various biological samples including plasma, urine, bile, dried blood spots (DBS), skin fibroblasts, skeletal and cardiac muscle, among others.[6-9] Researchers have found that acylcarnitine profiles vary dramatically depending on the type of sample studied and in some cases it is necessary to analyze more than one sample type to gather diagnostically relevant information as well as to confirm their findings.[4, 10]

Analysis of plasma constitutes a major challenge due to its composition. It is a heterogeneous mixture of proteins, lipids, metabolites and ionic species which may interact with each other in various ways, an example of which is the formation of metabolite-protein complexes.[11] Preparation of plasma samples for metabolomics studies involves the removal of many of these species especially proteins and lipids which can additionally cause severe matrix effects.

Analysis of whole blood also comes with its own considerations. In order to avoid some of the disadvantages of handling and storage of whole blood, researchers have turned to dried blood spots. Dried blood spots offer numerous advantages: first, sample acquisition is much less invasive (heel or finger prick). Second, most analytes on dried blood spots are stable at room temperature for a week which greatly simplifies storage.[12] Moreover, once the blood spots are dry they are no longer considered a biohazard.[13] The major aspect of dried blood spot analysis that needs to be considered is the drying process on the filter paper which causes protein denaturation and cell lysis. The implications of this are that intra-cellular metabolites as well as previously protein-bound metabolites are introduced into the sample. This may cause unexpected results, for example both red blood cells (RBC) and leukocytes contain high concentrations of free carnitine, causing an elevated whole blood free carnitine concentration.[5]

Upon centrifugation of whole blood, many metabolites which interact with RBC membranes through hydrophobic and electrostatic interactions may be lost. These metabolites such as long-chain acylcarnitines are important biomarkers for disorders such as very long-chain acyl-CoA dehydrogenase (VLCAD) deficiency

as well as peroxisomal disorders.[14, 15] Extracting these metabolites however, requires careful manipulation. The extraction solvent must dissolve the analytes of interest while not lysing the cells. Likewise, the amount of mechanical force applied should be enough to disrupt the interactions between metabolites and cells but not enough to disrupt the cells themselves.

In order to obtain a comprehensive and truly representative acylcarnitine profile of a certain individual at a particular time, it is necessary to analyze as many sample types as possible, since complementary as well as confirmatory information can be obtained. In this work, acylcarnitines were profiled using two UPLC-MS/MS methods, one targeting short and medium-chain species and the other focusing on long and very long-chain ones. Urine, plasma, dried blood spots and RBC pellets were analyzed and compared. It was found that by compiling all the data provided a more complete depiction of the carnitine pool in healthy individuals can be obtained.

3.2 Experimental

3.2.1 Chemicals and Reagents

Refer to Chapter 2 Section 2.2.1 for a complete list of chemicals and reagents used.

3.2.2 UPLC

Chromatographic separation was performed on an ACQUITY UPLC® system (Waters Corporation, Milford, MA) consisting of a binary solvent manger, a sample manager and a column compartment. Two distinct LC methods had to be developed; one was optimized for short and medium-chain acylcarnitines, while the other was optimized for long and very long-chain species. The column used for the short and medium-chain method was a BEH (Ethylene Bridged Hybrid) C_{18} 1.0 mm i.d. × 150 mm with 1.7 µm particle size. In the case of the long-chain method, the column used was a BEH (Ethylene Bridged Hybrid) C_{18} 2.1 mm i.d.

× 50 mm with 1.7 µm particle size. In both cases, a 5 µL sample aliquot was injected onto the column which was maintained at a temperature of 25 ˚C. A gradient elution with two mobile phases was used for both methods: 0.1% FA, 4% I in H_2O (eluent A) and 0.1% FA in I (eluent B). A flow rate of 50 µL/min was utilized for the short and medium chain method. The gradient sequence started by holding 0% B for 11 min, followed by an increase to 50% B in 90 min. The gradient was subsequently increased to 100% B over a period of 5 min and held for 10 min. At 105.10 min after injection, the system was returned to 100% A for 25 min at a flow rate of 75 µL/min to re-equilibrate the column. Finally, the flow rate was brought back down to 50 µL/min and held for 5 min in order to allow the pressure in the system to stabilize. For the long and very long-chain method, the flow rate used was 300 µL/min, the gradient sequence started by holding 50% B for 2.33 minutes, followed by an increase to 100% B in 21.68 minutes. This condition was held for an extra 2.45 minutes and the % of B was subsequently lowered back to 50% and held for 4.87 minutes to allow for the column to re-equilibrate.

3.2.3 ESI-MS

The MS system used was a 4000 QTRAP® MS/MS System (Applied Biosystems, Foster City, CA) equipped with a Turbo V™ ion source. Information dependent acquisitions (IDAs) were performed for both methods, using multiple reaction monitoring (MRM) as a survey scan. The method for short and medium chains contained 89 MRM transitions, which can be summarized as acylcarnitine $m/z \rightarrow 85$, each having a dwell time of 10 ms. These transitions were based on the results presented in Chapter 2 and literature searches. During the survey scan, for every data point acquired, the 4 most intense peaks were selected for subsequent enhanced product ion scan (i.e., MS/MS).

For the short and medium-chain method the ESI source was set to positive ion mode with the following settings: the curtain gas, 10 psi; the collision-activated dissociation (CAD) gas, high; the ion source voltage, 5000 V; the source

temperature, 350 °C; and gases 1 and 2 set to 20 and 15 psi, respectively. The declustering potential (DP) was set to 40 V. The collision energy (CE) was 37 V and the entrance potential (EP) was set to 8 V, while the collision cell exit potential (CXP) was set to 15 V. The resolution for both Q1 and Q3 was set to high. The enhanced product ion parameters in the linear ion trap were the followings: the CE, 32 V with a collision energy spread (CES) of 5 V; the Q3 entry barrier, 6 V; and the scan rate, 4000 Da/s for a scan range of 50 to 550 Da. Dynamic fill time was selected.

In the case of the long and very long-chain method, 99 MRM transitions were set with a dwell time of 10 ms each. The 4 most intense ions along each chromatographic data point were selected for subsequent MS/MS analysis. For ethyl ester detection in DBS, 28 amu where added to the original Q1 masses of all MRM transitions (corresponding to the added ethyl group).

The ESI source was set to positive ion mode with the following settings to accommodate for the higher flow rate used: the curtain gas, 15 psi; the collision-activated dissociation (CAD) gas, high; the ion source voltage, 4800 V; the source temperature, 500 °C; and gases 1 and 2 set to 35 and 30 psi, respectively. The declustering potential (DP) was set to 60 V. The collision energy (CE) was 45 V and the entrance potential (EP) was set to 11 V, while the collision cell exit potential (CXP) was set to 13 V. The resolution for both Q1 and Q3 was set to high. The enhanced product ion parameters in the linear ion trap were the followings: the CE, 37 V with a collision energy spread (CES) of 5 V; the Q3 entry barrier, 6 V; and the scan rate, 4000 Da/s for a scan range of 50 to 550 Da. Dynamic fill time was selected. A detailed description of the UPLC-MS/MS methods used can be found in the electronic Appendix.

3.2.4 Sample preparation

3.2.4.1 Urine and plasma samples

Please refer to Chapter 2 Sections 2.2.3 and 2.2.4 for a detailed protocol of urine sample preparation. Plasma samples were prepared as follows: Whole blood

was collected from five female healthy volunteers who were not on any special diet or taking any nutritional supplements. An informed consent was obtained from each volunteer and ethics approval for this work was obtained from the University of Alberta in compliance with the Arts, Science and Law Research Ethics Board policy. Whole blood samples in tri-potassium ethylenediaminetetraacetic acid (EDTA) were immediately centrifuged at 14,000 rpm for 10 min in order to separate the plasma. Protein precipitation/analyte extraction was performed by adding 200 µL of 20% H_2O, 80% acetonitrile (I) to 50 µL of plasma and incubating for 30 min at 4 °C. Samples were then centrifuged at 14,000 rpm for 10 min at 4 °C.

3.2.4.2 Dried blood spots

The same whole blood samples mentioned in Section 3.2.4.1 were used to prepared dried blood spots. Fifty microlitres of blood were pipetted onto Whatman 903 specimen collection papers and allowed to dry overnight at 4 °C. A 3 mm hole punch was used to punch out 2 disks per sample which were placed in microcentrifuge vials. Two hundred microlitres of methanol were added to the vials and the samples were sonicated for 30 minutes. The disks were removed and the solvent was evaporated to dryness in a Speedvac concentrator and reconstituted in 50 µL 0.1% FA, 50% I in H_2O. It was found that the peak intensities were quite low (see figure 3.3). Esterification was performed in an attempt to improve their detectability by redissolving the dried extract in 25 µL of ethanol, adding 0.5 µL of sulfuric acid and allowing the reaction to proceed at 50 °C for one hour. The solvent was then evaporated to dryness and reconstituted in 50 µL 0.1% FA, 50% I in H_2O.

3.2.4.3 Red blood cell pellets

After whole blood centrifugation of all five samples at 14,000 *g* for 10 minutes, 200 µL of methanol were added to the remaining RBC pellets. The vials were gently shaken for 5 minutes and the supernatant was transferred to a clean

vial. The samples were evaporated to dryness in a Speedvac concentrator and reconstituted in 50 μL 0.1% FA, 50% I in H_2O.

3.3 Results and Discussion

Acylcarnitine profiles varied dramatically depending on the biofluid studied. This is apparent by simple inspection of the Total Ion Chromatogram (TIC) of each analytical run. The top panel of Figure 3.1 shows a urinary acylcarnitine profile. As compared to the bottom panel, which shows a plasma acylcarnitine profile, it can be easily observed that while there are more species in urine than in plasma, there are more hydrophobic species (which are later-eluting) present in plasma than in urine. Upon further data inspection, it was noticed that there were many more phase I acylcarnitine metabolites such as hydroxyl-acylcarnitines found in urine than in plasma. This was expected since phase I metabolites are formed as part of the kidney excretion process especially for more hydrophobic species.[16]

In order to study and compare the presence of long-chain acylcarnitines in urine and plasma, representative urine and plasma samples were run using an UPLC-MS/MS method optimized for this particular type of species. Figure 3.2 shows an overlay of two Total Ion Chromatograms (TICs). It can be observed that species such as C16 and C18 as well as unsaturated derivatives of C18 are found in much higher abundance in plasma than in urine, a finding that agrees well with previously published results.[17] This supports the claim that in order to obtain an accurate depiction of an individual's acylcarnitine profile, more than one type of sample should be studied.

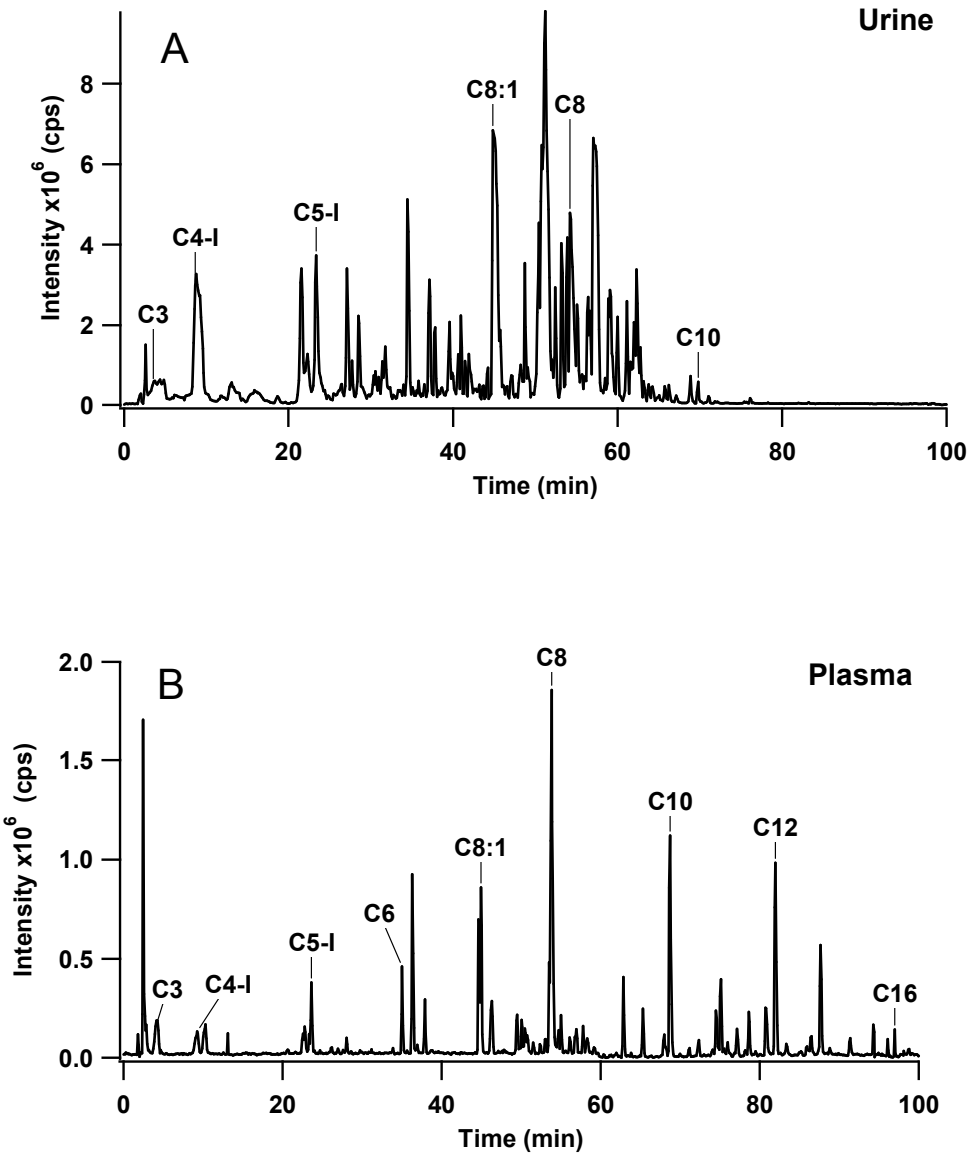

Figure 3.1 The differences in the acylcarnitine profile in urine (top) and plasma (bottom) is clear when comparing these Total Ion Chromatograms (TICs). Urine was found to contain more species overall while plasma contained more hydrophobic species.

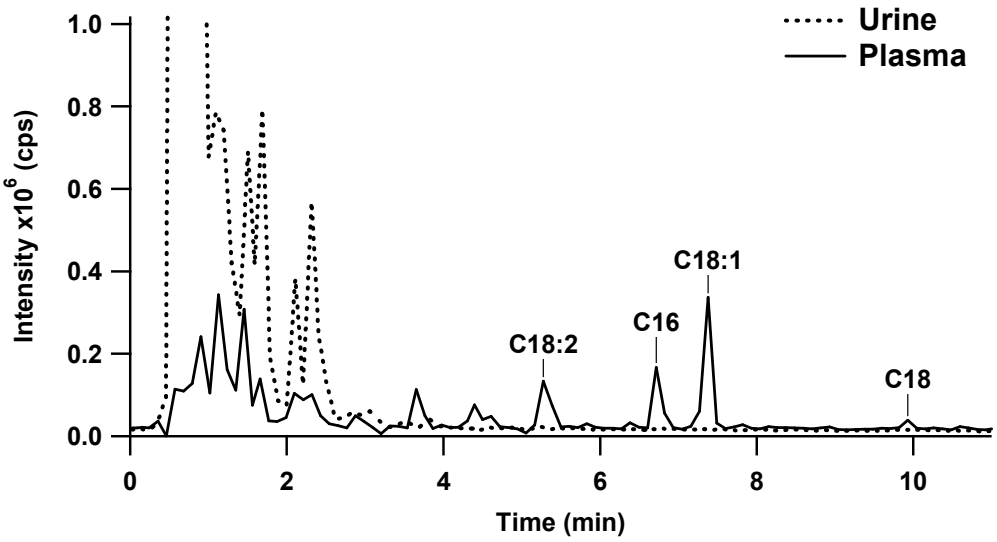

Figure 3.2 Overlay of two TICs obtained from a method optimized for long-chain species, displaying the higher abundance of C16 and C18 (and their derivatives) in plasma than in urine.

Various extraction solvents and methods including the use of heat, shaking and sonication were tested in order to extract as many acylcarnitines from DBS samples as possible. The best results were obtained from the conditions described in Section 3.2.4.2. It can be observed in Figure 3.3 however, that the peak intensities from the DBS sample without esterification were quite low. Esterification of these samples dramatically increased their peak intensities allowing for the detection of more than double the number of species. A total of 41 species were detected in the esterified DBS samples.

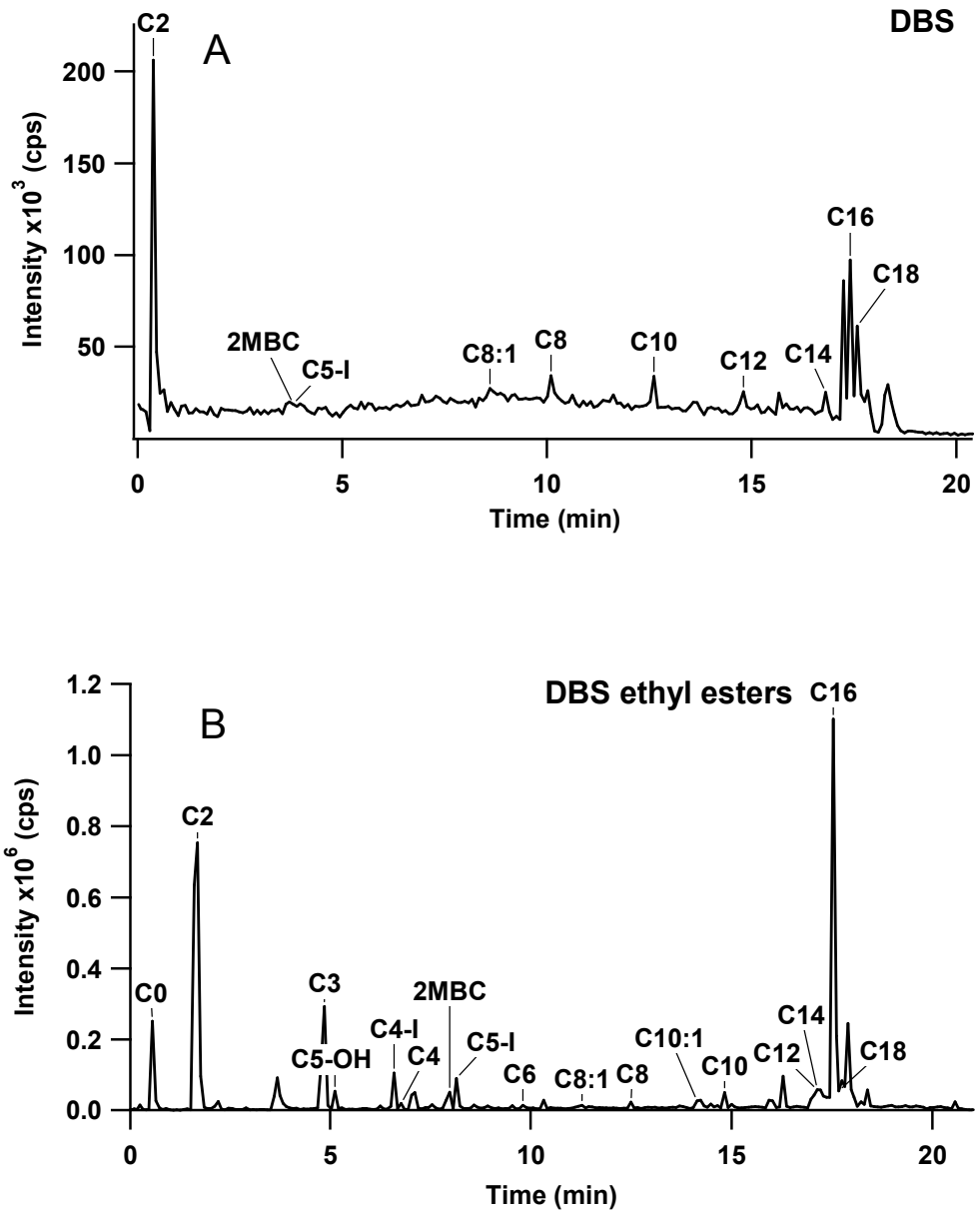

Figure 3.3 TICs of DBS with (bottom) and without (top) esterification. A significant signal enhancement was observed upon esterification of an extracted dried blood spot sample.

Analysis of red blood cell pellet washes revealed 22 long and very long-chain species, most of which were unsaturated derivatives. Interestingly, a species that seemed to be an acylcarnitine with a fatty acid chain of 17 carbons and its isomer were detected. Their structural assignment was achieved based on their relative retention time and MS/MS fragmentation pattern. Odd chain and

branched-chain acylcarnitines consisting of 5 carbons or less are products of amino acid metabolism.[18] Odd-chain acylcarnitines with longer chain lengths are not very common; β-oxidation of odd-chain fatty acids yields propionyl-CoA (instead of acetyl-CoA) which is not a citric acid cycle substrate.[19] Fatty acids with an odd number of carbon atoms usually come from exogenous sources such as gut microflora or from diet. It was thus speculated that both of these species were most likely branched. Figure 3.4 is a TIC of a RBC pellet methanol wash, note that only one C17 isomer was outlined on the TIC.

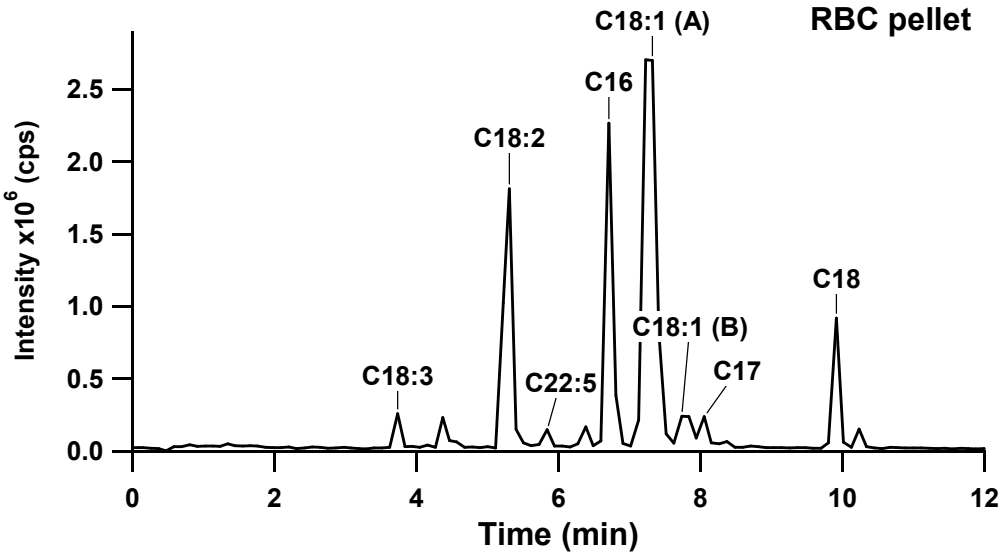

Figure 3.4 TIC of a RBC pellet methanol wash. Only long and very long-chain species were found.

Figure 3.5 is a Venn diagram describing the distribution of acylcarnitines in various biofluids; namely urine, plasma, dried blood spots and RBC pellet. Urine results are those described in Chapter 2. There were 436 species found in total (all sample types) with urine having the most detected (355 species). The RBC pellet contained strictly long and very long-chain acylcarnitines, so as expected, there were no species found both in urine and in RBC pellet. On the other hand, there were 251 species unique to urine, mostly phase I metabolites of acylcarnitines, species with at least one degree of unsaturation, as well as hydroxy

species. Isomeric species of many of these metabolites account for this high value. Plasma contained 50 unique species, which seemed to be mostly structural isomers of unsaturated medium-chain species, the isomers of which have not been previously reported in the literature. The DBS samples studied contained 7 unique species (mostly hydroxy metabolites of long-chain species). Interestingly, DBS samples contained the widest range of hydrophobicities, with compounds ranging from C0 to C26. The RBC pellet washes contained 5 acylcarnitines with unknown structures that were not found in any other biofluid. These results clearly demonstrate the diversity of acylcarnitines in various biofluids. Partial lists of acylcarnitines found in DBS, plasma and RBC pellet can be found in Appendix Sections 3.1, 3.3 and 3.5 respectively. Representative MS/MS spectra for each of these sample types can be found in Appendix Sections 3.2, 3.4 and 3.6. Complete tables and MS/MS libraries can be found in the electronic Appendix.

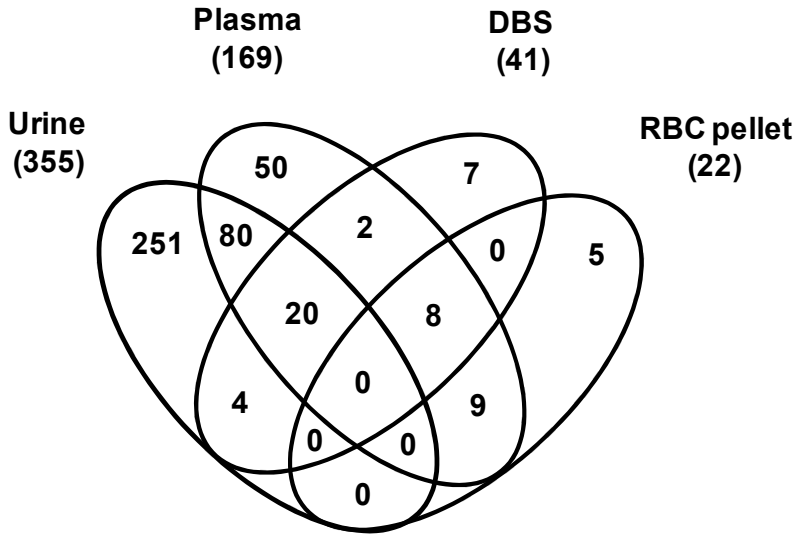

Figure 3.5 Venn diagram showing the distribution of acylcarnitines in urine, plasma, dried blood spots (DBS) and red blood cell (RBC) pellet. The totals for each sample type are shown in brackets.

3.4 Conclusions

Two UPLC-MS/MS methods were developed in order to comprehensively profile acylcarnitines in urine, plasma, dried blood spots and RBC pellets. Four hundred and thirty six unique species were detected, 355 of which were found in urine. There were 169 acylcarnitines found in plasma, 50 of which were unique to this biofluid. The 41 species found in DBS constituted the largest range of hydrophobicities found in one biofluid (C0 to C26). Red blood cell pellets contained a total of 22 different long and very long-chain species with only five being unique to this sample type. Only by compiling all this data can an extensive acylcarnitine pool be obtained.

3.5 Literature cited

(1) Reuter, S. E.; Evans, A. M.; Chace, D. H.; Fornasini, G. *Annals of Clinical Biochemistry* **2008**, *45*, 585-592.

(2) Reuter, S. E.; Evans, A. M.; Faull, R. J.; Chace, D. H.; Fornasini, G. *Annals of Clinical Biochemistry* **2005**, *42*, 387-393.

(3) Möder, M.; Kießling, A.; Löster, H.; Brüggemann, L. *Analytical and Bioanalytical Chemistry* **2003**, *375*, 200-210.

(4) Maeda, Y.; Ito, T.; Ohmi, H.; Yokoi, K.; Nakajima, Y.; Ueta, A.; Kurono, Y.; Togari, H.; Sugiyama, N. *Journal of Chromatography B* **2008**, *870*, 154-159.

(5) Bieber, L. L. *Annual Review of Biochemistry* **1988**, *57*, 261-283.

(6) Minkler, P. E.; Stoll, M. S. K.; Ingalls, S. T.; Yang, S.; Kerner, J.; Hoppel, C. L. *Clinical Chemistry* **2008**, *54*, 1451-1462.

(7) Okun, J. G.; Kölker, S.; Schulze, A.; Kohlmüller, D.; Olgemöller, K.; Lindner, M.; Hoffmann, G. F.; Wanders, R. J. A.; Mayatepek, E. *Biochimica et Biophysica Acta (BBA) – Molecular and Cell Biology of Lipids* **2002**, *1584*, 91-98.

(8) Dunnigan, A.; Staley, N. A.; Smith, S. A.; Ella Pierpont, M.; Judd, D.; Benditt, D. G.; Woodrow Benson Jr, D. *Journal of the American College of Cardiology* **1987**, *10*, 608-618.

(9) Chace, D. H.; Kalas, T. A.; Naylor, E. W. *Clinical Chemistry* **2003**, *49*, 1797-1817.

(10) Chace, D. H.; DiPerna, J. C.; Mitchell, B. L.; Sgroi, B.; Hofman, L. F.; Naylor, E. W. *Clinical Chemistry* **2001**, *47*, 1166-1182.

(11) Daykin, C. A.; Foxall, P. J. D.; Connor, S. C.; Lindon, J. C.; Nicholson, J. K. *Analytical Biochemistry* **2002**, *304*, 220-230.

(12) McDade, T. W.; Williams, S.; Snodgrass, J. J. *Demography* **2007**, *44*, 899-925.

(13) Spooner, N.; Lad, R.; Barfield, M. *Analytical Chemistry* **2009**, *81*, 1557-1563.

(14) Laforêt, P.; Acquaviva-Bourdain, C.; Rigal, O.; Brivet, M.; Penisson-Besnier, I.; Chabrol, B.; Chaigne, D.; Boespflug-Tanguy, O.; Laroche, C.; Bedat-Millet, A.-L.; Behin, A.; Delevaux, I.; Lombès, A.; Andresen, B. S.; Eymard, B.; Vianey-Saban, C. *Neuromuscular Disorders* **2009**, *19*, 324-329.

(15) R.J.A, W. *Molecular Genetics and Metabolism* **2004**, *83*, 16-27.

(16) Wen, B.; Nelson, S. D. In *Mass Spectrometry in Drug Metabolism and Disposition: Basic Principles and Applications*; Lee, M. S., Zhu, M., Eds.; John Wiley & Sons, Inc.: Singapore, 2011, pp 13-41.

(17) Costa, C. G.; Struys, E. A.; Bootsma, A.; ten Brink, H. J.; Dorland, L.; Tavares de Almeida, I.; Duran, M.; Jakobs, C. *Journal of Lipid Research* **1997**, *38*, 173-182.

(18) Bieber, L. L.; Choi, Y. R. *Proceedings of the National Academy of Sciences* **1977**, *74*, 2795-2798.

(19) Libert, R.; Van Hoof, F.; Thillaye, M.; Vincent, M.-F.; Nassogne, M.-C.; de Hoffmann, E.; Schanck, A. *Clinica Chimica Acta* **2000**, *295*, 87-96.

Chapter 4

Quantitative profiling of urinary acylcarnitines in healthy individuals by ultra-high performance liquid chromatography tandem mass spectrometry*

4.1 Introduction

Current research has shown that acylcarnitines are dysregulated in various diseased states other than inborn errors of metabolism, namely diabetes mellitus type II, multiple sclerosis, sepsis, pre-eclampsia, kidney cancer and narcolepsy.[1-8] Due to the biological significance of these compounds, interest in their quantification in various biofluids has persisted. For many reasons, plasma or dried blood spots have been the biological samples of choice when analyzing acylcarnitines. First, long-chain acylcarnitines can be more easily studied; secondly, a subject's water consumption does not have an effect on quantitative analyses as in the case of urine analysis. However, in order to obtain a truly comprehensive acylcarnitine profile, more than one biofluid may need to be studied.

* A form of this chapter is in preparation for publication as: Zuniga, A. and Li, L. "Quantitative profiling of urinary acylcarnitines in healthy individuals by ultra-high performance liquid chromatography tandem mass spectrometry"

Urinary metabolite concentrations are dependent on the amount of a compound in blood, the rate at which the chemical is excreted from the blood, and the volume of fluid excreted by the kidneys. Due to these reasons, correcting for the effects of urine volume on urinary concentration is necessary.[9] Metabolite concentrations can be quoted relative to a certain amount of creatinine since it is generally accepted that there is little excretory variance of creatinine in healthy individuals. By doing so, urine has been found to be a very useful substrate for the analysis of acylcarnitines, especially in cases where ambiguous results are obtained from blood or plasma and additional diagnostic tools are needed.[10-12] The distribution pattern of these species in urine, or the excretion of particular acylcarnitines, has been found particularly useful for studying metabolic diseases.[3, 13-15]

Acylcarnitines have been commonly analyzed as butyl[16] as well as 4'-bromophenacyl esters[17, 18] in order to increase their ionization efficiency. The derivatization step increases their hydrophobicity and blocks the potential negative charge that could arise from the carboxylic acid moiety (refer to Figure 4.1). In this work, acylcarnitine ethyl esters were synthesized and served double purpose: they improved ESI response and allowed the introduction of a $^{12}C_2$ or $^{13}C_2$ label. The heavy labeled acylcarnitine ethyl esters formed were subsequently used as internal standards. This presents a great advantage in that a separate set of isotopically labeled internal standards is not required. Another advantage of analyzing acylcarnitines as their ethyl ester derivatives is that a characteristic fragment ion at *m/z* 113 can be utilized as further confirmation of the identity of detected metabolites as acylcarnitine ethyl esters. Figure 4.1 shows a schematic of the esterification reaction.

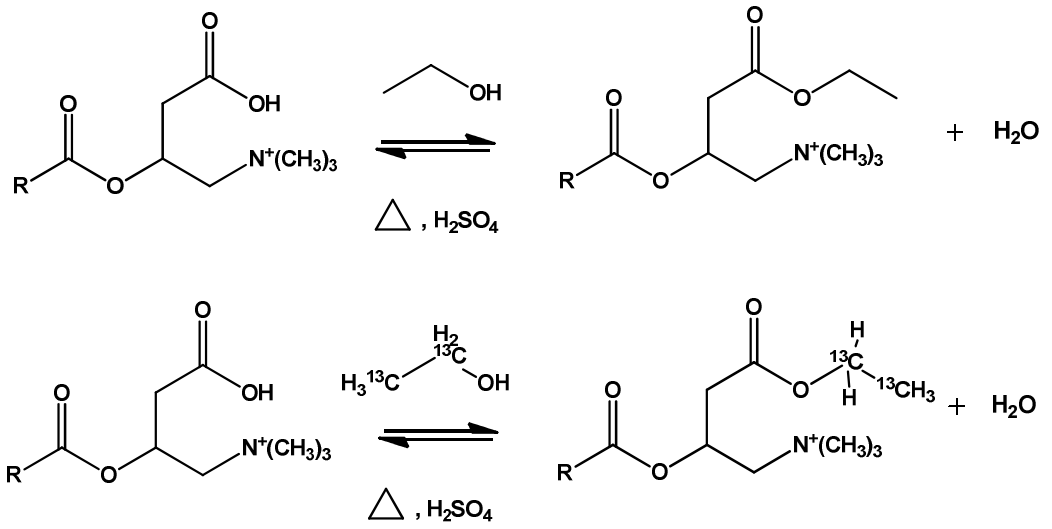

Figure 4.1 Reaction scheme. Addition of light or heavy labeled ethanol to acylcarnitines in the presence of H_2SO_4 and heat produces acylcarnitine ethyl esters and water.

Quantification of acylcarnitines has been routinely carried out by stable isotope dilution, usually using deuterated standards. A disadvantage of this approach is that a separate set of standards has to be purchased. Another major disadvantage is the isotope effect at the chromatographic level, due to the stronger binding of deuterium to carbon than hydrogen to carbon, which causes slight differences in the molecule's physico-chemical properties.[19, 20] It has been shown that the small difference in retention time between the analyte and the deuterated internal standard can cause changes in their ionization efficiencies, due to differences in matrix effects which can greatly affect quantitative studies.[21] However, this phenomenon has not been demonstrated for stable isotopes with ^{13}C instead of ^{12}C.[20, 22] In this work, internal standards were prepared from the original set of acylcarnitine standards by introducing a $^{13}C_2$ label via the addition of an ethyl group to the carboxylic acid moiety present in the carnitine backbone.

Acylcarnitines, being endogenous metabolites, present a significant challenge in terms of their quantification in comparison to metabolites from exogenous sources. Due to the lack of analyte-free matrices, calibration curves have to be built using surrogate analytes or a surrogate matrix.[23-26] In this work,

the latter approach was employed using unesterified urine as a surrogate matrix. Calibration curves in unesterified urine had slopes that were not found to be statistically different from those built using esterified urine and were therefore expected to provide accurate results. This was confirmed by analyzing quality control samples, comparing results to those from standard addition experiments and comparing results with previously published data. The absolute quantification results obtained from this study correlated well with previously published data on acylcarnitine profiling in healthy individuals.

There are many acylcarnitines for which there are no commercially available standards; relative rather than absolute quantification was performed on these compounds. Relative quantification data was collected for a total of 64 acylcarnitines. This information is important in order to obtain a more comprehensive urinary acylcarnitine profile that can be more indicative of a diseased state than only evaluating a few compounds at a time. Moreover, in many cases, data are reported as concentration ratios since the relative concentration of a particular species in comparison with another is more useful than the absolute concentration itself.[27]

In this study, a fully validated analytical method is presented for the quantification of acylcarnitines in urine. Accuracy, precision, linearity, stability, carry over, and matrix effects were investigated. Samples from 20 healthy volunteers (10 males, 10 females) collected over three consecutive days were analyzed. The results obtained were consistent with previously published values. The effect of gender and body mass index (BMI) on acylcarnitine profiles was also studied.

4.2 Experimental

4.2.1 Chemicals and reagents

Chapter 2 Section 2.2.1 includes a list of chemicals and reagents used for this work. 1, 2-$^{13}C_2$ Ethanol (99% isotopic purity) was generously donated by Cambridge Isotopes (Andover, Massachusetts). Deuterated free carnitine (C0-d_3) was purchased from C/D/N Isotopes Inc. (Pointe-Claire, Quebec). Millex-GV Filters (0.22 µm, PVDF, 33 mm) were purchased from Millipore (Billerica, MA).

4.2.2 Urine samples

Urine was collected from twenty healthy volunteers who were not on any special diet or taking any nutritional supplements. An informed consent was obtained from each volunteer and ethics approval for this work was obtained from the University of Alberta in compliance with the Arts, Science and Law Research Ethics Board policy. The volunteers were all adults, ten male and ten female, with BMI values ranging from 18.0 to 34.3 kg/m^2. All urine samples were collected as second morning void samples for three consecutive days, providing a total of 60 samples. Urine samples were centrifuged for 10 min at 14,000 *g* to remove any solids and were then filtered with Millex-GV Filters (0.22 µm, PVDF, 33 mm). All urine samples were immediately stored at -80 °C pending further sample preparation. The creatinine concentration of all urine samples was determined using a commercially available creatinine assay kit (BioAssay Systems, Hayward, California). A table including creatinine values for all samples can be found in the electronic Appendix. A volume of urine corresponding to 200 nmol of creatinine was used for all analyses without the need to perform any further sample clean-up steps such as solid-phase extraction. Samples were evaporated to dryness with a vacuum concentrator system (Thermo Fisher Scientific, Nepean, Ontario) and underwent esterification to form ethyl esters. The samples were evaporated to dryness after the reaction was completed and reconstituted in 48 µL of 0.1% formic acid (FA), 20% acetonitrile (I) in water, two microlitres of internal standard solution were subsequently added, yielding a final volume of 50 µL.

4.2.3 Ethyl ester synthesis reaction optimization

Fischer esterification reactions are known to be robust and have high yields (> 80%). Urine was utilized for all reaction optimization experiments since there are many organic acids in urine[28] which can also be esterified and can thus compete with acylcarnitines for available reagents. It was therefore necessary to be certain that all reagents used were present in excess. At the time these experiments were performed, 1,2-$^{13}C_2$ ethanol was not available and so it was not possible to use internal standards for reaction optimization. Instead, analyte peaks were normalized by dividing their areas by the total ion chromatogram (TIC) area. The precision of the experiments was not as high as when using an internal standard, however, it was found that changes in the reaction conditions did not have a dramatic effect on efficiency since esterification reactions are very robust. An equal volume of urine from all 60 samples was pooled together, 25 µL of which were used for all optimization reactions, which were in turn performed in triplicate. Reaction temperature, time and volume of ethanol were optimized and the use of an acid catalyst and a drying agent were studied. Preliminary results suggested that a two hour reaction at 60 °C was appropriate and these were used as the starting conditions for optimization experiments.

4.2.3.1 Acid catalyst

Acidic conditions were used in order to drive the reaction forward. The use of concentrated hydrochloric (HCl) and sulfuric acid (H_2SO_4) was investigated. Sulfuric acid is known to be a water scavenger[29] and its use as a catalyst provided better results than hydrochloric acid. The volume of acid used was then optimized. Two percent v/v was found to be optimal and thus this volume of sulfuric acid was used for all subsequent experiments.

4.2.3.2 Drying agent

Water is a by-product of the esterification reaction (Figure 4.1), so any water present in the sample or produced from the reaction will shift the

equilibrium of the reaction towards the reactants' side (Le Châtelier's principle), which is detrimental to efficiency of the reaction. It was speculated that introducing a drying agent to the reaction vessel might drive the reaction to the products' side, increasing the efficiency of the reaction. The use of silica gel as an extra drying agent was assessed. Reactions with and without silica gel were carried out.

4.2.3.3 Volume of ethanol

In this reaction, ethanol acts both as a solvent and as a reagent. Ethanol needs to be present in enough excess to fully label all acylcarnitines as well as to re-dissolve completely the dried urine residues. Adding it in stoichiometric excess is also advantageous since it shifts the equilibrium of the reaction to the products' side. It is challenging, however, to estimate the molar amount of acids in urine. Moreover, the cost of 1,2-$^{13}C_2$-ethanol was the limiting factor as to how much ethanol could be used for each reaction. Reactions using 15 µL, 25 µL and 50 µL of ethanol were performed. It was found that 25 µL of ethanol (4.29×10^{-4} mol) was enough to provide good labeling efficiency.

4.2.3.4 Reaction temperature

The ester linkage already present in acylcarnitines is susceptible to hydrolysis at high temperatures, so a reaction temperature that allowed high reaction efficiency while minimizing the hydrolysis of this ester linkage was necessary. The boiling point of ethanol (78 °C) also limited the high end of the range of temperatures tested. Temperatures of 40 °C, 50 °C, 60 °C and 70 °C were tested.

4.2.3.5 Reaction time

The total reaction time was also optimized. Reactions were allowed to proceed for 0.5, 1, 2 and 3 hours at 50 °C.

4.2.3.6 Esterification of urine samples

The volume of urine equivalent to 200 nmol of creatinine was evaporated to dryness using a vacuum concentrator system. The solid residue was re-dissolved in 25 µL of anhydrous ethanol and 0.5 µL of concentrated H_2SO_4 were subsequently added. The vials were capped and introduced into a water bath that had been preheated to 50 °C. The reaction was allowed to proceed for one hour. All samples were then evaporated to dryness and reconstituted in 0.1% FA, 20% I in H_2O, 2 µL of internal standard solution were subsequently added to yield a final volume of 50 µL.

4.2.4 Standard and internal standard stock solution preparation

A calibration stock solution was prepared by esterifying a previously dried 10 µM acylcarnitine standard mix (C2 concentration was 50 µM) using 340 µL of ethanol, 7 µL of H_2SO_4 and allowing the reaction to take place at 50 °C for one hour. An internal standard (IS) stock solution was also prepared by esterifying a previously dried 2.5 µM acylcarnitine standard mix (C2, C4 and C4-I concentration was 12.5 µM, C3 concentration was 6.25 µM) using 150 µL of $^{13}C_2$- ethanol and 3 µL of H_2SO_4 at 50 °C for one hour, giving rise to $^{13}C_2$-labeled acylcarnitines. These reactions were scaled up from a 1 µM mix of 15 acylcarnitines where no unesterified species were detected. Calibration solutions were prepared by spiking 10 µL of a previously prepared standard (of different concentrations) and 2 µL of IS solution to 48 µL of surrogate matrix.

4.2.5 UHPLC-MS/MS

Chromatographic separation was performed on an Agilent UHPLC 1290 Infinity system (Agilent Technologies, Mississauga, Ontario) consisting of two high-pressure binary pumps, an autosampler and a column compartment containing a 10-port valve that allowed switching between two analytical columns. The two C_{18} columns used were 2.1 × 50 mm with a particle size of 1.7 µm and a pore size of 100 Å (Phenomenex, Torrance, California). A 5 µL sample

aliquot was injected onto either column with the column temperature maintained at 25 ˚C. The flow rate used was 300 µL/min. Mobile phase A consisted of 2% I, 0.1% FA in H_2O, whereas mobile phase B contained 2% H_2O, 0.1% FA in I. The gradient used was the following: the column was equilibrated at 15% B, solvent B was increased to 22.5% in 8 min and it was further increased to 100% in 28 minutes. Solvent B was held at 100% for 5 min, and the solvent system was returned to initial conditions for an extra minute to re-fill the solvent line with 15% B. The total run time was 34 minutes. The two binary pump system allowed full re-equilibration of one column while the other performed the analytical separation, greatly reducing analysis time.

The mass spectrometer used was a 4000 QTRAP® MS/MS System (Applied Biosystems, Foster City, California) equipped with a Turbo V™ ion source. Two UHPLC-MS/MS methods were developed: one for quantification and one for qualitative confirmation of the presence of acylcarnitines in the sample. Three experimental replicates of each urine sample were prepared and analyzed once each with the quantitative method, followed by the analysis of one of the replicates using the qualitative method to obtain MS/MS information. Both methods had the same ESI source and compound-specific parameters, which can be summarized as follows: Q1 and Q3 resolution were set to unit, GS1 was set to 40 psi, GS2 was set to 35 psi, CAD gas was set to high, the curtain gas was set to 10 psi, the IS voltage was 4800 V, the source temperature was set to 400 °C, the declustering potential (DP) was set to 60 V, the entrance potential (EP) was set to 11 V and the collision cell exit potential (CXP) was set to 13 V.

The quantitative method was developed using multiple reaction monitoring (MRM). The method contained a total of 118 MRM transitions, which can be summarized as acylcarnitine ethyl ester $m/z \rightarrow 85$, each having a dwell time of 10 ms. The Q1 mass for the MRM transitions were calculated using *m/z* ratios corresponding to acylcarnitines obtained from previous studies of urine[30] and plasma and adding 28 to each *m/z* ratio (corresponding to the mass of the ethyl group). The transition corresponding to C0 was set to $m/z \rightarrow 103$ since it

provided a more intense response. Transitions associated with the $^{13}C_2$-labeled acylcarnitine ethyl esters were also included. Due to background interference, most likely due to endogenous acylcarnitines present in underivatized urine, the transitions for C2, C3 and C4 were changed to $m/z \rightarrow 113$, which was observed to have a lower background signal. The collision energy (CE) used was compound dependent and was determined in the following way: the CE necessary to fragment 90% of the precursor ion was used (data obtained using synthetic standards). That is, the CE needed to decrease the intensity of the precursor ion to 10% of its original value was used. Compounds for which standards were not available were grouped and the CE used for the standard closest in mass, but not exceeding it was used (see electronic Appendix).

In order to confirm the identity of the detected metabolites as acylcarnitines, a qualitative, information dependent acquisition (IDA) method containing two dependent MS/MS scans was developed. The MRM survey scan was the same as that of the quantitative method except the dwell time of each transition was set to 2 ms. For every data point acquired along the chromatographic peaks, the two most intense ions were selected for subsequent enhanced product ion (EPI) scans (i.e. MS/MS). The parameters used for the EPI scans were the following: the Q1 resolution was set to unit, the Q3 entry barrier was set to 6 V, the scan rate was 4000 amu/s for a scan range of m/z 50 to 600. The collision energy (CE) was set to 30 V with a spread (CES) of 5 V. Dynamic fill time was selected. More detailed information is included in the electronic Appendix.

4.3 Method validation

4.3.1 Hydrolysis/Quantification of free carnitine (C0)

The conditions of the esterification reaction employed were found to be harsh enough to cause the ester linkage already present in acylcarnitines to

hydrolyze. The free carnitine formed is also esterified during the reaction giving rise to a peak at *m/z* 190 (see Figure 4.2). The formation of free carnitine during the esterification reaction complicates the quantification of endogenous free carnitine in urine by causing an overestimation of this compound. The extent of hydrolysis per acylcarnitine species resulting from the esterification reaction was assessed by quantifying the amount of free carnitine formed using neat standards. It was found that acylcarnitines of different chain lengths hydrolyze to different extents. For this reason, as well as the large number of acylcarnitine species found in urine, it was not possible to accurately quantify the amount of endogenous free carnitine in these samples. Consequently, quantification of free carnitine was not performed in this work.

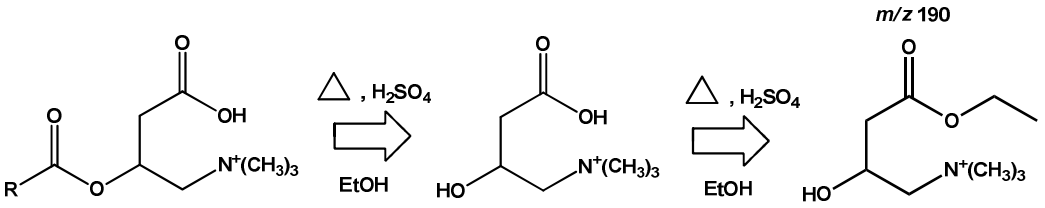

Figure 4.2 Formation of free carnitine ethyl ester upon derivatization gives rise to a peak at *m/z* 190.

4.3.2 Selection of a surrogate matrix

Quantification of endogenous metabolites is challenging due to the unavailability of analyte-free matrices. Researchers have in these cases used surrogate matrices such as phosphate-buffered bovine serum albumin solution[31] or synthetic urine.[32] In this work, underivatized urine that was pooled from all 60 samples was utilized as a surrogate matrix. The slopes of calibration curves prepared in derivatized pooled urine were compared to those in underivatized pooled urine using a specialized Student's t-test.[33] The equations are described below (Equations 4.1 to 4.3). If the calculated value of *t* is higher than the tabulated value for a particular confidence interval and a determined number of degrees of freedom, the two slopes are said to be statistically different. The results showed that there was no statistically significant difference between the two

slopes for any of the analytes studied and thus calibration curves constructed in a surrogate matrix were found to be suitable for all further studies.

$$t = \frac{\mathbf{b1} - \mathbf{b2}}{S_{b1-b2}} \tag{4.1}$$

Where

$$S_{b1-b2} = \sqrt{\frac{(S^2_{y\cdot x})\ p}{(\Sigma x^2)_1}} + \sqrt{\frac{(S^2_{y\cdot x})\ p}{(\Sigma x^2)_2}} \tag{4.2}$$

And

$$(S^2_{y\cdot x})\ p = \frac{(residual\ SS)_1 + (residual\ SS)_2}{(residual\ DF)_1 + (residual\ DF)_2} \tag{4.3}$$

Subscripts 1 and 2 refer to calibration curves 1 and 2, respectively and *b* is the slope of the calibration curve. In Equation 4.2, *x* is the difference between the mean of the concentrations of the standards used and each of the individual concentrations. In Equation 4.3, *residual SS* is the residual sum of squares and *residual DF* is the degrees of freedom.

4.3.3 $^{12}C_2$ vs. $^{13}C_2$ response

Before utilizing an internal standard it is necessary to determine whether all analytes behave in the same way as their corresponding internal standards when spiked into the matrix of choice. It is widely accepted that different MRM transitions may have more interference than others, especially when dealing with complex matrices. In order to verify the utility of $^{13}C_2$-labeled acylcarnitines as internal standards, the response (in terms of absolute peak area counts) of these species was compared to that of $^{12}C_2$-labeled species when spiked at increasing concentrations into the surrogate matrix. The surrogate matrix does not contain either type of species, so as long as there are no matrix effects that may cause a

difference in response of one type of species relative to the other, their response curves should be the same. The slopes of the response curves were compared using the Student's t-test described above. The results of these comparisons can be found in the electronic Appendix.

4.3.4 Calibration curves and matrix effects

Multiple-point calibration curves were prepared both in neat solvents and in underivatized urine. Least-squares regression was performed using R software. It was noted that the data obtained was heteroscedastic and therefore weighted linear regression had to be performed. Various weighting factors were evaluated and weighting of 1/y was found to provide the lowest value for the sum of residuals squared and was therefore used to create calibration curves for all analytes. Matrix effects were assessed by comparing the slope of the calibration curve of each analyte in neat solvents to the slope of the curve in an underivatized pooled urine sample using Equation (4.4) with the result expressed as a percentage.

$$\frac{\boldsymbol{Slope\ in\ urine}}{\boldsymbol{Slope\ in\ neat\ solvent}} \times \mathbf{100\%} - \mathbf{100\%} \qquad (4.4)$$

4.3.5 Reproducibility of the analytical platform

In order to assess repeatability of the entire experimental protocol, five 25 µL aliquots of a previously pooled and dried urine sample were esterified in parallel using the reaction described above and analyzed once each.

4.3.6 Reproducibility (intra-day and inter-day)

Intra-day reproducibility was assessed by analyzing the same esterified urine sample ten times during the course of one day (n =10). The inter-day precision was calculated by analyzing that same sample 10 times/day over a three day period (n =30).

4.3.7 Linear dynamic range

The linear dynamic range of these compounds was assessed in underivatized urine. The linear range of a calibration curve was found by inspecting the residuals within the range of concentrations used in the calibration curves.

4.3.8 Limit of detection and lower limit of quantification

The limit of detection (LOD) was calculated by using the following equation: LOD= 3.3σ/S. The lower limit of quantification or LLOQ was set equal to 10 σ/S, where σ is the standard error of the y-intercept and S is the slope of the calibration curve, both being obtained by linear regression analysis. This definition of LLOQ was chosen since it takes into consideration the background signal per compound in the sample of interest that is reflected in the error of the y-intercept of the calibration curves.[34]

4.3.9 Accuracy

Accuracy was assessed by analyzing quality control (QC) samples prepared at three different concentrations in derivatized urine and calculating the relative error. Another strategy to assess the accuracy of this method was to compare the results obtained to those from a standard addition experiment. In this case the concentration of acylcarnitines in a derivatized pooled urine sample was calculated using the calibration curves obtained in underivatized urine and compared to results from a standard addition experiment performed on an aliquot of the same urine sample.

4.3.10 Stability

The stability of post-preparatory samples was evaluated at three different temperature conditions: at room temperature, at 4 °C and -20 °C, as well as after each of three freeze-thaw cycles. Three QC-low sample aliquots were analyzed immediately after sample preparation and were used as controls. Three sample aliquots were left at room temperature for four hours, which is the maximum time

needed to prepare samples (including solvent evaporation in a liquid concentrator). Another set of replicates were stored at 4°C for 18 hours, which is the longest time a particular sample would remain in the autosampler of the LC system pending analysis. A last set of aliquots was analyzed after each of three freeze-thaw cycles that were performed at 18-hour intervals. Medium- and long-term storage were assessed by analyzing a sample after storage at -20 °C for two and eight weeks, respectively.

4.3.11 Absolute quantification

A total of 12 internal standards were prepared by esterifying an acylcarnitine standard stock solution with heavy-labeled ethanol. The final concentration of IS used for each compound varied and was determined by the endogenous amount of the compound present in the urine sample (in order to avoid signal suppression of the internal standard by the analyte itself). The final concentration of internal standards in the samples was 0.1 μM for all acylcarnitines except C2, C3 and C4s, which were at 0.5, 0.25 and 0.5μM, respectively. Absolute quantification was performed using calibration curves prepared in a surrogate matrix.

4.3.12 Relative quantification

There were many acylcarnitines detected in urine for which standards are not commercially available. In order to perform relative quantification of these compounds, a specific internal standard was assigned to each compound according to its retention time. These compounds were quantified using the calibration curve corresponding to the internal standard chosen. Using this method, 64 acylcarnitine species were relatively quantified. It is worth noting that although many acylcarnitines were detected, only compounds that were consistently found in most urine samples and for which good quality MS/MS spectra were obtained were quantified.

4.4 Results and discussion

4.4.1 Esterification reaction optimization

4.4.1.1 Catalyst and drying agent

The use of HCl and H_2SO_4 as catalysts was evaluated. It was found that the precision of the results when using H_2SO_4 was higher than when HCl was utilized. Moreover, sulfuric acid is known to be a water scavenger. For those reasons sulfuric acid was utilized as a catalyst for all subsequent reactions. The use of silica gel as an extra drying agent was also assessed. However, there was no significant improvement found. Silica gel was therefore not used for subsequent experiments. Figure 4.3 shows a comparison of HCl and H_2SO_4 as catalysts for the esterification of four representative acylcarnitines.

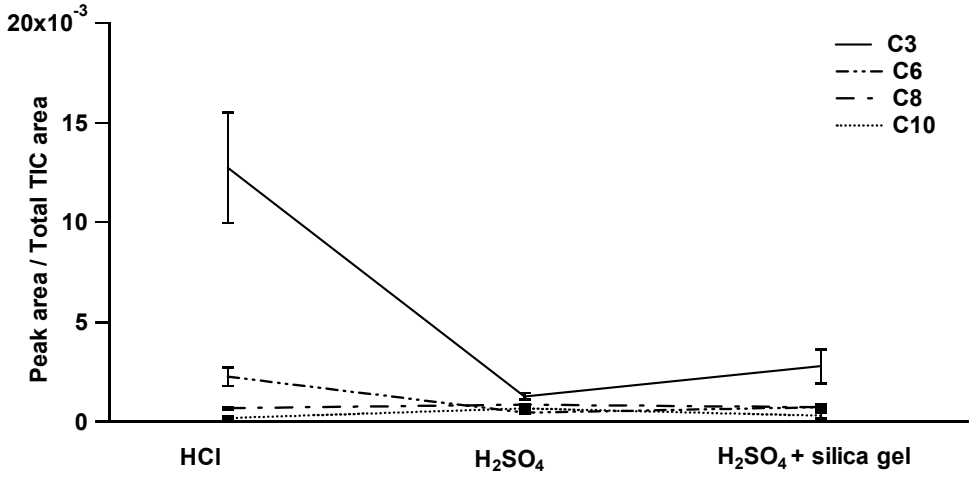

Figure 4.3 Use of a catalyst and drying agent. More reproducible results were obtained when using H_2SO_4. The use of silica gel did not significantly improve the reaction efficiency. The reactions were carried out at 60 °C for 2 hours.

4.4.1.2 Volume of ethanol

The volume of ethanol used was optimized taking a number of factors into consideration; ethanol needed to be present in excess so that it did not

become the limiting reagent, the volume also needed to be enough for re-dissolving the dried urine samples. On the other hand, the cost of $^{13}C_2$- ethanol also needed to be considered, since reactions with $^{13}C_2$-ethanol to create internal standards needed to be performed in the same way as those with $^{12}C_2$-ethanol. There was no significant improvement found when using 50 µL, so 25 µL of ethanol were used for all subsequent experiments. Figure 4.4 shows a comparison of reaction efficiency relative to volume of ethanol used.

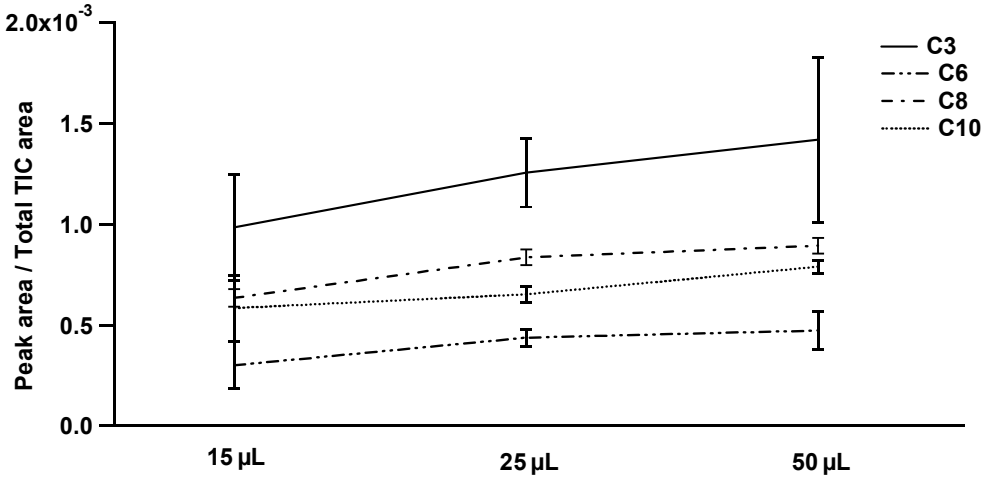

Figure 4.4 Volume of ethanol used. Ethanol is used both as a solvent and as a reagent so its volume used needs to be carefully controlled.

4.4.1.3 Reaction temperature

The reaction temperature was optimized to maximize its yield as well as to minimize hydrolysis of the ester linkage found in acylcarnitines. It was found that a temperatures between 40 °C and 60 °C provided similar results. The efficiency of the reaction at 70 °C decreased notably, likely due to hydrolysis. A temperature of 50 °C was chosen for all further experiments. Figure 4.5 summarized the results.

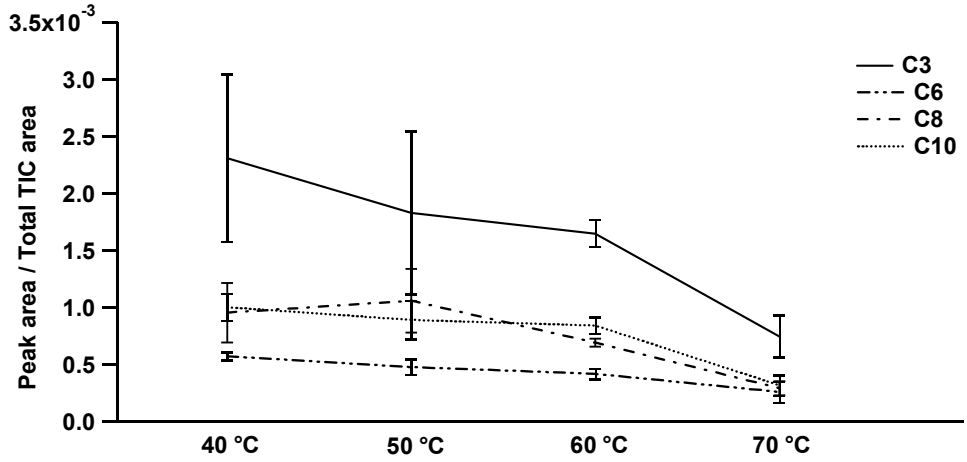

Figure 4.5 Reaction temperature optimization. Reactions were allowed to proceed for 2 hours.

4.4.1.4 Reaction time

The length of time the reaction was allowed to proceed for was also optimized. A one-hour reaction at 50 °C was found to provide better results than any of the other reaction times tested. However, the differences were marginal; in many cases they were within a standard deviation, providing further evidence of the robustness of this reaction. The results are shown in Figure 4.6.

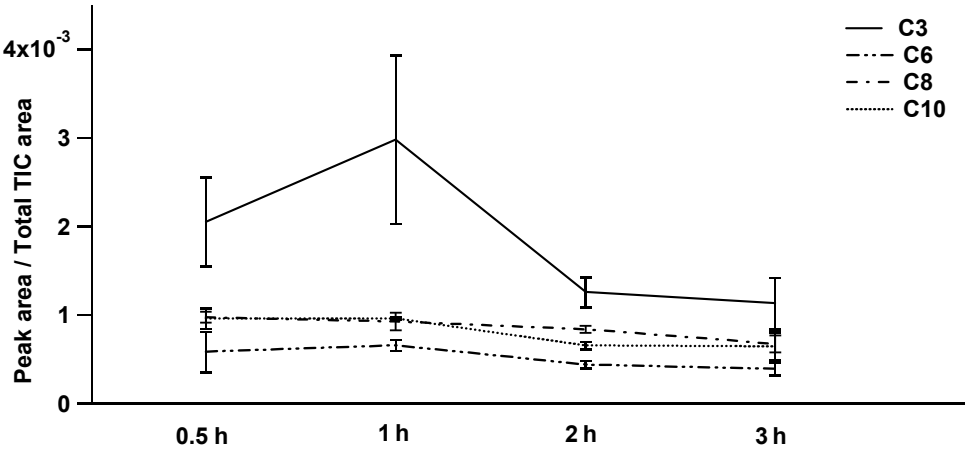

Figure 4.6 Optimization of reaction time. One hour was found to be the optimal reaction time and so it was used for all subsequent experiments. The reactions were carried out at 50 °C.

4.4.1.5 Comparison of optimized results

The optimized conditions (50 °C for one hour) were compared to a two-hour reaction at 50 and 60 °C to be certain that these conditions in fact were better than the preliminary conditions used. This was found to be the case, so all subsequent esterification reactions were performed at 50 °C for one hour. Figure 4.7 summarizes the results.

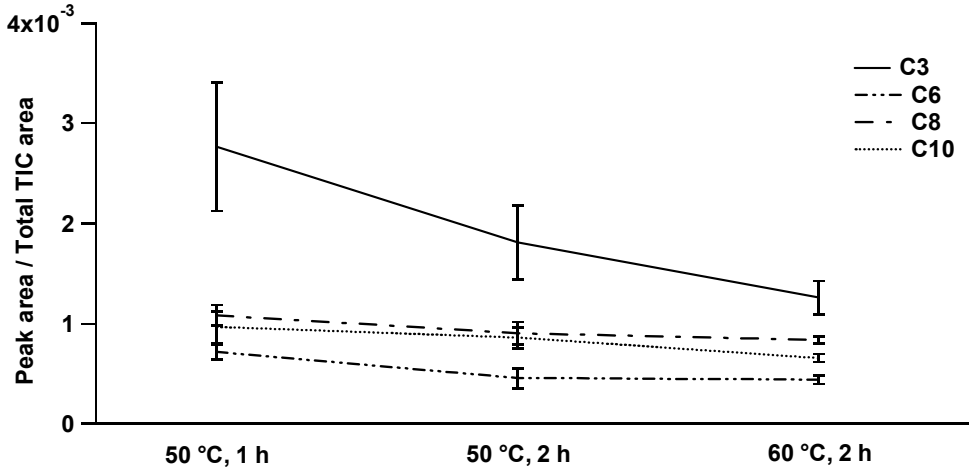

Figure 4.7 To make certain that the conditions selected were optimal, the reaction was carried out again and compared to a two-hour reaction at 50 and 60 °C.

4.4.2 Quantitative and qualitative UHPLC-MS/MS methods

Monitoring over 100 MRM transitions requires the use of short dwell times. However, as dwell times fall below 10 ms, precision as well as sensitivity of the instrument starts to suffer. Moreover, it was found that when transitions were set to monitor the same fragment ion in the third quadrupole, with a dwell time of less than 10 ms, cross-talk in the collision cell made it impossible to perform accurate quantification. For these reasons, in this work, two separate MS methods had to be developed: one for quantification and one to obtain qualitative data for structure elucidation. With a dwell time of 10 ms per transition and including two dependent EPI scans, the total scan time would be too high to adequately define UHPLC peaks with a width of 10 to 15 s at the base. For

quantification, at least 10 points per peak are preferred, which would correspond to a total scan time of 1 s. This is not feasible if two dependent MS/MS scans need to be included (≈0.5 s each using a scan rate of 4000 amu/s).

As a result, a quantitative method was developed in an attempt to find a compromise between sensitivity and obtaining well-defined chromatographic peaks. A dwell time of 10 ms was used for all MRM transitions and no dependent MS/MS scans were included. The qualitative method that was subsequently developed in order to obtain fragmentation information for the compounds of interest consisted of dwell times of 2 ms per MRM transition and 2 dependent MS/MS scans. In this case, less than 10 points per peak were found to be acceptable since only qualitative information was obtained from this method. The details of both methods are included in the electronic Appendix.

4.4.3 Acylcarnitine ethyl ester fragmentation and structure elucidation

The masses of acylcarnitine ethyl esters may overlap with those of underivatized acylcarnitines. However, it is straight-forward to distinguish between them due to the presence of a prominent fragment ion at *m/z* 113 present only in the MS/MS spectra of the esterified form of these compounds (Figure 4.8). This fragment ion, analogous to the fragment ion at *m/z* 85 present in underivatized acylcarnitines, corresponds to a McLafferty rearrangement followed by the loss of the trimethylamine group. It is also worth noting that the fragment ion at *m/z* 113 upon further fragmentation can also give rise to the peak at *m/z* 85 and, in most cases, both are present in the MS/MS spectra of derivatized acylcarnitines. This characteristic fragment from the esterified form can also be used as further confirmation of the identity of these compounds as acylcarnitines. In the case of heavy labeled acylcarnitine ethyl esters, the fragment ion at *m/z* 113 becomes *m/z* 115.

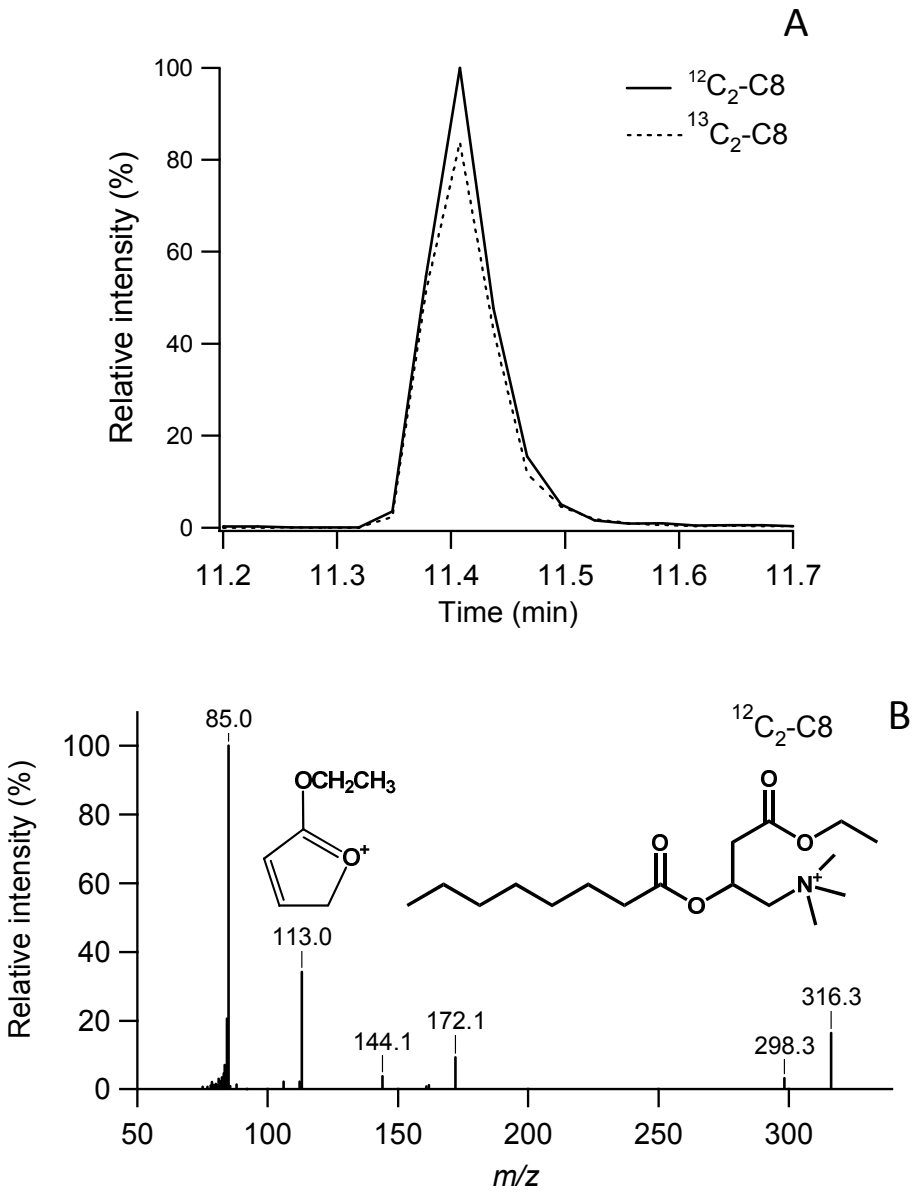

Figure 4.8 (A) Overlay of extracted ion chromatograms (XICs) of MRM transitions corresponding to light and heavy labeled C8 ethyl ester showing the co-elution of both species. (B) MS/MS spectrum of light-labeled octanoylcarnitine (C8) ethyl ester, displaying fragment ion at *m/z* 113 used as further evidence for identification of compounds as acylcarnitines.

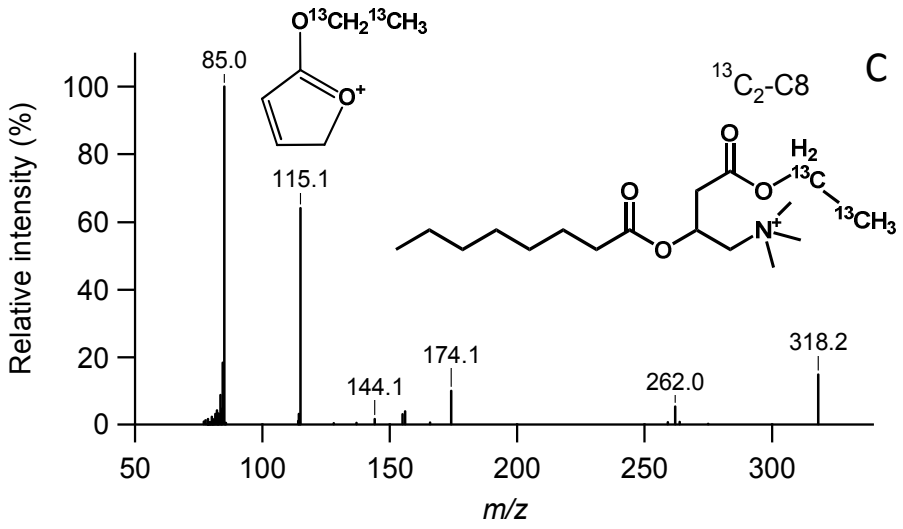

Figure 4.9 MS/MS of heavy-labeled C8 ethyl ester, with fragment ion at *m/z* 115.

Putative identification of these compounds was achieved by manual analysis of their MS/MS spectra by following the fragmentation trends found in a previously reported study.[30] Representative MS/MS spectra are included in Section 4.8 of the Appendix. A complete MS/MS library of all quantified compounds can be found in the electronic Appendix. It was observed that acylcarnitine ethyl esters typically displayed a few less fragments than underivatized acylcarnitines. It is also noteworthy that although it was simple to identify compounds as acylcarnitines, in many cases further structure elucidation was difficult, since during low-energy collision-induced dissociation, the organic acid chain conjugated to carnitine could not be fragmented further and, thus, it was not possible to pinpoint the location of a double bond or a hydroxyl group. Similarly, structural isomers could not be distinguished.

4.4.4 Chromatographic separation of C4 and C5 isomers

Separation of two C4 and five C5 isomers was achieved in standards and in most urine samples. Figure 4.9 (A) shows the separation of iso- and butyrylcarnitine. It can be observed that when the two are equimolar (as in the case of the internal standards) these are almost base-line resolved. However, since isobutyrylcarnitine was 10-20 times higher in concentration than butyrylcarnitine in the urine samples studied, the C4 signal was in some cases overwhelmed by that of C4-I. Peak integration had to be carefully performed in order not to include the signal from C4-I. In the case of the C5 isomers, pivaloylcarnitine, 2MBC, C5-I and C5 were all almost base-line resolved. In most urine samples, the *I* and *(S)* diastereomers (carnitine contains a chiral center of its own) of 2-methylbutyrylcarnitine (2MBC) were also resolved. The *I* isomer eluted after pivaloylcarnitine and before the *(S)* isomer of 2MBC. The 2MBC standard obtained from VU Medical Centre was optically pure (*(S)* form only), which simplified the assignment of these optical isomers. The two diastereomers were integrated together for quantification purposes since researchers have found that the sum of the two is more diagnostically significant.[35] Figure 4.9 (B) shows an example of a urine sample where all five C5 isomers were separated.

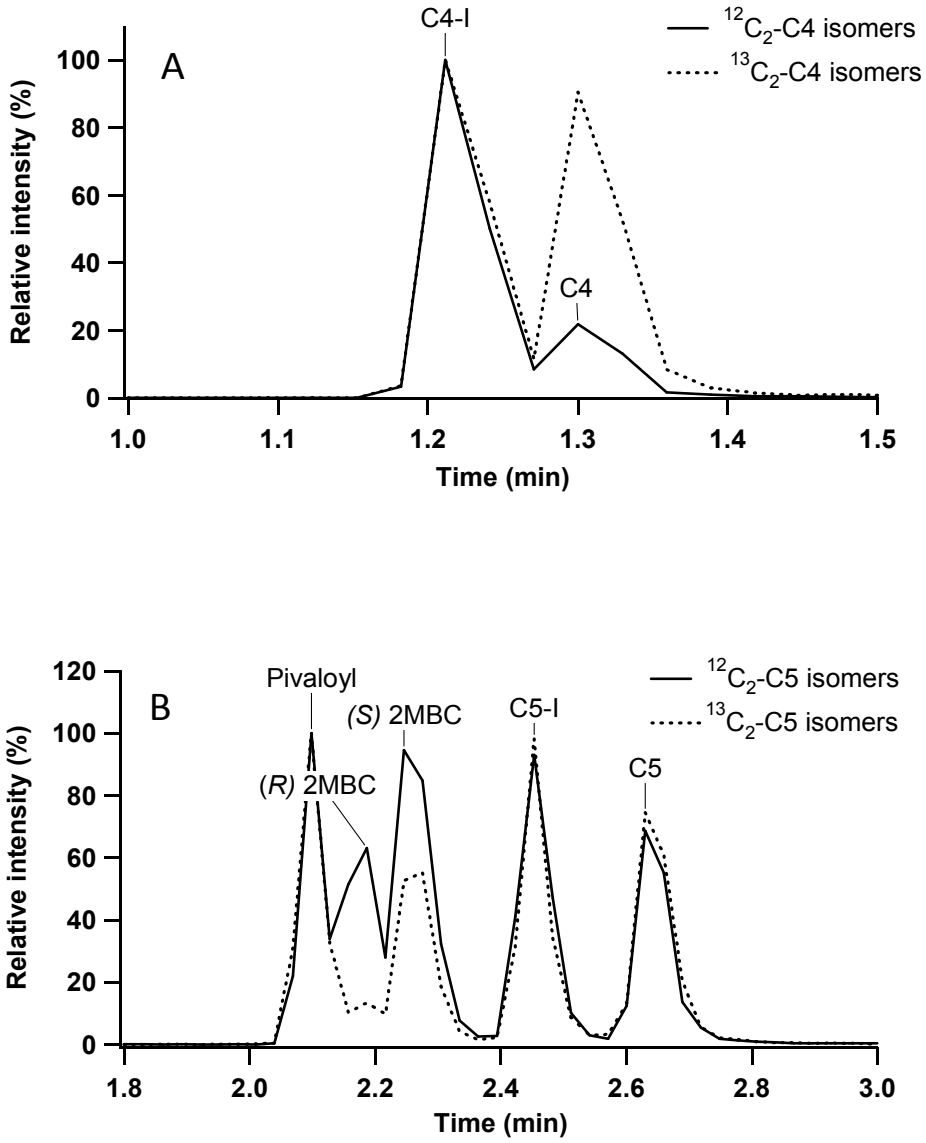

Figure 4.10 Chromatographic separation of C4 and C5 isomers in a derivatized urine sample. (A) Overlay of extracted ion chromatograms (XICs) for MRM transitions corresponding to C4 isomers and their corresponding internal standards. (B) Overlay of XICs for MRM transitions corresponding to C5 isomers and their corresponding internal standards. Separation of 2MBC *I* and *(S)* diastereomers was achieved in most urine samples; however these species were integrated together for quantification purposes.

4.4.5 Hydrolysis/free carnitine quantification

The extent of hydrolysis was assessed by quantifying the amount of free carnitine formed upon esterification of each individual acylcarnitine standard at two concentrations, 0.04 μM (QC-low) and 0.4 μM (QC-high). Deuterated C0 was utilized as an internal standard in order to avoid using a $^{13}C_2$-labeled C0 ethyl ester which would have to undergo a second esterification reaction and is much more costly. By using a deuterated species as an internal standard, both C0 species can be esterified simultaneously. An internal standard solution was prepared to spike into the calibration standards by esterifying a 5 μM deuterated C0 solution with regular ethanol using the protocol described in Section 4.2.4. Calibration standard solutions were prepared in 20% I, 0.1% FA in H_2O and were spiked with deuterated esterified C0 internal standard. A calibration curve was obtained and used to quantify the amount of C0 present after the esterification of each of the acylcarnitine standards.

It was found that short-chain as well as longer-chain species (>C5) hydrolyzed more than medium chains at both concentrations. It was also noted that the final concentration of esterified C0 was, in some cases, higher than the concentration of standard used; see 0.04 μM C10 standard in figure 4.10. This is very possibly due to C0 already present in the pre-esterified standards. The method utilized to synthesize the acylcarnitine standards themselves involves acylation of free carnitine, a reaction with 88-97% yield[36], so it is possible that there is residual C0 present in the standards. To investigate this further, all pre-esterified standards at both concentrations were analyzed for free carnitine. No detectable signals were present corresponding to free carnitine; however, the ionization efficiency of unesterified free carnitine is quite low due to its high hydrophilicity, which may be the reason why it was not detected. Due to the large number of acylcarnitines found in urine and their varying extents of hydrolysis (dependent on acyl chain length), C0 was not quantified using this approach.

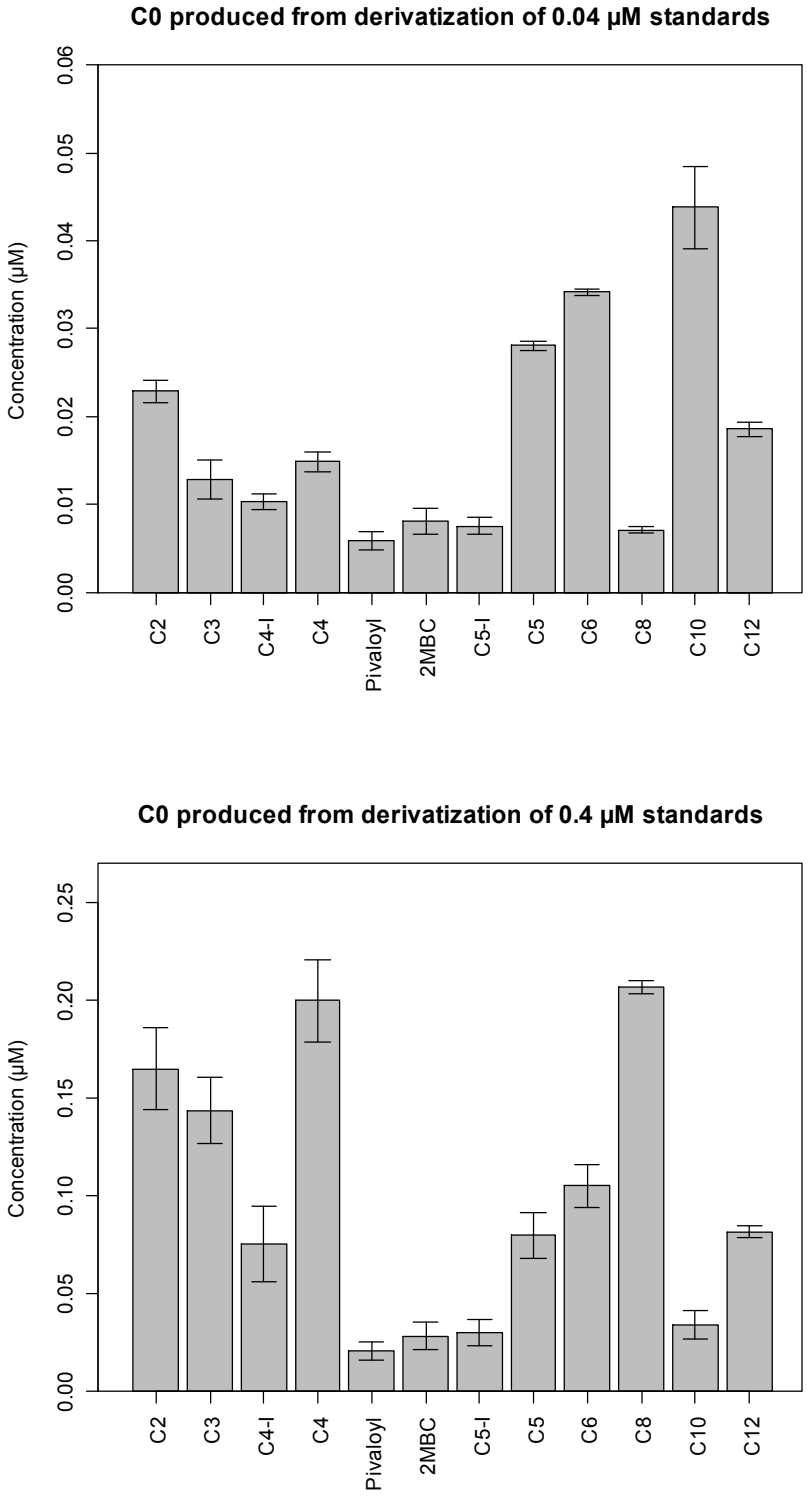

Figure 4.11. Formation of free carnitine (C0) ethyl ester upon derivatization of neat standards giving rise to a peak at *m/z* 190. C0 formed from derivatization of 0.04 µM standards (A) and from 0.4 µM standards (B).

4.4.6 Calibration curves and matrix effects

In order to assess matrix effects, calibration curves were prepared in neat solvents as well as in underivatized urine. The slopes of the calibration curves obtained were compared. Tables 4.1 and 4.2 summarize the details of the calibration curves prepared in neat solvents and underivatized urine, respectively. Representative calibration curves prepared in neat solvents and in unesterified urine can be found in Appendix Sections 4.1 and 4.3, respectively. Linear regression information for these calibration curves can be found in Appendix Sections 4.2 and 4.4. The signal-to-noise ratios for all solutions at the LLOQ were found to be higher or equal to 20. Table 4.3 summarizes the matrix effects study. Signal enhancement was observed in most cases except for C3 and C4. The results of the specialized Student's t-test used to compare the slopes in surrogate (unesterified) and authentic (esterified) matrix used to assess the suitability of the surrogate matrix approach are presented in Table 4.4. It can be observed that all calculated t values are well below tabulated t values at a 95% confidence limit, which demonstrates that underivatized urine is suitable as a surrogate matrix.

4.4.7 Precision

4.4.7.1 Method precision

The overall method precision was evaluated by analyzing five experimental replicates (five esterified urine samples prepared in parallel). It was found to range from 5.7 to 15.0%. The results are summarized in Table 4.5.

Table 4.1. Linear regression data for 12 standards dissolved in 0.1% FA, 20% I in H_2O. Average precision corresponds to the average % CV for the entire calibration range.

AC	Calibration equation	Linear range (µM)	Linearity (R^2)	Average precision (CV %)	LOD (µM)	LLOQ (µM)
C2	y= 1.59x + 0.04	0.025 – 1.25	0.987	15.7	0.04	0.12
C3	y= 7.1x + 0.05	0.005 – 0.5	0.987	16.1	0.01	0.03
C4-I	y= 1.74x + 0.010	0.005 – 1	0.991	15.9	0.011	0.034
C4	y= 1.85x + 0.004	0.005 – 2	0.998	15.5	0.006	0.018
Pivaloyl	y= 9.0x – 0.001	0.005 – 0.5	0.999	12.9	0.002	0.007
2MBC	y= 7.6x + 0.026	0.005 – 0.5	0.991	14.6	0.008	0.024
C5-I	y= 8.3x + 0.01	0.005 – 0.5	0.997	12.2	0.004	0.01
C5	y= 9.4 + 0.001	0.005 – 0.5	0.997	12.6	0.004	0.013
C6	y= 7.6x + 0.01	0.005 – 0.5	0.987	14.7	0.01	0.03
C8	y= 9.5x + 0.004	0.005 – 0.5	0.994	10.8	0.006	0.018
C10	y= 7.5x + 0.08	0.005 – 1	0.996	15.5	0.009	0.03
C12	y= 6.7x + 0.01	0.005 – 1	0.995	12.5	0.008	0.03

Table 4.2 Linear regression data for 12 standards spiked into surrogate matrix. Calibration curves for C2 and C4-I were performed in underivatized urine, diluted 1:5 (v/v).

AC	Calibration equation	Linear range (µM)	Linearity (R^2)	Average precision (CV %)	LOD (µM)	LLOQ (µM)	LLOQ (µmol/g creatinine)
C2	y= 1.86x + 0.015	0.025 – 1.25	0.998	9.0	0.015	0.045	0.098
C3	y= 3.8x + 0.005	0.005 – 0.5	0.997	7.7	0.005	0.014	0.030
C4-I	y= 1.84x + 0.004	0.005 – 1	0.999	17.1	0.003	0.009	0.021
C4	y= 1.70x + 0.004	0.005 – 2	0.995	8.5	0.010	0.030	0.066
Pivaloyl	y= 9.2x + 0.03	0.005 – 0.5	0.983	12.5	0.01	0.03	0.07
2MBC	y= 9.7x + 0.09	0.005 – 0.5	0.985	17.5	0.01	0.04	0.08
C5-I	y= 10.5x + 0.02	0.005 – 0.5	0.998	9.5	0.004	0.011	0.025
C5	y= 10.0x + 0.08	0.005 – 0.5	0.986	13.4	0.01	0.03	0.08
C6	y= 9.4x+ 0.008	0.005 – 0.5	0.996	16.0	0.005	0.015	0.032
C8	y= 9.7x + 0.10	0.005 – 0.5	0.996	6.6	0.01	0.03	0.07
C10	y= 8.9x – 0.02	0.005 – 1	0.998	10.5	0.004	0.01	0.03
C12	y= 9.0x – 0.06	0.005 – 1	0.981	8.1	0.01	0.03	0.07

Table 4.3 Comparison of slopes of calibration curves in solvent and urine.

AC	Sensitivity (μM^{-1}) in 20%ACN	Sensitivity (μM^{-1}) in urine	Suppression (-) or enhancement (+) (%)
C2	1.59	1.86	+ 16.8
C3	7.1	3.8	- 47.1
C4-I	1.74	1.84	+ 5.6
C4	1.85	1.70	- 8.3
Pivaloyl	9.0	9.2	+ 2.2
2MBC	7.6	9.7	+ 28.9
C5-I	8.3	10.5	+ 27.8
C5	9.4	10.0	+ 5.7
C6	7.6	9.4	+ 22.2
C8	9.5	9.7	+ 2.3
C10	7.5	8.9	+ 18.6
C12	6.7	9.0	+ 35.7

Table 4.4 Comparison of slopes of calibration curves in authentic and surrogate matrix.

AC	Slope in authentic matrix	Slope in surrogate matrix	Degrees of freedom	Calculated t value	Tabulated t value (95% C.I)
C2	1.82	1.86	7	0.459	2.365
C3	3.5	3.8	10	1.902	2.228
C4-I	1.84	1.84	11	0.183	2.201
C4	1.70	1.70	12	0.027	2.179
Pivaloyl	9.5	9.2	10	0.836	2.228
2MBC	9.8	9.7	10	0.119	2.228
C5-I	10.4	10.5	10	1.214	2.228
C5	9.5	10.0	10	1.535	2.228
C6	9.2	9.4	10	0.645	2.228
C8	9.5	9.7	10	0.849	2.228
C10	8.9	8.9	12	0.293	2.179
C12	9.5	9.0	12	1.468	2.179

Table 4.5 CVs (%) based on five experimental replicates.

AC	CV (%) in urine
Acetylcarnitine (C2)	10.1
Propionylcarnitine (C3)	8.9
Isobutyrylcarnitine (C4-I)	13.4
Butyrylcarnitine (C4)	7.4
Pivaloylcarnitine	11.7
2-Methylbutyrylcarnitine (2MBC)	14.9
Isovalerylcarnitine (C5-I)	15.0
Valerylcarnitine (C5)	11.7
Hexanoylcarnitine (C6)	8.3
Octanoylcarnitine (C8)	5.7
Decanoylcarnitine (C10)	10.3
Dodecanoylcarnitine (C12)	13.5

4.4.7.2 Intra-day and inter-day reproducibility

Intra-day reproducibility was assessed by analyzing the same derivatized urine sample ten times in the course of one day. The coefficients of variation (CVs) were found to range from 5.3 to 11%. Inter-day precision was assessed by analyzing the same urine sample ten times per day over the course of three consecutive days. The CVs ranged from 6.2 to 12.7%, based on a total of 30 replicate analyses. The CVs per compound are summarized in Table 4.6.

Table 4.6 CVs (%) upon analysis of the same pooled urine sample 10 times per day over a three day period.

AC	Intra-day precision CV (%) *n=10*	Inter-day precision CV (%) *n=30*
C2	6.0	7.5
C3	8.1	8.1
C4-I	6.2	9.8
C4	7.7	12.7
Pivaloyl	8.8	9.8
2MBC	5.9	8.1
C5-I	7.6	8.4
C5	11.0	12.0
C6	5.4	9.3
C8	5.7	6.2
C10	8.8	9.1
C12	5.3	7.1

4.4.8 Accuracy

4.4.8.1 Comparison to standard addition

Accuracy of the experimental approach was assessed by calculating the concentration of acylcarnitine ethyl esters in an esterified pooled urine sample both by standard addition and by using the calibration equations constructed in underivatized urine. The relative error was calculated by subtracting the concentration obtained by standard addition from that obtained by using the calibration equation, dividing by the latter and multiplying by 100%. The absolute value for the relative error was less than 15% in all cases. The results are summarized in Table 4.7 and in Figure 4.11.

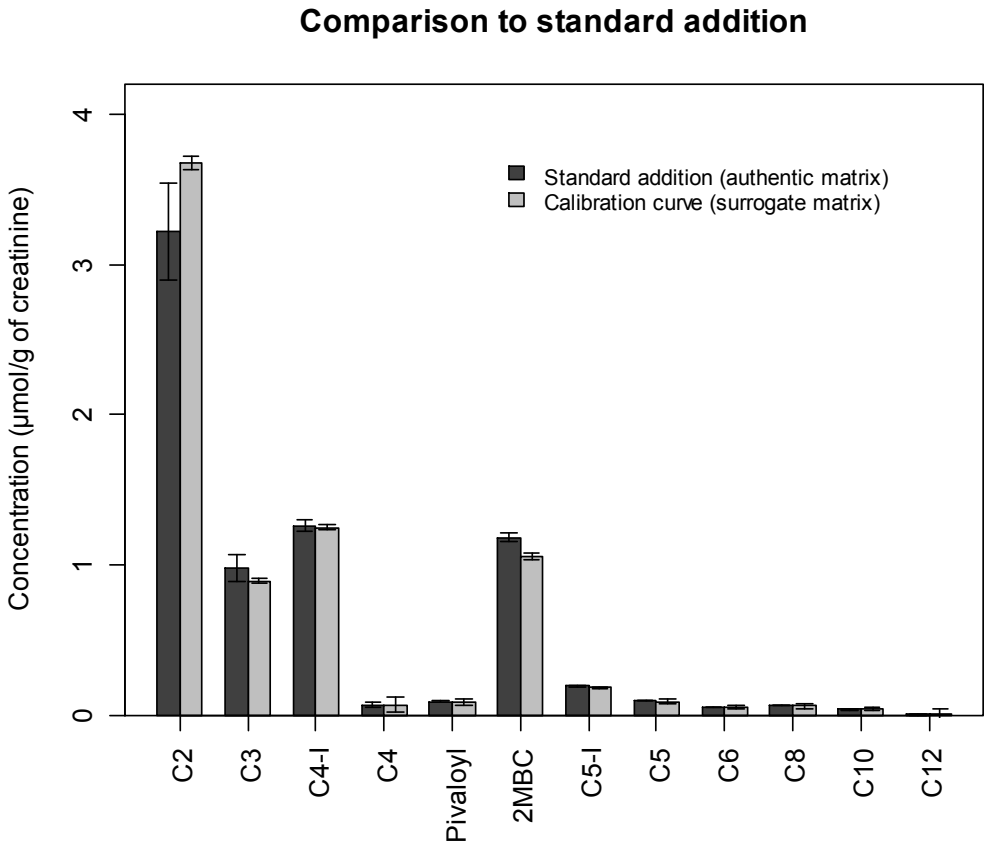

Figure 4.12 Comparison to standard addition. Acylcarnitines in a pooled urine sample were quantified using a standard addition approach and by using the calibration curves constructed in surrogate matrix. The results from both approaches were within 15% in all cases.

Table 4.7 Comparison of concentration determined by calibration equations in surrogate matrix and by standard addition experiments in authentic matrix.

AC	Concentration (µmol/g of creatinine) (By standard addition in authentic matrix)	Concentration (µmol/g of creatinine) (Calibration curve in surrogate matrix)	% RE
C2	3.2 ± 0.3	3.68 ± 0.04	15.0
C3	0.98 ± 0.09	0.89 ± 0.02	-9.2
C4-I	1.26 ± 0.04	1.25 ± 0.01	-0.8
C4	0.07 ± 0.02	0.07 ± 0.05	-1.8
Pivaloyl	0.088 ± 0.006	0.08 ± 0.02	-9.1
2MBC	1.18 ± 0.03	1.06 ± 0.02	-10.2
C5-I	0.193 ± 0.004	0.181 ± 0.008	-6.2
C5	0.097 ± 0.003	0.09 ± 0.02	-7.2
C6	0.053 ± 0.002	0.05 ± 0.01	-5.7
C8	0.065 ± 0.003	0.06 ± 0.02	-7.7
C10	0.040 ± 0.005	0.04 ± 0.01	9.3
C12	0.002 ± 0.005	0.003 ± 0.03	7.0

4.4.8.2 QC sample accuracy

Three quality control (QC) samples were prepared in esterified urine, diluted 1:5 (v/v) and spiked at different concentrations: a QC-low solution was prepared by spiking a standard corresponding to an added concentration of 0.04 µM (except for C2, which was spiked at 0.2 µM); QC-medium solution was prepared by adding 0.2 µM (except C2, which was spiked at 1 µM); and QC-high, which was spiked at 0.4 µM (except C2, which was spiked at 2 µM). All results were based on 5 consecutive analyses of the same QC sample. Relative error (RE) was calculated by subtracting the endogenous concentration from the calculated one, dividing by the theoretical (added concentration) and multiplying by 100%. Accuracy and precision results are summarized in Table 4.8.

Table 4.8 QC values in authentic matrix, diluted 1:5 (v/v).

AC	QC Low (C2: 0.2µM, others: 0.04µM)		QC Medium (C2: 1µM, others: 0.2µM)		QC High (C2: 2µM, others: 0.4µM)	
	CV (%)	% RE	CV (%)	% RE	CV (%)	% RE
C2	11.8	7.8	5.9	-12.3	5.4	-18.9
C3	8.2	-7.2	18.9	-11.7	6.3	-13.0
C4-I	11.6	-0.1	13.5	0.3	3.7	-8.8
C4	10.4	9.3	12.3	8.0	5.2	2.2
Pivaloyl	13.2	14.3	2.9	9.2	8.6	5.5
2MBC	6.0	3.3	13.5	3.7	6.4	-5.4
C5-I	6.0	-2.1	10.0	-8.2	12.4	-8.4
C5	16.9	0.4	10.7	-5.7	8.4	-7.8
C6	9.7	1.7	10.3	-8.1	8.1	-6.4
C8	13.6	-18.5	14.7	-14.1	7.1	-11.4
C10	14.8	-11.7	12.0	-8.7	12.9	-7.2
C12	18.8	-10.3	10.2	8.8	4.4	2.1

4.4.9 Carryover

It is important to verify the absence of carryover of material from sample to sample as part of the method validation process. Blank solutions consisting of 20% I, 0.1% FA in H_2O were analyzed after the analysis of standards, calibration solutions, quality control samples and esterified urine samples from the 20 volunteers. No carryover was observed in any of the cases mentioned above. Figure 4.12 shows a Total Ion Chromatogram (TIC) of a blank solution analyzed immediately after an esterified pooled urine sample. No carryover was detected.

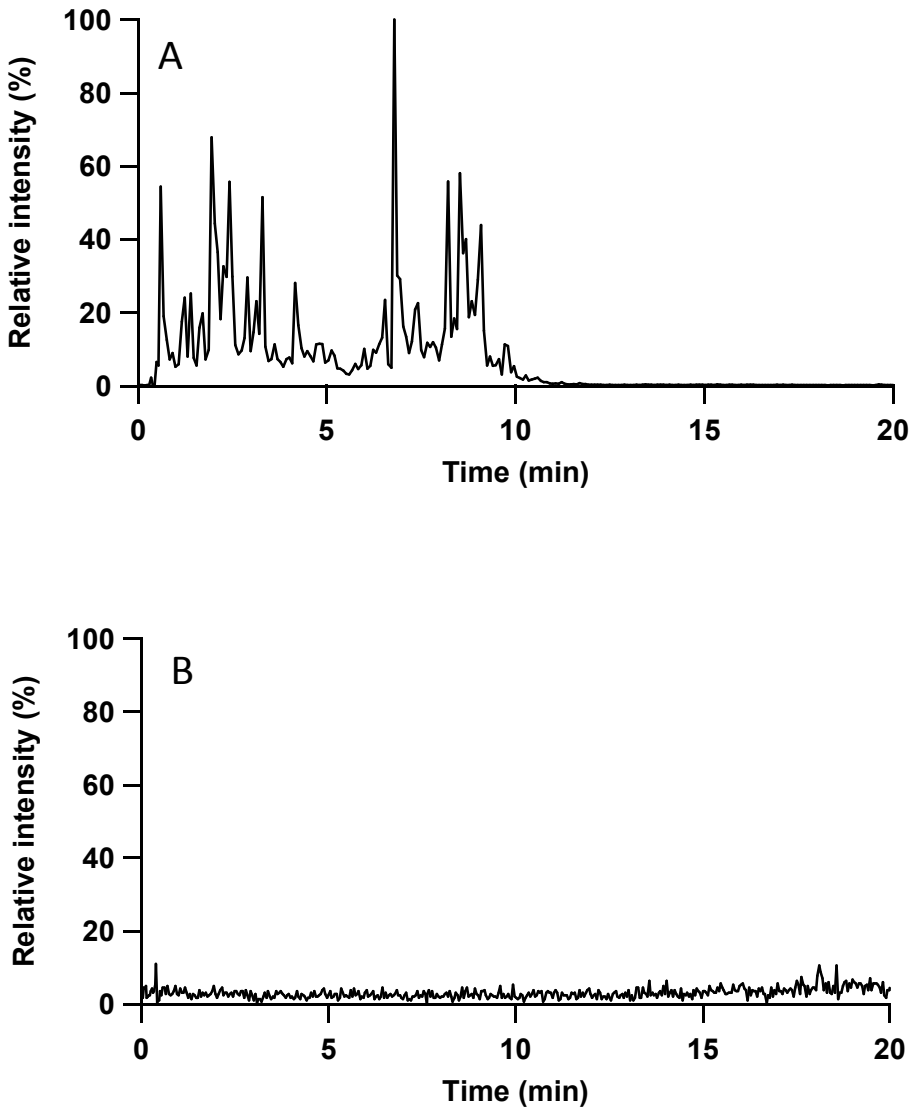

Figure 4.13 Carryover test. Blank solutions consisting of 20% I in H_2O were analyzed immediately after standards, calibration solutions, quality control samples and derivatized urine samples. (A) Example of a Total Ion Chromatogram (TIC) of an esterified pooled urine sample. (B) TIC of blank solution analyzed immediately after the pooled urine sample shown in (A) and plotted relative to the total signal in (A). No carryover was detected.

4.4.10 Comparison of ESI response

A dried pooled urine sample was divided into two aliquots. One was reconstituted in 20% I, 0.1% FA in H_2O, while the other was esterified first and then reconstituted with the same solution. The acylcarnitine ESI response in both samples was assessed by comparing their corresponding peak areas in five analytical replicates. Esterified carnitine dicarboxylic acid conjugates showed the most signal enhancement compared to their unesterified counterparts, likely due to the incorporation of two ethyl groups (one per carboxylic acid group) instead of just one. In the case of unsubstituted acylcarnitines, the esterified counterparts showed marginally increased signal intensity, except for C4-I which had a lower response (possibly due to matrix interferences). The marginal increase in response of esterified acylcarnitines as compared to unesterified species is probably due to the fact that acylcarnitines themselves already possess a good ESI response. This is due to the high hydrophobic character of the organic acid chain and the permanent positive charge of the quaternary amine in the carnitine backbone.

Matrix differences make it difficult to directly compare peak areas of esterified and unesterified acylcarnitines. That is, a particular unesterified acylcarnitine in underivatized urine might have a different response from that same acylcarnitine ethyl ester in derivatized urine, depending on the number and type of co-eluting species present. However, it was considered important to assess signal enhancement in actual samples (rather than neat standards), which is the reason why these experiments were carried out in urine. Figure 4.13 shows a summary of the results.

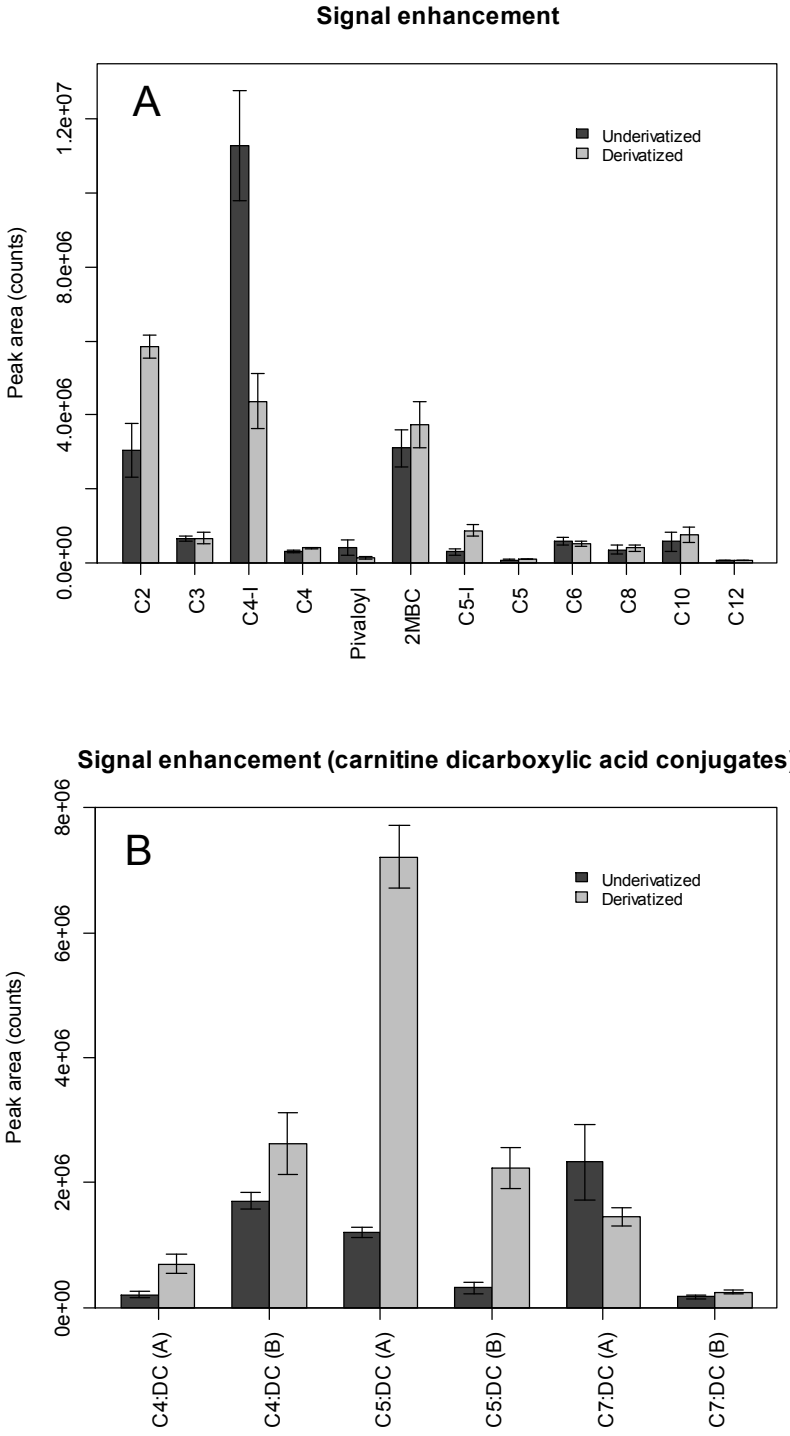

Figure 4.14 Signal enhancement. Peak areas corresponding to derivatized and underivatized acylcarnitines were compared. Carnitine dicarboxylic acid conjugates (B) showed the more enhancement compared to unsubstituted species (A), possibly due to the presence of two added ethyl groups instead of one. Results were based on five replicates.

4.4.11 Stability

The stability of post-preparatory samples was assessed at three different temperature conditions: at room temperature, at 4 °C and -20 °C, as well as after three freeze-thaw cycles. Three QC-low sample aliquots were analyzed immediately after sample preparation and were used as controls. Three sample aliquots were left at room temperature for four hours, which is the maximum time needed to prepare samples (including solvent evaporation in a liquid concentrator). Another set of experimental replicates were stored at 4 °C for 18 hours, which is the longest period a particular sample would remain in the autosampler of the LC system pending analysis. A last set of aliquots were analyzed after each of 3 freeze-thaw cycles which were performed at 18-hour intervals. Medium- and long-term storage were assessed by analyzing a sample after two and eight weeks of storage at -20 °C, respectively. The analyte response obtained following storage under certain conditions was compared to that of freshly prepared QC-low sample aliquots and results were expressed as a percentage difference from the freshly analyzed sample. In most cases, the results obtained were within ± 15% of the freshly analyzed sample, indicating that the stability of these analytes is adequate for the purposes of this study. Figure 4.14 shows a summary of the results.

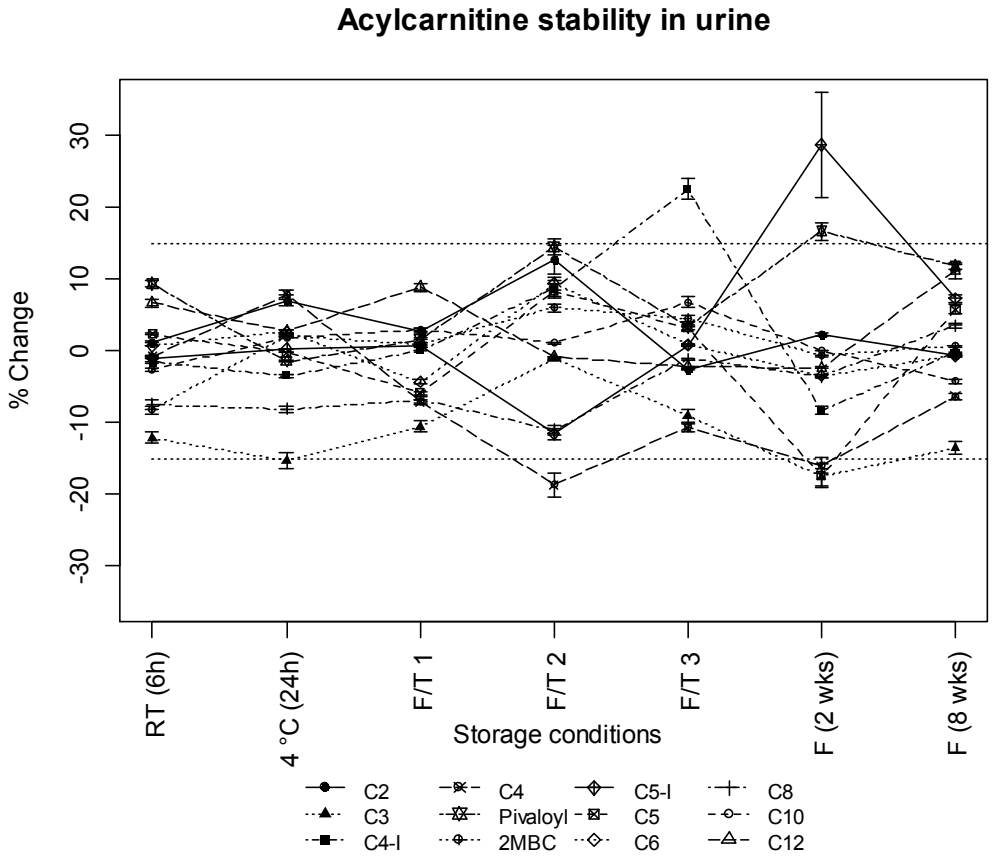

Figure 4.15 Acylcarnitine stability. The stability of a QC-low sample was analyzed under several conditions. RT (6 h), room temperature for 6 hours; 4 °C (24 h), 4°C for 24 h; F/T 1, first freeze/thaw cycle; F/T 2, second freeze/thaw cycle; F/T 3, third freeze/thaw cycle; F (2 wks), frozen for 2 weeks; F (8 wks), frozen for 8 weeks. The dotted lines represent ±15%.

4.4.12 Comparison with previously published methods

Maeda *et al.*[15] developed an LC-MS/MS method for acylcarnitine quantification in urine and plasma which did not include a derivatization step. They reported LLOQ values in neat solvents of 0.1 μM for methylmalonylcarnitine and 0.05 μM for all other acylcarnitines. Vernez *et al.*[37] reported an LC-MS/MS method for urinary acylcarnitine quantification without derivatization for which LLOQ values were 5 μM for C0, 2.5 μM for C2 and 0.75 μM for C3, C5-I, C6 and C8. They defined LLOQ as the lowest concentration with a relative deviation of replicate runs of less than 20%. Minkler *et al.*[31] did

not explicitly report LLOQ values for their LC-MS/MS method. The LLOQs for the method described herein were found to be lower than those described above and ranged from 0.007 to 0.034 μM, with the exception of C2, which was found to be 0.120 μM. The definition of LLOQ used in this work is 10 σ/S, where σ is the standard error of the y-intercept and S is the slope of the calibration curve. Using this definition, the S/N ratio for all analytes was equal to or greater than 20. Even when using different definitions, the LLOQs for the method described herein are considerably lower than those previously reported.

4.4.13 Urine of 20 individuals

Absolute quantification was performed on 12 acylcarnitines for which standards are commercially available using calibration curves constructed in unesterified urine. The 60 samples collected were analyzed in triplicate; that is, each urine sample was divided into three aliquots which were prepared in a parallel fashion and analyzed once each (experimental replicates). The results obtained were converted from μM concentrations to μmol/g of creatinine. Representative results of absolute quantification experiments can be found in Appendix Section 4.6, complete results tables can be found in the electronic Appendix.

4.4.13.1 Comparison with previously reported values

The values reported in this study correlate well with those published by Minkler *et al*.[31], who provided cut-off values based on a pool of 392 samples, as well as those by Maeda *et al.*[15], who provided a range of values based on 5 healthy volunteers. The results are summarized in Table 4.9. Complete tables with detailed results, including day-to-day fluctuations within individuals as well as variations between individuals, are included in the electronic Appendix.

Table 4.9 Comparison to previously reported values.

AC	Maeda *et al.* [15] (µmol/g of creatinine) *(n=5)*	Minkler *et al.* [31] (µmol/g of creatinine) *(n=392)*	This work (µmol/g of creatinine) *(n=20)*
C2	0.82 – 67.2	<44.2	1.21 – 67.3
C3	0.78 – 3.72	<2.80	0.13 – 4.56
C4-I	<LLOQ – 0.13	<13.9	2.16 – 16.4
C4	0.04 – 0.07	<0.28	<LLOQ - 0.92
Pivaloyl	N/A	N/A	<LLOQ – 0.72
2MBC	<LLOQ – 3.95	<3.79	0.62 - 4.99
C5-I	<LLOQ – 0.14	<0.70	0.04 - 1.07
C5	N/A	<0.03	<LLOQ – 0.20
C6	<LLOQ – 0.04	<0.34	<LLOQ – 0.13
C8	<LLOQ – 0.14	<0.36	<LLOQ – 0.22
C10	<LLOQ	<0.26	<LLOQ – 0.12
C12	<LLOQ	<LLOQ	<LLOQ – 0.17

4.4.13.2 Effect of gender and BMI

The body mass index (BMI) values for the ten female volunteers ranged from 18.0 to 34.2 with an average of 22.2 kg/m^2. The range of values for males was 19.4 to 33.9 with an average of 23.2 kg/m^2. Table 4.10 lists volunteers' gender and BMI values. Volunteers were divided into 4 groups (underweight, normal weight, overweight and obese) according to the Canadian guidelines for body weight classification in adults. The similarity in the average BMI values in males and females makes it easier to determine whether gender has an effect on urinary acylcarnitine profile. It was found, however, that although females had a marginally elevated acylcarnitine profile compared to males, this difference was not statistically significant. The only exception was pivaloylcarnitine, which was found to be below the LLOQ for all males except for one but was detected in all females. Pivalic acid and pivalate compounds are commonly found in prescription as well as over-the-counter skin lotions and ointments. Once absorbed into the body, pivalic acid can conjugate to carnitine forming pivaloylcarnitine. It is

possible that females are more likely to apply lotions and ointments than males and so it speculated that this could be the source of excreted pivaloylcarnitine. This speculation was investigated further but no definite source of pivalic acid was found. There was also no clear correlati2on found between BMI and acylcarnitine concentration. These results agree with previously reported studies.[3] Figures 4.15 and 4.16 illustrate this further.

Table 4.10 Volunteers' gender and BMI information.

Individual	Gender	BMI (kg/m^2)
001	F	19.1
004	F	27.0
005	F	34.2
008	F	20.8
009	F	23.2
018	F	19.7
019	F	22.4
024	F	18.0
027	F	18.9
032	F	18.5
010	M	24.8
011	M	23.0
015	M	20.7
016	M	22.7
021	M	22.0
023	M	22.0
025	M	20.6
026	M	19.4
029	M	33.9
030	M	25.6

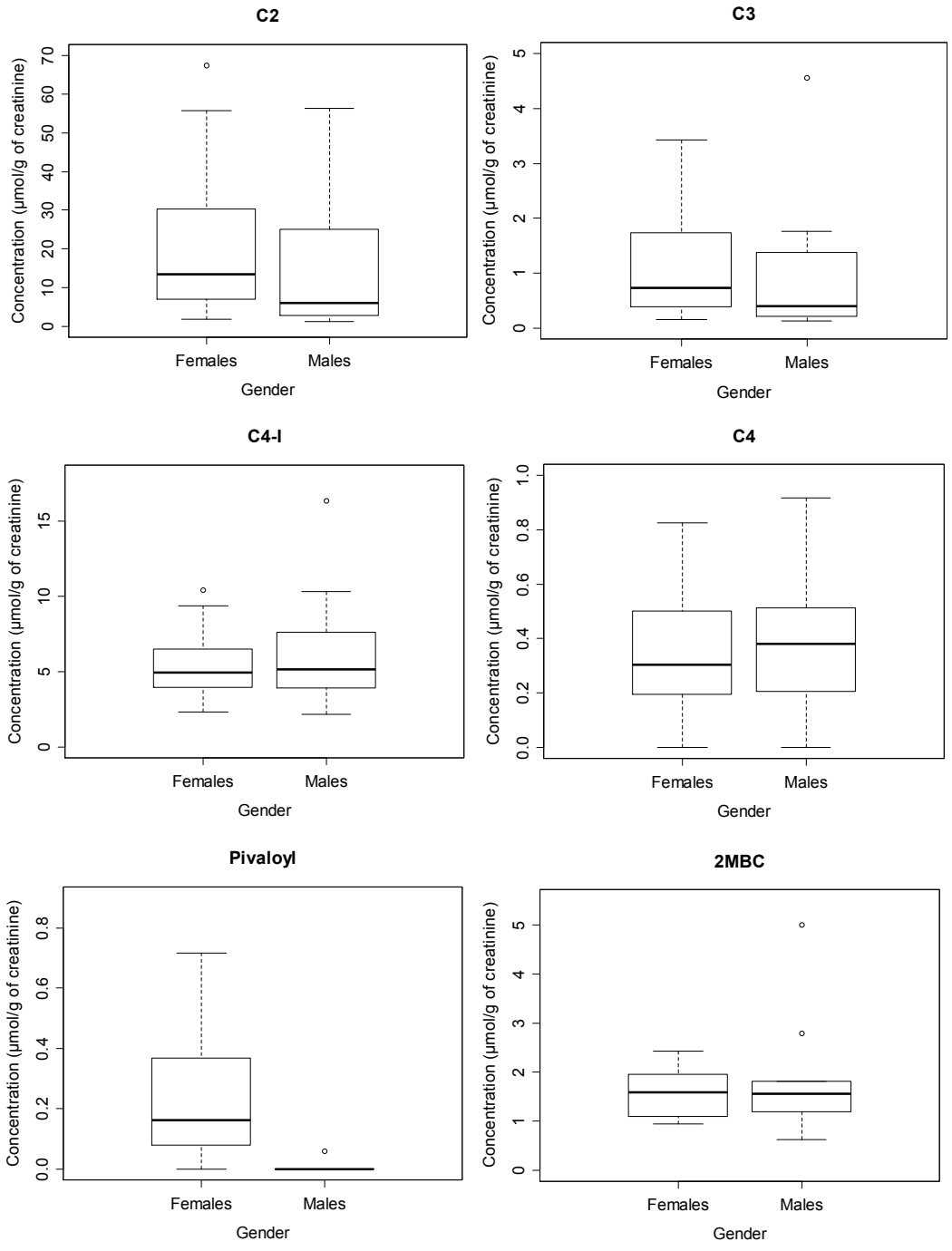

Figure 4.16 Influence of gender. The urine of ten males and ten females was analyzed. Box plots were created for all 12 acylcarnitines. The horizontal line inside each box represents the median value. Possible outliers are displayed as empty circles (± 1.5x inter-quartile range). Horizontal lines at 0.00 concentration indicate that the concentration is below the LLOQ.

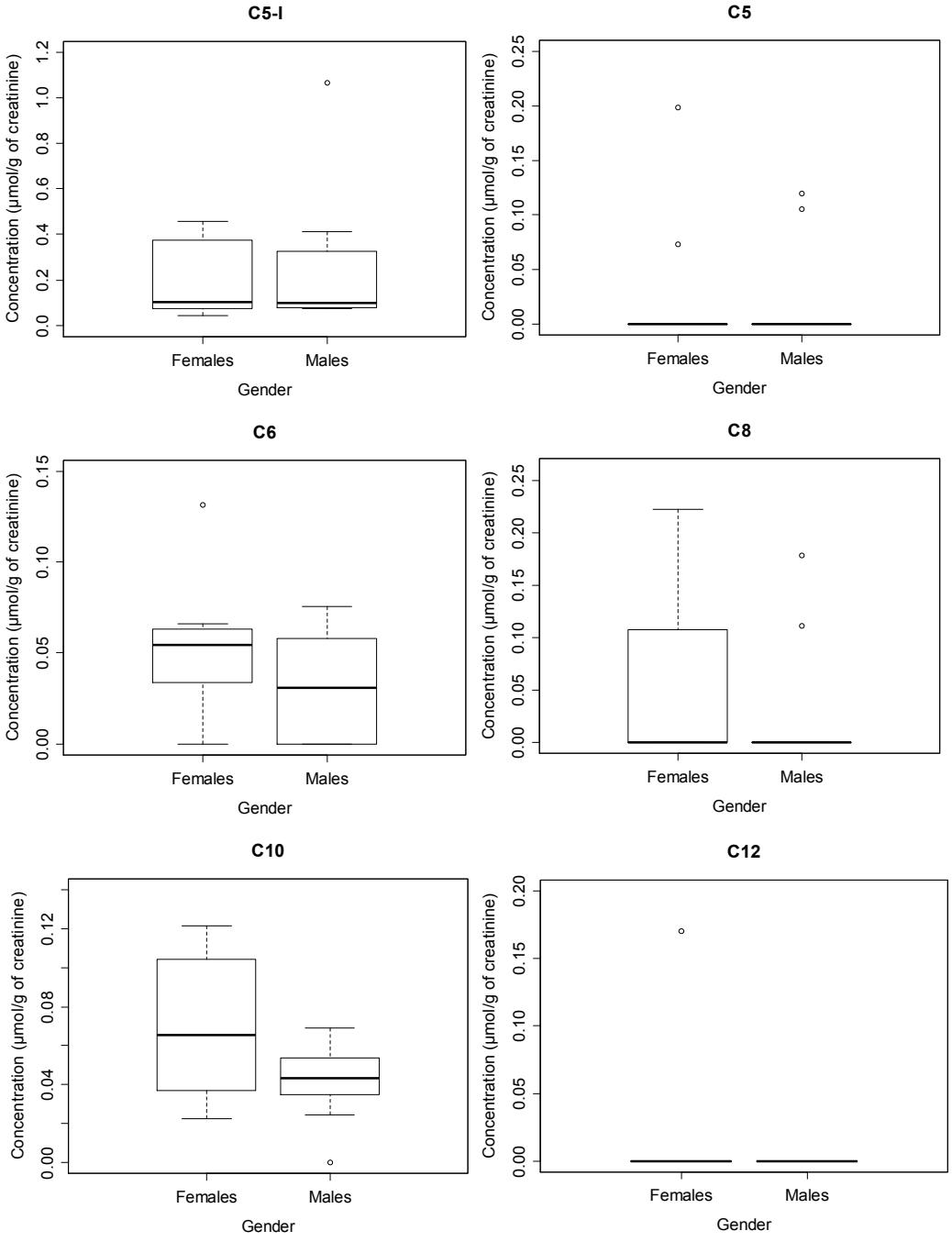

Figure 4.17 Influence of gender (continued). The urine of ten males and ten females was analyzed. Box plots were created for all 12 acylcarnitines. The horizontal line inside each box represents the median value. Possible outliers are displayed as empty circles (± 1.5x inter-quartile range). Horizontal lines at 0.00 concentration indicate that the concentration is below the LLOQ.

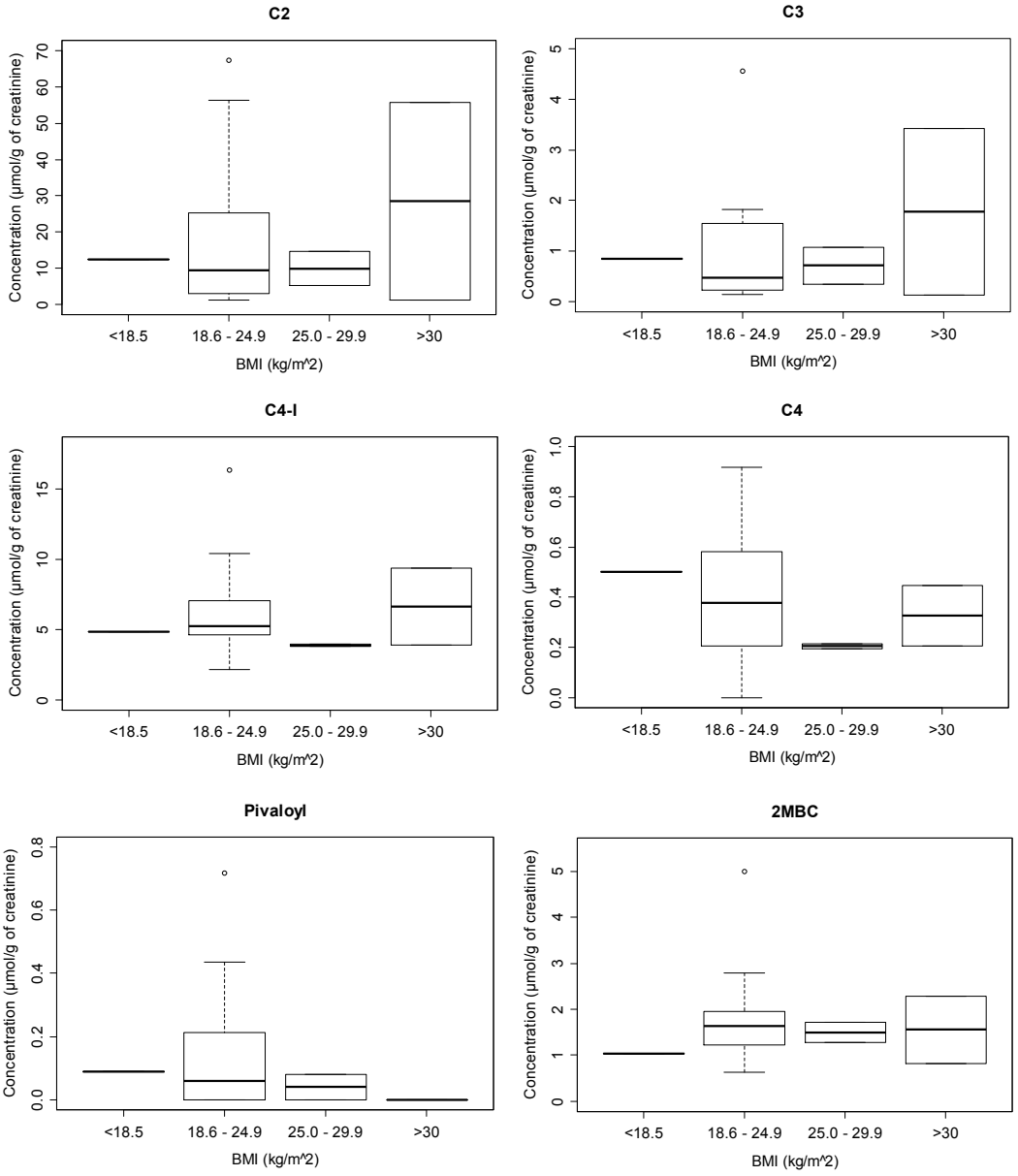

Figure 4.18 Effect of BMI. Results were arranged into four groups according to the volunteers' BMI. The group with BMI <18.5 kg/m^2 (underweight) consisted of only one volunteer, the groups with BMIs 25.0-29.9 (overweight) and >30 kg/m^2 (obese) consisted of only 2 volunteers each. The rest of the volunteers had BMI values that ranged from 18.6 to 24.9 kg/m^2 (normal weight). The horizontal line inside each box represents the median. Possible outliers are displayed as empty circles (± 1.5x inter-quartile range).

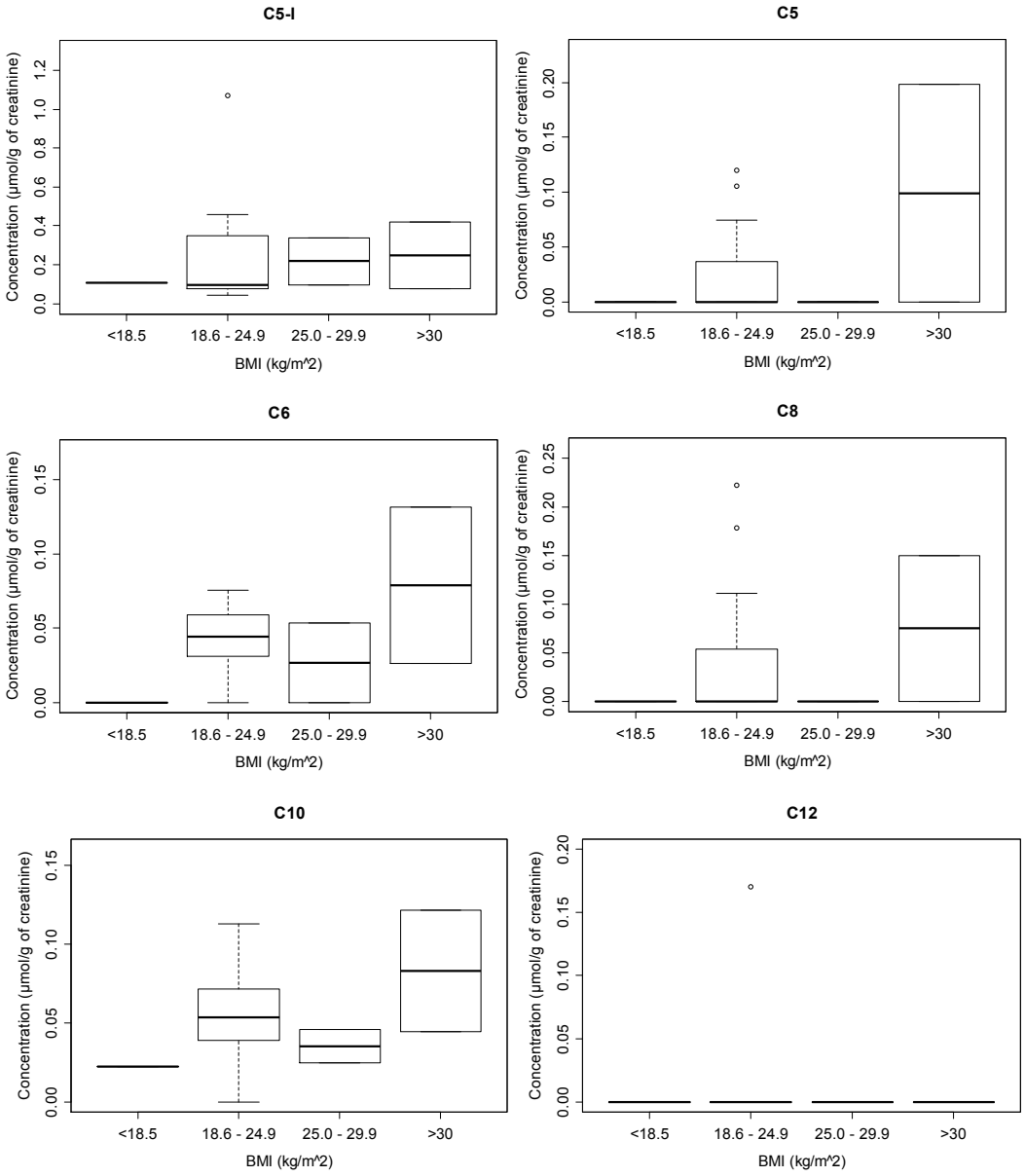

Figure 4.19 Effect of BMI (continued). Results were arranged into four groups according to the volunteers' BMI. The group with BMI <18.5 kg/m^2 (underweight) consisted of only one volunteer, the groups with BMIs 25.0-29.9 (overweight) and >30 kg/m^2 (obese) consisted of only 2 volunteers each. The rest of the volunteers had BMI values that ranged from 18.6 to 24.9 kg/m^2 (normal weight). The horizontal line inside each box represents the median. Possible outliers are displayed as empty circles (± 1.5x inter-quartile range).

Table 4.11 Effect of BMI and gender on acylcarnitine concentration.

	BMI (kg/m^2)				**Gender**	
AC (µmol/g of creatinine)	**<18.5 underweight *(n=1)***	**18.6 – 24.9 normal weight *(n=15)***	**25.0 – 29.9 overweight *(n=2)***	**>30.0 obese *(n=2)***	**Female *(n=10)***	**Male *(n=10)***
C2	12.3	1.21 – 67.3	5.15 – 14.5	1.22 – 55.7	1.76 – 67.3	1.21 – 56.4
C3	0.84	0.14 – 4.56	0.34 – 1.08	0.13 – 3.42	0.15 – 3.42	0.13 – 4.56
C4-I	4.86	2.16 – 16.3	3.79 – 3.94	3.92 – 9.36	2.31 – 10.4	2.16 – 16.3
C4	0.50	<LLOQ – 0.92	0.20 – 0.22	0.21 – 0.45	<LLOQ – 0.82	<LLOQ – 0.92
Pivaloyl	0.09	<LLOQ – 0.72	<LLOQ – 0.08	<LLOQ	<LLOQ – 0.72	<LLOQ – 0.06
2MBC	1.04	0.62 – 4.99	1.28 – 1.72	0.81 – 2.28	0.93 – 2.42	0.62 – 4.99
C5-I	0.11	<LLOQ – 1.07	0.095 – 0.34	0.08 – 0.42	<LLOQ – 0.46	0.07 – 1.07
C5	<LLOQ	<LLOQ – 0.12	<LLOQ	<LLOQ – 0.20	<LLOQ – 0.20	<LLOQ – 0.11
C6	<LLOQ	<LLOQ – 0.08	<LLOQ – 0.05	0.03 – 0.13	<LLOQ – 0.13	<LLOQ – 0.08
C8	<LLOQ	<LLOQ – 0.22	<LLOQ	<LLOQ – 0.15	<LLOQ – 0.22	<LLOQ – 0.18
C10	0.02	<LLOQ – 0.11	0.02 – 0.05	0.04 – 0.12	0.03 – 0.12	<LLOQ – 0.07
C12	<LLOQ	<LLOQ	<LLOQ	<LLOQ	<LLOQ	<LLOQ

4.4.13.3 Relative quantification of 64 additional acylcarnitines

Compounds for which standards were not commercially available were quantified by assigning them one of the available internal standards. It has been shown that the choice of internal standard can have a dramatic effect on the accuracy of results[38] and so internal standards should be chosen as carefully as possible. In this work, internal standards were assigned based on retention time since electrospray response is directly related to a compound's hydrophobicity. As far as possible, compounds that appeared to be structural isomers of each other (same *m/z* ratio and similar retention time) were assigned the same internal standard. Table 4.12 lists the internal standards used according to retention time range.

Table 4.12 Internal standard assignment based on retention time for relative quantification studies.

Retention time (min)	IS used
<0.61	C2
0.62 - 1.10	C3
1.11 – 2.00	C4-I
2.01 – 5.00	C5
5.01 – 11.20	C6
11.21 – 13.50	C8
13.51 – 15.50	C10
>15.50	C12

It was found that some acylcarnitines, such as acylcarnitine with *m/z* 402 and retention time 11.82 min, did not seem to vary much from day to day or even between individuals, while others varied in intensity as much as 2 orders of magnitude, such as acylcarnitine with *m/z* 402 and retention time of 13.84 min.

Factors such as diet, fasting as well as physical activity have been found to have a large effect on acylcarnitine profile[39-41] and may be the cause of the differences observed. A partial table of relative quantification results can be found in Appendix Section 4.7. An Excel spreadsheet summarizing all relative quantification results is included in the electronic Appendix. A partial table of all quantified compounds, including their putative identification can be found in Appendix Section 4.5. A complete table of all quantified compounds including their putative identification can be found in the electronic Appendix.

This work comprises the most comprehensive quantitative profile of acylcarnitines in healthy volunteers published to date (76 acylcarnitines in total). Although most compounds were only putatively identified, this information may still be useful for biomarker discovery studies. Once a compound is identified as being a potential biomarker, extraction and pre-concentration can be performed and further structure elucidation can be achieved by other techniques such as NMR. Alternatively, analysis by GC-MS with electron impact ionization could provide the fragmentation necessary to further elucidate the structures of the quantified compounds. A more costly approach would be to synthesize standards in order to obtain definitive identification.

4.5 Conclusions

In this study, a UHPLC-MS/MS method to obtain a comprehensive quantitative profile of urinary acylcarnitines was developed and validated. Acylcarnitine ethyl esters were synthesized in order to increase their ESI response as well as to introduce a $^{13}C_2$ label to prepare a set of internal standards. A surrogate approach was utilized where unesterified urine was used as a surrogate matrix to construct calibration curves. Preparation of urine samples required no additional clean-up steps apart from the initial filtration step. Absolute quantification was performed on 12 acylcarnitines and relative quantification was carried out on an additional 64. The urine of 20 volunteers collected over the

course of three days was analyzed. This study describes the most comprehensive quantitative profile of acylcarnitines in healthy volunteers published to date (76 acylcarnitines in total). There were no statistically significant effects found on urinary acylcarnitine profile as a result of differences in gender or BMI values. Future work includes the analysis of clinical samples with the aim of discovering new biomarkers for disorders such as diabetes mellitus type II, sepsis and multiple sclerosis, among others.

4.6 Literature cited

(1) Khovidhunkit, W.; Kim, M.-S.; Memon, R. A.; Shigenaga, J. K.; Moser, A. H.; Feingold, K. R.; Grunfeld, C. *Journal of Lipid Research* **2004**, *45*, 1169-1196.

(2) Eaton, S.; Pierro, A. *Monatshefte für Chemie / Chemical Monthly* **2005**, *136*, 1483-1492.

(3) Moder, M.; Kiessling, A.; Loster, H.; Bruggemann, L. *Analytical and Bioanalytical Chemistry* **2003**, *375*, 200-210.

(4) Chalmers, R. A.; Roe, C. R.; Stacey, T. E.; Hoppel, C. L. *Pediatric Research* **1984**, *18*, 1325-1328.

(5) Calabrese, V.; Scapagnini, G.; Ravagna, A.; Bella, R.; Butterfield, D. A.; Calvani, M.; Pennisi, G.; Giuffrida Stella, A. M. *Neurochemical Research* **2003**, *28*, 1321-1328.

(6) Illsinger, S.; Janzen, N.; Sander, S.; Schmidt, K.-H.; Bednarczyk, J.; Mallunat, L.; Bode, J.; Hagebölling, F.; Hoy, L.; Lücke, T.; Hass, R.; Das, A. M. *Reproductive Sciences* **2010**, *17*, 219-226.

(7) Ganti, S.; Taylor, S. L.; Kim, K.; Hoppel, C. L.; Guo, L.; Yang, J.; Evans, C.; Weiss, R. H. *International Journal of Cancer* **2011**, *In Press*.

(8) Miyagawa, T.; Miyadera, H.; Tanaka, S.; Kawashima, M.; Shimada, M.; Honda, Y.; Tokunaga, K.; Honda, M. *SLEEP* **2011**, *34*, 349-353.

(9) Ryan, D.; Robards, K.; Prenzler, P. D.; Kendall, M. *Analytica Chimica Acta* **2011**, *684*, 17-29.

(10) Kobayashi, H.; Hasegawa, Y.; Endo, M.; Purevsuren, J.; Yamaguchi, S. *Journal of Chromatography B* **2007**, *855*, 80-87.

(11) Abdenur, J. E.; Chamoles, N. A.; Guinle, A. E.; Schenone, A. B.; Fuertes, A. N. J. *Journal of Inherited Metabolic Disease* **1998**, *21*, 624-630.

(12) Matern, D.; Tortorelli, S.; Oglesbee, D.; Gavrilov, D.; Rinaldo, P. *Journal of Inherited Metabolic Disease* **2007**, *30*, 585-592.

(13) Smith, E. H.; Thomas, C.; McHugh, D.; Gavrilov, D.; Raymond, K.; Rinaldo, P.; Tortorelli, S.; Matern, D.; Highsmith, W. E.; Oglesbee, D. *Molecular Genetics and Metabolism* **2010**, *100*, 241-250.

(14) Maeda, Y.; Ito, T.; Ohmi, H.; Yokoi, K.; Nakajima, Y.; Ueta, A.; Kurono, Y.; Togari, H.; Sugiyama, N. *Journal of Chromatography B* **2008**, *870*, 154-159.

(15) Maeda, Y.; Ito, T.; Suzuki, A.; Kurono, Y.; Ueta, A.; Yokoi, K.; Sumi, S.; Togari, H.; Sugiyama, N. *Rapid Communications in Mass Spectrometry* **2007**, *21*, 799-806.

(16) Millington, D. S.; Kodo, N.; Terada, N.; Roe, D.; Chace, D. H. *International Journal of Mass Spectrometry and Ion Processes* **1991**, *111*, 211-228.

(17) Minkler, P. E.; Ingalls, S. T.; Hoppel, C. L. *Analytical Chemistry* **2005**, *77*, 1448-1457.

(18) Poorthuis, B. J. H. M.; Jille-Vlcková, T.; Onkenhout, W. *Clinica Chimica Acta* **1993**, *216*, 53-61.

(19) Turowski, M.; Yamakawa, N.; Meller, J.; Kimata, K.; Ikegami, T.; Hosoya, K.; Tanaka, N.; Thornton, E. R. *Journal of the American Chemical Society* **2003**, *125*, 13836-13849.

(20) Wieling, J. *Chromatographia* **2002**, *55*, S107-S113.

(21) Wang, S.; Cyronak, M.; Yang, E. *Journal of Pharmaceutical and Biomedical Analysis* **2007**, *43*, 701-707.

(22) Lowes, S.; Jersey, J.; Shoup, R.; Garofolo, F.; Savoie, N.; Mortz, E.; Needham, S.; Caturla, M. C.; Steffen, R.; Sheldon, C.; Hayes, R.; Samuels, T.; Di Donato, L.; Kamerud, J.; Michael, S.; Lin, Z.; Hillier, J.; Moussallie, M.; de Souza Teixeira, L.; Rocci, M.; Buonarati, M.; Truog, J.; Hussain, S.; Lundberg, R.; Breau, A.; Zhang, T.; Jonker, J.; Berger, N.; Gagnon-Carignan, S.; Nehls, C.; Nicholson, R.; Hilhorst, M.; Karnik, S.; de Boer, T.; Houghton, R.; Smith, K.; Cojocaru, L.; Allen, M.; Harter, T.;

Fatmi, S.; Sayyarpour, F.; Vija, J.; Malone, M.; Heller, D. *Bioanalysis* **2011**, *3*, 1323-1332.

(23) Penner, N.; Ramanathan, R.; Zgoda-Pols, J.; Chowdhury, S. *Journal of Pharmaceutical and Biomedical Analysis* **2010**, *52*, 534-543.

(24) Peng, L.; Jiang, T.; Rong, Z.; Liu, T.; Wang, H.; Shao, B.; Ma, J.; Yang, L.; Kang, L.; Shen, Y.; Li, H.; Qi, H.; Chen, H. *Journal of Chromatography B* **2011**, *879*, 3927-3931.

(25) Bogialli, S.; D'Ascenzo, G.; Di Corcia, A.; Laganà , A.; Nicolardi, S. *Food Chemistry* **2008**, *108*, 354-360.

(26) Berna, M.; Ackermann, B. *Analytical Chemistry* **2009**, *81*, 3950-3956.

(27) Mohamed S, R. *Journal of Chromatography B* **2001**, *758*, 27-48.

(28) Kuhara, T. *Mass Spectrometry Reviews* **2005**, *24*, 814-827.

(29) Stalhandske, C. *Acta Crystallographica Section B* **1980**, *36*, 23-26.

(30) Zuniga, A.; Li, L. *Analytica Chimica Acta* **2011**, *689*, 77-84.

(31) Minkler, P. E.; Stoll, M. S. K.; Ingalls, S. T.; Yang, S.; Kerner, J.; Hoppel, C. L. *Clinical Chemistry* **2008**, *54*, 1451-1462.

(32) Khymenets, O.; Farré, M.; Pujadas, M.; Ortiz, E.; Joglar, J.; Covas, M. I.; de la Torre, R. *Food Chemistry* **2011**, *126*, 306-314.

(33) Zar, J. H. *Biostatistical Analysis*, 5th ed.; Pearson Prentice Hall: New Jersey, 2010.

(34) Rosing, H.; Man, W.; Doyle, E.; Bult, A.; Beijnen, J. *Journal of Liquid Chromatography & Related Technologies* **2000**, *23*, 329-354.

(35) Forni, S.; Fu, X.; Palmer, S. E.; Sweetman, L. *Molecular Genetics and Metabolism*, *101*, 25-32.

(36) Ziegler, H. J.; Bruckner, P.; Binon, F. *The Journal of Organic Chemistry* **1967**, *32*, 3989-3991.

(37) Vernez, L.; Hopfgartner, G.; Wenk, M.; Krähenbühl, S. *Journal of Chromatography A* **2003**, *984*, 203-213.

(38) Stokvis, E.; Rosing, H.; Beijnen, J. H. *Rapid Communications in Mass Spectrometry* **2005**, *19*, 401-407.

(39) Hoppel, C. L.; Genuth, S. M. *American Journal of Physiology - Endocrinology And Metabolism* **1980**, *238*, E409-E415.

(40) Cederblad, G. *The American Journal of Clinical Nutrition* **1987**, *45*, 725-729.

(41) Lehmann, R.; Zhao, X.; Weigert, C.; Simon, P.; Fehrenbach, E.; Fritsche, J.; Machann, J.; Schick, F.; Wang, J.; Hoene, M.; Schleicher, E. D.; Häring, H.-U.; Xu, G.; Niess, A. M. *PLoS ONE*, *5*, e11519.

Chapter 5

Quantitative analysis of acylcarnitines as their ethyl esters derivatives in the plasma of healthy individuals by Ultra-high performance liquid chromatography tandem mass spectrometry*

5.1 Introduction

Plasma acylcarnitines have been routinely analyzed since the early 1990's in studies involving inborn errors of metabolism including organic acidurias and fatty acid oxidation disorders.[1-4] Recent studies however, have shown acylcarnitines to be dysregulated in various other diseases such as diabetes mellitus type II, obesity, narcolepsy and biotin deficiency.[5-9] Interestingly, acylcarnitines have also been found to be decreased in patients with dysregulated immune systems such as patients suffering from sepsis, systemic sclerosis, chronic fatigue and those tested positive for human immunodeficiency virus (HIV). This might be due to the fact that immune cells under stress can lose acylcarnitines or may present an increased carnitine demand.[10] These recent findings have maintained interest in acylcarnitine research.

* A form of this Chapter is in preparation as: Zuniga, A. and Li, L. "Quantitative analysis of acylcarnitines as their ethyl esters derivatives in the plasma of healthy individuals by Ultra-high performance liquid chromatography tandem mass spectrometry"

Recently, acylcarnitine research has focused on the development of platforms using novel analytical techniques in order to improve accuracy and precision. A recent report describes the use of hydrophilic interaction liquid chromatography (HILIC) coupled to mass spectrometry for the accurate quantification of free and total carnitine in human plasma.[11] Capillary electrophoresis with contactless conductivity detection has also been used for the determination of carnitine and acylcarnitines in clinical samples, albeit with limited sensitivity.[12] The application of different ionization techniques such as atmospheric pressure thermal desorption chemical ionization (APCI) to analyze acylcarnitines in dried blood spot extracts has also been recently studied.[13] However, acylcarnitine thermal dissociation made it impossible to detect molecular ions. The work presented herein describes the development and validation of a quantitative UHPLC-MS/MS method for plasma acylcarnitines.

This UHPLC-MS/MS method allows for the accurate and precise absolute quantification of 13 acylcarnitines including structural isomers. Internal standards were prepared by esterifying acylcarnitine standards with 1,2-$^{13}C_2$ ethanol overcoming the need to purchase a separate set of internal standards. A surrogate matrix approach was employed where calibration curves were prepared by spiking acylcarnitine ethyl esters into unesterified plasma. This was found to be an effective way to overcome the lack of acylcarnitine-free plasma. There was no statistically significant difference found between the calibration curve slopes prepared in esterified and unesterified plasma. This suggests that unesterified plasma is a suitable matrix which may provide more accurate results than using other surrogate matrices typically used such as phosphate-buffered bovine serum albumin solution. Relative quantification was performed on an additional 19 compounds for which standards are not commercially available.

Carrying out relative rather than absolute quantification of detected metabolites may still be of great value since a more comprehensive acylcarnitine profile can be attained, providing insight into the carnitine status of an individual at a particular time. In many cases the ratio of one acylcarnitine to another has

been found to be more significant than the absolute concentration of acylcarnitines themselves.[14] Analyzing a larger number of acylcarnitines in healthy individuals may provide a more accurate representation of a healthy acylcarnitine profile. Moreover, obtaining reliable reference values for acylcarnitines in healthy individuals is critical since it would greatly facilitate disease diagnosis as well as biomarker discovery studies.[15]

5.2 Experimental

5.2.1 Chemicals and reagents

Chemicals and reagents used in this work are summarized in Chapter 2 Section 2.2.1. Three deuterated standards (C3-d_3, C10-d_3 and C16-d_3) were used for extraction efficiency studies and were purchased from C/D/N Isotopes Inc. (Pointe-Claire, Quebec).

5.2.2 Plasma sample preparation

Whole blood was collected from five male and five female healthy volunteers who were not on any special diet or taking any nutritional supplements. An informed consent was obtained from each volunteer and ethics approval for this work was obtained from the University of Alberta in compliance with the Arts, Science and Law Research Ethics Board policy. Whole blood samples were immediately centrifuged at 14,000 rpm for 10 min in order to separate the plasma. Protein precipitation/analyte extraction was performed by adding 200 µL of 20% H_2O, 80% acetonitrile (I) to 50 µL of plasma and incubating for 30 min at 4 °C. Samples were then centrifuged at 14,000 rpm for 10 min at 4 °C. Plasma samples were esterified using a previously optimized reaction which is summarized in the next section. Finally, 2 µL of the internal standard solution was spiked to each plasma sample.

5.2.3 Esterification of plasma samples

Following analyte extraction, plasma samples were evaporated to dryness using a vacuum concentrator system (Thermo Fisher Scientific, Nepean, Ontario). The reaction conditions described in Chapter 4 Section 4.2.3 were utilized. The solid residue was re-dissolved in 25 µL of anhydrous ethanol and 0.5 µL of concentrated H_2SO_4 were subsequently added. The vials were capped and introduced into a water bath that had been previously preheated to 50 °C. The reaction was allowed to proceed for one hour. All samples were then evaporated to dryness and reconstituted in 48 µL of 0.1% formic acid (FA), 50% I in H_2O, 2 µL of internal standard solution were then spiked to yield a final volume of 50 µL. Fifty percent acetonitrile was chosen for sample reconstitution since it was found to dissolve long-chain species well while also allowing for the chromatographic separation of all short-chain species and their structural isomers. Three experimental triplicates of each plasma sample were prepared and analyzed.

5.2.4 Standard and internal standard stock solution preparation

A calibration stock solution was prepared by esterifying a previously dried 10 µM acylcarnitine standard mix (C2 concentration was 50 µM) using 340 µL of ethanol, 7 µL of H_2SO_4 and allowing the reaction to take place at 50 °C for one hour. An internal standard stock solution was also prepared by esterifying a previously dried 2.5 µM acylcarnitine standard mix (C2, C4 and C4-I concentration was 12.5 µM, C3 concentration was 6.25 µM) using 150 µL of $^{13}C_2$- ethanol, 3 µL of H_2SO_4 at 50 °C for one hour in order to obtain $^{13}C_2$-labeled acylcarnitines. To prepare the calibration solutions, the standard stock was diluted as necessary and 10 µL of each solution was added to the 48 µL of matrix to provide the correct final concentration, 2 µL of IS solution were subsequently added.

5.2.5 UHPLC-MS/MS

Chromatographic separation was performed on an Agilent UHPLC 1290 Infinity system (Agilent Technologies, Mississauga, Ontario) consisting of two binary pumps, an autosampler, and a column compartment containing a 10-port valve that allows to switch between two analytical columns. The two C_{18} columns used were 2.1 × 50 mm long with a particle size of 1.7 µm and a pore size of 100 Å (Phenomenex, Torrance, California). A 5 µL sample aliquot was injected onto the column with the column temperature maintained at 25 °C. The flow rate used was 300 µL/min. Mobile phase A consisted of 2% I, 0.1% FA in H_2O, whereas mobile phase B contained 2% H_2O, 0.1% FA in I. The gradient used was the following; the column was equilibrated at 15% B, solvent B was increased to 22.5% in 8 min and it was further increased to 100% in 28 minutes. Solvent B was held at 100% for 5 minutes, and the solvent system was returned to initial conditions for an extra minute to re-fill the solvent line with 15% B. The total run time was 34 minutes. The two binary pump system allowed for full re-equilibration of one column while the other performed the analytical separation.

The MS system used was a 4000 QTRAP® MS/MS System (Applied Biosystems, Foster City, California) equipped with a Turbo V™ ion source. Two UHPLC-MS/MS methods were developed, one for quantification and one for qualitative confirmation of the presence of acylcarnitines in the sample. These methods are very similar to those previously developed for urine analysis (described in Chapter 4) with some minor differences. Three experimental replicates of each plasma sample were prepared and analyzed once each with the quantitative method, followed by the analysis of one of the replicates using the qualitative method to obtain MS/MS information. Both methods had the same ESI source and compound-specific parameters that can be summarized as follows; Q1 and Q3 resolution were set to unit, GS1 was set to 40 psi, GS2 was set to 35 psi, CAD gas was set to high, the curtain gas was set 10 psi, the IS voltage was 4800 V, the source temperature was set to 400 °C, the declustering potential (DP) was

set to 60 V, the entrance potential (EP) was set to 11 V and the collision cell exit potential (CXP) was set to 13 V.

The quantitative method was developed using multiple reaction monitoring (MRM). The method contained a total of 122 MRM transitions, which can be summarized as acylcarnitine ethyl ester *m/z* → 85, each having a dwell time of 10 ms. The Q1 mass for the MRM transitions were calculated using *m/z* ratios corresponding to acylcarnitines obtained from previous studies of urine[16] and plasma and adding 28 to each *m/z* ratio (corresponding to the ethyl group). Transitions associated with the $^{13}C_2$-labeled acylcarnitine ethyl esters were also included. Due to background interference, the transitions for C2, C3, C4, C14, C16 and C18 were changed to *m/z* → 113 which showed a lower background signal. The collision energy (CE) used was compound dependent and was obtained in the following way; the CE necessary to fragment 90% of the precursor ion was used (data obtained using synthetic standards). That is, the CE needed to decrease the intensity of the precursor ion to 10% of its original value was used. Compounds for which standards were not available were grouped and the CE used for the standard closest in mass but not exceeding it was used. In order to confirm the identity of the quantified compounds as acylcarnitines, a qualitative, information dependent acquisition (IDA) method containing two dependent MS/MS scans was developed. The MRM survey scan was the same as that of the quantitative method except the dwell time of each transition was set to 2 ms. For every data point acquired along the chromatographic peak, the 2 most intense ions were selected for subsequent enhanced product ion (EPI) scan (i.e. MS/MS). The parameters used for the EPI scans were the following; the Q1 resolution was set to unit, the Q3 entry barrier was set to 6 V, the scan rate was 4000 amu/s for a scan range of m/z 50 to 600. The collision energy (CE) was set to 37 V with a spread (CES) of 6 V. Dynamic fill time was selected. The details of these methods can be found in the electronic Appendix.

5.3 Method validation

5.3.1 Analyte extraction efficiency

In order to assess the analyte extraction efficiency during the protein precipitation step of the sample preparation process, three deuterated standards were utilized as surrogate analytes (propionylcarnitine-d_3, decanoylcarnitine-d_3 and palmitoylcarnitine- d_3) and spiked at two different concentrations into underivatized plasma. $^{12}C_2$ acylcarnitine ethyl esters were not used for this purpose since they would be hydrolyzed during the esterification process and the plasma sample is esterified after protein precipitation. Percent recovery was calculated as the peak area ratio of the deuterated standard to the internal standard when the deuterated standards were spiked before protein precipitation divided by peak area ratio when spiked after protein precipitation and multiplied by 100%.

5.3.2 Calibration curves and matrix effects

Multiple-point calibration curves were prepared both in neat solvents and in underivatized plasma (surrogate matrix). Least-squares regression was performed using R software. Weighting was found to be necessary due to the heteroscedastic nature of the data. Weighting of 1/y was found to provide the lowest value for the sum of residuals squared and was therefore used to create calibration curves for all analytes. Matrix effects were assessed by comparing the slope of the calibration curve of each analyte in neat solvents to the slope of the curve in an underivatized pooled plasma sample using Equation (5.1) with the result expressed as a percentage.

$$\frac{\boldsymbol{Slope\ in\ plasma}}{\boldsymbol{Slope\ in\ neat\ solvent}} \times \mathbf{100\%} - \mathbf{100\%} \qquad (5.1)$$

5.3.3 Intra-day and inter-day reproducibility

Intra-day reproducibility was assessed by analyzing the same esterified plasma sample ten times in the course of one day (n = 10). The inter-day precision was calculated by analyzing that same sample 10 times/day over a three day period (n = 30).

5.3.4 Linear dynamic range

The linear dynamic range of these compounds was assessed in underivatized plasma. The linear range of the calibration curves was found by preparing and inspecting residual plots within the range of concentrations used in the calibration curves. The ranges for all analytes are listed in Table 5.3.

5.3.5 Limit of detection and lower limit of quantification

The limit of detection (LOD) was calculated by using the following equation; LOD = 3.3σ/S. The lower limit of quantification or LLOQ was set equal to 10 σ/S, where σ is the standard error of the y-intercept and S is the slope of the calibration curve in unesterified plasma (obtained from linear regression analysis). This definition of LOD and LLOQ has been found to be more accurate for the quantification of endogenous metabolites, since it takes into consideration the background from the sample of interest which is reflected in the error of the y-intercept.

5.3.6 Accuracy

Accuracy was assessed by analyzing quality control samples spiked at three different concentrations in esterified plasma (authentic matrix). Also, the concentration of acylcarnitines in a derivatized pooled plasma sample was calculated using the calibration curves obtained in surrogate matrix and compared to results from a standard addition experiment performed on an aliquot of the same plasma sample. Finally, the results obtained from the plasma of ten healthy volunteers were compared to previously published values.

5.3.7 Stability

The stability of post-preparatory samples was assessed at three different temperature conditions; at room temperature, at 4 °C and after three freeze-thaw cycles at -20 °C. Three low-concentration QC sample aliquots analyzed immediately after sample preparation were used as controls. Three sample aliquots were left at room temperature for four hours which was the maximum time needed to prepare samples (including solvent evaporation in a liquid concentrator). Another set of experimental replicates were stored at 4 °C for 18 hours which was the longest period of time a particular sample would remain in the autosampler of the LC system pending analysis. A last set of aliquots were analyzed after each of three 3 freeze-thaw cycles that were performed at 18-hour intervals.

5.3.8 Absolute quantification

A total of 15 internal standards were prepared by esterifying an acylcarnitine standard stock solution with heavy-labeled ethanol. The final concentration of IS used for each compound varied and was determined by the endogenous amount of the compound present in the plasma sample (in order to avoid signal suppression of the internal standard by the analyte itself). The final concentration of internal standards in the samples was 0.1 μM for all acylcarnitines except C2, C3 and C4s (which were at 0.5, 0.25 and 0.5 μM, respectively). Absolute quantification was performed using multiple-point calibration curves prepared in the surrogate matrix.

5.3.9 Relative quantification

There were certain acylcarnitines detected in plasma for which there are no commercially available standards. In order to perform relative quantification of these compounds, a specific internal standard was assigned to each of them according to retention time. Table 5.10 is a list of each compound and the internal standard used. These compounds were quantified using the calibration curve corresponding to the internal standard chosen. Using this method, and additional

19 acylcarnitine species were semi-quantified. Only acylcarnitines which were in high enough concentration to provide good quality MS/MS spectra were quantified.

5.4 Results and Discussion

5.4.1 Challenges of analyzing plasma acylcarnitines

The main challenge of analyzing acylcarnitines in plasma is the wide range of hydrophobicities found in this family of compounds. First, it is difficult to find a solvent that will dissolve all species to the same extent; inevitably some species will dissolve in the chosen solvent better than others. The percentage of organic solvent used has to be low enough in order to avoid peak broadening of early-eluting species in the chromatographic separation, while still being high enough to adequately dissolve long-chain acylcarnitines. It was found that 50% I in H_2O was an adequate solvent. The wide range of hydrophobicities also played a role when optimizing ESI as well as MS parameters, it was found that hydrophilic species required different ESI and MS conditions compared to hydrophobic ones, it was therefore necessary to find conditions that will satisfy the requirements of all species.

Another challenge that was encountered when analyzing acylcarnitines in plasma is carryover both in the LC system as well as in the C_{18} column used. Thirty second needle washes using a solution of isopropanol and acetonitrile (40:60 v/v respectively) were performed before every injection. Also, a wash step with 100% B was found to be needed at the end of every chromatographic run. Additionally, a 30 min isopropanol/acetonitrile wash (40:60 v/v respectively) was performed after every 30 injections in order to wash off any hydrophobic compounds (mainly lipids and some proteins) that may have been tightly bound to the C_{18} column during analysis.

5.4.2 Metabolite extraction efficiency studies

Protein precipitation was performed before esterification as part of the sample preparation protocol employed; it was therefore necessary to assess the recovery of acylcarnitines during this step. It was not possible to do this by spiking heavy-labeled acylcarnitine ethyl esters into the plasma sample before sample preparation since the internal standards are already esterified and undergoing a second esterification reaction would cause hydrolysis of both ester linkages present in these compounds. Moreover, $^{13}C_2$-labeled species are required as internal standards. Instead, three deuterated standards C3-d_3, C10-d_3 and C16-d_3 (one short, one medium and one long-chain) were used as surrogate analytes to assess analyte recovery during the protein precipitation procedure. A QC-low and a QC-high sample were spiked with the deuterated standards before and after protein precipitation (prepared in triplicates). Both sets of replicates were esterified in parallel and were then spiked with the $^{13}C_2$-labeled internal standards. Percent recovery was calculated as the peak area ratio of the deuterated standard to the internal standard when spiked before protein precipitation divided by peak area ratio when spiked after protein precipitation and multiplied by 100%. Percent recoveries ranged between 93 to 109% for all three compounds at both concentrations. The results for all three analytes are summarized in Table 5.1.

Table 5.1 Analyte recovery upon protein precipitation (results based on three experimental replicates).

AC	**% Recovery**	
	QC-low (C2: 0.2 µM, others: 0.04 µM)	QC-high (C2: 2 µM, others: 0.4 µM)
C3-d_3	96 ± 7	107 ± 8
C10-d_3	100 ± 7	109 ± 7
C16-d_3	93 ± 6	98 ± 10

5.4.3 Calibration curves and matrix effects

Calibration curves were constructed in underivatized plasma for all 15 acylcarnitines. All calibration curves contained at least 5 points with each point containing five replicates. Table 5.2 summarizes all the linear regression analysis results. Average precision refers to the average precision for the entire calibration range. Sample calibration curves can be found in the Appendix Section 5.1, the complete set of calibration curves are included in the electronic Appendix. A summary of linear regression data can be found in Appendix Section 5.2.

In order to assess matrix effects, calibration curves constructed in neat solvents and unesterified plasma were compared. Matrix effects were calculated using Equation 5.1 and expressed in terms of slope enhancement and/or suppression. Most species displayed a reduced calibration curve slope in plasma as compared to neat solvents, especially the short- and medium-chain species. Table 5.3 summarizes the results.

With the purpose of assessing the suitability of underivatized plasma as a surrogate matrix, the calibration curve slopes in surrogate and authentic matrix were compared using a specialized Student's t test.[17] All calculated t values were lower than the critical values at the 95% confidence interval which demonstrates that underivatized plasma is a suitable surrogate matrix for this method. Results for the Student's t test are presented in Table 5.4. The accuracy of the calibration curves prepared in surrogate matrix was further assessed by comparing the results obtained with this approach with those from a standard addition experiment.

Table 5.2 Summary of linear regression for calibration curves prepared in surrogate matrix.

AC	Calibration equation	Linear range (µM)	Linearity (R^2)	Average precision (CV %)	LOD (µM)	LLOQ (µM)
C2	y= 0.51x +0.007	0.025-2.5	0.997	6.6	0.026	0.077
C3	y= 0.90x + 0.002	0.005-0.5	0.994	8.8	0.007	0.020
C4-I	y= 0.63x + 0.003	0.005-0.5	0.995	11.9	0.006	0.018
C4	y= 0.90x + 0.005	0.005-0.5	0.998	9.6	0.004	0.013
Pivaloyl	y= 4.4x + 0.013	0.005-0.5	0.998	8.6	0.004	0.013
2MBC	y= 4.15x + 0.014	0.005-0.5	0.998	9.6	0.004	0.012
C5-I	y= 3.73x + 0.016	0.005-0.5	0.997	11.1	0.005	0.015
C5	y= 4.1x + 0.012	0.005-0.5	0.996	10.6	0.006	0.017
C6	y= 4.20x + 0.009	0.005-0.5	0.999	5.9	0.003	0.009
C8	y= 7.4x + 0.03	0.005-0.5	0.997	7.8	0.005	0.02
C10	y= 6.6x + 0.026	0.005-0.5	0.998	5.9	0.004	0.013
C12	y= 8.1x + 0.061	0.005-0.5	0.999	7.1	0.003	0.010
C14	y= 9.0x + 0.03	0.005-0.5	0.998	6.1	0.004	0.01
C16	y= 11.7x + 0.04	0.01-0.25	0.991	8.0	0.009	0.03
C18	y= 12.8x – 0.01	0.01-0.25	0.999	6.3	0.003	0.010

Table 5.3 Comparison of slopes of calibration curves in solvent and plasma.

AC	Sensitivity (μM^{-1}) in solvent	Sensitivity (μM^{-1}) in plasma	Suppression (-) or enhancement (+) (%)
C2	1.59	0.51	-68.1
C3	7.1	0.90	-87.4
C4-I	1.74	0.63	-63.8
C4	1.85	0.90	-51.4
Pivaloyl	9.0	4.4	-50.8
2MBC	7.6	4.15	-45.1
C5-I	8.3	3.73	-54.8
C5	9.4	4.1	-56.7
C6	7.6	4.20	-45.0
C8	9.5	7.4	-22.0
C10	7.5	6.6	-11.4
C12	6.7	8.1	17.2
C14	7.4	9.0	21.4
C16	11.5	11.7	1.7
C18	20.1	12.8	-36.3

Table 5.4 Comparison of response in surrogate and in authentic matrix.

AC	Slope in authentic matrix	Slope in surrogate matrix	Degrees of freedom	Calculated t value	Tabulated t value (95% C.I)
C2	0.52	0.51	11	0.362	2.201
C3	0.89	0.90	11	0.364	2.201
C4-I	0.63	0.63	11	0.088	2.201
C4	0.89	0.90	11	0.676	2.201
Pivaloyl	4.5	4.4	11	0.356	2.201
2MBC	4.17	4.15	11	0.398	2.201
C5-I	3.77	3.73	11	0.735	2.201
C5	4.1	4.1	11	0.344	2.201
C6	4.15	4.20	11	0.0317	2.201
C8	7.3	7.4	11	1.5475	2.201
C10	6.6	6.6	11	0.012	2.201
C12	8.1	8.1	11	0.943	2.201
C14	8.9	9.0	11	-1.656	2.201
C16	11.7	11.7	8	0.040	2.262
C18	12.8	12.8	8	0.325	2.262

5.4.4 Intra-day and inter-day precision

Intra-day reproducibility was assessed by analyzing the same esterified pooled plasma sample ten times (n = 10). The inter-day precision was calculated by analyzing that same sample 10 times per day over a three day period (n = 30). The CV for intra-day precision was found to be less than 9%, while that for inter-day precision was less than 10%. Table 5.5 summarizes the results. Pivaloylcarnitine and valerylcarnitine were found to be below the LLOQ.

Table 5.5 CVs (%) upon analysis of a pooled plasma sample analyzed 10 times per day over a three day period.

AC	**Intra-day precision (% CV) *n=10***	**Inter-day precision (% CV) *n=30***
C2	4.6	6.2
C3	5.3	5.6
C4-I	8.0	8.6
C4	7.0	9.2
Pivaloyl	<LLOQ	<LLOQ
2MBC	6.1	7.8
C5-I	8.8	9.7
C5	<LLOQ	<LLOQ
C6	4.9	4.9
C8	5.2	5.9
C10	3.8	5.4
C12	6.1	5.5
C14	6.7	6.8
C16	4.6	6.4
C18	4.7	7.7

5.4.5 Accuracy

5.4.5.1 Comparison to standard addition

Accuracy was assessed by calculating the concentration of acylcarnitine ethyl esters in a pooled plasma sample both by standard addition and by using the calibration equations constructed in surrogate matrix. The percent relative error was calculated by subtracting the concentration obtained by standard addition from that obtained by using the calibration equation, dividing by the latter and multiplying by 100%. The RE values were within ± 13% in all cases except 2MBC which was 21.2%. The results are summarized Figure 5.1 and Table 5.6.

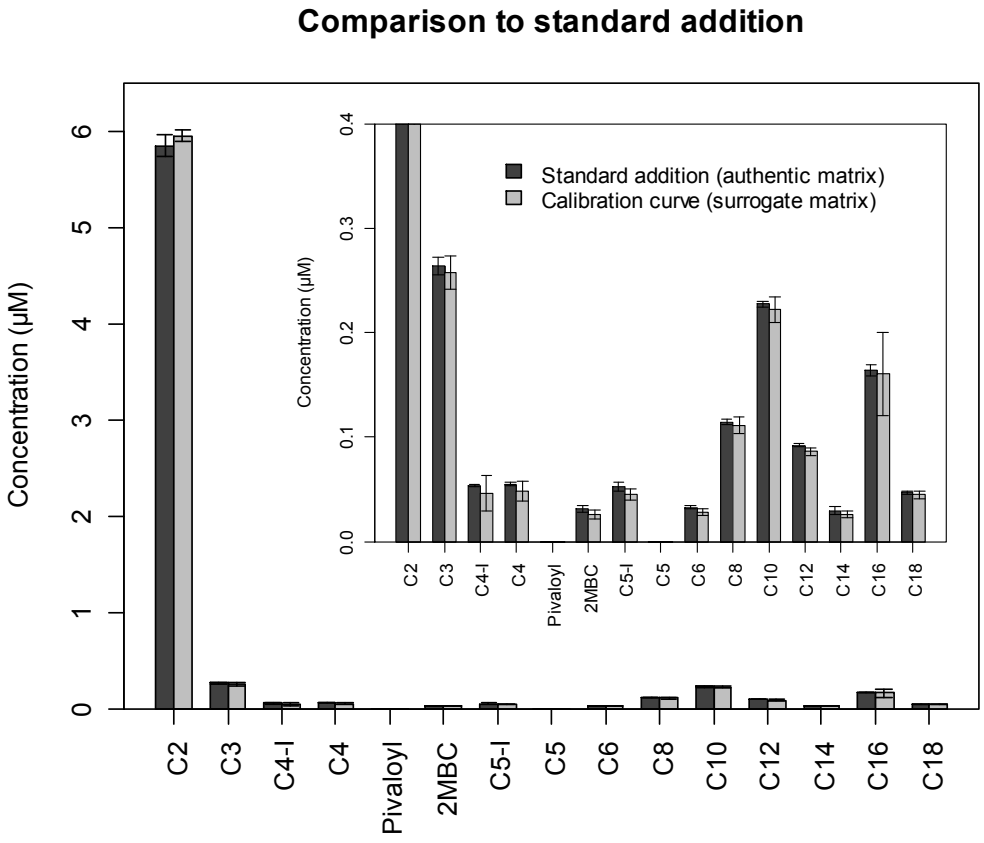

Figure 5.1 Comparison to standard addition. Acylcarnitines in a pooled plasma sample were quantified using a standard addition approach as well as using the calibration curves constructed in surrogate matrix. The insert shows a zoomed-in region of the bar chart.

Table 5.6 Comparison to standard addition.

AC	Concentration (µM) (By standard addition in authentic matrix)	Concentration (µM) (Calibration curve in surrogate matrix)	% RE
C2	5.9 ± 0.1	5.96 ± 0.05	1.0
C3	0.264 ± 0.008	0.26 ± 0.02	- 1.5
C4-I	0.054 ± 0.001	0.05 ± 0.02	- 7.4
C4	0.055 ± 0.002	0.05 ± 0.01	- 9.1
Pivaloyl	<LLOQ	<LLOQ	N/A
2MBC	0.033 ± 0.003	0.026 ± 0.004	- 21.2
C5-I	0.052 ± 0.004	0.046 ± 0.006	- 11.5
C5	<LLOQ	<LLOQ	N/A
C6	0.033 ± 0.002	0.029 ± 0.003	- 12.1
C8	0.115 ± 0.003	0.111 ± 0.008	- 3.4
C10	0.228 ± 0.003	0.22 ± 0.01	- 3.5
C12	0.093 ± 0.002	0.087 ± 0.004	- 6.4
C14	0.030 ± 0.003	0.026 ± 0.003	- 13.3
C16	0.164 ± 0.005	0.16 ± 0.04	- 2.4
C18	0.047 ± 0.001	0.045 ± 0.004	- 4.3

5.4.5.2 QC sample accuracy

Quality control samples were prepared in authentic matrix at three different concentrations. The QC-low sample was prepared at 0.04 µM except for C2 which was spiked at 0.2 µM, the QC-mid sample was prepared at 0.2 µM except for C2 which was spiked at 1 µM and finally the QC-high sample was prepared at 0.4 µM except for C2 which was spiked at 2 µM. Each sample was analyzed five times. All % CVs were less than 11%. All % Res were found to be less than 12%. QC-high was outside the linear dynamic range for C16 and C18; these compounds were thus not quantified at this concentration. Moreover, the concentration of these compounds in the plasma of healthy individuals is well below 0.4 µM. The results are summarized in Table 5.7.

Table 5.7 Accuracy and precision of quality control samples. QC-high is outside the linear dynamic range for C16 and C18 and thus were not quantified.

AC	QC-low (C2: 0.2 µM, others: 0.04 µM)		QC-medium (C2: 1 µM, others: 0.2 µM)		QC-high (C2: 2 µM, others: 0.4 µM)	
	CV (%)	% RE	CV (%)	% RE	CV (%)	% RE
C2	7.3	-2.1	5.9	3.3	4.1	1.8
C3	5.0	11.1	3.5	7.7	7.4	9.4
C4-I	5.7	- 8.7	5.9	-7.9	4.6	0.2
C4	7.1	- 2.1	3.5	0.1	7.8	6.6
Pivaloyl	5.6	- 3.8	10.9	3.8	4.2	- 3.3
2MBC	8.1	2.2	6.6	10.0	7.8	7.7
C5-I	9.9	7.9	3.4	- 4.4	8.4	6.6
C5	7.5	- 7.8	7.6	-8.1	10.7	- 4.9
C6	5.7	- 1.4	5.6	- 5.8	3.4	- 8.5
C8	4.1	3.3	6.0	8.3	4.4	- 5.1
C10	2.2	2.6	2.9	8.3	4.0	8.9
C12	3.4	- 9.9	2.0	7.1	3.5	4.3
C14	2.6	- 9.4	2.4	8.6	4.7	10.8
C16	4.1	7.2	3.3	- 4.5	N/A	N/A
C18	6.4	7.9	2.2	5.3	N/A	N/A

5.4.5.3 Comparison to previously reported values

The concentration ranges obtained from the analysis of plasma samples from ten healthy individuals were compared to previously published values of plasma acylcarnitines in healthy volunteers. The values obtained from this study correlated well with the values reported by Maeda *et al.*[18] and Ghoshal *et al.*[19] as can be observed in Table 5.8. The concentration range for all analytes was found to be within the reference limits reported by Minkler *et al*.[20] (using a cohort of 1748 samples) except those for C8, C10, C12 and C14 which were marginally higher.

Table 5.8 Comparison to previously reported values. The number of volunteers is given in brackets.

AC	Maeda *et al.*[18] (µM) *(n=5)*	Minkler *et al.*[20] (µM) *(n=1748)*	Ghoshal *et al.*[19] (µM)	Zuniga *et al.* (µM) *(n=10)*
C2	4.88 – 10.9	3.01-13.5	9.37	0.50 – 13.2
C3	0.22 – 31.8	<0.64	1.07	0.046 – 0.22
C4-I	0.05 – 0.13	<0.21	N/A	<LLOQ – 0.066
C4	<LLOQ – 0.17	<0.23	0.29	<LLOQ – 0.060
Pivaloyl	N/A	N/A	N/A	<LLOQ
2MBC	<LLOQ – 0.14	<0.09	N/A	<LLOQ – 0.031
C5-I	<LLOQ – 0.10	<0.13	0.15	<LLOQ – 0.044
C5	<LLOQ	<0.03	N/A	<LLOQ
C6	<LLOQ – 0.17	<0.12	0.06	<LLOQ – 0.067
C8	<LLOQ – 0.18	<0.24	0.14	0.013 – 0.25
C10	N/A	<0.33	0.30	0.058 – 0.54
C12	N/A	<0.12	0.09	0.020 – 0.19
C14	N/A	<0.05	0.04	<LLOQ – 0.075
C16	N/A	<0.16	0.15	0.037 – 0.15
C18	N/A	<0.07	0.02	0.014 – 0.066

5.4.6 Stability

The stability of a QC-low sample was assessed under several storage conditions described under the method validation section. Figure 5.2 shows that the percent change under all conditions was found to be within ± 15% with the exception of C2 upon storage at -20 °C for two weeks. This suggests that the stability of acylcarnitine ethyl esters in plasma is suitable for the purposes of this study.

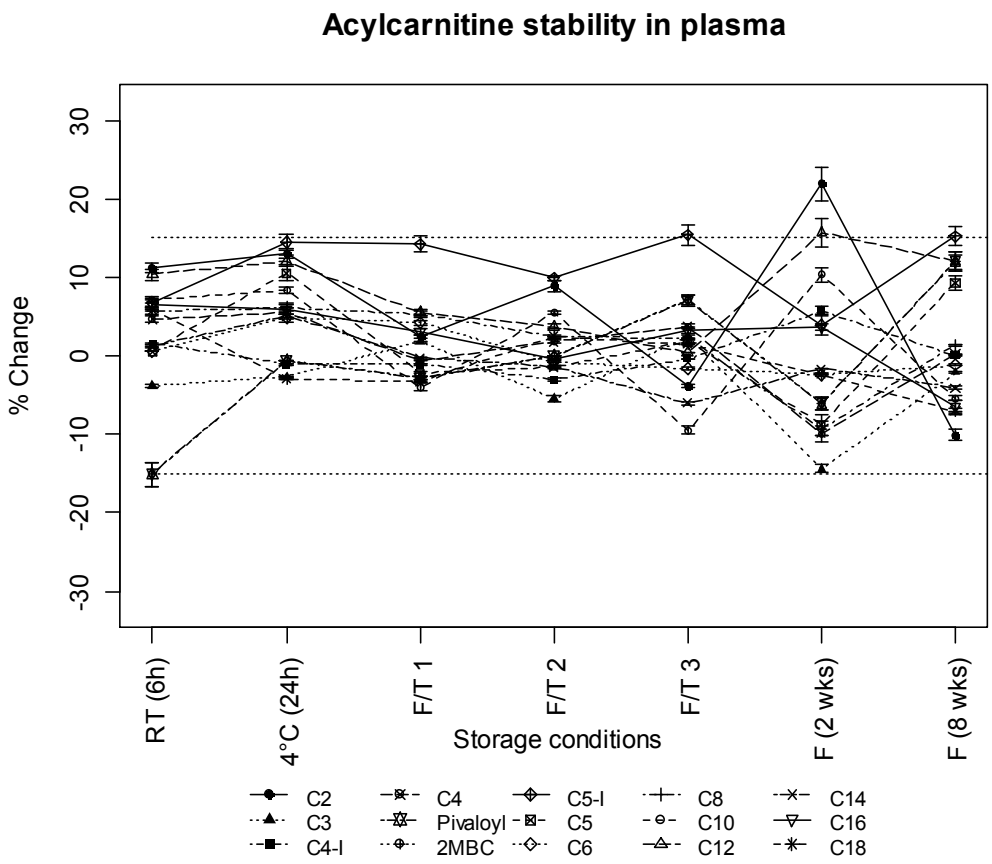

Figure 5.2 Acylcarnitine stability. The stability of a QC-low sample was analyzed under several conditions. RT (6h), room temperature for 6 hours; 4°C (24h), 4°C for 24h; F/T 1, first freeze/thaw cycle; F/T 2, second freeze/thaw cycle; F/T 3, third freeze/thaw cycle; F (2 wks), frozen for 2 weeks; F (8 wks), frozen for 8 weeks. The dotted lines represent ±15%.

5.4.7 Acylcarnitine profile in ten healthy individuals

5.4.7.1 Long- and very long-chain acylcarnitines

Several long and very long-chain acylcarnitine species were either found in very low abundance or not detected at all in the plasma samples analyzed. These highly hydrophobic species are known to interact with hydrophobic proteins as well as with the membranes of red blood cells. It was thus speculated that these species were probably lost in the centrifugation step. In order to confirm this speculation, upon centrifugation of a whole blood sample, the red blood cell

(RBC) pellet was washed with methanol and analyzed using a high-throughput 15-min UHPLC-MS/MS method that was optimized for long-chain acylcarnitines species. Many of these species were found in higher abundance in the RBC pellet as compared to plasma. Figure 5.3 is an overlay of the total ion chromatogram (TIC) from the analysis of the RBC pellet and that of the analysis of a plasma sample. Species ranging from C16 to C22:5 were considerably higher in the RBC pellet than in plasma. Further analysis of RBC pellets was not undertaken due to the possible damage that they may have on reversed phase columns, especially C_{18} columns. It was found that the column performance suffered even with the use of a guard column and after thorough column regeneration.

5.4.7.2 Absolute quantification

Absolute quantification was performed on 13 acylcarnitines for which standards were commercially available. Free carnitine (C0) was not quantified using this method since the esterification reaction conditions utilized were found to be harsh enough to hydrolyze the ester linkage already present in acylcarnitines. The free carnitine produced due to hydrolysis would cause an overestimation of the endogenous free carnitine in the samples. Please refer to Chapter 4 Sections 4.3.1 and 4.4.4 for more details. Calibration curves constructed in unesterified plasma were utilized for this purpose. All plasma samples were prepared and analyzed in triplicate. Pivaloylcarnitine as well as valerylcarnitine were found to be below the LLOQ. A sample of the absolute quantification of C2 in all individuals can be found in Appendix Section 5.3. A detailed summary of the rest of the absolute quantification results can be found in the electronic Appendix. There was no major variation found in the plasma acylcarnitine profile among individuals, with the exception of individual 9 (a female) which had consistently higher concentrations of these 13 acylcarnitines.

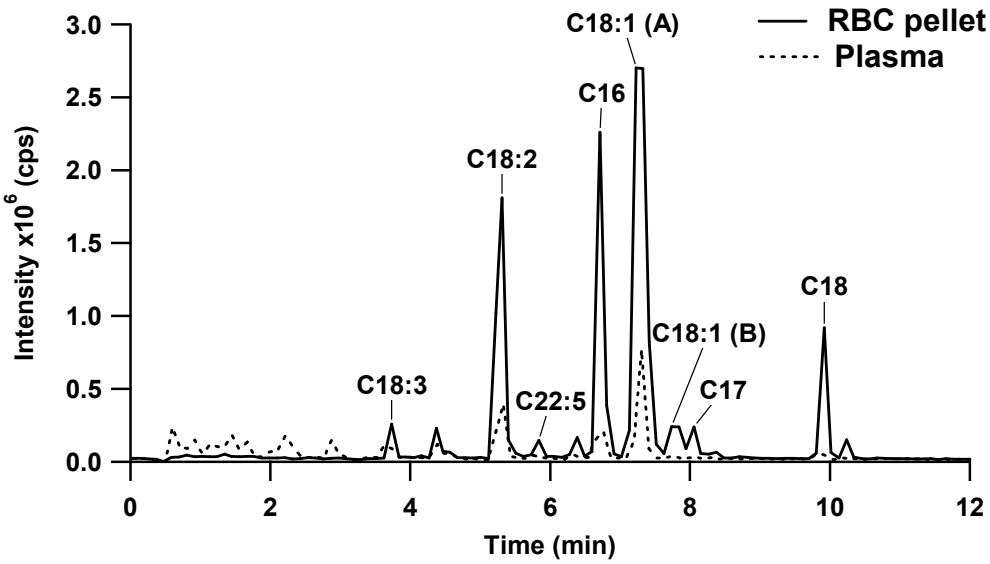

Figure 5.3 Long and very long-chain acylcarnitines. Overlay of two Total Ion Chromatograms (TICs), one from red blood cell (RBC) pellet analysis and the second from plasma analysis. Due to their interaction with red blood cells (RBCs), upon centrifugation of whole blood, hydrophobic species were more abundant in the RBC pellet than in plasma.

5.4.7.3 Effect of gender

The results from the absolute quantification experiments were further analyzed in order to investigate the effect of gender on the plasma acylcarnitine profile of healthy individuals. It was found that acetylcarnitine was generally higher in females than in males; however, due to the wide range of concentrations (0.68 - 13.24 μM) within females, this difference was not found to be statistically significant. Overall, there was no statistically significant difference found due to differences in gender (according to a two-tailed t-test at the 95% confidence limit). Figure 5.4 and Table 5.9 summarize the results.

Table 5.9 Effect of gender on acylcarnitine profile.

AC	Concentration range (µM)	
	Female *(n=5)*	Male *(n=5)*
C2	0.69 - 13.24	0.50 - 1.96
C3	0.046 - 0.22	0.067 - 0.18
C4-I	0.010 - 0.066	<LLOQ - 0.031
C4	<LLOQ - 0.060	<LLOQ - 0.019
Pivaloyl	<LLOQ	<LLOQ
2MBC	<LLOQ - 0.031	<LLOQ - 0.023
C5-I	<LLOQ - 0.031	0.010 - 0.044
C5	<LLOQ	<LLOQ
C6	0.015 - 0.067	<LLOQ - 0.016
C8	0.078 - 0.25	0.013 - 0.091
C10	0.14 - 0.54	0.058 - 0.21
C12	0.036 - 0.19	0.020 - 0.085
C14	<LLOQ - 0.075	<LLOQ - 0.016
C16	0.037 - 0.15	0.046 - 0.080
C18	0.014 - 0.066	0.015 - 0.027

5.4.7.4 Relative quantification

Nine-teen acylcarnitines for which there are no commercial synthetic standards available were semi-quantified. Internal standards were assigned to each analyte based on retention time since electrospray response is directly related to a compounds' hydrophobicity. Table 5.10 shows quantified compounds along with the internal standard used. Some of the reported values were marginally lower than their respective LLOQs; however, all signal to noise ratios were higher than 10 and the % CVs were within acceptable limits (± 15%). The results of the relative quantification experiments for individual 9 can be found in Appendix Section 5.4, the full version of the results including data from all 10 individuals can be found in the electronic Appendix.

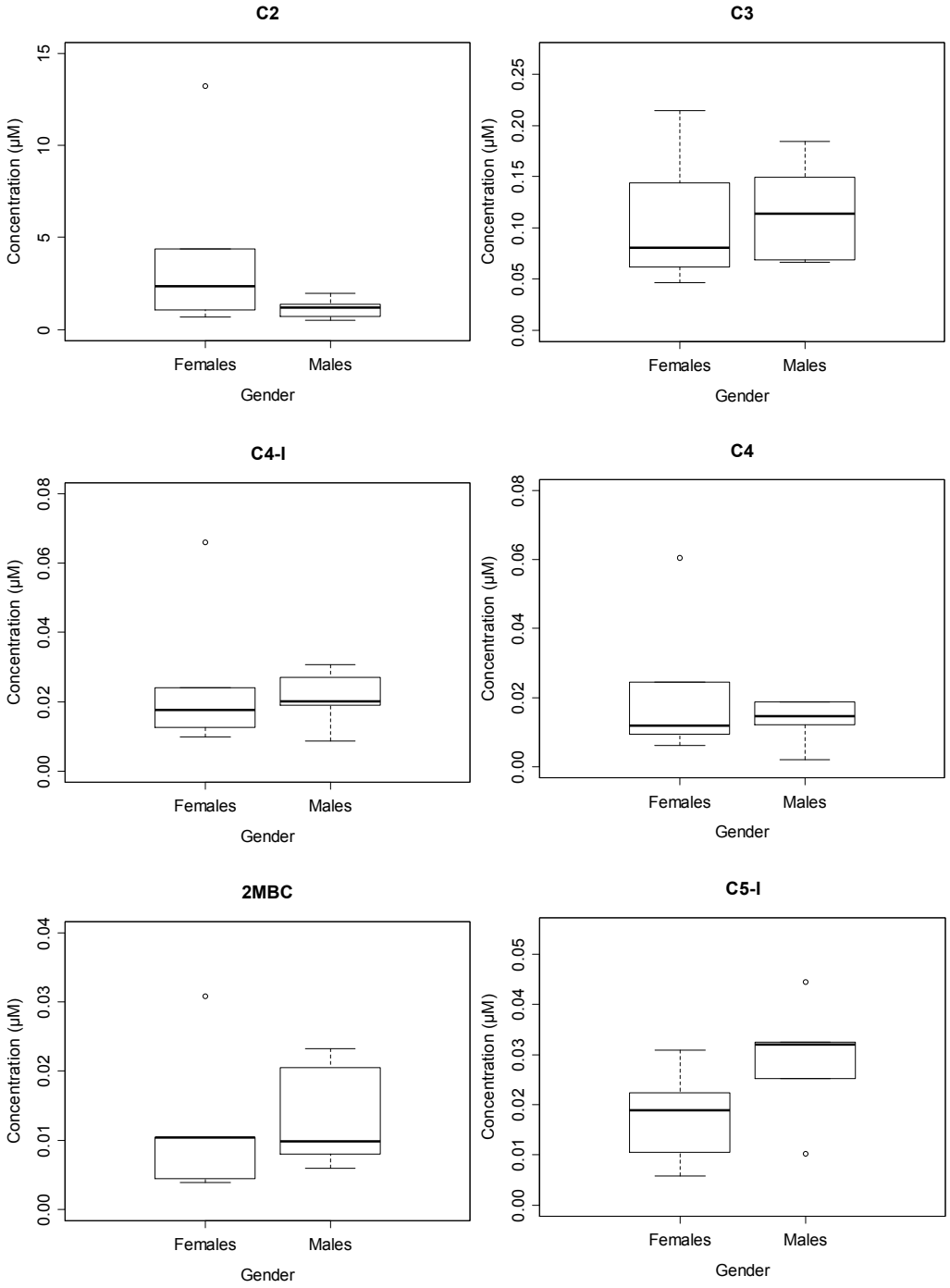

Figure 5.4 Effect of gender. The plasma of 5 male and 5 female samples were analyzed. Box plots were created for all acylcarnitines for which standards are available except pivaloylcarnitine and valerylcarnitine since they were below the LLOQ. The horizontal line inside each box represents the median. Possible outliers are displayed as empty circles (± 1.5x inter-quartile range).

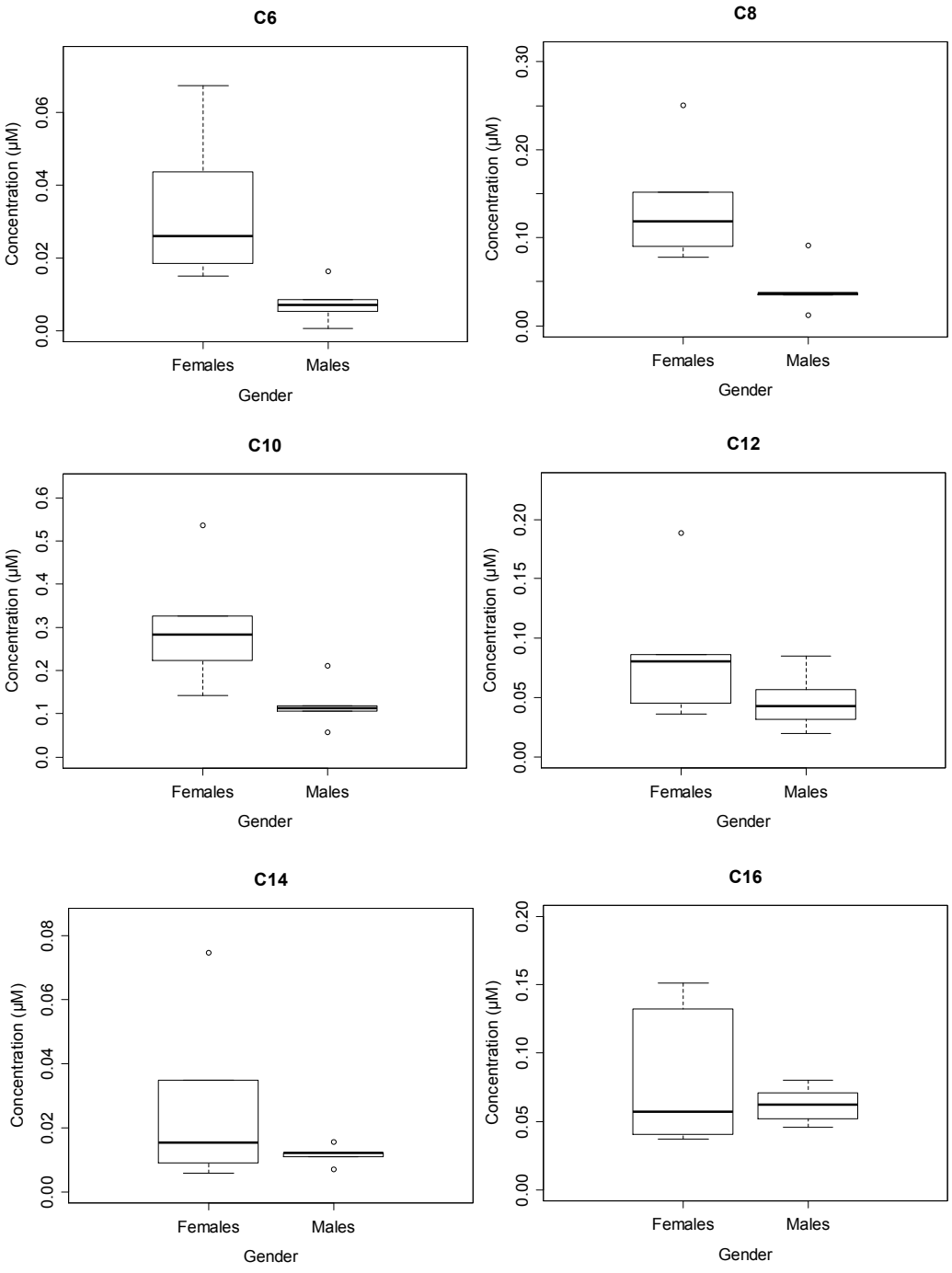

Figure 5.5 Effect of gender (continued). The plasma of 5 male and 5 female samples were analyzed. Box plots were created for all acylcarnitines for which standards are available except pivaloylcarnitine and valerylcarnitine since they were below the LLOQ. The horizontal line inside each box represents the median. Possible outliers are displayed as empty circles (± 1.5x inter-quartile range).

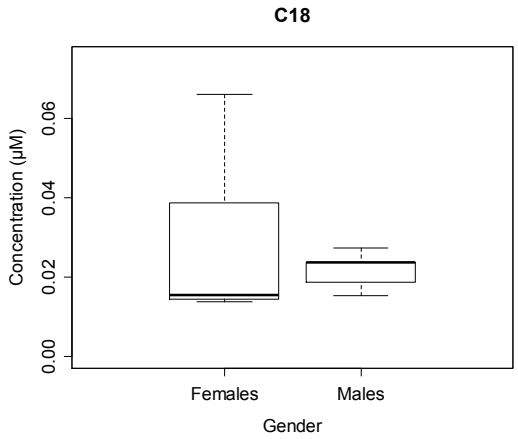

Figure 5.6 Effect of gender (continued). The plasma of 5 male and 5 female samples were analyzed. Box plots were created for all acylcarnitines for which standards are available except pivaloylcarnitine and valerylcarnitine since they were below the LLOQ. The horizontal line inside each box represents the median. Possible outliers are displayed as empty circles (± 1.5x inter-quartile range).

The relative quantification data revealed that Individual 9 (a female) again had consistently higher plasma acylcarnitine concentrations than the rest of the volunteers (regardless of gender). Factors such as diet or physical activity are known to influence acylcarnitine patterns[21-23] so there is a possibility that these factors could be the cause of the differences observed. However, all volunteers that participated in this study remained anonymous; it was therefore not possible to obtain any additional information from the volunteers regarding diet or general lifestyle. As a result, no definitive explanation to these findings was obtained.

Table 5.10 Internal standard assignment.

AC (*m/z*)	RT (min)	IS used
284	0.98	C3
304	1.10	C3
272	1.62	C4-I
332 (A)	1.96	C4-I
332 (B)	4.41	C6
332 (C)	5.29	C6
360 (A)	5.38	C6
412	5.53	C6
360 (B)	5.90	C6
388	10.62	C8
360 (C)	10.88	C8
330 (A)	11.97	C8
330 (B)	12.20	C8
342	12.75	C8
416 (A)	13.20	C10
416 (B)	13.40	C10
358	14.39	C12
386	16.33	C14
454	19.97	C16

Table 5.11 is a list of all quantified acylcarnitine ethyl esters (AC EEs) with retention time (RT) information as well as their putative identification. The number following the letter C corresponds to the number of carbon atoms in the organic acid chain conjugated to carnitine. The nomenclature "+OH" corresponds to a hydroxyl group added to the organic acid chain conjugated to carnitine. A dicarboxylic acid carnitine conjugate is described as ": DC". Finally, a colon

followed by a number corresponds to the degrees of unsaturation along the organic acid chain (for example :1 corresponds one degree of unsaturation).

An MS/MS spectral library including common fragment ions for all quantified acylcarnitines was also included in the electronic Appendix. Four representative annotated MS/MS spectra are included in Appendix Section 5.5.

Table 5.11 Putative identification of all quantified metabolites.

AC EE (*m/z*)	AC (*m/z*)	RT (min)	Putative ID
232	204	0.61	C2 (confirmed with standard)
246	218	0.77	C3 (confirmed with standard)
260 (A)	232	1.22	C4-I (confirmed with standard)
260 (B)	232	1.28	C4 (confirmed with standard)
272	244	1.62	C5:1-M (3-methylcrotonyl) or C5:1-T (tiglyl)
274 (A)	246	2.09	2MBC (confirmed with standard)
274 (B)	246	2.27	C5-I (confirmed with standard)
284	256	0.98	
288	260	4.58	C6 (confirmed with standard)
304	276	1.10	C5:DC
316	288	11.31	C8 (confirmed with standard)
330 (A)	302	11.97	C9 isomer
330 (B)	302	12.20	C9
332 (A)	304	1.96	Doubly labeled C5:DC
332 (B)	304	4.41	Doubly labeled C5:DC (isomer)
332(C)	304	5.29	
342	314	12.75	C10:1
344	316	13.74	C10 (confirmed with standard)
358	330	14.39	C11
360 (A)	304	5.39	Doubly labeled C7:DC (isomer)
360 (B)	304	5.90	Doubly labeled C7:DC (isomer)
360 (C)	332	10.88	C10+OH
372	344	15.71	C12 (confirmed with standard)
386	358	16.33	
388	360	10.62	C12+OH
400	372	17.65	C14 (confirmed with standard)
412	384	5.53	
416 (A)	388	13.00	C14+OH

416 (B)	388	13.40	C14+OH (isomer)
428	400	19.35	C16 (confirmed with standard)
454	426	19.97	C18:1
456	428	21.11	C18 (confirmed with standard)

5.5 Conclusions

An accurate and precise UHPLC-MS/MS method for the quantification of plasma acylcarnitines was developed. A fast and robust esterification reaction was used to introduce a light or heavy label in order to obtain a series of acylcarnitine ethyl ester standards and their respective $^{13}C_2$- labeled internal standards (without the need to buy a separate set of internal standards). A surrogate approach was employed were unesterified plasma was used as a surrogate matrix to build calibration curves. The plasma of ten healthy volunteers was analyzed in triplicate with results that correlated well with previously published values. A total of 32 acylcarnitines species were quantified. An advantage of this method is the use of ^{13}C instead of ^{2}H labels avoiding the occurrence of isotope effect at the chromatographic level. Moreover, the addition of a small labeling group such as an ethyl group has the advantage of not changing the fragmentation patterns of acylcarnitines which allows for the identification of novel acylcarnitine species. Using this method, detection of novel isomers of unsaturated medium-chain species was accomplished. An additional advantage is the use of actual human urine (unesterified) as a surrogate matrix instead of utilizing commonly used ones such as synthetic urine or a bovine serum albumin solution, which only attempt to mimic real human urine. This method could be useful for biomarker discovery studies for diseases such as diabetes mellitus type II and biotin deficiency.

5.6 Literature cited

(1) Hove, J. L. K.; Chace, D. H.; Kahler, S. G.; Millington, D. S. *Journal of Inherited Metabolic Disease* **1993**, *16*, 361-367.

(2) Chace, D. H.; Hillman, S. L.; Van Hove, J. L. K.; Naylor, E. W. *Clinical Chemistry* **1997**, *43*, 2106-2113.

(3) Bennett, M. J.; Coates, P. M.; Hale, D. E.; Millington, D. S.; Pollitt, R. J.; Rinaldo, P.; Roe, C. R.; Tanaka, K. *Journal of Inherited Metabolic Disease* **1990**, *13*, 707-715.

(4) Millington, D. S.; Kodo, N.; Norwood, D. L.; Roe, C. R. *Journal of Inherited Metabolic Disease* **1990**, *13*, 321-324.

(5) Stratton, S. L.; Horvath, T. D.; Bogusiewicz, A.; Matthews, N. I.; Henrich, C. L.; Spencer, H. J.; Moran, J. H.; Mock, D. M. *The American Journal of Clinical Nutrition* **2010**, *92*, 1399-1405.

(6) Ganti, S.; Taylor, S. L.; Kim, K.; Hoppel, C. L.; Guo, L.; Yang, J.; Evans, C.; Weiss, R. H. *International Journal of Cancer* **2011**, *In Press*.

(7) Adams, S. H.; Hoppel, C. L.; Lok, K. H.; Zhao, L.; Wong, S. W.; Minkler, P. E.; Hwang, D. H.; Newman, J. W.; Garvey, W. T. *The Journal of Nutrition* **2009**, *139*, 1073-1081.

(8) Mihalik, S. J.; Goodpaster, B. H.; Kelley, D. E.; Chace, D. H.; Vockley, J.; Toledo, F. G. S.; DeLany, J. P. *Obesity* **2010**, *18*, 1695-1700.

(9) Miyagawa, T.; Miyadera, H.; Tanaka, S.; Kawashima, M.; Shimada, M.; Honda, Y.; Tokunaga, K.; Honda, M. *SLEEP* **2011**, *34*, 349-353.

(10) Famularo, G.; de Simone, C.; Trinchieri, V.; Mosca, L.; Blackwell Publishing Ltd, 2004; Vol. 1033, pp 132-138.

(11) Sowell, J.; Fuqua, M.; Wood, T. *Journal of Chromatographic Science* **2011**, *49*, 463-468.

(12) Pormsila, W.; Morand, R. j.; Krähenbühl, S.; Hauser, P. C. *Journal of Chromatography B* **2011**, *879*, 921-926.

(13) Corso, G.; D'Apolito, O.; Garofalo, D.; Paglia, G.; Dello Russo, A. *Biochimica et Biophysica Acta (BBA) - Molecular and Cell Biology of Lipids* **2011**, *1811*, 669-679.

(14) Mohamed S, R. *Journal of Chromatography B: Biomedical Sciences and Applications* **2001**, *758*, 27-48.

(15) Reuter, S. E.; Evans, A. M.; Chace, D. H.; Fornasini, G. *Annals of Clinical Biochemistry* **2008**, *45*, 585-592.

(16) Zuniga, A.; Li, L. *Analytica Chimica Acta* **2011**, *689*, 77-84.

(17) Zar, J. H. *Biostatistical Analysis*, 5th ed.; Pearson Prentice Hall: New Jersey, 2010.

(18) Maeda, Y.; Ito, T.; Suzuki, A.; Kurono, Y.; Ueta, A.; Yokoi, K.; Sumi, S.; Togari, H.; Sugiyama, N. *Rapid Communications in Mass Spectrometry* **2007**, *21*, 799-806.

(19) Ghoshal, A. K.; Guo, T.; Soukhova, N.; Soldin, S. J. *Clinica Chimica Acta* **2005**, *358*, 104-112.

(20) Minkler, P. E.; Stoll, M. S. K.; Ingalls, S. T.; Yang, S.; Kerner, J.; Hoppel, C. L. *Clinical Chemistry* **2008**, *54*, 1451-1462.

(21) Hoppel, C. L.; Genuth, S. M. *American Journal of Physiology - Endocrinology And Metabolism* **1980**, *238*, E409-E415.

(22) Cederblad, G. *The American Journal of Clinical Nutrition* **1987**, *45*, 725-729.

(23) Lehmann, R.; Zhao, X.; Weigert, C.; Simon, P.; Fehrenbach, E.; Fritsche, J.; Machann, J.; Schick, F.; Wang, J.; Hoene, M.; Schleicher, E. D.; Häring, H.-U.; Xu, G.; Niess, A. M. *PLoS ONE* **2010**, *5*, e11519.

Chapter 6

MyCompoundID: Using an Evidence-based Metabolome Library for Metabolite Identification*

6.1 Introduction

Metabolomics is a rapidly growing field which plays an important role in many areas of research, including the study of biological systems and biomarker discovery.[1, 2] Advances in metabolomics are largely driven by the development of new analytical techniques, such as liquid chromatography mass spectrometry (LC-MS) which are tailored to large scale profiling of the metabolome. The number of spectral features or detectable analytes in a biological sample has increased steadily in the past few years due to the introduction of sensitive LC-MS methods. Metabolite identification however, remains to be a major challenge.[3, 4] The vast majority of spectral features observed cannot be assigned unequivocally to known compounds.[5-7]

* A form of this chapter has been submitted for publication as: Liang Li, Jianjun Zhou, Azeret Zuniga *et al*. 2012, "MyCompoundID: Using an Evidence-based Metabolome Library for Metabolite Identification" My contribution to this work was the development of the LC-MS methods used to analyze samples, the performance assessment of the tool using the dataset obtained from the plasma sample, generation of tables and figures as well as editorial support.

One approach for metabolite identification is database searching. There are several metabolomics databases available in the public domain, including the Human Metabolome Database (HMDB)[8, 9], the METLIN Metabolite Database[10], the Madison Metabolomics Consortium Database (MMCD)[3] and MassBank.[11] Accurate mass searching is useful, but will not usually lead to a unique elemental formula. Even if a formula is deduced, many chemical structures can be proposed. On the other hand, spectral searching against a spectral library created from standard compounds of known structures can potentially result in definitive compound identification. Unfortunately, the availability of metabolite standards is limited. For example, for human endogenous metabolites, about 900 compounds are available commercially. NMR and MS/MS spectral libraries of these compounds are accessible from HMDB (www.hmdb.ca). However, compared to the current 8021 metabolite entries in HMDB (as of 2012) as well as tens of thousands of spectral features detectable from human biofluids by LC-MS, it is clear that these standards only cover a small fraction of the human metabolome.

In cases where standards are not available, an MS search can be used to screen for metabolite candidates from a library of compounds. In addition, the fragmentation pattern deduced from the MS/MS spectrum of the ion of interest can be interpreted against the structures of metabolite candidates. In some instances, this can narrow down the list of candidates into one or a few unique structures. If definitive identification is required, authentic standards may be synthesized for comparison. In cases where the standards of putatively identified metabolites are difficult to synthesize, the use of microsome- or other cell/tissue-based biotransformations of structurally related standards may be explored.[12] Reducing the number of possible metabolite candidates by combining accurate mass searching followed by MS/MS interpretation, or MS+MS/MS, is the main goal of the web-based tool (MyCompoundID) described herein.

The success of this MS+MS/MS approach for putative metabolite identification is, however, very much dependent on the size and quality of the metabolite library. Many compound databases such as the Kyoto Encyclopedia of

Genes and Genomes (KEGG)[13] contain a mixture of known metabolites and synthetic molecules. Most applications however, target the analysis of endogenous metabolites present in a biological sample. In an effort to expand current libraries of endogenous metabolites to achieve more possible hits, an evidence-based metabolome library (EML) has been constructed. This library is composed of known, previously-published metabolites as well as their possible metabolic products that are predicted based on biotransformation reactions commonly encountered in metabolism. The potential existence of the predicted metabolites in a given species is based on the fact that they are derived from known metabolites and metabolic reactions. The rationale is that a known metabolite can be involved in various metabolic reactions in biological systems, producing different metabolic products. Our hypothesis is that, by including as many metabolic products in the library as possible, many unknowns that are structurally related to known metabolites can potentially be identified using the MS+MS/MS approach. In this work, a web-based tool for metabolite identification built upon an evidence-based metabolite library is described.

6.2 Experimental

6.2.1 Creation and use of the metabolite library and web-based tool

The 8,021 entries in the HMDB were used to create the EML. Upon careful literature searching, 76 common metabolic reactions were identified and are listed in Table 6.1. Based on these reactions, *in silico* biotransformations of the 8,021 metabolites were performed. A product is generated with the addition or subtraction of an expected group (e.g., +O in oxidation or -O in de-oxidation) from the reactant; a known metabolite. Several possible structures of the product (such as isomers) could exist, but all with a characteristic mass shift from the added or subtracted group. Some redundancies could arise from this process which could be difficult to differentiate from unique entries in the library. However, after a mass search, these entries can be readily sorted out. The number

of new entries in EML with one metabolic reaction is 375,809; impossible transformations (e.g., -O from a metabolite containing no oxygen) have been excluded during the construction of the library. There is also an option of generating the library with two metabolic reactions [e.g., a metabolite undergoes methylation (+CH2) and then oxidation (+O) or a metabolite undergoes demethylation (-CH2) and then oxidation (+O)], which produces a library with 10,583,901 entries.

Table 6.1 List of common metabolic reactions.

Reaction	Mass Difference (Da)	Description
$-H_2$	-2.015650	dehydrogenation
$+H_2$	2.015650	hydrogenation
$-CH_2$	-14.015650	demethylation
$+CH_2$	14.015650	methylation
-NH	-15.010899	loss of NH
+NH	15.010899	addition of NH
-O	-15.994915	loss of oxygen
+O	15.994915	oxidation
$-NH_3$	-17.026549	loss of ammonia
$+NH_3$	17.026549	addition of ammonia
$-H_2O$	-18.010565	loss of water
$+H_2O$	18.010565	addition of water
-CO	-27.994915	loss of CO
+CO	27.994915	addition of CO
$-C_2H_4$	-28.031300	loss of C_2H_4
$+C_2H_4$	28.031300	addition of C_2H_4
$-C_2H_2O$	-42.010565	deacetylation
$+C_2H_2O$	42.010565	acetylation
$-CO_2$	-43.989830	loss of CO_2
$+CO_2$	43.989830	addition of CO_2
SO_3H->SH	-47.984745	sulfonic acid to thiol
SH->SO_3H	47.984745	thiol to sulfonic acid
$-C_2H_3NO$	-57.021464	loss of glycine
$+C_2H_3NO$	57.021464	glycine conjugation
$-SO_3$	-79.956817	loss of sulfate
$+SO_3$	79.956817	sulfate conjugation
$-HPO_3$	-79.966333	loss of phosphate

$+HPO_3$	79.966333	addition of phosphate
$-C_4H_3N_3$	-93.032697	loss of cytosine
$+C_4H_3N_3$	93.032697	addition of cytosine
$-C_4H_2N_2O$	-94.016713	loss of uracil
$+C_4H_2N_2O$	94.016713	addition of uracil
$-C_3H_5NOS$	-103.009186	loss of cysteine
$+C_3H_5NOS$	103.009186	cysteine conjugation
$-C_2H_5NO_2S$	-107.004101	loss of taurine
$+C_2H_5NO_2S$	107.004101	taurine conjugation
$-C_5H_4N_2O$	-108.032363	loss of thymine
$+C_5H_4N_2O$	108.032363	addition of thymine
$-(C_5H_5N_5 - H_2O)$	-117.043930	loss of adenine
$+(C_5H_5N_5 - H_2O)$	117.043930	addition of adenine
$-C_3H_5NO_2S$	-119.004101	loss of S-cysteine
$+C_3H_5NO_2S$	119.004101	S-cysteine conjugation
$-C_5H_8O_4$	-132.042260	loss of D-ribose
$+C_5H_8O_4$	132.042260	addition of D-ribose
$-C_5H_3N_5$	-133.038845	loss of guanine
$+C_5H_3N_5$	133.038845	addition of guanine
$-C_7H_{13}NO_2$	-143.094629	loss of carnitine
$+C_7H_{13}NO_2$	143.094629	addition of carnitine
$-C_5H_7NO_3S$	-161.014666	loss of N-acetyl-S-cysteine
$+C_5H_7NO_3S$	161.014666	addition of N-acetyl-S-cysteine
$-C_6H_{10}O_5$	-162.052825	loss of hexose
$+C_6H_{10}O_5$	162.052825	addition of hexose
$-C_6H_8O_6$	-176.032090	loss of glucuronic acid
$+C_6H_8O_6$	176.032090	addition of glucuronic acid
$-C_{10}H_{12}N_2O_4$	-224.079708	loss of thymidine
$+C_{10}H_{12}N_2O_4$	224.079708	addition of thymidine
$-C_9H_{11}N_3O_4$	-225.074957	loss of cytidine
$+C_9H_{11}N_3O_4$	225.074957	addition of cytidine
$-C_9H_{10}N_2O_5$	-226.058973	loss of uridine
$+C_9H_{10}N_2O_5$	226.058973	addition of uridine
$-C_{16}H_{30}O$	-238.229665	loss of palmitic acid
$+C_{16}H_{30}O$	238.229665	addition of palmitic acid
$-C_6H_{11}O_8P$	-242.019158	loss of glucose-6-phosphate
$+C_6H_{11}O_8P$	242.019158	addition of glucose-6-phosphate
$-C_{10}H_{11}N_5O_3$	-249.086190	loss of adenosine

$+C_{10}H_{11}N_5O_3$	249.086190	addition of adenosine
$-C_{10}H_{11}N_5O_4$	-265.081105	loss of guanosine
$+C_{10}H_{11}N_5O_4$	265.081105	addition of guanosine
$-C_{10}H_{15}N_3O_5S$	-289.073244	loss of glutathione
$+C_{10}H_{15}N_3O_5S$	289.073244	addition of glutathione
$-C_{10}H_{15}N_3O_6S$	-305.068159	loss of S-glutathione
$+C_{10}H_{15}N_3O_6S$	305.068159	addition of S-glutathione
$-C_{12}H_{20}O_{10}$	-324.105650	loss of di-hexose
$+C_{12}H_{20}O_{10}$	324.105650	addition of di-hexose
$-C_{18}H_{30}O_{15}$	-486.158475	loss of tri-hexose
$+C_{18}H_{30}O_{15}$	486.158475	addition of tri-hexose

In order to use the EML library for metabolite identification, a web-based search and data interpretation program called MyCompoundID (www.mycompoundid.org) has been developed. All known human endogenous metabolites are imported from the HMDB and stored in a local MySQL database. These metabolites and their one- or two-reaction products are indexed using the molecular masses up to the millionth precision. The web server for this tool was constructed within Apache using Java and JavaScript to ensure the most efficiency and the largest platform compatibility. The 76 commonly encountered metabolic reactions previously mentioned were implemented in the web server, which accepts single and batch queries with 0, 1 and 2 allowed metabolic reactions. Reactions where a certain atom or group is removed from the original structure are logically validated using the compound's MOL files. The web server interacts with the local computer to allow the users to exclude any output entry and to associate an output entry to any experimental evidence. Such post-curated query results can then be exported to a local archive. All these functions are enabled and efficiently executed in Java and JavaScript, with extendibility for further development.

The initial step when using MyCompoundID is to generate both MS and MS/MS spectra of a biological sample using one or more high performance mass spectrometers, such as a Time-of-flight (TOF) MS and a quadrupole linear trap (QTRAP®) tandem MS. Once the user is on the web interface, he/she may enter a

mass (either a single entry or multiple entries in batch mode) and a mass tolerance value determined by the mass accuracy of the instrument used. The next step is to select the reaction number (0, 1, or 2). The program searches the EML to find any matches of library entries with the query mass within the defined mass tolerance limits. The search results are displayed in an interactive table and the matched entries can be sorted (e.g. by increasing mass error). One important functionality of the program is the ability to upload the chemical structure of the parent metabolite into ChemDraw or a free-ware ChemDraw Plugin. Both ChemDraw and ChemDraw Plugin allow the user to add or subtract a reaction group in the uploaded structure to create a new one. Furthermore, the user can use the Mass fragmentation tool therein to break chemical bond(s) to generate fragment ion structures and obtain their masses. Using the MS/MS spectrum produced from the precursor ion of the query mass, the user can examine the spectral fragmentation pattern and compare it to the fragment ions generated by the Mass fragmentation tool. If the pattern matches, putative metabolite identification can be made on the query mass. A drawback of this approach is that the user must have some knowledge of common biotransformation reactions in order to add or subtract the required group from the right location on the reactant molecule (the known metabolite). Moreover, the user must also have experience with collision-induced fragmentation patterns of small molecules. However, if these requirements are met, MyCompoundID can dramatically speed up the time-consuming process of *de novo* MS/MS spectral interpretation.

To document the identification process, all metadata, including the structure of the proposed match, the experimental MS/MS spectrum, fragment ion structures and fragmentation pathways can be saved to the matched entry. Finally, the results can be exported to a spreadsheet for presentation and other uses. An example of the process described above as well as a detailed tutorial for the use of the program can be found in the electronic Appendix. Figure 6.1 is an overview of the strategy and workflow of MyCompoundID.

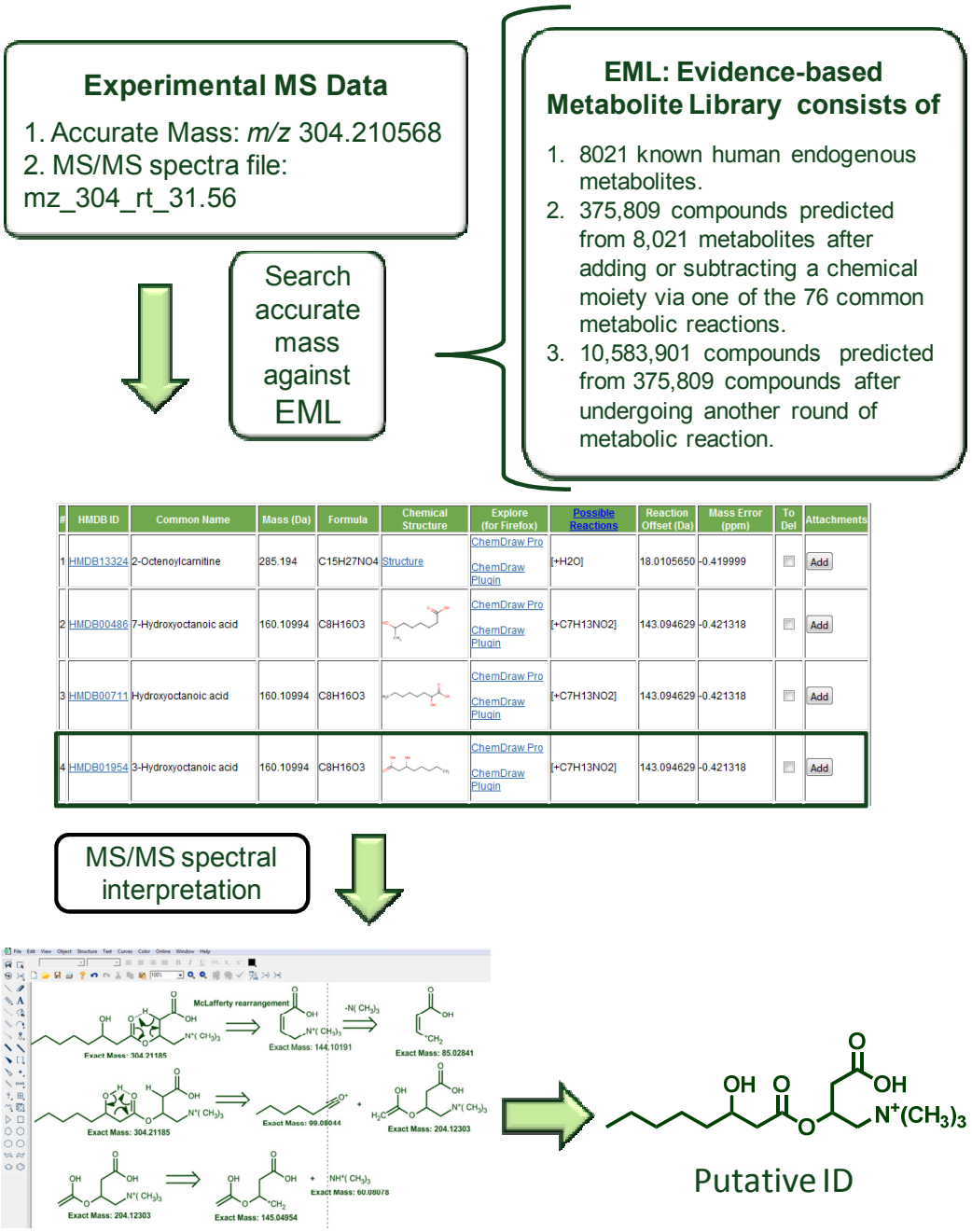

#	HMDB ID	Common Name	Mass (Da)	Formula	Chemical Structure	Explore (for Firefox)	Possible Reactions	Reaction Offset (Da)	Mass Error (ppm)	To Del	Attachments
1	HMDB13324	2-Octenoylcarnitine	285.194	C15H27NO4	Structure	ChemDraw Pro ChemDraw Plugin	[+H2O]	18.0105650	-0.419999		Add
2	HMDB00486	7-Hydroxyoctanoic acid	160.10994	C8H16O3		ChemDraw Pro ChemDraw Plugin	[+C7H13NO2]	143.094629	-0.421318		Add
3	HMDB00711	Hydroxyoctanoic acid	160.10994	C8H16O3		ChemDraw Pro ChemDraw Plugin	[+C7H13NO2]	143.094629	-0.421318		Add
4	HMDB01954	3-Hydroxyoctanoic acid	160.10994	C8H16O3		ChemDraw Pro ChemDraw Plugin	[+C7H13NO2]	143.094629	-0.421318		Add

Figure 6.1 Strategy and workflow of MyCompoundID.

6.2.2 Plasma and urine sample preparation

A whole blood and urine sample were obtained from a healthy volunteer who was not on any special diet or taking any nutritional supplements. An

informed consent was obtained and ethics approval for this work was obtained from the University of in compliance with the Arts, Science and Law Research Ethics Board policy. The whole blood sample in tri-potassium ethylenediaminetetraacetic acid (EDTA) was immediately centrifuged at 14,000 rpm for 10 min in order to separate the plasma. The urine sample was also centrifuged under the same conditions with the purpose of removing any solids.

Solid-phase extraction (SPE) was performed on 1 mL of biofluid (urine or plasma) using Waters Oasis HLB SPE cartridges (with a volume of 3 cc, sorbent weight of 60 mg and 3 μm particle size). These cartridges were chosen since they contain a hydrophilic-lipophilic balance reversed-phase sorbent which retains both hydrophobic and polar analytes. The cartridge was conditioned with 1mL of methanol and was subsequently equilibrated with 1 mL of water. One millilitre of biofluid was then loaded onto the cartridge. A washing step was performed by adding 1 mL of water and finally the sample was eluted with 1mL of methanol. The eluate was evaporated to dryness in a Savant SpeedVac concentrator system (Global Medical Instrumentation or GMI, Ramsey, Minnesota). The urine sample was reconstituted in 100 μL of mobile phase A (0.1% formic acid, 4% acetonitrile in H_2O) while the plasma sample was reconstituted in 100 μL of 0.1% formic acid, 40% acetonitrile in H_2O in order to dissolve lipids and other hydrophobic species.

6.2.3 LC-MS parameters

6.2.3.1 LC system

Five microlitres of each sample were injected into a 1200 series High Performance Liquid Chromatography system (Agilent Technologies, Santa Clara, CA). The chromatography column used was a BEH (ethylene bridged hybrid) 2.1 X 50 mm, 1.7 μm C_{18} column (Waters Corporation, Milford, MA). Mobile phase A consisted of 0.1% formic acid, 4% acetonitrile in H_2O, while mobile phase B consisted of 0.1% formic acid in acetonitrile. The flow rate utilized was 100 μL/min. The gradient conditions used were the following; the column was

equilibrated at 0% B prior to sample injection and was held under these conditions for the first ten minutes of the separation. The percentage of mobile phase B was increased to 80% in 50 minutes and subsequently increased to 100% in 55 minutes. The percentage of mobile phase B was held at 100% for 5 minutes before decreasing it back to the starting conditions for column re-equilibration to take place for 20 minutes. The total run time was 80 minutes.

6.2.3.2 Time of flight (TOF) MS system

A 6220 orthogonal time of flight (TOF) mass spectrometer (Agilent Technologies, Santa Clara, CA) was utilized in the positive ion mode to obtain high-resolution, high-accuracy mass spectral data for all detected metabolites in both biofluids. The scan range was set from 54.0114583359894 to 999.270141364876. The optics parameters can be summarized as follows; Oct1 DC = 34.2 Volts, Bot Slit= 17.10 Volts, Horiz Q = 25.70 Volts, Ion Focus= -152.0 Volts, Oct2 DC= 32.9 Volts, Slicer= -9.5 Volts, Top Slit = 17.00 Volts and Q= 26.00 Volts. The ESI source parameters are the following; Drying Gas= 9.9 L/min, Fragmentor:1 = 120 Volts, Fragmentor:2 = 0 Volts, Fragmentor:3= 0 Volts, Fragmentor:4= 0 Volts, Gas Temp= 325 °C, Nebulizer= 20 psi, Oct 1 RF Vpp:1= 250 Volts, Oct 1 RF Vpp:2= 0 Volts, Oct 1 RF Vpp:3= 0 Volts, Oct 1 RF Vpp:4= 0 Volts, Sheath Gas Flow= 0.0 L/min, Skimmer:1= 63.0 Volts, Skimmer:2= 0.0 Volts, Skimmer:3= 0.0 Volts, Skimmer:4,= 0.0 Volts, Vaporizer/Sheath Gas Temp = 40 °C, VCap:1= 3200 Volts, VCap:2= 0 Volts, V_{Cap}:3= 0 Volts, VCap:4= 0 Volts. Finally the TOF parameters used were the following; Acc Focus= -1950 Volts, Mirror Back= 1650 Volts, Mirror .Front= -6500 Volts, Mirror Mid= -1391.0 Volts, Puller= -800 Volts, Puller Offset= 21 Volts, Pusher= 1250 Volts.

6.2.3.3 QTRAP® MS system

A 4000 QTRAP® MS/MS System (Applied Biosystems, Foster City, California) equipped with a Turbo V™ ion source was used in the positive ion mode to obtain MS/MS spectra of all detected metabolites. Enhanced MS mode

was utilized as a survey scan with a scan range of *m/z* 50-1000 and a scan rate of 1000 Da/s. For every data point acquired along a chromatographic peak, the 4 most intense ions were selected for subsequent enhanced product ion (EPI) scan (i.e. MS/MS). The parameters used for the EPI scans were the following; the Q1 resolution was set to unit, the Q3 entry barrier was set to 8 V, the scan rate was 4000 amu/s for a scan range of *m/z* 50 to 600. The collision energy (CE) was set to 37 V with a spread (CES) of 6 V. Dynamic fill time was selected. ESI source and compound-specific parameters that can be summarized as follows; Q1 and Q3 resolution were set to unit, GS1 was set to 25 psi, GS2 was set to 15 psi, CAD gas was set to high, the curtain gas was set 10 psi, the IS voltage was 4800 V, the source temperature was set to 250 °C and the declustering potential (DP) was set to 50 V.

6.2.4 Data extraction and processing

A mass list with retention time information was manually extracted from the QTRAP® data using Analyst software. A mass list was obtained from the TOF instrument by exporting the raw data as a .mzdata file and processing it using R software (free software environment for statistical computing and graphics) and XCMS Analyte Profiling Software[14] using the following parameters; full width at half maximum= 30, step= 0.005, signal to noise= 2. These parameters were optimized by assessing the mass accuracy of the exported data from a 1 μM acylcarnitine standard mix.

6.3 Results and Discussion

6.3.1 Features

The mass list containing retention time information obtained from the QTRAP® data was compared to that obtained from the TOF data. Only features with the same nominal mass and similar retention times were utilized for further

data analysis. Additionally, a careful inspection of the data was performed to find and delete as many fragment ions as possible from this list of features.

6.3.2 Observations

It was observed that the sorbent type of the SPE cartridge utilized, which contains benzene rings, introduced a slight bias in the compounds detected and identified in both biofluids. It was found that aromatic compounds were preferentially retained on the sorbent bed over aliphatic ones, especially in urine. Figure 6.2 shows the chemical properties of the sorbent bed. Moreover, samples were only analyzed in the positive ion mode which also limits the number of features found. Glucoronide, taurine and sulfate conjugates as well as acidic compounds which are readily found in urine display a higher ionization efficiency in the negative ion mode. In order to obtain a more comprehensive list of metabolites, a combination of different SPE sorbent chemistries as well as analysis in both the positive and negative ionization mode would be necessary.

Also noteworthy is that structural isomers could not be distinguished based on fragmentation patterns. Upon low-energy collision-induced dissociation, aliphatic chains cannot be fragmented and so double-bond and substituent positions cannot be determined.

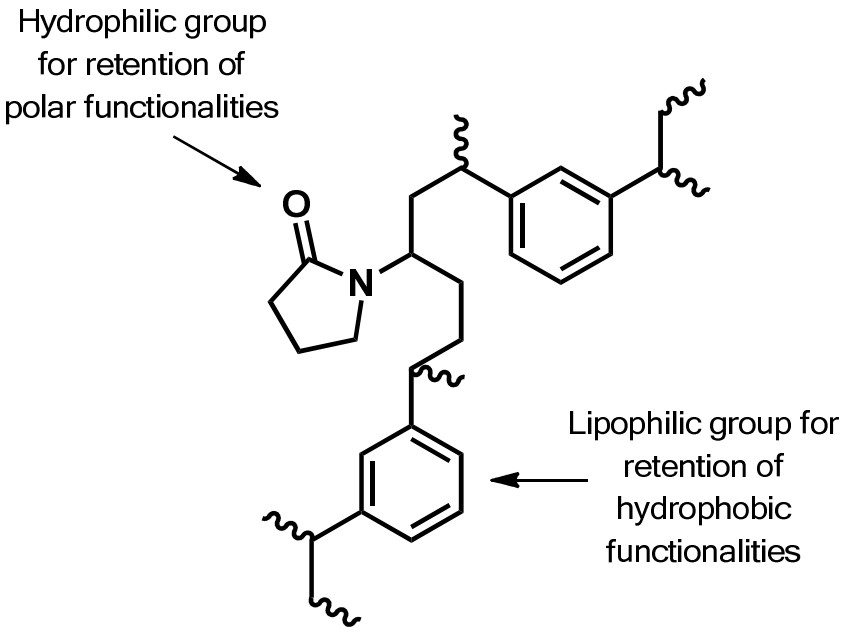

Figure 6.2 Waters Oasis HLB SPE sorbent chemistry. Adapted from Waters website.

6.3.3 Plasma and urine metabolites

Under positive ion mode using a simple extraction, 347 peaks were found in urine and 116 found in plasma that were commonly detected by TOF-MS, QTRAP-MS, and QTRAP-MS/MS (see electronic Appendix). To identify these metabolites, a search against the HMDB was carried out using accurate mass (<5 ppm) and MS/MS spectra against a library of about 900 metabolite standards. Only 8 metabolites were identified in urine and 7 in plasma (see Tables 6.2 and 6.3). This low rate of success reflects the current status of metabolite identification by LC-MS, i.e., many peaks detected cannot be readily identified using current databases.[3, 8, 10, 11, 13] The next step was to utilize MyCompoundID to search the accurate masses of the remaining features against the 8021 known metabolites to generate a list of mass-matches, followed by MS/MS spectral interpretation of individual matches. Fourteen metabolites were putatively identified in urine and 34 metabolites in plasma. Tables summarizing these results can be found in Appendix Sections 6.1 and 6.4, respectively. MyCompoundID was utilized again to search the accurate masses of the remaining features against EML with one biotransformation reaction. In conjunction with MS/MS spectral

interpretation, 41 metabolites were putatively identified in urine and 14 in plasma (Sections 6.2 and 6.5 of the Appendix). The use of EML with two reactions only led to the putative identification of 3 metabolites in urine (Appendix Section 6.3) and none in plasma. This low rate of identification was due to the presence of many hits for each matched mass, complicating the manual spectral interpretation process for structure assignment.

Future work includes the development of an automated spectral interpretation program that may facilitate metabolite identification using EML with two or more reactions. Nevertheless, using MyCompoundID, an additional 58 metabolites were putatively identified in urine and 48 in plasma, compared to 8 and 7 metabolites identified using the standard HMDB library, respectively. These results illustrate that MyCompoundID can significantly increase the number of identifiable metabolites in different biofluids.

Table 6.2 Metabolites identified in urine by direct comparison with experimental data obtained from HMDB (reaction number = 0).

Feature ID #	Accurate *m/z* TOF	RT range (min) TOF	*m/z* QTRAP	RT (min) QTRAP	Ion Type	Putative ID	Error (ppm)	Structure
1	107.0493	16.70 - 17.60	107.0	17.92	$[M + H]^+$	Benzaldehyde	1.29	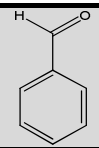
2	246.1697	21.30 - 21.70	246.2	21.30	$[M + H]^+$	2-Methylbutyroylcarnitine or isomers	-1.34	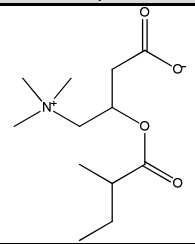
3	255.0655	34.00 - 34.50	255.1	34.79	$[M + H]^+$	Daidzein	1.24	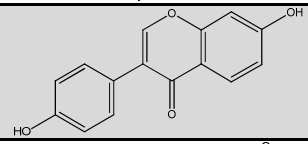
4	288.2170	34.70 - 35.20	288.2	35.18	$[M + H]^+$	Octanoylcarnitine or isomers	0.35	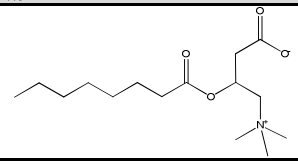

5	288.2167	35.50 - 35.80	288.2	35.87	$[M + H]^+$	Octanoylcarnitine or isomers	-0.92	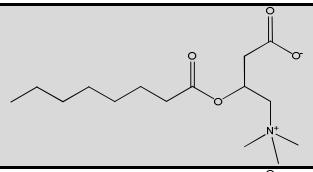
6	288.2166	36.60 - 37.00	288.1	37.08	$[M + H]^+$	Octanoylcarnitine or isomers	-1.19	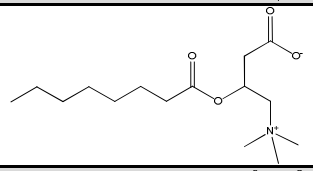
7	316.2484	40.00 - 40.60	316.2	40.53	$[M + H]^+$	Decanoylcarnitine or isomers	0.41	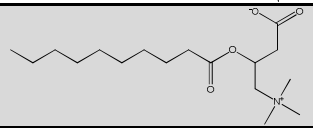
8	316.2485	41.20 - 41.60	316.1	41.57	$[M + H]^+$	Decanoylcarnitine or isomers	0.91	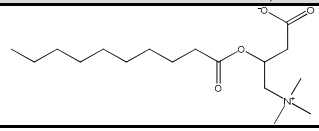

Table 6.3 Metabolites identified in plasma by direct comparison with experimental data obtained from HMDB (reaction number = 0).

Feature ID #	Accurate *m/z* TOF	RT range (min) TOF	*m/z* QTRAP	RT (min) QTRAP	Ion type	Putative ID	error (ppm)	Structure
1	181.0722	3.60 - 4.10	181.0	3.40	$[M+H]^+$	Theobromine	0.91	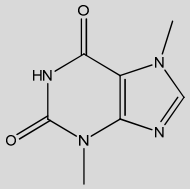
2	260.1855	28.20 - 28.80	260.2	30.80	$[M+H]^+$	Hexanoylcarnitine	-0.63	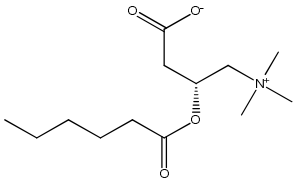
3	288.2172	36.30 - 36.80	288.2	37.00	$[M+H]^+$	Octanoylcarnitine	1.03	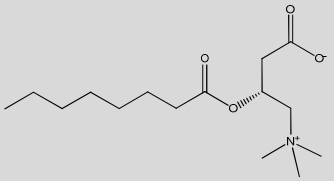

4	316.2488	40.70 - 41.20	316.2	41.50	$[M+H]^+$	Decanoylcarnitine	1.65	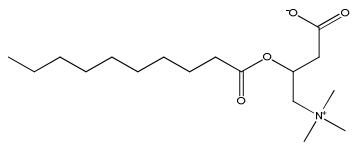
5	361.2009	35.10 - 35.60	361.2	35.90	$[M+H]^+$	Cortisone	-0.24	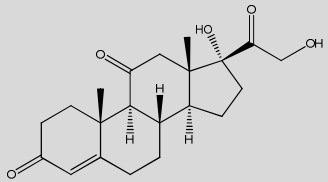
6	391.2838	66.30 - 66.80	391.3	66.30	$[M+H]^+$	7a-Hydroxy-3-oxo-5b-cholanoic acid	-1.27	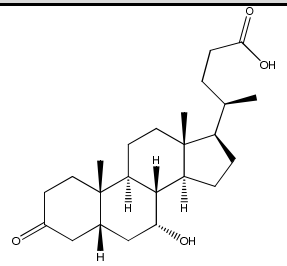
7	400.3418	52.80 - 53.30	400.4	53.70	$[M+H]^+$	Palmitoylcarnitine	-0.90	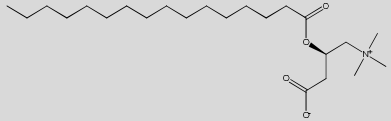

It should be noted that MyCompoundID only allows the user to putatively identify a metabolite based on matching both accurate molecular mass and fragment ions based on a proposed chemical structure. However, using this approach the user can narrow down the list of metabolite candidates into one or a few unique structures. If positive identification is required (e.g., a potentially useful biomarker of a disease), an authentic standard may be synthesized for comparison. Reducing the number of possible metabolite candidates by this combination of mass search and MS/MS interpretation, or MS+MS/MS, in combination with the EML could potentially save a user time and effort.

6.3.4 Metabolites from exogenous sources

Surfactants have been used for many applications such as cosmetics, pharmaceuticals, household cleaners and textiles among others.[15] However, it hasn't been until the last couple of decade that their toxicity and environmental fate has been tested. Researchers have recently detected these compounds in human bodily fluids. For example, polyethylene glycol (PEG) is used extensively in foods, drugs, cosmetics, and ointments, and since it is not metabolized by colonic bacteria, it is readily found in human urine.[16] Alkylphenol polyethoxylates have been used for more than 40 years in household and industrial detergents.[17] Another example are cocodiethanolamides which are readily used in shampoos.[18]

MyCompoundID allowed the putative identification of a series of exogenous metabolites based on accurate mass, relative retention time and characteristic fragmentation patterns. Interestingly, some of these compounds were detected only in urine while others were detected only in plasma. In detail, ten polyethylene glycol (PEG) analogues and three polyethoxylates were found in urine only. Appendix Section 6.6 contains a list of all PEG analogues detected in urine and plasma. Two cocodiethanolamides (CDEAs) were found only in plasma, while two others were found in both fluids. A list of all detected CDEAs can be found in Appendix Section 6.7. There was also a set of nine unidentified urine metabolites which had very similar fragmentation patterns and were thus

regarded as being related. A list of these compounds can be found in Appendix Section 6.8. Additionally, a group of seven unknown urine metabolites displayed the same neutral losses upon fragmentation. A list of these metabolites can be found in Section 6.9 of the Appendix. The fact that many of these metabolites remained unidentified is proof of the complexity of human metabolism and how difficult it can be to predict it. There were also 16 metabolites found in urine which, based on their fragmentation pattern, seemed to be glucoronide conjugates. Appendix Section 6.10 contains a list of all metabolites found in urine which exhibited the characteristic fragmentation pattern of glucoronide conjugates.

6.4 Conclusions

A publicly accessible web-based tool has been developed that can facilitate the identification of unknown metabolites for more reliable metabolome profiling. In combination with LC-MS, it is shown to be useful for identifying many more metabolites in human urine and plasma samples than using a standard library. MyCompoundID features a dynamic compound library that can be expanded in the future by inclusion of metabolites and their predicted metabolic products from different origins including human, microbes, plants, food, etc. We anticipate that an expanded compound library will increase the number of metabolites identifiable from human biofluids and open the possibility of using MyCompoundID for analyzing the metabolomes of other species. We also plan to add the functionality for data sharing among the researchers who are interested in chemical identification (e.g., deposition of MS/MS spectra and their interpretation and spectral assignment for newly identified compounds).

6.5 Literature cited

(1) Sreekumar, A.; Poisson, L. M.; Rajendiran, T. M.; Khan, A. P.; Cao, Q.; Yu, J.; Laxman, B.; Mehra, R.; Lonigro, R. J.; Li, Y.; Nyati, M. K.; Ahsan, A.; Kalyana-Sundaram, S.; Han, B.; Cao, X.; Byun, J.; Omenn, G. S.; Ghosh, D.; Pennathur, S.; Alexander, D. C.; Berger, A.; Shuster, J. R.; Wei, J. T.; Varambally, S.; Beecher, C.; Chinnaiyan, A. M. *Nature* **2009**, *457*, 910-914.

(2) Jenkins, H.; Hardy, N.; Beckmann, M.; Draper, J.; Smith, A. R.; Taylor, J.; Fiehn, O.; Goodacre, R.; Bino, R. J.; Hall, R.; Kopka, J.; Lane, G. A.; Lange, B. M.; Liu, J. R.; Mendes, P.; Nikolau, B. J.; Oliver, S. G.; Paton, N. W.; Rhee, S.; Roessner-Tunali, U.; Saito, K.; Smedsgaard, J.; Sumner, L. W.; Wang, T.; Walsh, S.; Wurtele, E. S.; Kell, D. B. *Nature Biotechnology* **2004**, *22*, 1601-1606.

(3) Cui, Q.; Lewis, I. A.; Hegeman, A. D.; Anderson, M. E.; Li, J.; Schulte, C. F.; Westler, W. M.; Eghbalnia, H. R.; Sussman, M. R.; Markley, J. L. *Nature Biotechnology* **2008**, *26*, 162-164.

(4) Han, X.; Yang, K.; Gross, R. W. *Mass Spectrometry Reviews* **2012**, *31*, 134-178.

(5) Want, E. J.; Wilson, I. D.; Gika, H.; Theodoridis, G.; Plumb, R. S.; Shockcor, J.; Holmes, E.; Nicholson, J. K. *Nature Protocols* **2010**, *5*, 1005-1018.

(6) Zehethofer, N.; Pinto, D. M. *Analytica Chimica Acta* **2008**, *627*, 62-70.

(7) Guo, K.; Li, L. *Analytical Chemistry* **2010**, *82*, 8789-8793.

(8) Wishart, D. S.; Tzur, D.; Knox, C.; Eisner, R.; Guo, A. C.; Young, N.; Cheng, D.; Jewell, K.; Arndt, D.; Sawhney, S.; Fung, C.; Nikolai, L.; Lewis, M.; Coutouly, M.-A.; Forsythe, I.; Tang, P.; Shrivastava, S.; Jeroncic, K.; Stothard, P.; Amegbey, G.; Block, D.; Hau, D. D.; Wagner, J.; Miniaci, J.; Clements, M.; Gebremedhin, M.; Guo, N.; Zhang, Y.; Duggan, G. E.; MacInnis, G. D.; Weljie, A. M.; Dowlatabadi, R.; Bamforth, F.; Clive, D.; Greiner, R.; Li, L.; Marrie, T.; Sykes, B. D.; Vogel, H. J.; Querengesser, L. *Nucleic Acids Research* **2007**, *35*, D521-D526.

(9) Wishart, D. S.; Knox, C.; Guo, A. C.; Eisner, R.; Young, N.; Gautam, B.; Hau, D. D.; Psychogios, N.; Dong, E.; Bouatra, S.; Mandal, R.; Sinelnikov, I.; Xia, J.; Jia, L.; Cruz, J. A.; Lim, E.; Sobsey, C. A.; Shrivastava, S.; Huang, P.; Liu, P.; Fang, L.; Peng, J.; Fradette, R.; Cheng,

D.; Tzur, D.; Clements, M.; Lewis, A.; De Souza, A.; Zuniga, A.; Dawe, M.; Xiong, Y.; Clive, D.; Greiner, R.; Nazyrova, A.; Shaykhutdinov, R.; Li, L.; Vogel, H. J.; Forsythe, I. *Nucleic Acids Research* **2009**, *37*, D603-D610.

(10) Smith, C. A.; Maille, G. O.; Want, E. J.; Qin, C.; Trauger, S. A.; Brandon, T. R.; Custodio, D. E.; Abagyan, R.; Siuzdak, G. *Therapeutic Drug Monitoring* **2005**, *27*, 747-751.

(11) Horai, H.; Arita, M.; Kanaya, S.; Nihei, Y.; Ikeda, T.; Suwa, K.; Ojima, Y.; Tanaka, K.; Tanaka, S.; Aoshima, K.; Oda, Y.; Kakazu, Y.; Kusano, M.; Tohge, T.; Matsuda, F.; Sawada, Y.; Hirai, M. Y.; Nakanishi, H.; Ikeda, K.; Akimoto, N.; Maoka, T.; Takahashi, H.; Ara, T.; Sakurai, N.; Suzuki, H.; Shibata, D.; Neumann, S.; Iida, T.; Tanaka, K.; Funatsu, K.; Matsuura, F.; Soga, T.; Taguchi, R.; Saito, K.; Nishioka, T. *Journal of Mass Spectrometry* **2010**, *45*, 703-714.

(12) Clements, M.; Li, L. *Analytica Chimica Acta* **2011**, *685*, 36-44.

(13) Kanehisa, M.; Araki, M.; Goto, S.; Hattori, M.; Hirakawa, M.; Itoh, M.; Katayama, T.; Kawashima, S.; Okuda, S.; Tokimatsu, T.; Yamanishi, Y. *Nucleic Acids Research* **2008**, *36*, D480-D484.

(14) Smith, C. A.; Want, E. J.; O'Maille, G.; Abagyan, R.; Siuzdak, G. *Analytical Chemistry* **2006**, *78*, 779-787.

(15) Prieto-Blanco, M. C.; Lopez-Mahia, P.; Muniategui-Lorenzo, S.; Prada Rodriguez, D. In *Analysis of cosmetic products,* 1st ed.; Elsevier: Oxford, 2007.

(16) Hollander, D.; Delahunty, T. *Clinical Chemistry* **1986**, *32*, 351-353.

(17) Montgomery-Brown, J.; Reinhard, M. *Environmental Engineering Science* **2003**, *20*, 471-486.

(18) Carolei, L.; Gutz, I. G. R. *Talanta* **2005**, *66*, 118-124.

Chapter 7

Conclusions and Future Work

Two of the main challenges of metabolic profiling by LC-MS that still persist up to this day are compound identification and accurate quantification of endogenous metabolites. The overall objective of my research was to develop qualitative and quantitative UHPLC-MS/MS methods to detect, identify and quantify endogenous metabolites in complex biological samples. Due to their important biological functions, carnitine and its acyl derivatives were chosen as a model system to test these methodologies on.

In Chapter 2, the development and application of a selective and reproducible analytical platform for urinary acylcarnitine profiling in healthy volunteers was described. The ability of this UPLC-MS/MS method to resolve acylcarnitine structural isomers and decrease the number of false positives was demonstrated; thereby providing an accurate and comprehensive acylcarnitine profile in urine. Human liver microsome incubations were successfully used to create reference standards for acylcarnitine phase I metabolites, which was illustrated using an octanoylcarnitine incubation as an example. A total of 355 species were detected, including hydroxyacylcarnitines as well as carnitine dicarboxylic acid conjugates. Only 43 of these species had been previously reported in the urine of healthy individuals.

In Chapter 3, comprehensive profiling of acylcarnitines was performed in various biofluids, including plasma, dried blood spots (DBS) as well as red blood cell (RBC) pellets. The results obtained were compared to those from Chapter 2. It was found that acylcarnitine profiles varied quite dramatically based on the

biofluid studied. There were 169 acylcarnitines found in plasma, 41 species were found in DBS and 22 were found in RBC pellet. Only long-chain species were found in the RBC pellets and thus there were no species found in common between the pellets and urine. Species with a large range of hydrophobicities were found in DBS (C0 to C26). The results obtained suggested that in order to obtain a truly comprehensive acylcarnitine profile, more than one biofluid needs to be analyzed.

Chapter 4 describes an analytical platform developed for the quantification of urinary acylcarnitines in healthy individuals. A rapid and robust esterification reaction was implemented to introduce a $^{12}C_2$ or $^{13}C_2$ label to endogenous acylcarnitines in order to obtain a set of reference and internal standards. Since acylcarnitines are endogenous metabolites, it is not possible to find acylcarnitine-free urine; quantification was thus achieved using a surrogate matrix approach where underivatized urine was used for the construction of calibration curves. Twelve acylcarnitines were quantified in the urine of 20 individuals collected over the course of three consecutive days. Relative quantification was performed on an additional 64 acylcarnitines. This work describes the most comprehensive quantitative profile of acylcarnitines in healthy volunteers published to date (76 acylcarnitines in total). The effect of volunteers' gender and BMI on acylcarnitine profile was evaluated; however, differences found were not statistically significant, which agrees with previously published results. The only exception was pivaloylcarnitine which was detected in the urine of all female volunteers but only in the urine of one out of ten males. Pivalate is found in over-the-counter lotions and ointments and it was thus speculated that these products are the source of pivaloylcarnitine in females.

Chapter 5 focused on the accurate and precise quantification of acylcarnitines in the plasma of ten healthy volunteers. The UHPLC-MS/MS method was developed based on the method described in Chapter 4 with some differences. Thirteen acylcarnitines were quantified using this method and relative quantification was performed on an additional 19 acylcarnitines. As compared to

urine, plasma was found to contain more hydrophobic acylcarnitines, namely long-chain species. The plasma of a female volunteer showed consistently high acylcarnitine concentrations compared to the rest of the volunteers (regardless of gender). Diet and/or physical activity could account for such differences.

The development and application of a web-based tool for metabolite identification was described in Chapter 6. This tool features a dynamic compound library based on the Human Metabolome Database (HMDB). The library incorporated into MyCompoundID consists of the 900 compounds found in the HMDB plus the products of either one or two metabolic reactions (either phase I or phase II). Under positive ion mode, 347 metabolite features were found in urine and 116 found in plasma. When searching against the HMDB alone (using accurate mass (<5 ppm) and MS/MS), only 8 metabolites were matched in urine and 7 in plasma. When MyCompoundID was utilized, followed by MS/MS spectral interpretation of individual matches, 14 metabolites were putatively identified in urine and 34 in plasma. MyCompoundID was utilized in "one reaction mode" to search the accurate masses of the remaining features. In conjunction with MS/MS spectral interpretation, 41 metabolites were putatively identified in urine and 14 in plasma. The use of the library in "two reaction mode" only led to the tentative identification of 3 metabolites in urine and none in plasma. In summary, using MyCompoundID an additional 58 metabolites were putatively identified in urine and 48 in plasma. This is a major improvement from a regular HMDB search, where only 8 compounds were identified in urine and 7 in plasma. These results illustrate how MyCompoundID can significantly increase the number of putatively identified metabolites in various biofluids. This web-based tool also allowed for the putative identification of exogenous metabolites in urine and plasma such as polyethylene glycol derivatives, cocoethanolamides as well as glucoronide conjugates.

The possibilities for future work in the area of LC-MS-based metabolomics are vast. Effort has been directed in the past two decades towards the analysis of dried biofluid spots, whether it is whole blood, plasma, urine or

breast milk.[1-6] Dried biofluid spots are prepared by applying a biofluid to a high quality cotton-based filter paper and allowing it to dry. This type of samples exhibits numerous advantages such as long shelf-life and easy transport. Moreover, obtaining the sample is typically minimally invasive and only small sample volumes are needed.[7] However, handling such small sample volumes (a few micolitres) may translate into low signal intensities. Moreover, analyte extraction from the filter paper is not 100% efficient. The extraction efficiency must therefore be determined early in the method development stages and taken into account when carrying out quantitative studies. Also, when dealing with whole blood, the hematocrit or packed cell volume can have a considerable effect on the accuracy of the results obtained.[8]

In order to assess the applicability of dried biofluid spots for the analysis of acylcarnitines, simple methanol extractions were performed on dried blood, plasma and urine spots that had been previously allowed to dry overnight. All samples together with a regular plasma and urine sample were esterified using the method described in Chapter 4. Analyte extraction was carried out by sonicating the dried spots for 10 minutes in 200 μL of methanol. The results are presented in Figure 6.1. Panel (A) shows the TIC of an esterified dried blood spot (DBS). It can be observed by comparing panels (B) and (C) that the extraction of acylcarnitines from dried plasma spots (DPS) needs to be optimized further, especially for medium-chain species. The extraction from dried urine spots (DUS), however, seemed to have a higher efficiency, with results being comparable to a regular esterified urine sample of the same volume. It is not clear why the extraction efficiencies in DPS and DUS are not comparable; it may be due to other compounds (possibly proteins) present in plasma which hinder the extraction process.

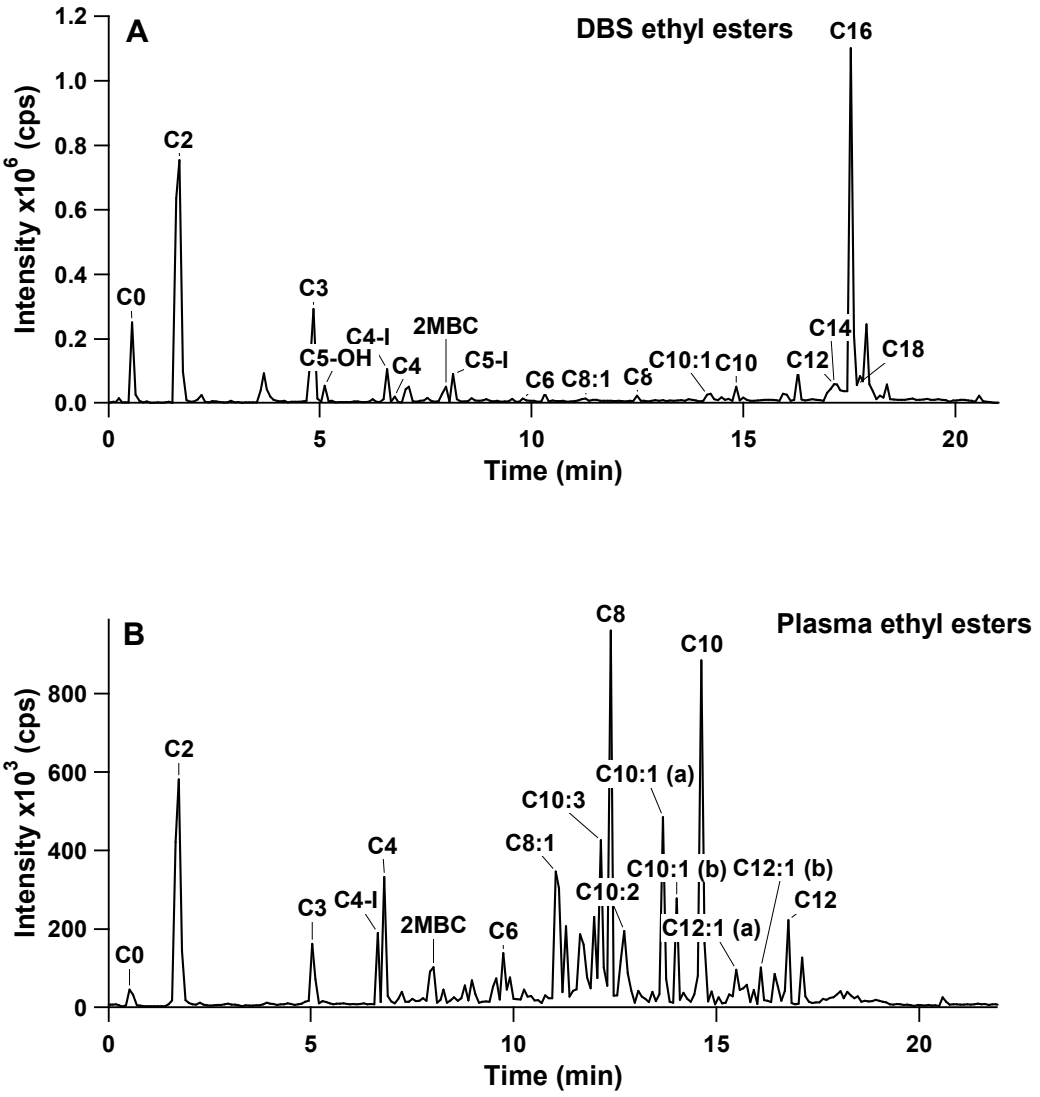

Figure 7.1 Development of dried biofluid spots. (A) Acylcarnitines with a wide range of hydrophobicities were detected in an esterified dried blood spot (DBS) sample. (B)-(C) Plasma and dried plasma spot (DPS) samples. Peak intensities were higher in the regular plasma sample, possibly due to losses from analyte extraction form the filter paper. (D)-(E) Urine and dried urine spot (DUS) samples showed very similar acylcarnitine profiles. Representative acylcarnitines have been labeled in all panels.

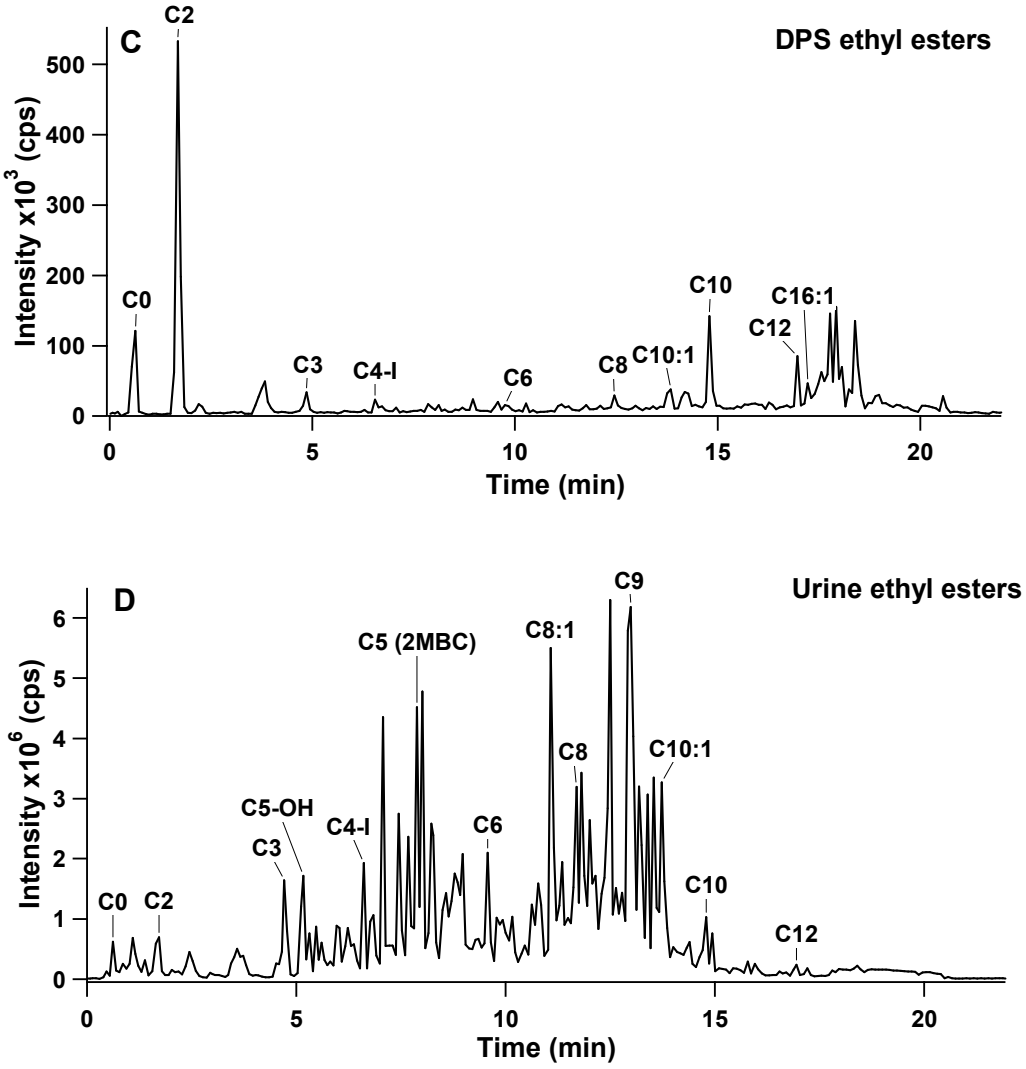

Figure 7.2 Development of dried biofluid spots (continued). (A) Acylcarnitines with a wide range of hydrophobicities were detected in an esterified dried blood spot (DBS) sample. (B)-(C) Plasma and dried plasma spot (DPS) samples. Peak intensities were higher in the regular plasma sample, possibly due to losses from analyte extraction form the filter paper. (D)-(E) Urine and dried urine spot (DUS) samples showed very similar acylcarnitine profiles. Representative acylcarnitines have been labeled in all panels.

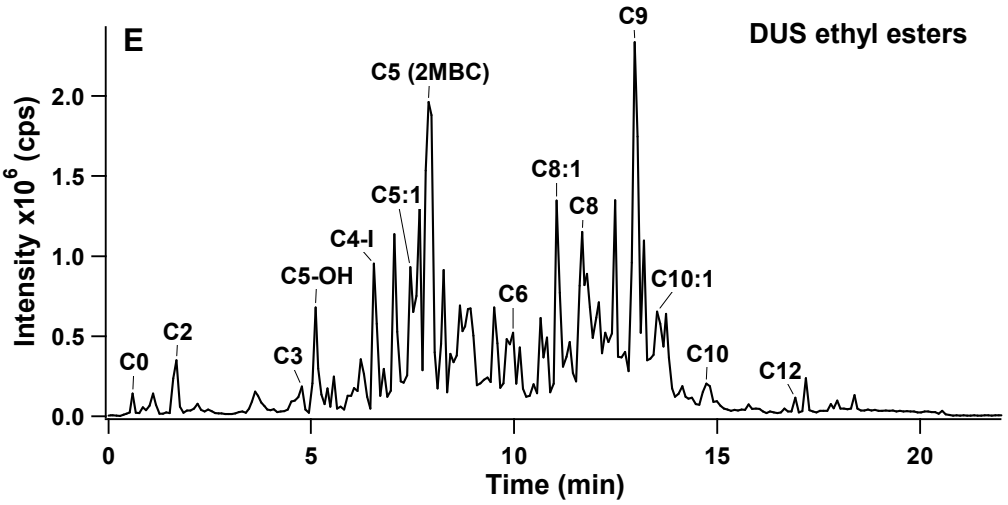

Figure 7.3 Development of dried biofluid spots (continued). (A) Acylcarnitines with a wide range of hydrophobicities were detected in an esterified dried blood spot (DBS) sample. (B)-(C) Plasma and dried plasma spot (DPS) samples. Peak intensities were higher in the regular plasma sample, possibly due to losses from analyte extraction form the filter paper. (D)-(E) Urine and dried urine spot (DUS) samples showed very similar acylcarnitine profiles. Representative acylcarnitines have been labeled in all panels.

One possibility to improve the extraction efficiency of acylcarnitines from filter paper as well as to increase the throughput of the sample preparation process is to utilize microwave technology. Microwave-assisted metabolite extractions[9] and derivatization reactions[10, 11] have proved to be successful, but there are not many reports were a microwave is utilized for both purposes, especially for dried biofluid spot applications. Microwave technology is advantageous due to its inherent rapid heating which can allow for short sample preparation times. This rapid heating is due to friction produced from the alignment of solvent molecules' dipoles with the electromagnetic field from the microwave. Heat can subsequently be transferred from the solvent to the analyte molecules. Heating can also originate from ionic conduction in the case when the molecules of interest are charged. Microwaves cause ions in solution to oscillate and collide with others producing heat. When using closed vessels, the solvent can be heated to temperatures well above its boiling point, increasing the efficiency of the reaction by increasing the rate of partitioning of the analyte molecules from the sample to

the solvent. In the case where the analyte molecules themselves are polar or ionic (and the volume of the solution is large enough) they can interact directly with the microwaves.[12]

The main goal of using this approach would be to optimize the conditions in such a way to carry out the extraction and derivatization in a single step, thereby speeding up considerably the sample preparation process (a few minutes instead of an hour for an esterification reaction). This methodology could also be applied to other derivatization techniques developed in our laboratory which target amine and carboxylic acid-containing metabolites.

Another aspect that should be investigated is the applicability of the developed analytical platforms to clinical samples in the search for new biomarkers for diseases such as inborn errors of metabolism, pre-eclampsia, sepsis and multiple sclerosis among others.

Improvement of the tool MyCompoundID described in Chapter 6 could include expanding the library with various types of metabolites such as exogenous compounds and metabolites from other living species. This would dramatically increase the number of metabolites identifiable in humans and open the possibility of using this tool for analyzing the metabolomes of other species. There are also ongoing plans to add the functionality for data sharing among researchers who are interested in chemical identification (e.g., uploading annotated MS/MS spectra of newly identified compounds). Finally, there is also interest in developing an automated spectral interpretation program that would facilitate the current process for metabolite identification using MyCompoundID.

Literature cited

(1) Chace, D. H.; Adam, B. W.; Smith, S. J.; Alexander, J. R.; Hillman, S. L.; Hannon, W. H. *Clinical Chemistry* **1999**, *45*, 1269-1277.

(2) Chace, D. H.; Kalas, T. A.; Naylor, E. W. *Clinical Chemistry* **2003**, *49*, 1797-1817.

(3) Blau, N.; Kierat, L.; Heizmann, C.; Endres, W.; Giudici, T.; Wang, M. *Journal of Inherited Metabolic Disease* **1992**, *15*, 402-404.

(4) Fu, X.-w.; Iga, M.; Kimura, M.; Yamaguchi, S. *Early human development* **2000**, *58*, 41-55.

(5) Cassol, S.; Gill, M. J.; Pilon, R.; Cormier, M.; Voigt, R. F.; Willoughby, B.; Forbes, J. *Journal of Clinical Microbiology* **1997**, *35*, 2795-2801.

(6) Ayele, W.; Schuurman, R.; Messele, T.; Dorigo-Zetsma, W.; Mengistu, Y.; Goudsmit, J.; Paxton, W. A.; de Baar, M. P.; Pollakis, G. *Journal of Clinical Microbiology* **2007**, *45*, 891-896.

(7) McDade, T.; Williams, S.; Snodgrass, J. *Demography* **2007**, *44*, 899-925.

(8) Mei, J. V.; Alexander, J. R.; Adam, B. W.; Hannon, W. H. *The Journal of Nutrition* **2001**, *131*, 1631S-1636S.

(9) Sparr Eskilsson, C.; Björklund, E. *Journal of Chromatography A* **2000**, *902*, 227-250.

(10) Amendola, L.; Colamonici, C.; Mazzarino, M.; Botrè, F. *Analytica Chimica Acta* **2003**, *475*, 125-136.

(11) Deng, C.; Ji, J.; Zhang, L.; Zhang, X. *Rapid Communications in Mass Spectrometry* **2005**, *19*, 2974-2978.

(12) Stuerga, D. In *Microwaves in Organic Synthesis*; Loupy, A., Ed.; Wiley-VCH Verlag GmbH: Paris, 2008, pp 1-57.

Appendix

This appendix is divided into sections corresponding to each of the Chapters in this Thesis. It contains partial tables and sample MS/MS spectra as well as sample calibration curves. Full tables, complete MS/MS spectral libraries, a complete set of calibration curves as well as any additional supporting information can be found in the electronic Appendix which is available from Dr. Liang Li (liang.li@ualberta.ca).

Chapter 2

2.1 Partial list of acylcarnitines found in the urine of six healthy individuals.*

AC *m/z*	Retention time (min)	Proposed or confirmed (C) structure
144	2.51 ± 0.05 (n=6)	Crotonobetaine (C)
162	2.12 ± 0.03 (n=6)	Free carnitine (C)
172	1.86 ± 0.02 (n=4)	
176	2.05 ± 0.03 (n=6)	
190 (A)	2.06 ± 0.02 (n=6)	
190 (B)	2.59 ± 0.04 (n=5)	C1**
204 (A)	2.59 ± 0.03 (n=6)	C2 (acetyl) (C)
204 (B)	30.86 ± 0.06 (n=3)	
204 (C)	32.05 ± 0.12 (n=3)	
218	4.20 ± 0.09 (n=5)	C3 (C)
222	4.54 ± 0.33 (n=3)	
230	5.39 ± 0.36 (n=6)	C4:1
232 (A)	9.45 ± 0.36 (n=6)	C4 (isobutyryl) (C)
232 (B)	10.53 ± 0.81 (n=6)	C4 (butyryl) (C)
244	22.10 ± 0.38 (n=6)	C5:1-M (3-methylcrotonyl), C5:1-T (tiglyl)
246 (A)	22.96 ± 0.29 (n=6)	C5 (2-methylbutyryl) (C)
246 (B)	23.92 ± 0.32 (n=6)	C5 (isovaleryl) (C)
246 (C)	24.89 ± 0.31 (n=6)	C5 (valeryl) (C)
248	3.13 ± 0.04 (n=6)	C4+OH
252	40.06 ± 0.36 (n=2)	

256 (A)	6.65 ± 0.39 (n=6)	
256 (B)	59.52 ± 0.09 (n=2)	
258 (A)	28.14 ± 0.15 (n=6)	C6:1
258 (B)	29.20 ± 0.21 (n=5)	C6:1
258 (C)	30.97 ± 0.16 (n=6)	C6:1
258 (D)	63.19 ± 0.68 (n=3)	
260 (A)	4.11 ± 0.24 (n=6)	C5+=O (C)
260 (B)	31.75 ± 0.11 (n=6)	C6 isomer
260 (C)	32.97 ± 0.36 (n=6)	C6 (4-methylvaleryl)
260 (D)	36.05 ± 0.21 (n=6)	C6 (hexanoyl) (C)
262 (A)	2.81 ± 0.11 (n=6)	
262 (B)	4.41 ± 0.29 (n=6)	C4:DC (succinyl) or methylmalonyl
266	27.59 ± 0.20 (n=6)	benzoyl
270	21.39 ± 0.65 (n=5)	C7:2
272 (A)	34.79 ± 0.24 (n=6)	C7:1
272 (B)	36.76 ± 0.19 (n=6)	C7:1
272 (C)	37.40 ± 0.24 (n=6)	C7:1
272 (D)	39.01 ± 0.24 (n=5)	C7:1
272 (E)	39.77 ± 0.26 (n=6)	C7:1
274 (A)	10.39 ± 0.40 (n=5)	C5:1:DC
274 (B)	15.14 ± 0.53 (n=5)	
274 (C)	40.21 ± 0.36 (n=6)	C7
274 (D)	41.13 ± 0.36 (n=5)	C7
274 (E)	42.39 ± 0.31 (n=6)	C7
274 (F)	43.29 ± 0.0 (n=2)	C7
276 (A)	3.98 ± 0.27 (n=6)	C5:DC (glutaryl or ethylmalonyl)
276 (B)	14.39 ± 0.52 (n=5)	C6+OH
276 (C)	19.39 ± 0.22 (n=5)	C6+OH
276 (D)	21.23 ± 0.42 (n=5)	C6+OH (C)
276 (E)	26.42 ± 0.32 (n=5)	C6+OH
276 (F)	30.45 ± 0.15 (n=6)	C6+OH
280	29.21 ± 0.05 (n=5)	phenylacetyl
284 (A)	37.33 ± 0.22 (n=6)	C8:2
284 (B)	38.03 ± 0.18 (n=5)	C8:2
284 (C)	39.11 ± 0.29 (n=4)	C8:2
284 (D)	39.68 ± 0.27 (n=6)	C8:2
284 (E)	41.38 ± 0.27 (n=6)	C8:2

*The MS/MS spectra of individual species sorted by m/z plus letter code can be found in the electronic Appendix.
**The following nomenclature is used.

(1) The number following the letter C corresponds to the number of carbon atoms in the fatty acid chain conjugated to carnitine;
(2) +OH corresponds to a hydroxyl group added to the fatty acid chain conjugated to carnitine;
(3) +=O corresponds to a carbonyl group added to the fatty acid chain conjugated to carnitine;
(4) :DC corresponds to a dicarboxylic acid conjugated to carnitine;
(5) A colon followed by a number corresponds to the degrees of unsaturation along the fatty acid chain (for example :1 corresponds one degree of unsaturation).

2.2 Representative annotated MS/MS spectra of acylcarnitines found in urine.

m/z 144 RT 2.51 min

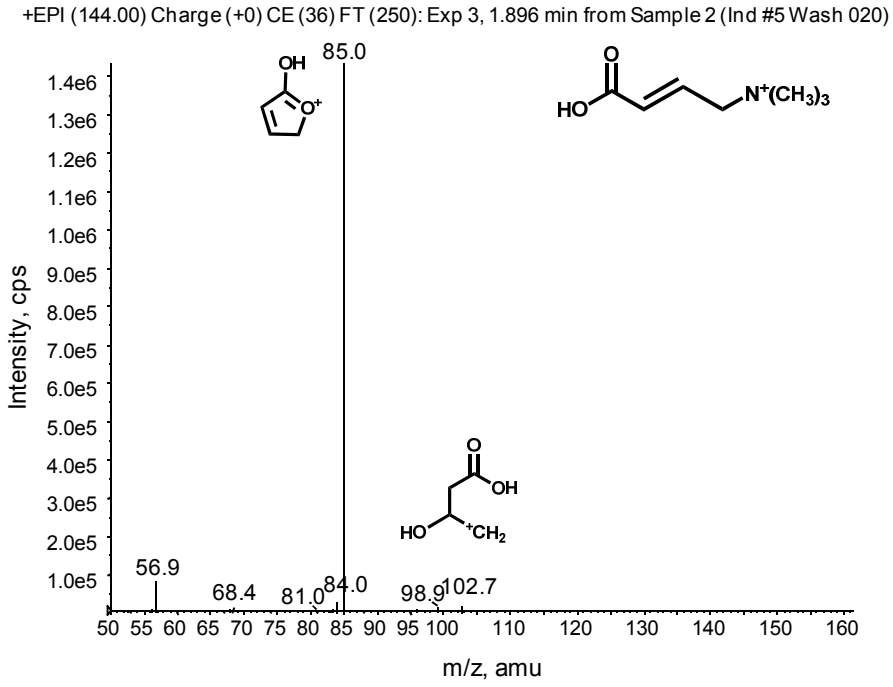

m/z 204 (A) RT 2.59 min

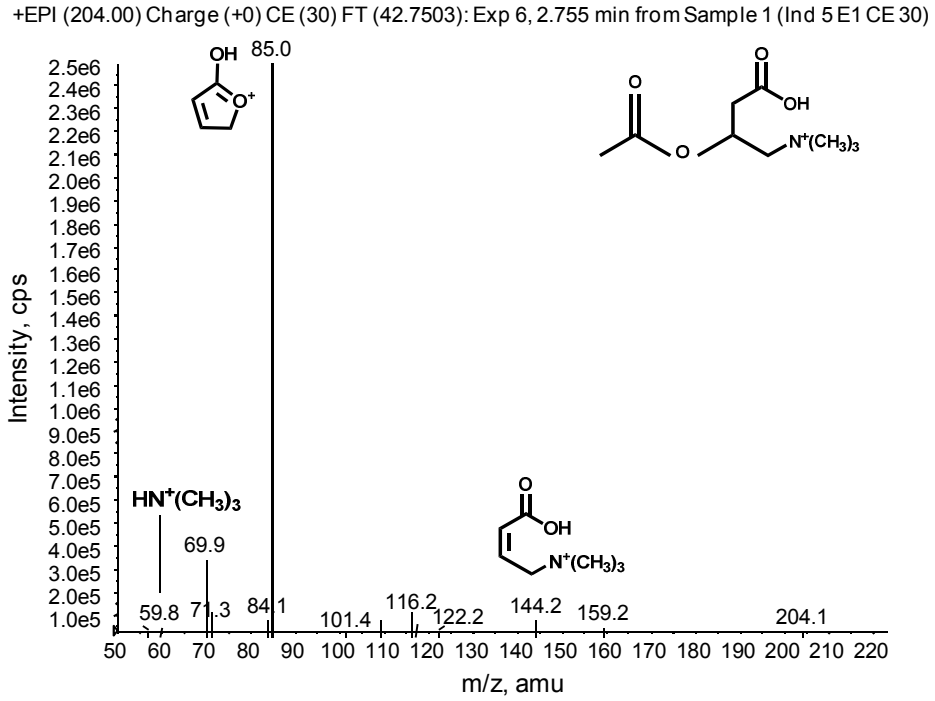

m/z 246 (A) RT 22.96 min

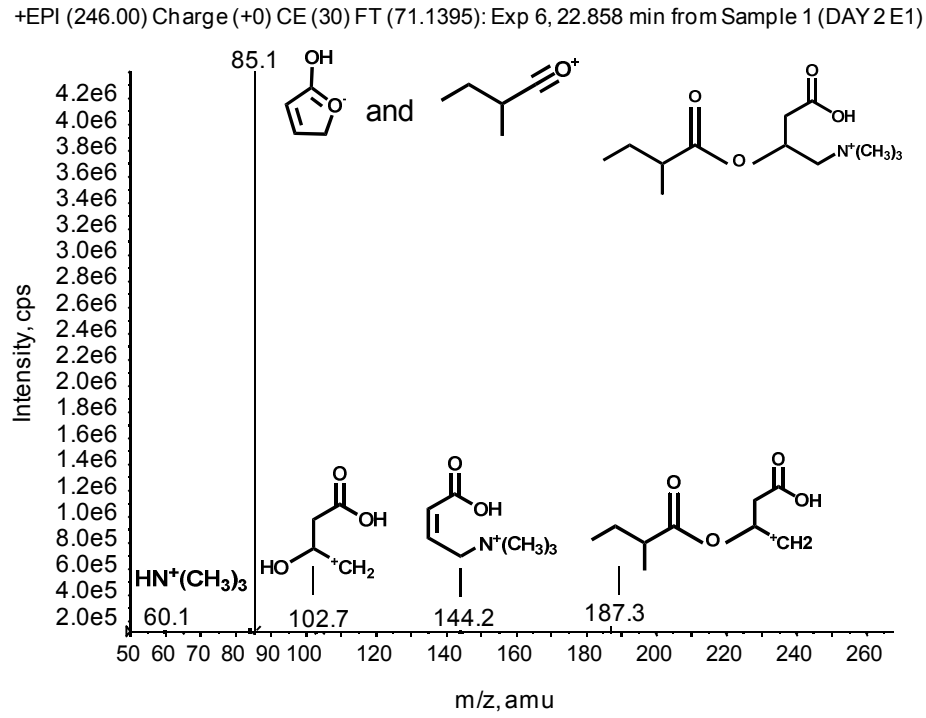

m/z 316 (K) RT 69.89 min

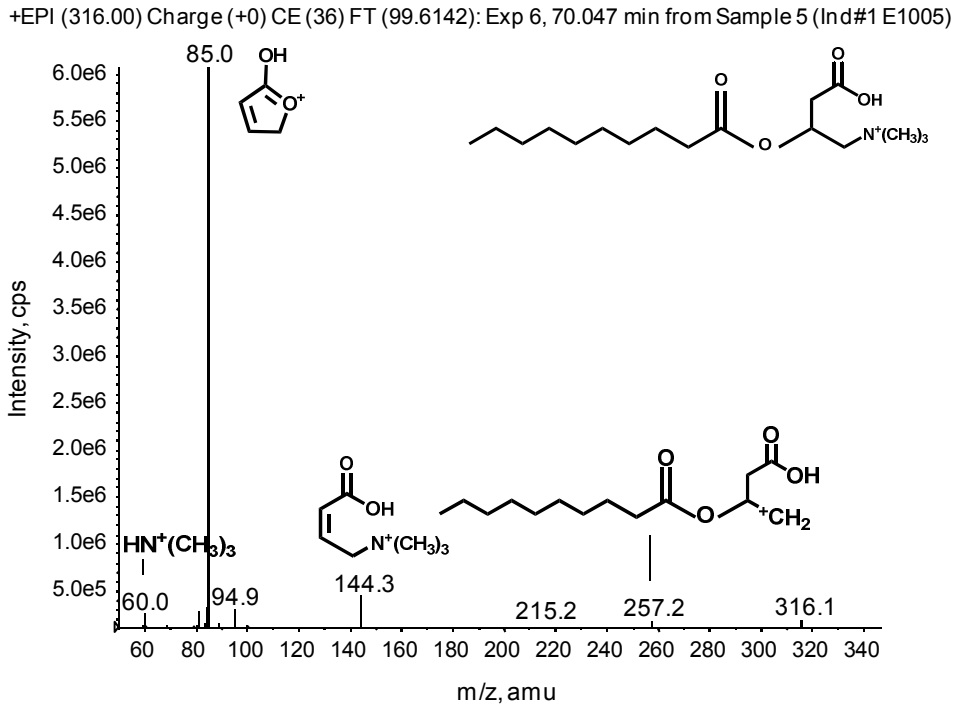

Chapter 3

3.1 Partial list of acylcarnitines found in dried blood spots.

AC EE *m/z*	AC *m/z*	RT (min)	Proposed or confirmed (C) structure
190	162	0.58	Free carnitine
232	204	1.67	C2
246	218	4.85	C3
260 (A)	232	6.6	C4-I
260 (B)	232	6.76	C4
272	244	7.53	C5:1
274 (A)	246	7.97	2MBC
274 (B)	246	8.15	C5-I
276	248	2.91	C4+OH
288	260	9.8	C6
290 (A)	262	2.5	C4:DC (single label)
290 (B)	262	5.12	C5+OH

294	266	8.24	Benzoyl
304	276	6.25	C6+OH
318	262	7.08	C4:DC (doubly labeled)/C6:DC (single label)
330	302	13	C9
342 (A)	314	13.78	C10:1
342 (B)	314	14.14	C10:1
344	316	14.83	C10
346 (A)	290	8.67	C6:DC (doubly labeled)/C8:DC (single label)
346 (B)	290	8.94	C6:DC (doubly labeled)/C8:DC (single label)
372	344	16.98	C12
398	370	3.12 (long chains)	C14:1
400	372	17.37	C14
414 (A)	386	4.87 (long chains)	C15
414 (B)	386	5.17 (long chains)	C15
426	398	4.88 (long chains)	C16:1
428	400	17.53	C16

3.2 Representative annotated MS/MS spectra of acylcarnitines found in dried blood spots.

m/z 190 RT 0.57 min

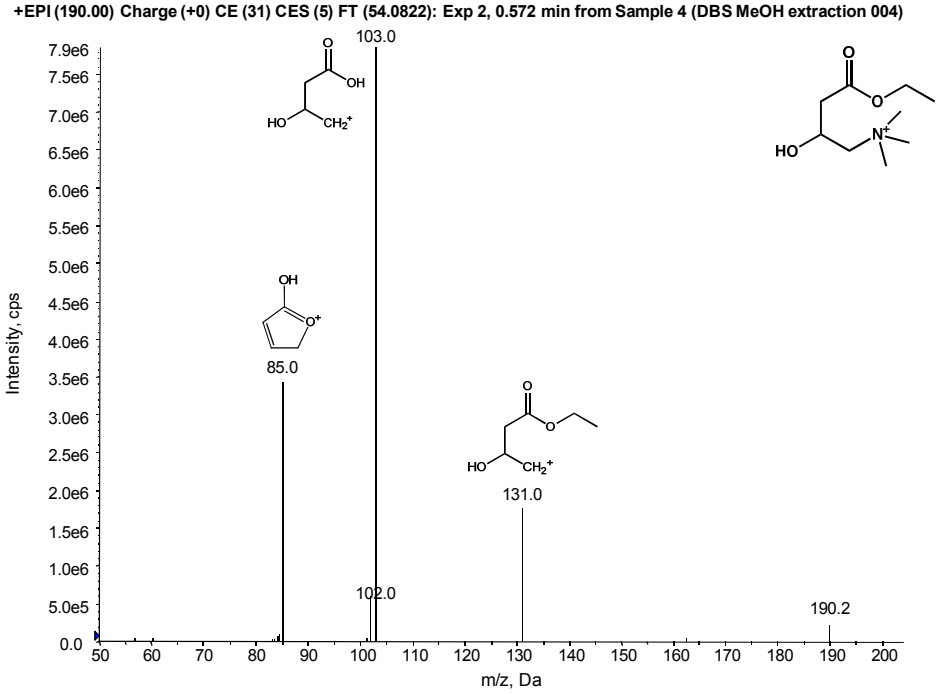

m/z 288 RT 9.80 min

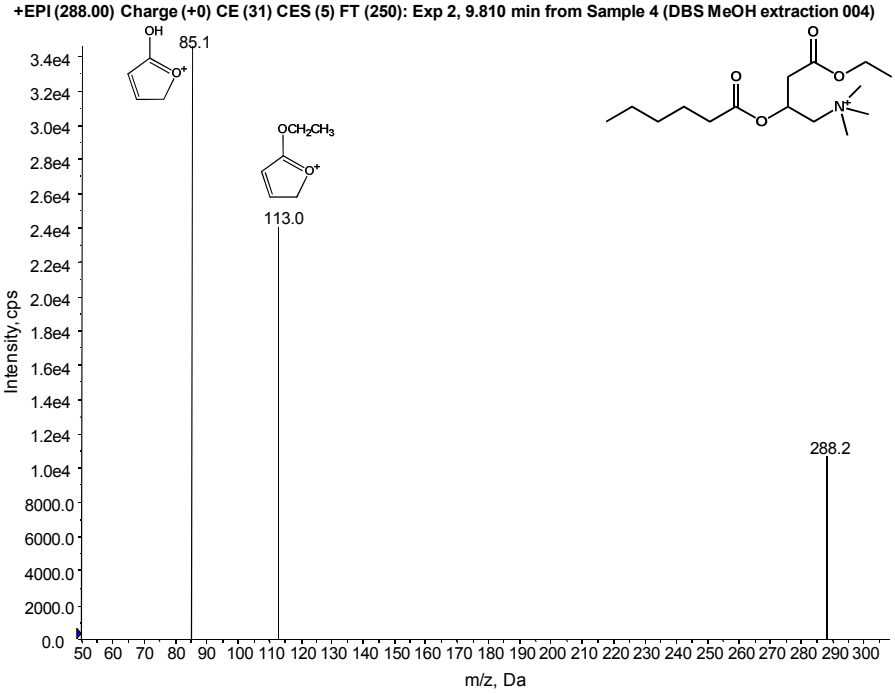

m/z 400 RT 17.37 min

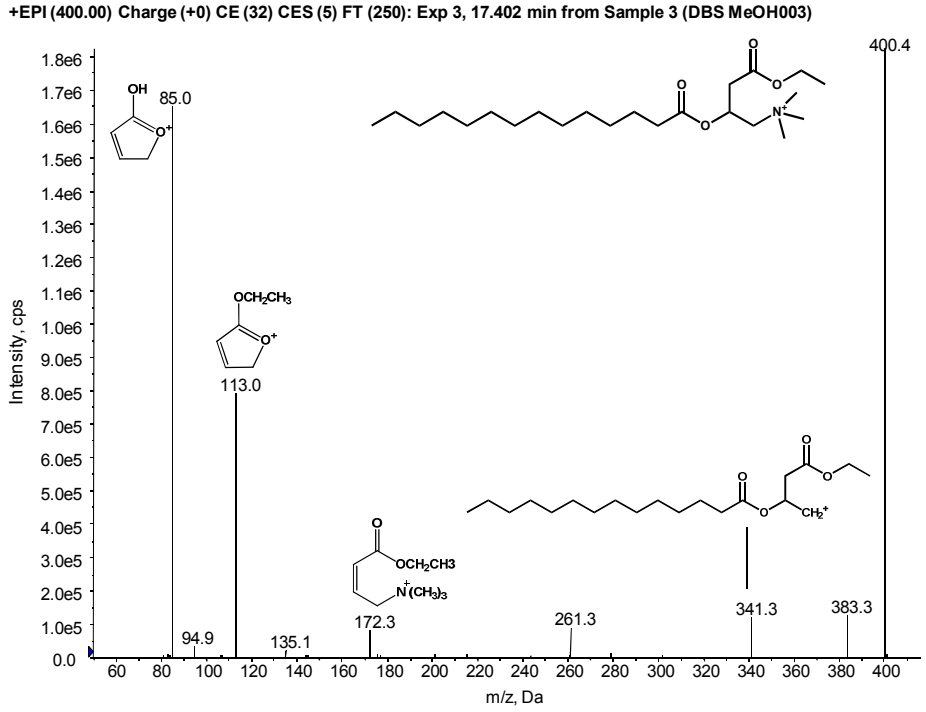

m/z 456 RT 17. 61min

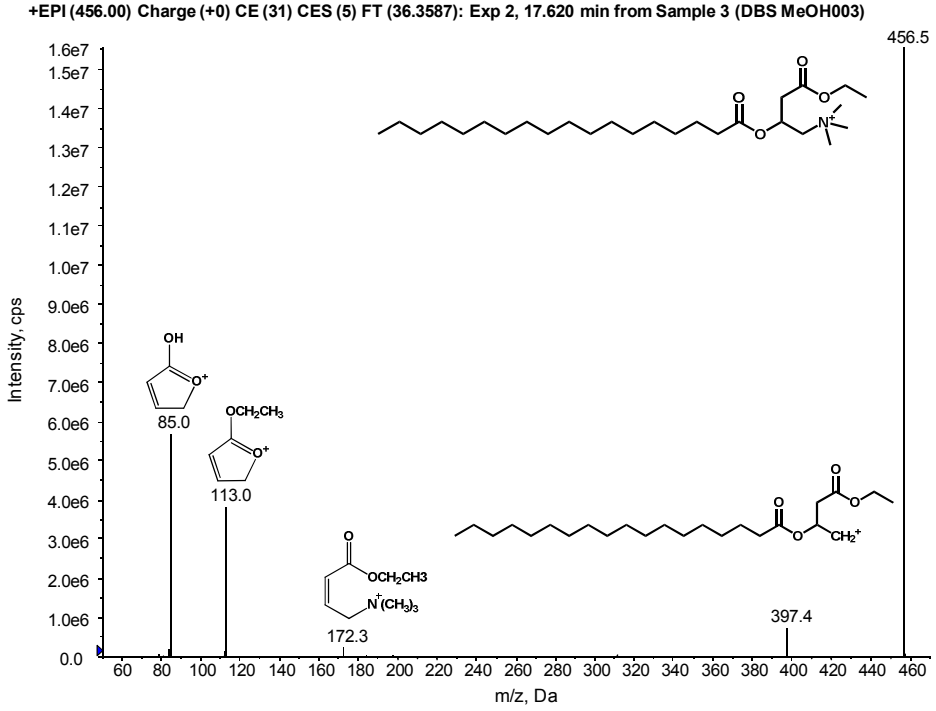

3.3 Partial list of acylcarnitines found in plasma.

AC *m/z*	RT (min)	Proposed or confirmed (C) structure
162	2.24	Free carnitine
204	2.51	C2 (acetyl) (C)
218	4.20	C3 (C)
232 (A)	9.3	C4-I (isobutyryl) (C)
232 (B)	10.3	C4(butyryl) (C)
244	21.57	C5:1-M (3-methylcrotonyl)/ C5:1-T (tiglyl)
246 (A)	22.82	2MBC (C)
246 (B)	23.65	C5-I (C)
246 (C)	24.71	C5 (valeryl) (C)
248	3.20	C4+OH
256	59.04	
258 (A)	26.97	C6:1
258 (B)	27.35	C6:1
258 (C)	28.95	C6:1
258 (D)	29.79	C6:1
260 (A)	31.34	C6 isomer
260 (B)	33.75	C6 (4-methylvaleryl)
260 (C)	35.05	C6 (hexanoyl) (C)
262	4.36	C4:DC(succinyl, methylmalonyl)
266	26.18	benzoyl
272 (A)	33.89	C7:1
272 (B)	36.44	C7:1(isomer)
274	42.57	C7
276 (A)	13.87	C6+OH
276 (B)	18.74	C6+OH
280	28.06	phenylacetyl
284 (A)	36.94	C8:2
284 (B)	37.32	C8:2
284 (C)	39.11	C8:2

3.4 Representative annotated MS/MS spectra of acylcarnitines found in plasma.

m/z 218 RT 4.20 min.

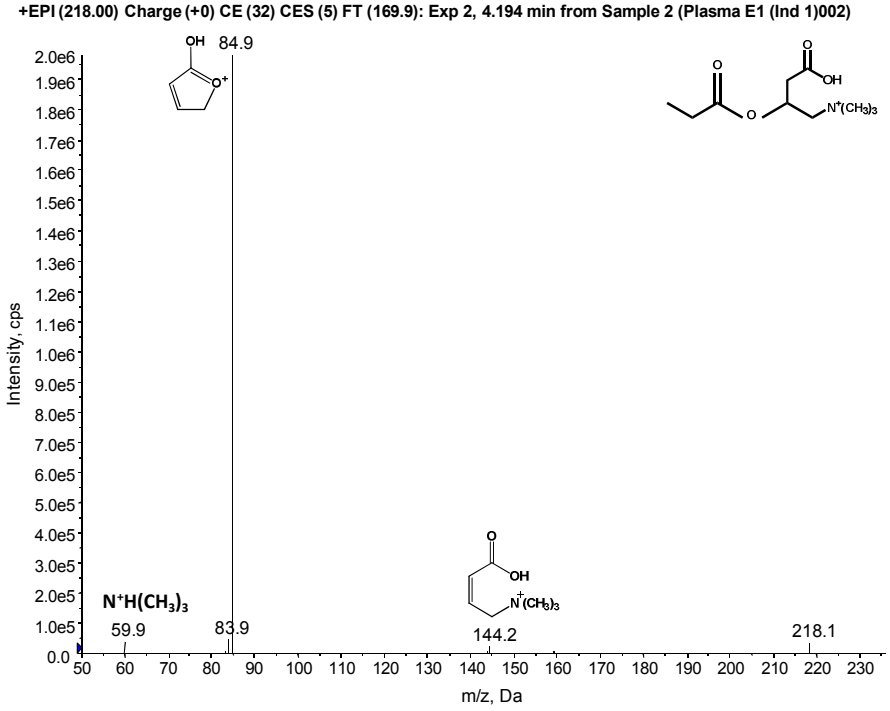

m/z 258 (A) RT 26.97 min

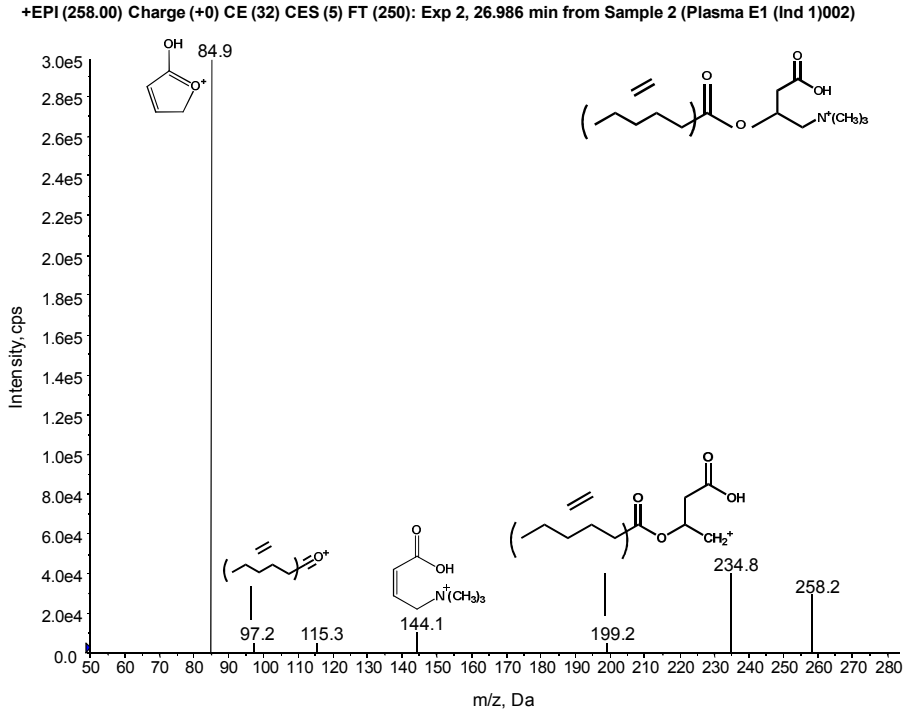

m/z 280 RT 28.06 min

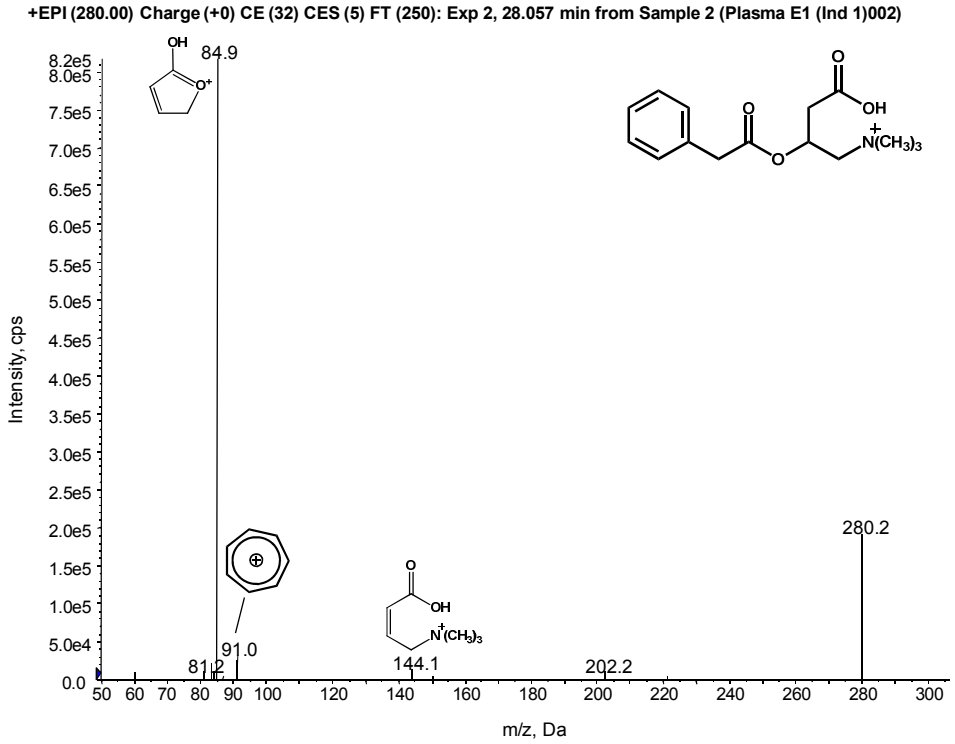

m/z 372 (B) RT 94.31 min

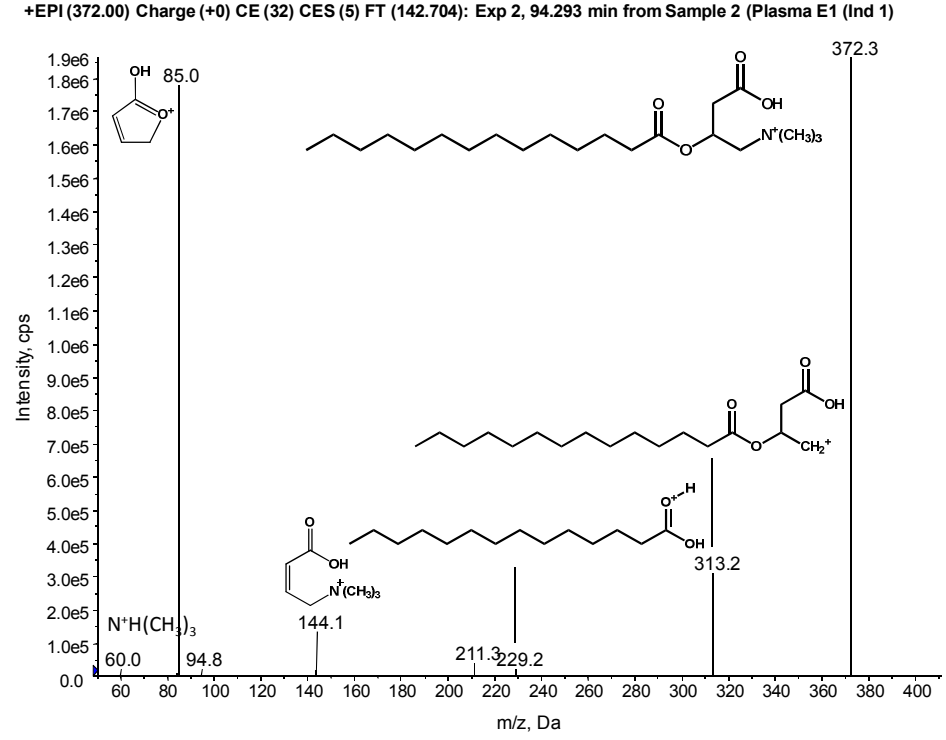

3.5 List of acylcarnitines found in red blood cell pellet.

AC *m/z*	RT (min)	Proposed or confirmed (C) structure
372	3.73	C14 (C)
386	5.21	C15
398	4.38	C16:1
400	6.71	C16 (C)
414 (A)	7.74	C17 (isomer)
414 (B)	8.36	C17
422 (A)	3.74	C18:3
422 (B)	3.95	C18:3
424 (A)	5.30	C18:2
424 (B)	5.84	C18:2
426 (A)	7.36	C18:1
426 (B)	7.84	C18:1
428	9.92	C18 (C)
440	8.79	
448	5.23	C20:4
450	6.38	C20:3
452	8.06	C20:2
454	10.24	C20:1
456	0.80	
472	5.01	C22:6
474	5.84	C22:5
476	7.51	C22:4

3.6 Representative annotated MS/MS spectra of acylcarnitines found in red blood cell pellet.

m/z 398 RT 4.38 min (long-chain method)

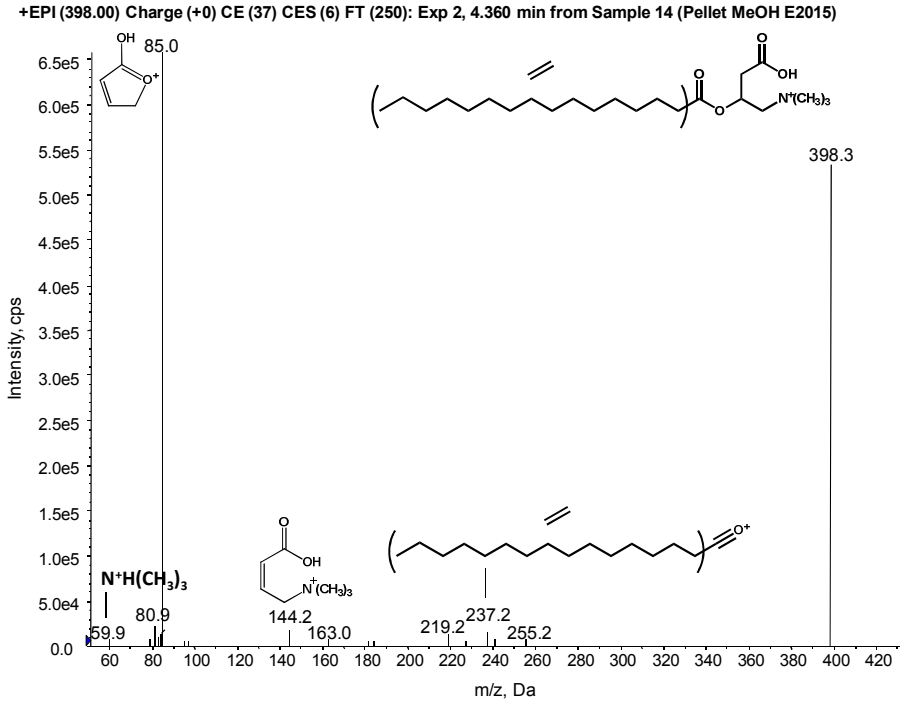

m/z 414 (B) RT 8.36 min (long-chain method)

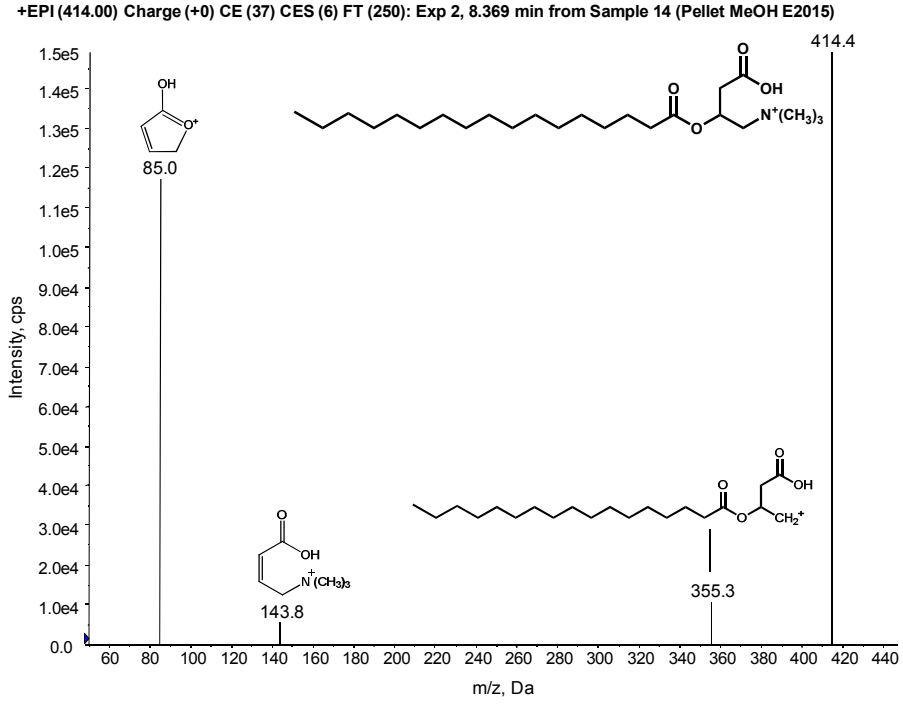

m/z 426 (A) RT 7.28 min (long-chain method)

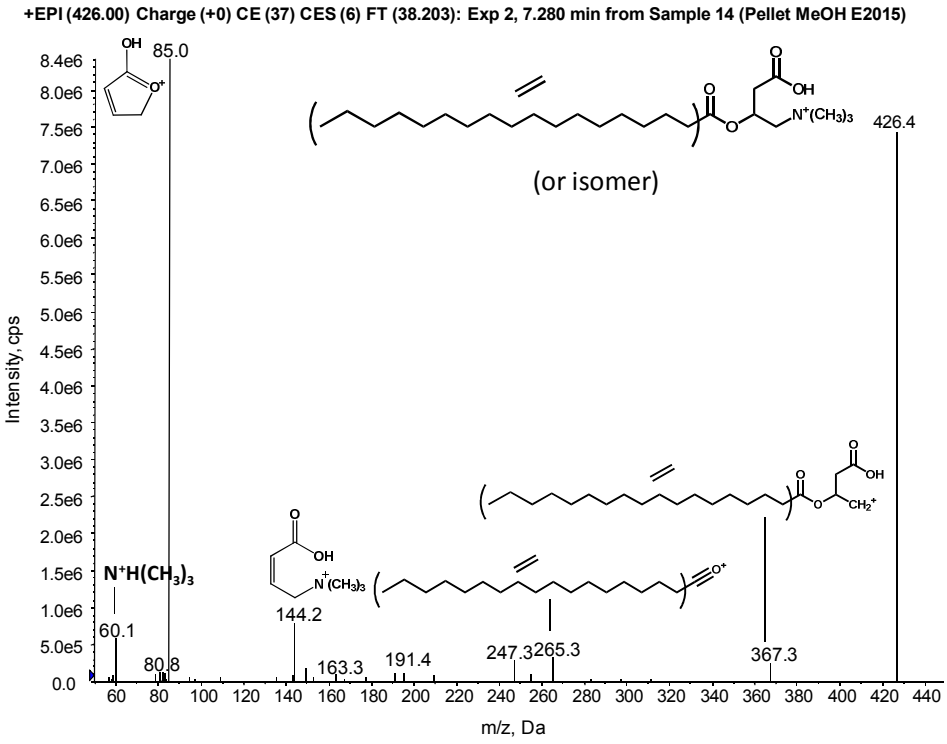

m/z 454 RT 10.24 min (long-chain method)

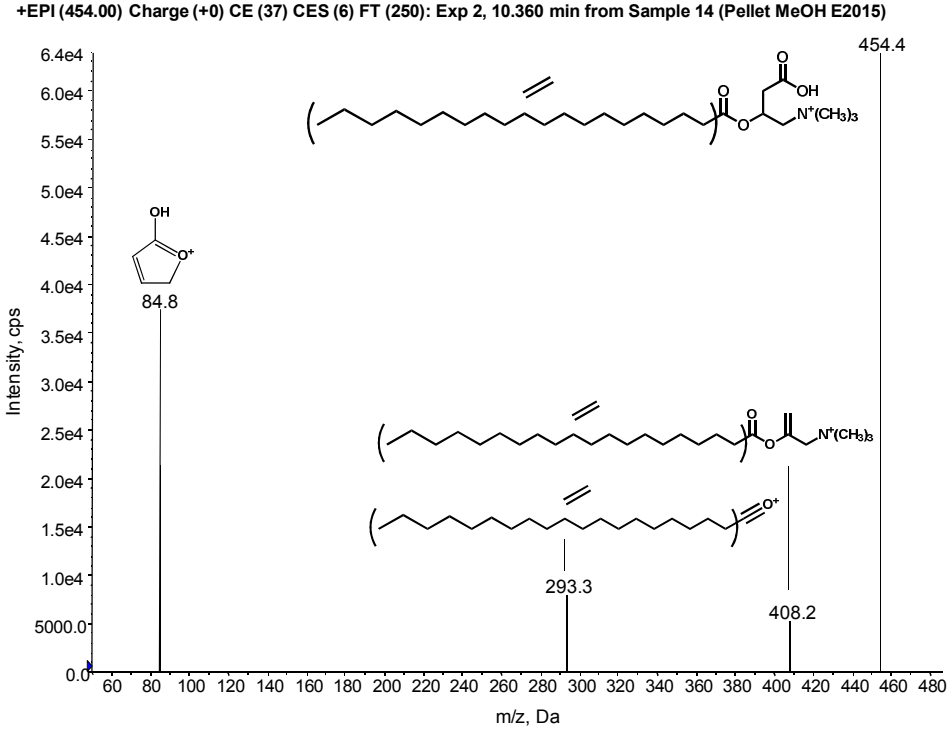

Chapter 4

4.1 Sample calibration curves in neat solvents

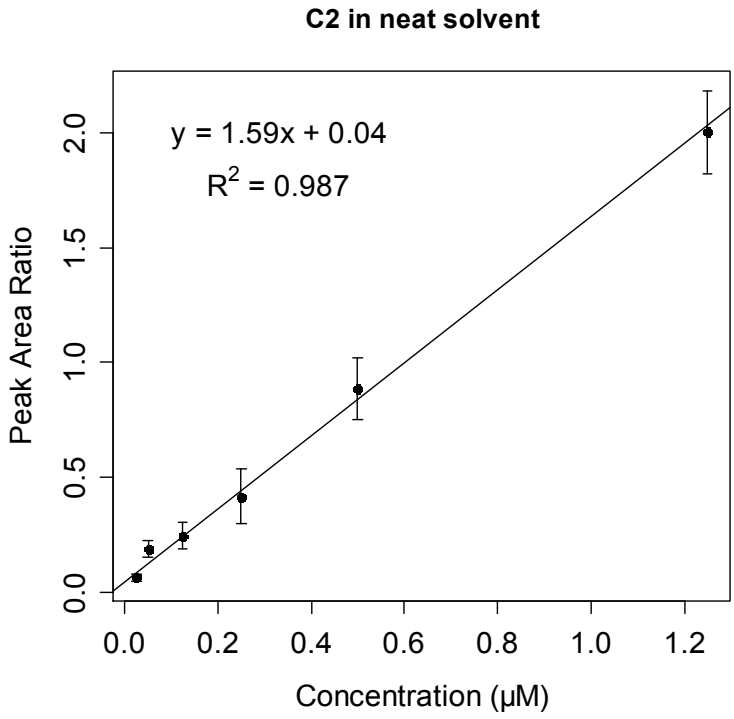

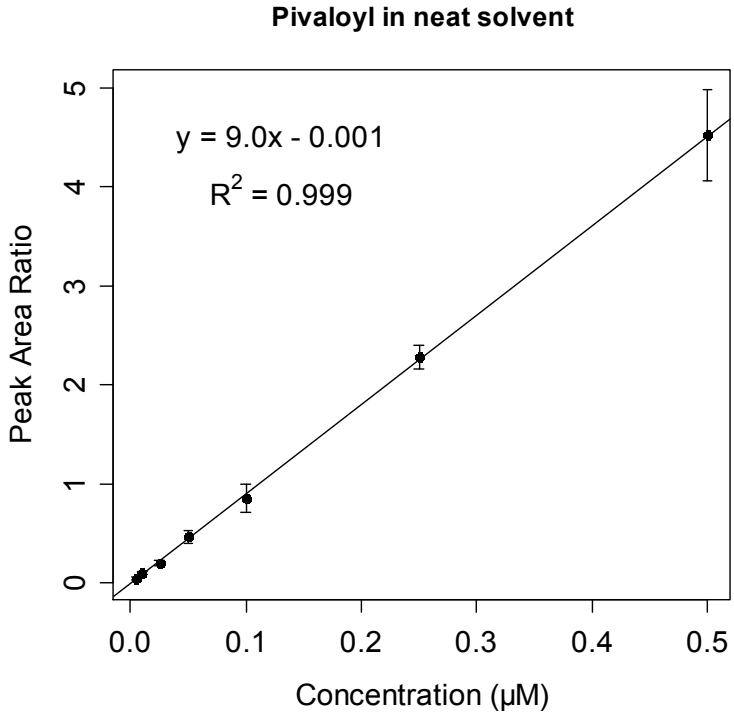

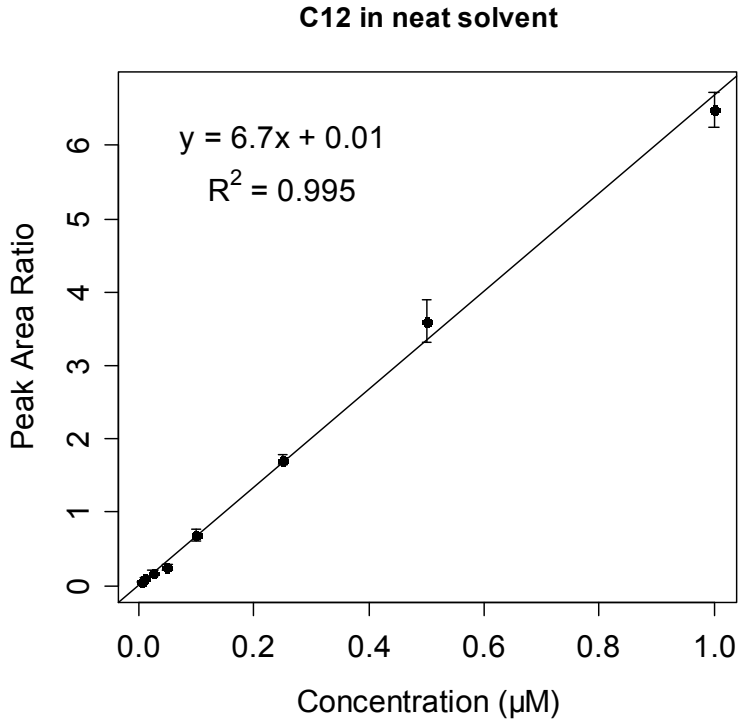

4.2 Summary of linear regression and statistics (neat solvent).

AC	Slope	Y-intercept	R^2	F-statistic	DF	P-value
C2	1.59 (0.09)	0.04 (0.02)	0.987	304.2	4	6.343e-05
C3	7.1 (0.4)	0.05 (0.02)	0.987	391.4	5	6.096e-06
C4-I	1.74 (0.07)	0.010 (0.006)	0.991	652	6	2.377e-07
C4	1.85 (0.03)	0.004 (0.003)	0.998	4118	7	5.865e-11
Pivaloyl	9.0 (0.1)	-0.001 (0.007)	0.999	4668	5	1.272e-08
2MBC	7.6 (0.3)	0.03 (0.02)	0.991	575.4	5	2.346e-06
C5-I	8.3 (0.2)	0.01 (0.01)	0.997	1615	5	1.8e-07
C5	9.4 (0.2)	0.001 (0.01)	0.997	1437	5	2.407e-07
C6	7.6 (0.4)	0.01 (0.02)	0.986	341.6	5	8.53e-06
C8	9.5 (0.3)	0.004 (0.02)	0.994	817.4	5	9.806e-07
C10	7.5 (0.2)	0.08 (0.02)	0.996	1641	6	1.512e-08
C12	6.7 (0.2)	0.01 (0.02)	0.995	1082	6	5.256e-08
C14	7.4 (0.2)	-0.0005 (0.01)	0.995	1065	5	5.081e-07
C16	11.5 (0.4)	-0.02 (0.02)	0.996	668.5	3	1.269e-4
C18	20.1 (0.8)	0.04 (0.04)	0.995	631.3	3	1.383e-4

4.3 Sample calibration curves in underivatized urine

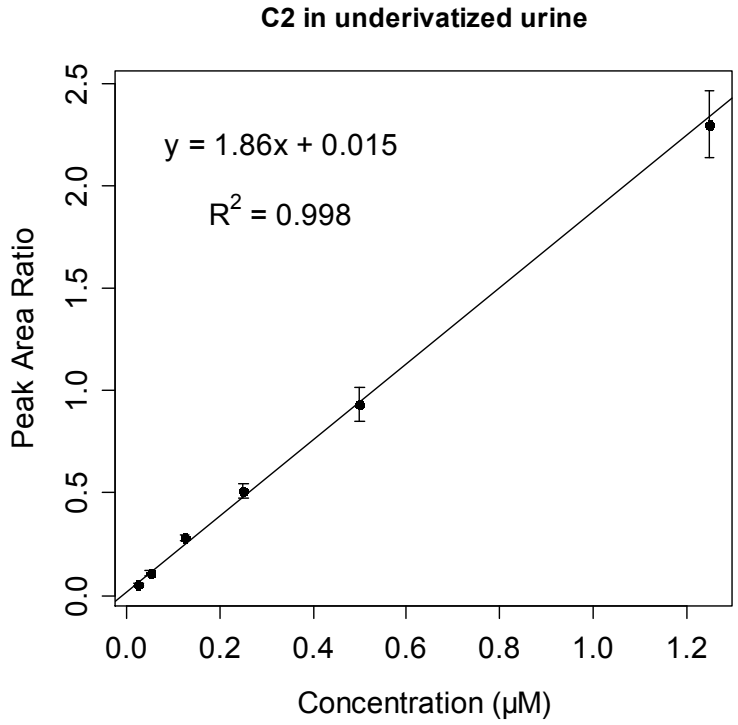

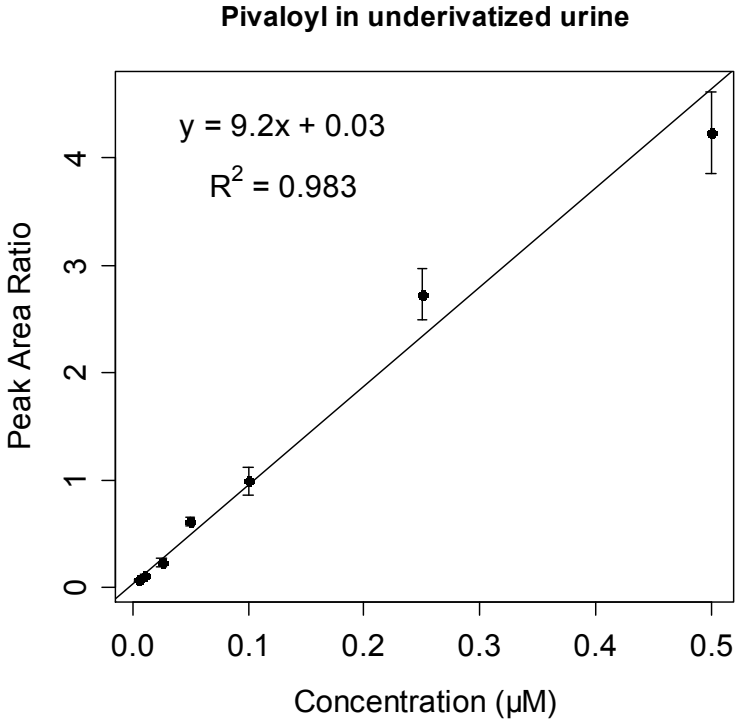

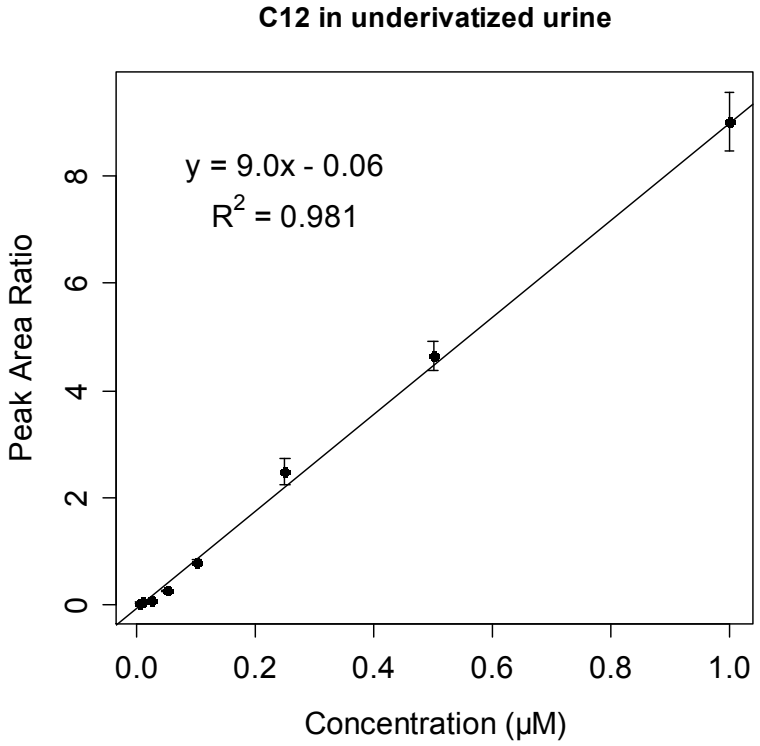

4.4 Summary of linear regression and statistics (urine).

AC	Slope	Y-intercept	R^2	F-statistic	DF	P-value
C2	1.86 (0.05)	0.015 (0.008)	0.998	1690	4	2.094e-06
C3	3.8 (0.1)	0.005 (0.005)	0.997	1469	5	2.176e-07
C4-I	1.84 (0.02)	0.004 (0.002)	0.999	7036	6	1.933e-10
C4	1.70 (0.05)	0.004 (0.005)	0.995	1350	7	2.878e-09
Pivaloyl	9.2 (0.5)	0.03 (0.03)	0.983	284.7	5	1.337e-05
2MBC	9.7 (0.5)	0.09 (0.04)	0.985	322.3	5	9.845e-06
C5-I	10.5 (0.2)	0.02 (0.01)	0.998	2282	5	7.591e-08
C5	10.0 (0.5)	0.08 (0.04)	0.986	345.2	5	8.314e-06
C6	9.4 (0.3)	0.008 (0.01)	0.996	1255	5	3.372e-07
C8	9.7 (0.4)	0.10 (0.03)	0.990	493.5	5	3.434e-06
C10	8.9 (0.2)	-0.02 (0.01)	0.998	2842	6	2.923e-09
C12	9.0 (0.5)	-0.06 (0.03)	0.981	305.4	6	2.251e-06

4.5 Partial list of quantified acylcarnitines in urine with putative identification.

AC EE *m/z*	AC *m/z*	RT (min)	Putative ID
232	204	0.61	C2** (confirmed with standard)
246	218	0.81	C3 (confirmed with standard)
260 (A)	232	1.30	C4-I (confirmed with standard)
260 (B)	232	1.38	C4 (confirmed with standard)
272	244	1.77	C5:1-M (3-methylcrotonyl) or C5:1-T (tiglyl)
274 (A)	246	2.12	Pivaloyl (confirmed with standard)
274 (B)	246	2.30	2MBC (confirmed with standard)
274 (C)	246	2.49	C5-I (confirmed with standard)
274 (D)	246	2.68	C5 (confirmed with standard)
286	258	2.9	C6:1
288 (A)	260	4.27	C6 (4-methylvaleryl)
288 (B)	260	5.25	C6 (confirmed with standard)
290	262	0.72	Singly labeled C4:DC
300 (A)	272	4.83	C7:1
300 (B)	272	5.47	C7:1 isomer
302 (A)	274	7.7	C7
302 (B)	274	7.9	C7 isomer
304	276	1.1	Singly labeled C5:DC
312	284	5.65	C8:2
314 (A)	286	8.9	C8:1
314 (B)	286	9.65	C8:1 isomer
316 (A)	288	10.10	C8 isomer (valproyl, 2- or 6-methylheptanoyl)
316 (B)	288	11.39	C8 (confirmed with standard)
318 (A)	262	0.95	Doubly labeled C4:DC (A)
318 (B)	262	1.47	Doubly labeled C4:DC (B)
328 (A)	300	10.84	C9:1
328 (B)	300	11.7	C9:1 isomer
330 (A)	302	12.01	C9 isomer
330 (B)	302	12.25	C9

4.6 Partial summary table of absolute quantification experiments. Concentrations are reported in µmol/g creatinine.

Individual	C6			C8		
	Day 1	Day 2	Day 3	Day 1	Day 2	Day 3
001	0.038 ± 0.002	0.028 ± 0.004	0.036 ± 0.003	<LLOQ	<LLOQ	<LLOQ
004	0.034 ± 0.003	0.030 ± 0.002	0.097 ± 0.002	<LLOQ	<LLOQ	0.092 ± 0.003
005	0.061 ± 0.008	0.24 ± 0.02	0.09 ± 0.01	0.114 ± 0.008	0.18 ± 0.01	0.16 ± 0.02
008	0.073 ± 0.006	0.047 ± 0.003	0.08 ± 0.01	<LLOQ	<LLOQ	<LLOQ
009	0.038 ± 0.003	0.078 ± 0.004	0.061 ± 0.003	0.075 ± 0.009	0.12 ± 0.01	0.122 ± 0.004
010	0.013 ± 0.002	0.09 ± 0.01	0.07 ± 0.01	<LLOQ	0.054 ± 0.006	0.08 ± 0.01
011	0.06 ± 0.02	0.08 ± 0.02	0.036 ± 0.006	0.054 ± 0.005	<LLOQ	<LLOQ
015	0.046 ± 0.005	<LLOQ	0.023 ± 0.003	<LLOQ	<LLOQ	<LLOQ
016	0.037 ± 0.003	0.053 ± 0.003	<LLOQ	0.090 ± 0.006	0.24 ± 0.02	<LLOQ
018	0.026 ± 0.003	0.113 ± 0.006	0.05 ± 0.02	0.052 ± 0.001	0.51 ± 0.01	0.103 ± 0.009

4.7 Partial summary table of relative quantification experiments for individual 001.

AC	Individual	IS	Day	Avg.Conc. (µmol/g creatinine)	Std. dev.
m/z 290 RT 0.72	001	C3	1	0.9	0.2
			2	0.65	0.06
			3	1.9	0.1
m/z 318 RT 0.95	001	C3	1	0.08	0.02
			2	0.0229	0.0003
			3	0.13	0.05
m/z 304 RT 1.1	001	C4-I	1	0.52	0.09
			2	0.28	0.03
			3	0.8	0.1
m/z 318 RT 1.47	001	C4-I	1	0.99	0.08
			2	1.5	0.2
			3	3.6	0.5
m/z 272 RT 1.77	001	C4-I	1	1.1	0.1
			2	1.0	0.2
			3	1.5	0.2
m/z 350 RT 1.91	001	C4-I	1	0.03	0.01
			2	0.009	0.002
			3	0.044	0.003
m/z 358 RT 2.0	001	C4-I	1	0.046	0.004
			2	0.02	0.01
			3	0.06	0.01

4.8 Representative MS/MS spectra of acylcarnitine ethyl esters detected and quantified in urine.

m/z 272 RT 1.77min

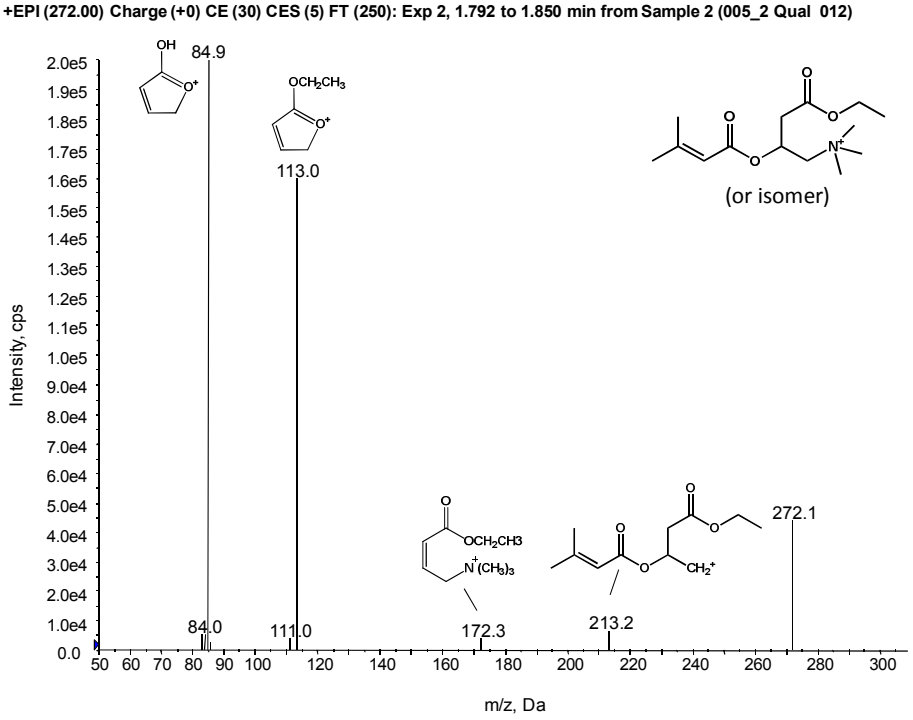

m/z 318 (B) RT 1.48min

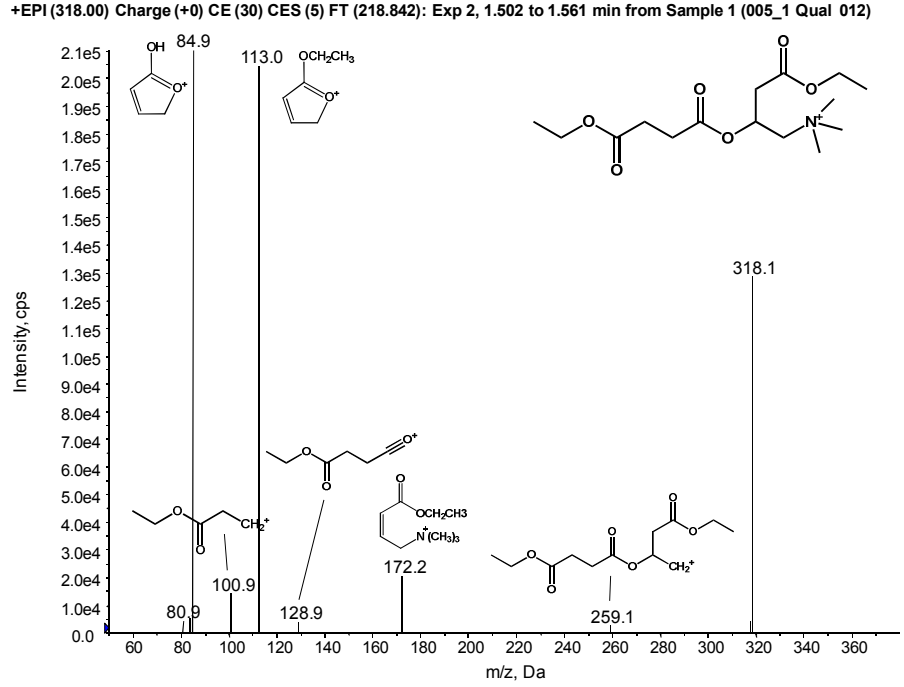

m/z 360 RT 4.95min

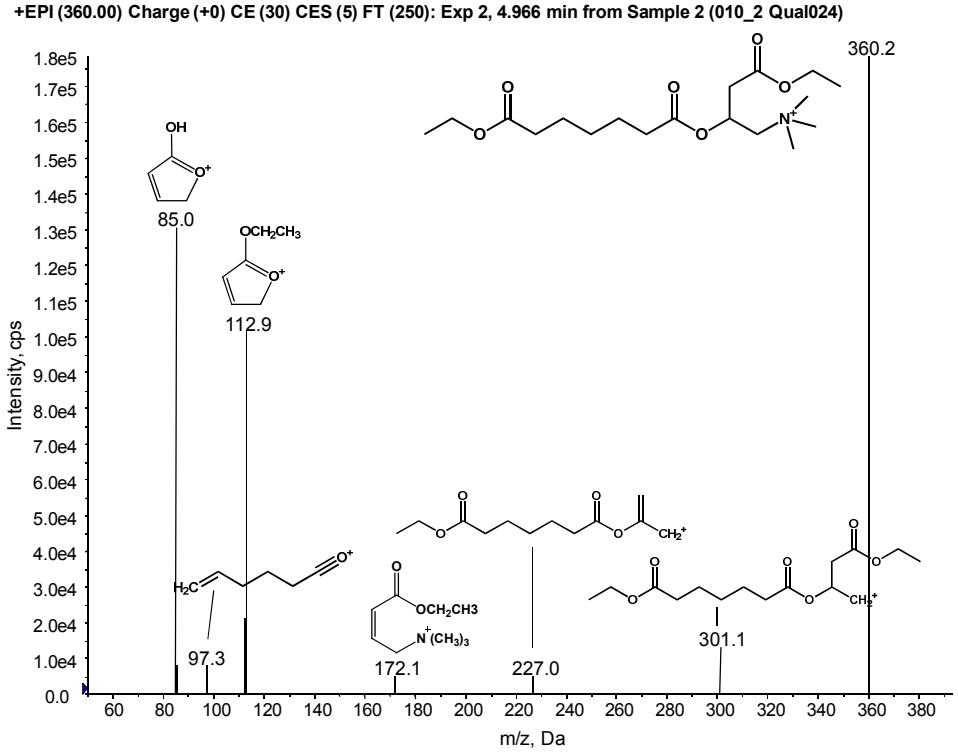

m/z 388 RT 10.13min

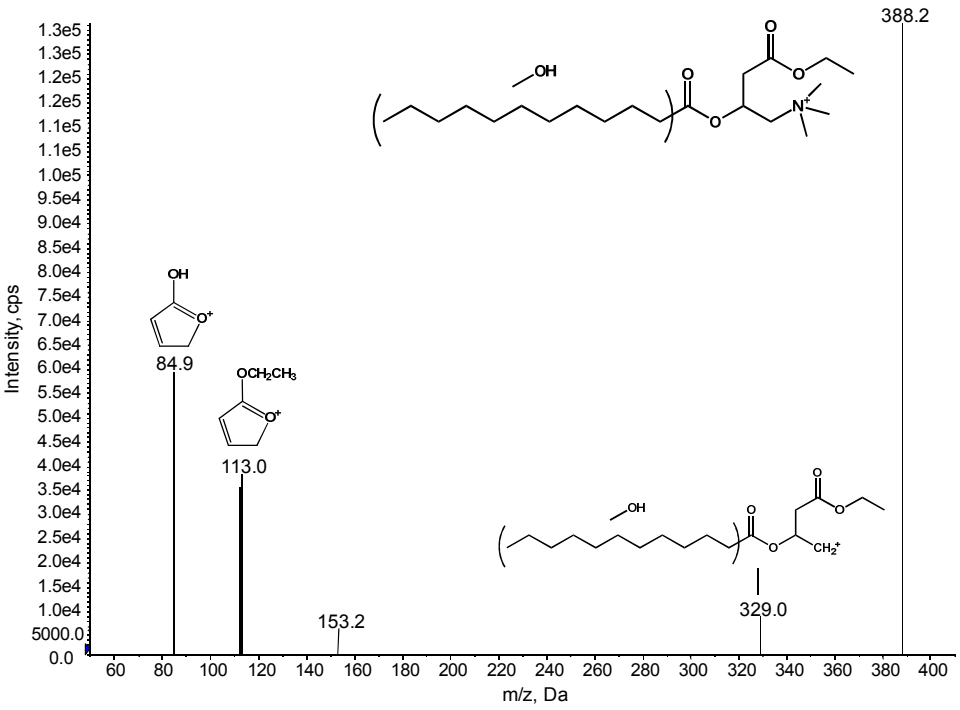

Chapter 5

5.1 Representative calibration curves in plasma.

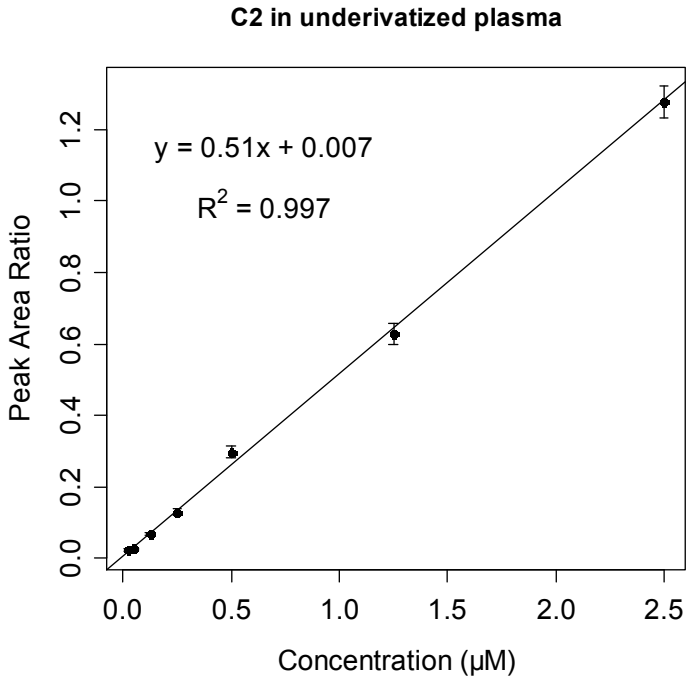

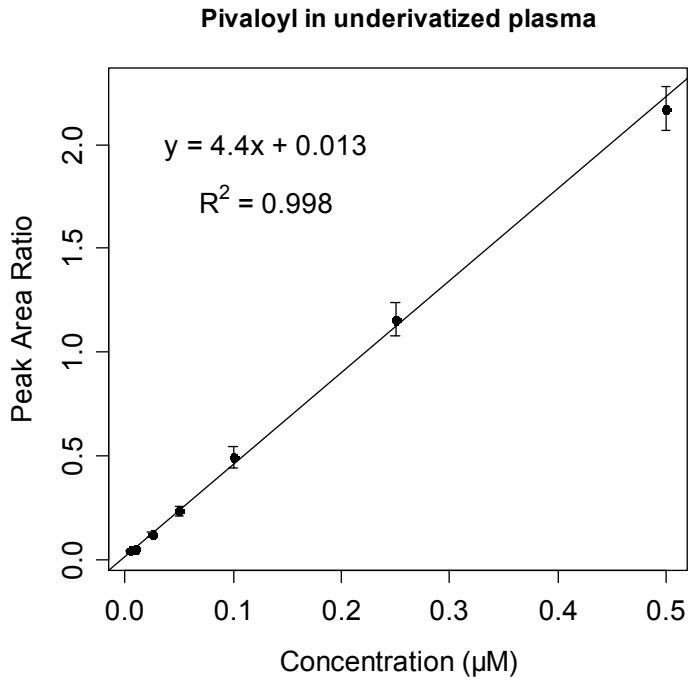
Pivaloyl in underivatized plasma
y = 4.4x + 0.013
R2 = 0.998
Peak Area Ratio
0.0
0.5
1.0
1.5
2.0
0.0
0.1
0.2
0.3
0.4
0.5
Concentration (µM)

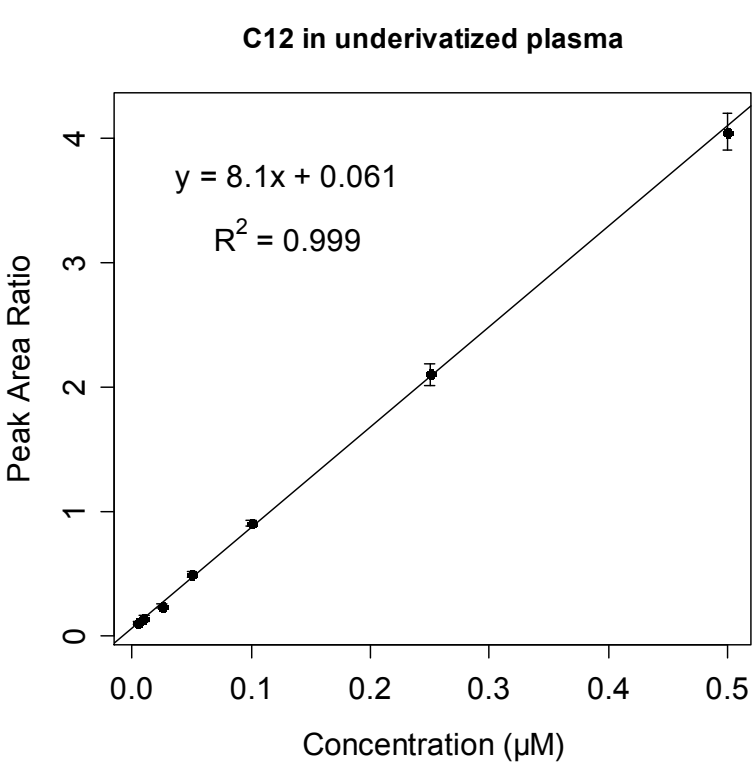
C12 in underivatized plasma
y = 8.1x + 0.061
R2 = 0.999
Peak Area Ratio
0
1
2
3
4
0.0
0.1
0.2
0.3
0.4
0.5
Concentration (µM)

5.2 Summary of linear regression and statistics (plasma).

AC	Slope	Y-intercept	R^2	F-statistic	DF	P-value
C2	0.51 (0.01)	0.007 (0.004)	0.997	1408	5	2.533e-07
C3	0.90 (0.03)	0.002 (0.002)	0.994	867.4	5	8.46e-07
C4-I	0.63 (0.02)	0.003 (0.001)	0.995	1077	5	4.942e-07
C4	0.90 (0.02)	0.005 (0.001)	0.998	2271	5	7.689e-08
Pivaloyl	4.4 (0.1)	0.013 (0.006)	0.998	2150	5	8.812e-08
2MBC	4.15 (0.08)	0.014 (0.005)	0.998	2533	5	5.855e-08
C5-I	3.73 (0.09)	0.016 (0.006)	0.997	1617	5	1.793e-07
C5	4.1 (0.1)	0.012 (0.007)	0.996	1216	5	3.645e-07
C6	4.20 (0.06)	0.009 (0.004)	0.999	4357	5	1.511e-08
C8	7.4 (0.2)	0.03 (0.01)	0.997	1504	5	2.147e-07
C10	6.6 (0.1)	0.026 (0.009)	0.998	2127	5	9.049e-08
C12	8.1 (0.1)	0.061 (0.008)	0.999	4823	5	1.172e-08
C14	9.0 (0.2)	0.03 (0.01)	0.998	2745	5	4.79e-08
C16	11.7 (0.6)	0.04 (0.03)	0.991	347.7	3	3.336e-4
C18	12.8 (0.2)	-0.01 (0.01)	0.999	2763	3	1.516e-05

5.3 Summary of results for absolute quantification of C2 in plasma.

Individual	Gender	Concentration (μM)	Std. dev.
1	Female	0.7	0.1
2	Male	0.5	0.1
3	Female	1.1	0.1
4	Male	1.2	0.3
5	Female	4.4	0.9
6	Male	0.7	0.1
7	Female	2.3	0.5
8	Male	2.0	0.5
9	Female	13	2
10	Male	1.4	0.3

5.4 Summary of results for relative quantification of acylcarnitines in plasma (individual 9).

AC	Concentration (μM)	Std. dev.
m/z 284 RT 0.98	<LLOQ	
m/z 304 RT 1.10	0.12	0.02
m/z 272 RT 1.62	0.005	0.001
m/z 332 (A) RT 1.96	0.023	0.003
m/z 332 (B) RT 4.41	0.13	0.02
m/z 332 (C) RT 5.29	0.037	0.006
m/z 360 (A) RT 5.38	0.014	0.002
m/z 412 RT 5.53	0.017	0.002
m/z 360 (B) RT 5.90	0.004	0.001
m/z 388 RT 10.62	0.033	0.003
m/z 360 (C) RT 10.88	0.043	0.005
m/z 330 (A) RT 11.97	0.006	0.001
m/z 330 (B) RT 12.20	0.006	0.001
m/z 342 RT 12.75	0.017	0.002
m/z 416 (A) RT 13.20	0.015	0.002
m/z 416 (B) RT 13.40	0.017	0.001
m/z 358 RT 14.39	0.0061	0.0004
m/z 386 RT 16.33	0.067	0.006
m/z 454 RT 19.97	0.032	0.004

5.5 Representative MS/MS spectra of acylcarnitine ethyl esters detected and quantified in plasma.

m/z 344 RT 13.74 min

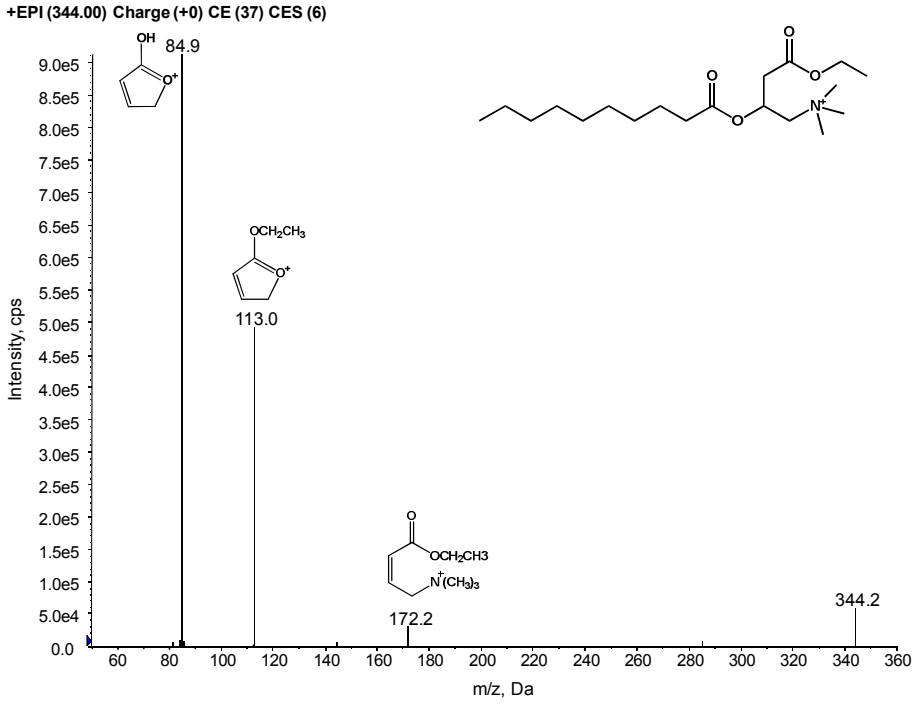

m/z 388 RT 10.62 min

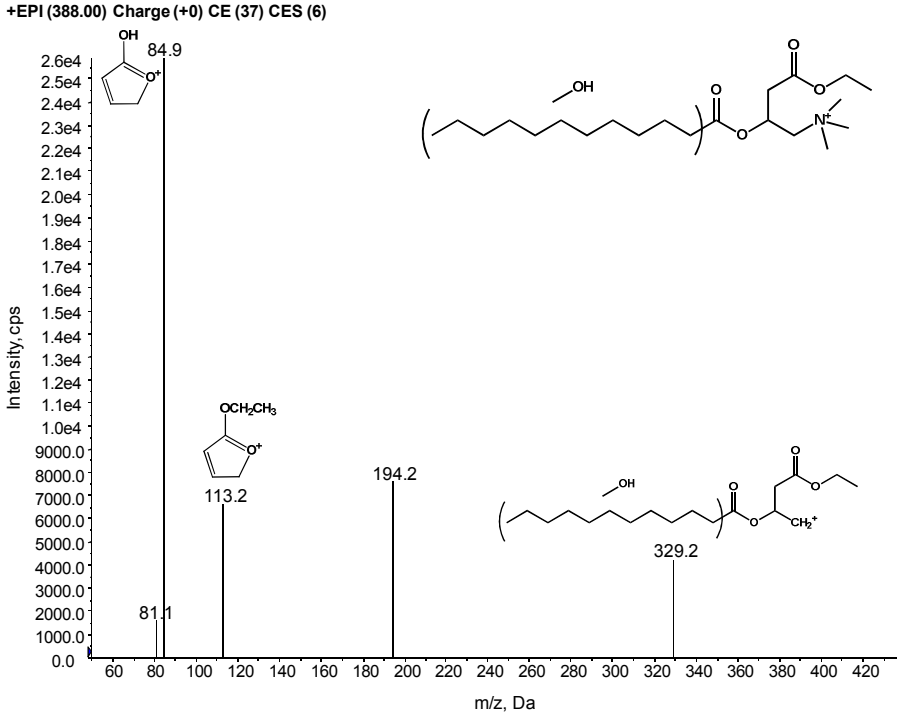

m/z 428 RT 19.35 min

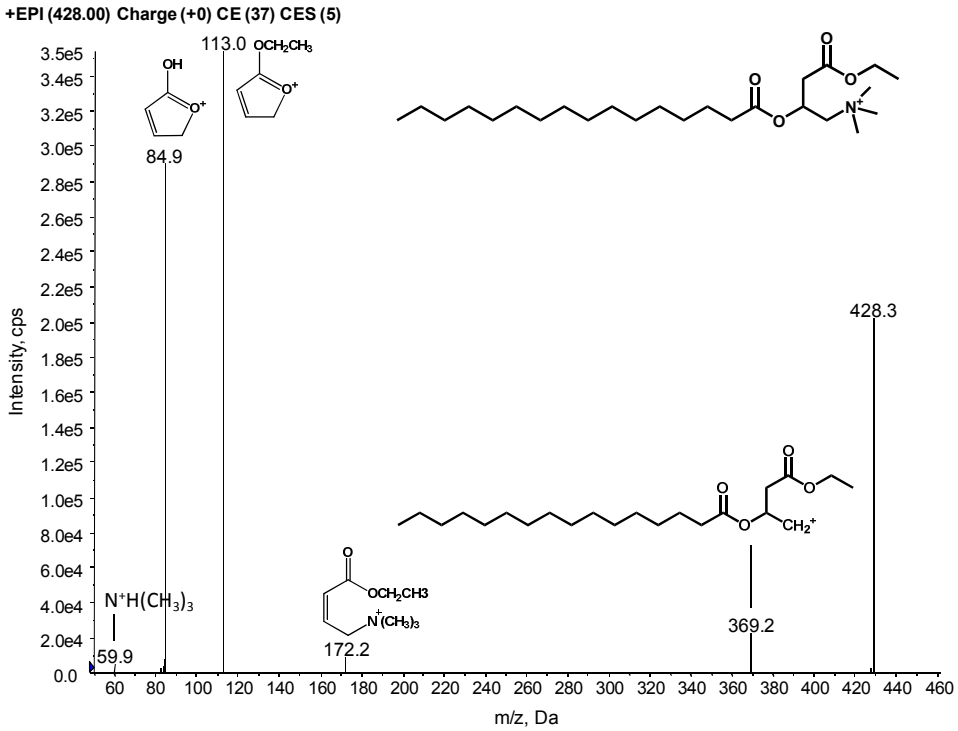

m/z 456 RT 21.11 min

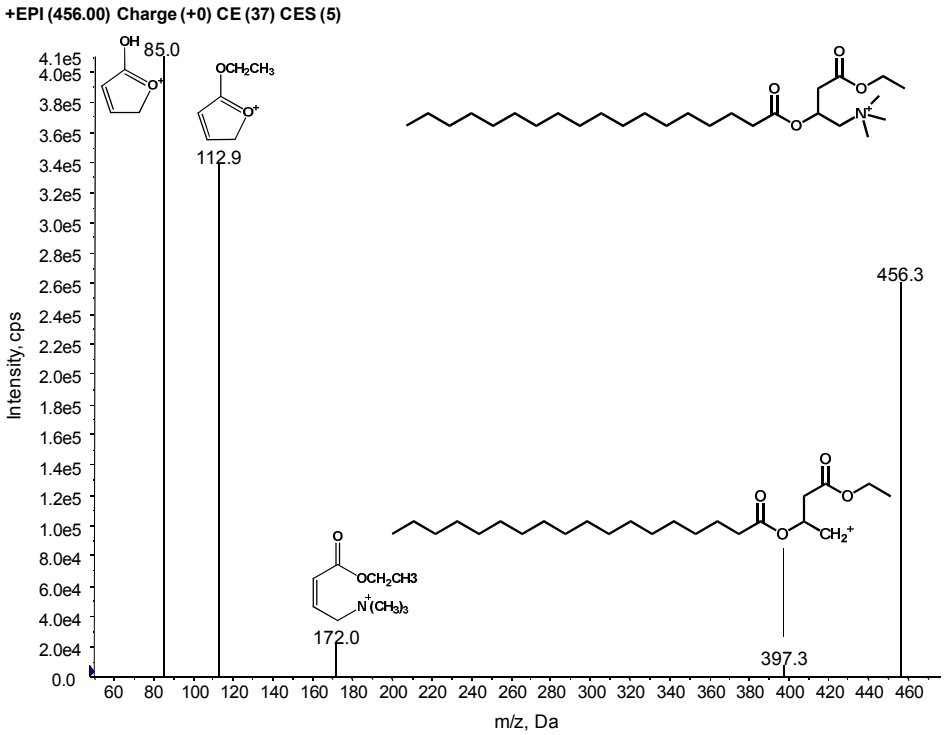

Chapter 6

6.1 Results from database searching of urine metabolite features using reaction = 0. No MS/MS spectra for these compounds were found in the HMDB database. MS/MS spectral interpretation was performed to confirm all structures.

Feature ID #	Accurate *m/z* (TOF)	RT range (min) TOF	*m/z* QTRAP	RT (min) QTRAP	Ion Type	Putative ID	Error (ppm)	Structure
1	162.0549	26.10 - 26.60	162.1	26.10	$[M + H]^+$	Indole-3-carboxylic acid or isomers	-0.15	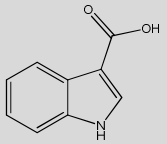
2	188.1749	1.50 - 2.00	188.2	1.22	$[M + H]^+$	N8-Acetylspermidine or isomers	-4.45	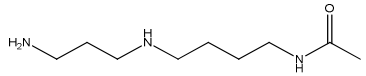
3	274.2002	31.90 - 32.30	274.2	32.68	$[M + H]^+$	Heptanoylcarnitine or isomer	-4.02	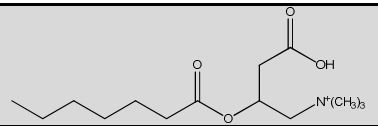
4	274.2009	32.60 - 33.10	274.1	33.29	$[M + H]^+$	Heptanoylcarnitine	-1.43	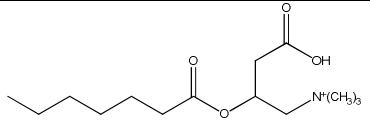

5	312.217	36.50 - 37.30	312.1	37.07	$[M + H]^+$	2-trans,4-cis-Decadienoylcarnitine	-0.02	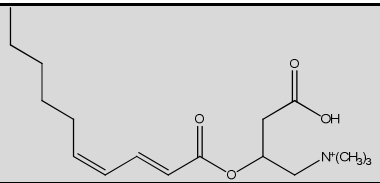
6	312.2175	38.10 - 38.60	312.2	38.57	$[M + H]^+$	2-trans,4-cis-Decadienoylcarnitine	1.75	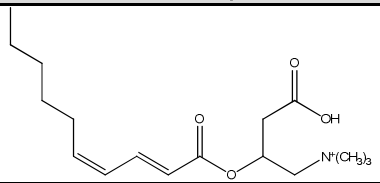
7	328.1030	26.30 - 26.90	328.1	26.49	$[M + H]^+$	Acetaminophen glucoronide	0.99	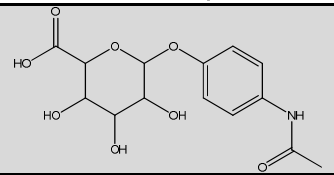
8	330.2273	33.10 - 33.60	330.1	33.79	$[M + H]^+$	6-Keto-decanoylcarnitine	-0.47	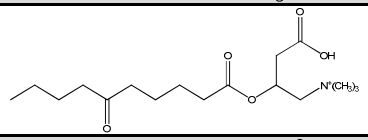
9	330.2263	34.60 - 35.10	330.2	35.16	$[M + H]^+$	6-Keto-decanoylcarnitine	-3.54	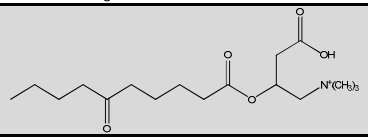
10	342.2638	43.00 - 43.50	342.2	43.46	$[M + H]^+$	trans-2-Dodecenoylcarnitine	-0.30	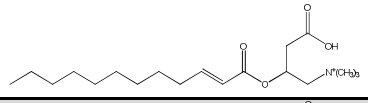
11	344.2789	45.20 - 45.70	344.3	45.63	$[M + H]^+$	Dodecanoylcarnitine	-1.94	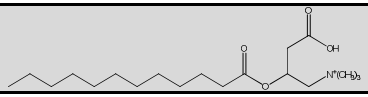

12	370.2945	46.80 - 47.50	370.3	47.45	$[M + H]^+$	Trans-2-Tetradecenoylcarnitine or isomer	-1.98	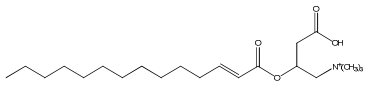
13	384.2746	41.90 - 42.40	384.3	42.33	$[M + H]^+$	3-Hydroxy-5, 8-tetradecadiencarnitine	0.36	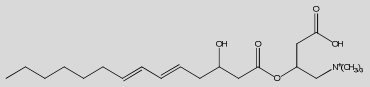
14	386.2892	43.60 - 44.20	386.3	44.10	$[M + H]^+$	3-Hydroxy-cis-5-tetradecenoylcarnitine	-2.37	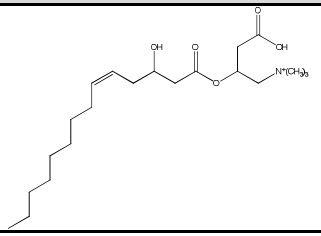

6.2 Results from database searching of urine metabolite features using reaction = 1. MS/MS spectral interpretation was performed to confirm all structures.

Feature ID #	Accurate *m/z* TOF	RT (min) TOF	*m/z* QTRAP	RT (min) QTRAP	Ion Type	Putative ID	Error (ppm)	Structure
1	156.1381	35.80 - 36.30	155.9	36.37	$[M + H]^+$	Gabapentin – O	-1.4	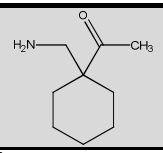
2	181.0600	5.80 - 6.30	181.2	6.35	$[M + H]^+$	Picolinic acid + C_2H_3NO (glycine) or isomer	-4.2	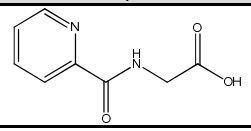

3	188.1276	10.70 - 11.20	188.2	11.00	$[M + H]^+$	N-Acetylleucine + CH_2	-2.9	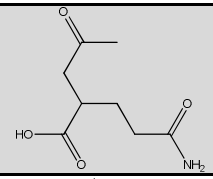
4	190.0858	16.70 - 17.90	190.3	17.45	$[M + H]^+$	N-Acetyl-L-phenylalanine - H_2O	-2.38	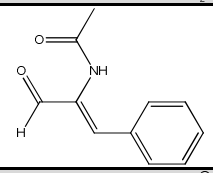
5	191.1071	30.80 - 31.30	191.1	31.16	$[M + H]^+$	Cuminaldehyde + C_2H_2O	2.12	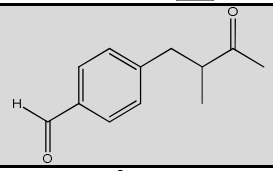
6	194.0811	22.10 - 23.00	194.2	22.49	$[M + H]^+$	3-Succinoylpyridine + CH_2	-0.36	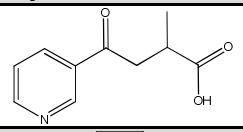
7	197.0961	47.00 - 47.60	197.2	47.74	$[M + H]^+$	(+)-(1R,2R)-1,2-Diphenylethane-1,2-diol – H_2O	-0.09	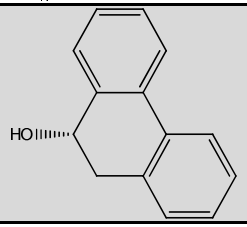
8	200.1283	33.60 - 34.10	200.2	34.21	$[M + H]^+$	Capryloylglycine + H_2	0.88	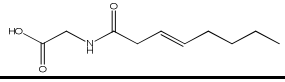

9	220.0602	26.30 - 26.80	220.2	26.36	$[M + H]^+$	5-Hydroxyindoleacetic acid + CO	-0.94	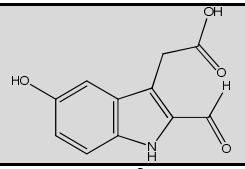
10	232.0273	6.40 - 7.00	232.1	7.29	$[M + H]^+$	Acetaminophen + SO_3	-0.72	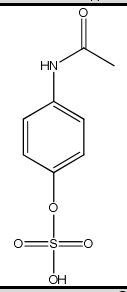
11	266.1390	25.80 - 26.40	266.1	26.08	$[M + H]^+$	Benzoic acid + $C_7H_{13}NO_2$ (carnitine)	1.32	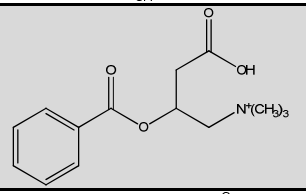
12	272.1849	29.80 - 30.30	272.2	30.58	$[M + H]^+$	Tiglylcarnitine + C_2H_4 or isomer	-2.59	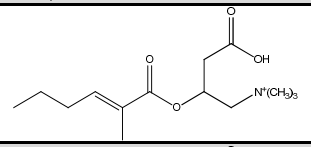
13	272.1845	30.90 - 31.40	272.1	31.61	$[M + H]^+$	Tiglylcarnitine + C_2H_4 or isomer	-4.05	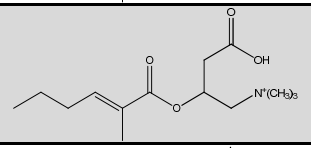
14	273.2206	41.90 - 42.40	273.2	42.38	$[M + H]^+$	Androstenol - H_2 or isomer	-2.47	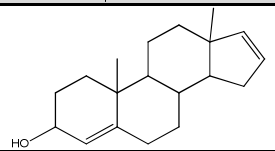

15	287.1994	36.20 - 36.80	287.2	36.82	$[M + H]^+$	Testosterone - H_2 or isomer	-2.02	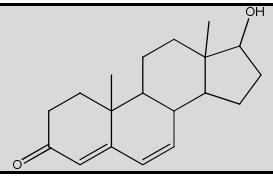
16	300.2174	36.70 - 37.20	300.1	37.21	$[M + H]^+$	2,6 dimethylheptanoyl carnitine - H_2 or isomer	1.50	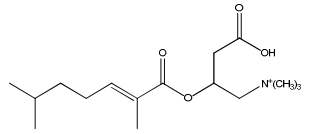
17	302.1976	27.80 - 28.40	302.2	28.50	$[M + H]^+$	2-Octenoylcarnitine + O or isomers	4.84	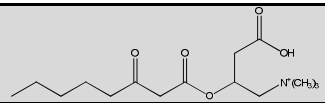
18	304.2106	30.90 - 31.30	304.1	31.51	$[M + H]^+$	3-Hydroxyoctanoic acid + $C_7H_{13}NO_2$ (carnitine) or isomer	-4.21	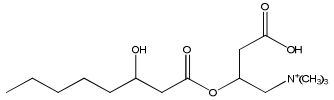
19	316.2111	30.30 - 30.80	316.1	31.01	$[M + H]^+$	6-Keto-decanoylcarnitine - CH_2 or isomer	-2.23	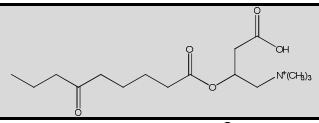
20	319.1911	41.70 - 42.20	319.2	42.19	$[M + H]^+$	11beta-hydroxyprogesterone - CH_2 or isomer	2.31	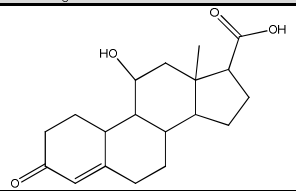
21	328.2105	30.00 - 30.50	328.1	30.26	$[M + H]^+$	2-trans,4-cis-Decadienoylcarnitine + O or isomer	-3.99	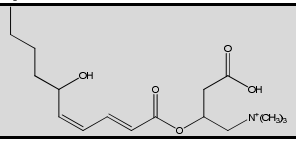

22	328.2118	32.60 - 33.10	328.2	33.23	$[M + H]^+$	2-trans,4-cis-Decadienoylcarnitine + O or isomer	-0.12	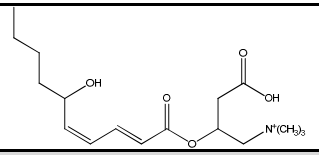
23	328.2467	39.70 - 40.30	328.2	40.29	$[M + H]^+$	4,8 dimethylnonanoyl carnitine -H_2 or isomer	-4.70	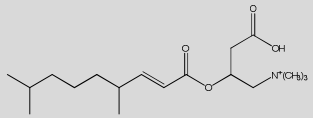
24	328.2489	40.90 - 41.30	328.2	41.28	$[M + H]^+$	4,8 dimethylnonanoyl carnitine -H_2 or isomer	1.96	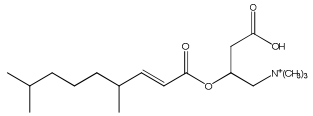
25	328.2484	41.70 - 42.00	328.2	41.95	$[M + H]^+$	4,8 dimethylnonanoyl carnitine -H_2 or isomer	0.51	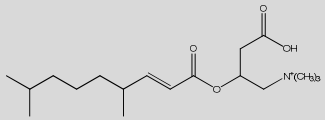
26	332.2066	29.40 - 30.00	332.2	30.23	$[M + H]^+$	Nonate + $C_7H_{13}NO_2$ (carnitine)	-0.57	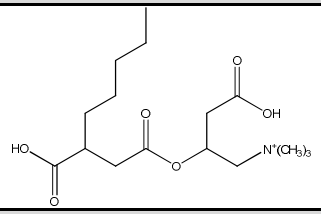
27	342.2280	31.90 - 32.40	341.9	32.58	$[M + H]^+$	9-Decenoylcarnitine + CO	1.42	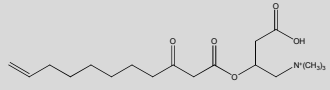
28	344.2061	30.90 - 31.40	344.2	31.37	$[M + H]^+$	Decenedioic acid + $C_7H_{13}NO_2$ (carnitine)	-1.79	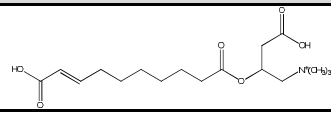

29	356.2437	34.80 - 35.30	356.2	35.35	$[M + H]^+$	3-Hydroxy-5, 8-tetradecadiencarnitine - C_2H_4 or isomer	1.62	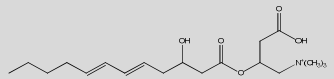
30	356.2426	37.20 - 37.70	356.4	37.62	$[M + H]^+$	3-Hydroxy-5, 8-tetradecadiencarnitine - C_2H_4 or isomer	-1.43	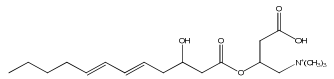
31	356.2437	38.50 - 39.10	356.1	38.92	$[M + H]^+$	3-Hydroxy-5, 8-tetradecadiencarnitine - C_2H_4 or isomer	1.65	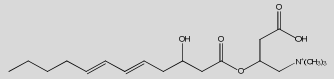
32	356.2786	44.90 - 45.40	356.3	45.27	$[M + H]^+$	trans-2-Dodecenoylcarnitine + CH_2 or isomer	-2.64	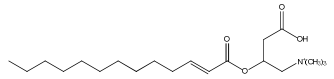
33	358.2221	32.30 - 33.10	358.2	32.97	$[M + H]^+$	9-Decenoylcarnitine + CO_2 or isomer	-0.91	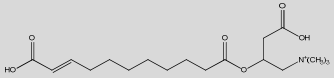
34	358.2583	36.20 - 36.90	358.2	36.71	$[M + H]^+$	trans-2-Dodecenoylcarnitine + O or isomer	-1.48	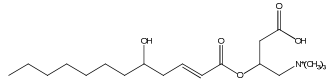
35	358.2587	38.80 - 39.30	357.8	39.27	$[M + H]^+$	trans-2-Dodecenoylcarnitine + O or isomer	-0.40	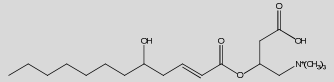
36	365.2319	35.20 - 35.70	365.1	35.72	$[M + H]^+$	Cortisol + H_2 or isomer	-1.05	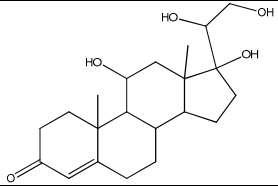

37	377.1062	28.10 - 28.50	377.2	28.01	$[M + Na]^+$	6,7-Dimethyl-8-(1-D-ribityl)lumazine + CO or isomer	-1.57	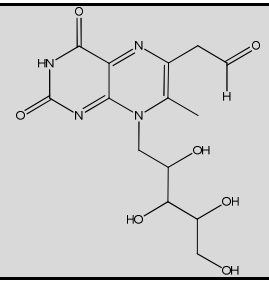
38	386.2535	35.80 - 36.30	386.2	36.36	$[M + H]^+$	trans-2-Dodecenoylcarnitine + CO_2 or isomer	-.070	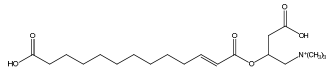
39	400.2695	34.70 - 35.20	400.2	35.22	$[M + H]^+$	3-Hydroxy-5, 8-tetradecadiencarnitine + O or isomer	0.34	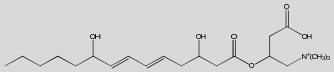
40	448.3056	40.70 - 41.30	448.3	41.16	$[M + H]^+$	Deoxycholic acid glycine conjugate - H_2 or isomer	-0.42	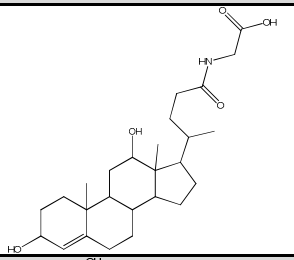
41	531.2201	43.60 - 44.10	531.3	44.05	$[M + Na]^+$	11beta-Hydroxyprogesterone + $C_6H_8O_6$ (glucuronic acid) or isomer	0.05	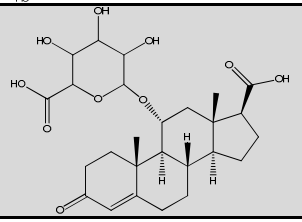

6.3 Results from database searching of urine metabolite features using reaction = 2. MS/MS spectral interpretation was performed to confirm all structures.

Feature ID #	Accurate *m/z* TOF	RT range (min) TOF	*m/z* QTRAP	RT (min) QTRAP	Ion Type	Putative ID	Error (ppm)	Structure
1	192.0986	6.10 - 6.60	192.2	6.28	$[M + H]^+$	L-Histidine + H_2O + H_2O	4.01	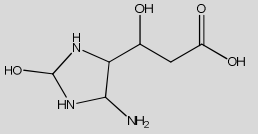
2	336.2174	36.90 - 37.40	336.1	37.44	$[M + H]^+$	5-Phenylvaleric acid + CH_2 + $C_7H_{13}NO_2$ (carnitine)	1.42	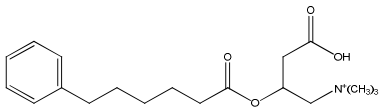
3	338.2330	38.50 - 39.00	338.1	39.03	$[M + H]^+$	Perillyl alcohol + C_2H_2O + $C_7H_{13}NO_2$ (carnitine)	1.28	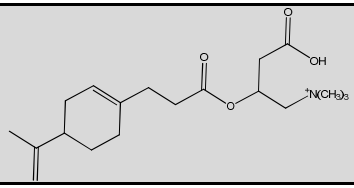

6.4 Results from database searching of plasma metabolite features using reaction = 0. No MS/MS spectra for these compounds were found in the HMDB database. MS/MS spectral interpretation was done to confirm structure.

Feature ID #	Accurate *m/z* TOF	RT range (min) TOF	*m/z* QTRAP	RT (min) QTRAP	Ion type	Putative ID	error (ppm)	Structure
1	153.0659	2.30 - 2.70	153.1	2.10	$[M+H]^+$	N1-Methyl-2-pyridone-5-carboxamide or N1-Methyl-4-pyridone-3-carboxamide	0.01	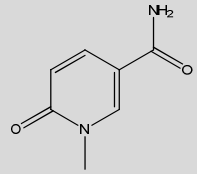
2	232.1544	3.60 - 4.20	232.2	4.40	$[M+H]^+$	Isobutyryl or butyrylcarnitine	0.29	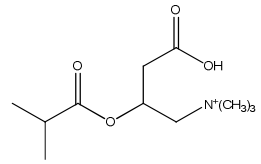
3	256.2630	58.90 - 59.50	256.2	59.60	$[M+H]^+$	Palmitic amide	-1.96	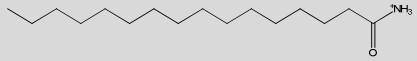

4	286.2014	33.20 - 33.70	286.2	34.30	$[M+H]^+$	2-octenoylcarnitine	0.49	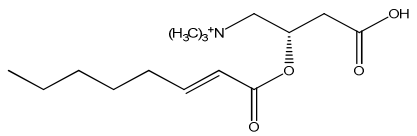
5	302.2322	37.20 - 37.60	302.2	37.90	$[M+H]^+$	2,6-dimethylheptanoylcarnitine Nonanoylcarnitine	1.27	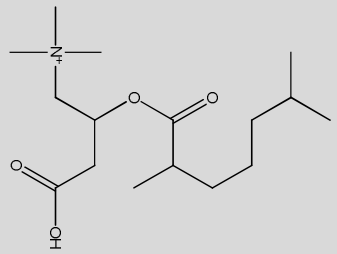
6	312.2168	37.00 - 37.40	312.2	37.80	$[M+H]^+$	2-trans,4-cis-Decadienoylcarnitine or isomer	-0.49	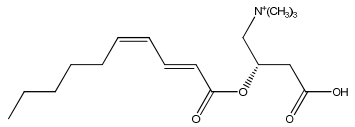
7	312.2165	37.60 - 38.00	312.2	38.30	$[M+H]^+$	2-trans,4-cis-Decadienoylcarnitine or isomer	-1.24	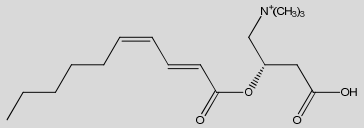

8	314.2328	38.90 - 39.40	314.2	39.80	$[M+H]^+$	9-Decenoylcarnitine or isomer	0.80	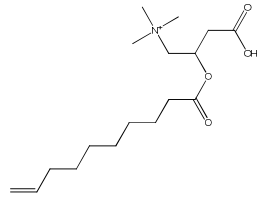
9	314.2322	39.80 - 40.20	314.2	40.50	$[M+H]^+$	9-Decenoylcarnitine or isomer	0.80	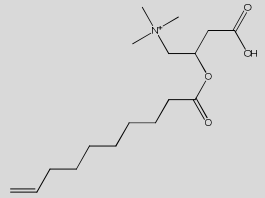
10	344.2793	44.70 - 45.20	344.3	45.70	$[M+H]^+$	Dodecanoylcarnitine	-0.80	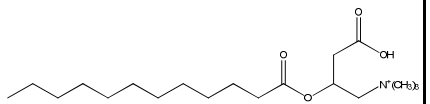
11	370.2951	46.40 - 46.90	370.3	47.50	$[M+H]^+$	trans-2-Tetradecenoylcarnitine or cis-5-Tetradecenoylcarnitine	-0.32	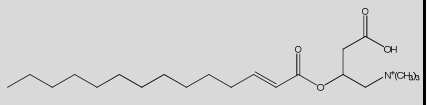

12	398.3260	49.70 - 50.40	398.3	50.80	$[M+H]^+$	trans-Hexadec-2-enoyl carnitine	-1.28	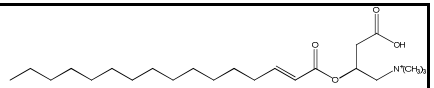
13	424.3419	50.90 - 51.40	424.3	51.90	$[M+H]^+$	Linoleylcarnitine or isomers	-0.62	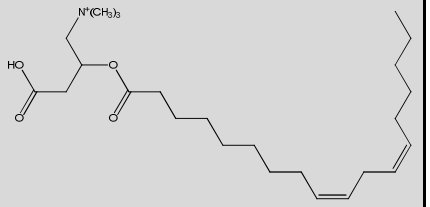
14	426.3572	53.60 - 54.10	426.4	54.50	$[M+H]^+$	Oleoylcarnitine or isomers	-1.25	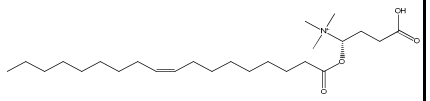
15	431.3147	49.00 - 49.50	431.3	50.10	$[M+H]^+$	7 alpha-Hydroxy-3-oxo-4-cholestenoate	-2.02	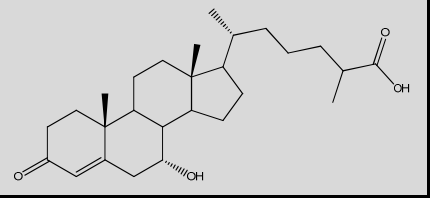

16	478.2927	48.50 - 49.00	478.3	49.50	$[M+H]^+$	LysoPE(0:0/18:2(9Z,12Z)) or LysoPE(18:2(9Z,12Z)/0:0)	-0.26	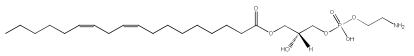
17	482.3238	48.20 - 48.70	482.3	49.30	$[M+H]^+$	LysoPC(15:0)	-0.59	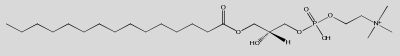
18	494.3244	47.30 - 47.90	494.3	48.30	$[M+H]^+$	LysoPC(16:1(9Z))	0.57	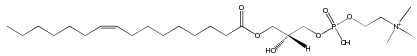
19	496.3406	49.50 - 49.80	496.3	50.60	$[M+H]^+$	LysoPC(16:0) isomer (branched)	1.67	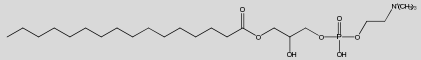
20	496.3377	50.30 - 50.90	496.4	51.40	$[M+H]^+$	LysoPC(16:0)	-4.23	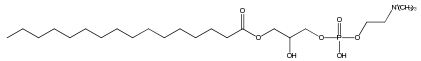

21	502.2930	48.60 - 49.10	502.4	49.00	$[M+H]^+$	LysoPE(0:0/20:4(5Z,8Z,11Z,14Z)), LysoPE(0:0/20:4(8Z,11Z,14Z,17Z)), LysoPE(20:4(5Z,8Z,11Z,14Z)/0:0) or LysoPE(20:4(8Z,11Z,14Z,17Z)/0:0)	0.47	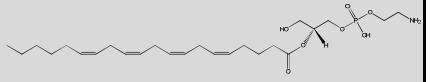
22	508.3756	52.20 - 52.70	508.4	53.30	$[M+H]^+$	LysoPC(P-18:0)	-1.05	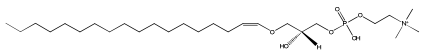
23	510.3549	52.60 - 53.10	510.4	53.70	$[M+H]^+$	LysoPC(17:0)	-0.98	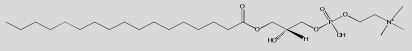
24	518.3216	49.50 - 49.80	518.3	50.60	$[M+Na]^+$	LysoPC(16:0) isomer	-0.32	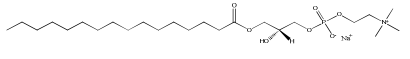

25	518.3225	50.30 - 50.90	518.3	51.40	$[M+Na]^+$	LysoPC(16:0)	1.55	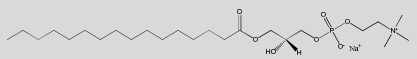
26	520.3380	48.60 - 49.20	520.3	49.00	$[M+H]^+$	LysoPC(18:2(9Z,12Z))	-3.45	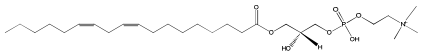
27	522.3555	51.30 - 51.90	522.4	52.40	$[M+H]^+$	LysoPC(18:1(9Z)) or LysoPC(18:1(11Z))	0.20	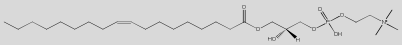
28	524.3721	55.00 - 55.60	524.4	55.20	$[M+H]^+$	LysoPC(18:0) or LysoPC(0:0/18:0)	1.90	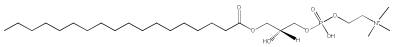

29	542.3219	48.60 - 49.20	542.6	49.00	$[M+Na]^+$	LysoPC(18:2(9Z,12Z))	0.37	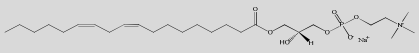
30	544.3403	48.70 - 49.20	544.6	49.74	$[M+H]^+$	LysoPC(20:4(5Z,8Z,11Z,14Z)) LysoPC(20:4(8Z,11Z,14Z,17Z))	0.95	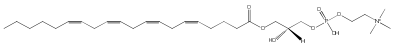
31	544.3374	51.30 - 51.90	544.6	52.40	$[M+Na]^+$	LysoPC(18:1(9Z)) or LysoPC(18:1(11Z))	0.14	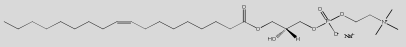
32	546.3551	50.20 - 50.70	546.7	51.20	$[M+H]^+$	LysoPC(20:3(5Z,8Z,11Z)) or LysoPC(20:3(8Z,11Z,14Z))	-0.60	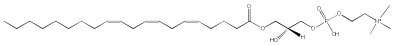
33	546.3529	55.00 - 55.60	546.8	56.10	$[M+Na]^+$	LysoPC(18:0) or LysoPC(0:0/18:0)	-0.26	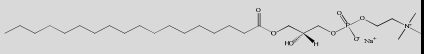

255	34	782.5659	63.30 - 64.00	782.7	63.30	$[M+H]^+$	Any of PC(14:0/22:4(7Z,10Z,13Z,16Z)), PC(16:0/20:4(5Z,8Z,11Z,14Z)), PC(16:0/20:4(8Z,11Z,14Z,17Z)), PC(16:1(9Z)/20:3(5Z,8Z,11Z)), PC(16:1(9Z)/20:3(8Z,11Z,14Z)), PC(18:0/18:4(6Z,9Z,12Z,15Z)), PC(18:1(11Z)/18:3(6Z,9Z,12Z)), PC(18:1(11Z)/18:3(9Z,12Z,15Z)), PC(18:1(9Z)/18:3(6Z,9Z,12Z)), PC(18:1(9Z)/18:3(9Z,12Z,15Z)), PC(18:2(9Z,12Z)/18:2(9Z,12Z)), PC(18:3(6Z,9Z,12Z)/18:1(11Z)), PC(18:3(6Z,9Z,12Z)/18:1(9Z)), PC(18:3(9Z,12Z,15Z)/18:1(11Z)), PC(18:3(9Z,12Z,15Z)/18:1(9Z)),	-4.45	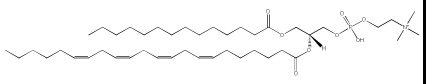

						PC(18:4(6Z,9Z,12Z,15Z)/18:0), PC(20:3(5Z,8Z,11Z)/16:1(9Z)), PC(20:3(8Z,11Z,14Z)/16:1(9Z)), PC(20:4(5Z,8Z,11Z,14Z)/16:0), PC(20:4(8Z,11Z,14Z,17Z)/16:0), PC(22:4(7Z,10Z,13Z,16Z)/14:0)		

6.5 Results from database searching of plasma metabolite features using reaction = 1. MS/MS spectral interpretation was done to confirm structure.

Feature ID #	Accurate *m/z* TOF	RT range (min) TOF	*m/z* QTRAP	RT (min) QTRAP	Ion type	Putative ID	error (ppm)	Structure
1	197.0962	46.70 - 47.20	197.1	47.90	$[M+H]^+$	(+)-(1R,2R)-1,2-Diphenylethane-1,2-diol – H_2O	0.51	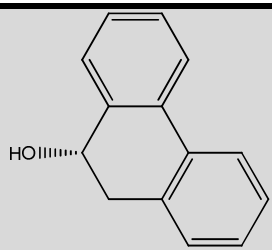
2	300.2163	35.20 - 35.70	300.1	36.00	$[M+H]^+$	2-Octenoylcarnitine + CH_2	-2.20	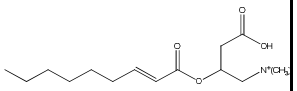
3	310.2008	36.10 - 36.70	310.1	36.90	$[M+H]^+$	2-trans,4-cis-Decadienoylcarnitine – H_2	-1.65	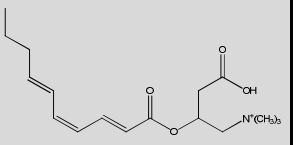

4	310.2009	35.00 - 35.50	310.2	35.90	$[M+H]^+$	2-trans,4-cis-Decadienoylcarnitine (isomer) $-H_2$	-1.65	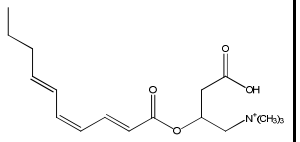
5	328.2481	40.50 - 40.90	328.2	41.30	$[M+H]^+$	trans-2-Dodecenoylcarnitine – CH_2	-0.31	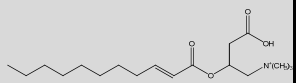
6	332.2427	36.30 - 36.80	332.2	37.00	$[M+H]^+$	(R)-3-Hydroxydecanoic acid + carnitine	-1.37	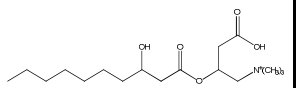
7	356.2795	44.40 - 44.80	356.2	45.30	$[M+H]^+$	trans-2-Dodecenoylcarnitine (or isomers) + CH_2	-0.26	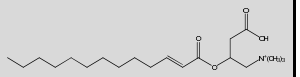

8	358.2586	39.10 - 39.60	358.2	39.90	$[M+H]^+$	3-Oxododecanoic acid (or isomers) + carnitine	-0.54	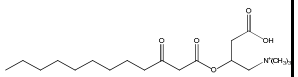
9	363.2522	34.80 - 35.40	363.2	35.60	$[M+H]^+$	Medroxyprogesterone + H_2O	-2.19	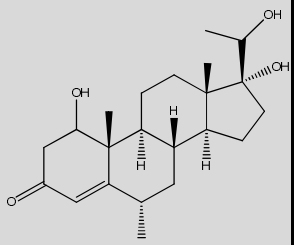
10	432.3106	41.80 - 42.30	432.3	42.70	$[M+H]^+$	Deoxycholic acid glycine conjugate (or isomer) – H_2O	-0.59	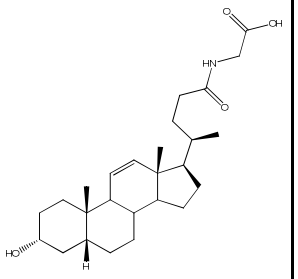
11	480.3103	51.10 - 51.60	480.3	52.70	$[M+H]^+$	LysoPC(15:0) – H_2	3.77	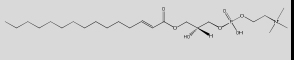

12	482.3591	51.20 - 51.70	482.3	52.30	$[M+H]^+$	LysoPC(O-18:0) – C_2H_4	-2.87	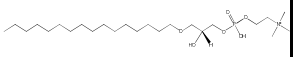
13	512.3342	40.40 - 41.00	512.4	41.30	$[M+H]^+$	LysoPC(16:1(9Z)) + H_2O	-0.97	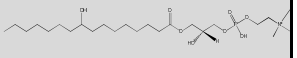
14	512.3342	47.00 - 47.50	512.3	48.10	$[M+H]^+$	LysoPC(16:0) + O	-0.99	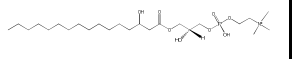

6.6 List of poly(ethylene glycol) (PEG) analogues found in urine and plasma. These compounds are not listed in the HMDB database and were therefore not found by MyCompoundID software.

Accurate *m/z* TOF	RT (min) TOF	*m/z* QTRAP	RT (min) QTRAP	PEG Analogue	Diagnostic fragments (*m/z*)	Matrix
371.2265	26.90 - 27.40	371.2	27.61	PEG_8	177, 133, 89	Urine
476.3281	28.60 – 29.10	476.2	29.16	$PEG_{10} + NH_4^+$	177, 89	Plasma
503.3043	29.00 - 29.40	503.3	29.67	PEG_{11}	177, 133, 89	Urine
520.3309	29.00 - 29.40	520.4	29.68	$PEG_{11} + NH_4^+$	177, 133, 89	Urine
534.3104	29.30 - 29.80	534.4	30.00	$MonomethoxyPEG_{11} + NH_4^+$	177, 147, 103, 89	Urine
547.3312	29.40 - 29.90	547.5	30.13	PEG_{12}	177, 133, 89	Urine
564.3584	29.40 - 29.90	564.4	30.13	$PEG_{12} + NH_4^+$	177, 89	Urine
578.3364	29.80 - 30.20	578.5	30.45	$MonomethoxyPEG_{12} + NH_4^+$	177, 147, 133, 103, 89	Urine
608.3839	29.90 - 30.40	608.5	30.54	$PEG_{13} + NH_4^+$	177, 89	Urine and plasma
622.3627	30.20 - 30.70	622.5	30.85	$MonomethoxyPEG_{13} + NH_4^+$	177, 147, 103, 89	Urine
652.4105	30.30 - 30.80	652.5	30.89	$PEG_{14} + NH_4^+$	177	Urine
666.3884	30.60 - 31.10	666.5	31.20	Monomethoxy PEG	177, 147	Urine
696.4364	30.60 - 31.10	696.5	31.22	$PEG_{15} + NH_4^+$	177	Urine

740.4617	31.00 - 31.50	740.5	31.53	$PEG_{16} + NH_4^+$	177	Urine

6.7 List of cocodiethanolamides (CDEAs) found in urine and plasma. These compounds are not listed in the HMDB database and were therefore not found by MyCompoundID software.

Accurate *m/z* TOF	RT (min) TOF	*m/z* QTRAP	RT (min) QTRAP	Diagnostic fragments (*m/z*)	Putative ID	Matrix
288.2896	43.60 – 44.0	288.3	44.52	88, 106, 227	$CDEA_{11}$	Urine and plasma
288.2897	44.40 – 44.80	288.3	45.21	88, 112, 227, 270	$CDEA_{11}$ (isomer)	Urine and plasma
316.3206	47.70 – 48.10	316.3	48.63	88, 106, 298	$CDEA_{13}$	Plasma
316.3206	48.40 – 48.80	316.3	49.34	88,188, 298	$CDEA_{13}$ (isomer)	Plasma

6.8 List of unknown metabolites found in urine sharing common diagnostic ions.

Accurate *m/z* TOF	RT (min) TOF	*m/z* QTRAP	RT (min) QTRAP	Diagnostic fragments (*m/z*)
369.2939	60.60 - 61.10	369.4	59.93	147, 189, 203
392.2791	44.90 - 45.70	393.3	45.33	149, 189
402.2836	34.90 -35.60	402.3	35.49	149, 187, 205
410.2894	45.00 - 45.50	410.3	44.46	147, 189, 203
421.2321	51.20 - 51.80	421.2	51.97	147, 203
504.2806	38.10 - 38.70	504.3	38.57	149, 185
529.2938	40.90 - 41.50	529.3	41.28	145, 187, 205
555.3055	41.70 - 42.00	555.1	42.44	147, 189, 203
555.3102	42.60 - 43.10	555.5	42.95	147, 189, 203

6.9 List of unknown metabolites found in urine sharing common neutral losses. None of these masses yielded any hits on the HMDB database.

Accurate *m/z* TOF	RT (min) TOF	*m/z* QTRAP	RT (min) QTRAP	Diagnostic neutral losses (Da)
431.1977	29.00 - 29.40	431.2	29.05	59, 135, 176, 180, 264, 282
431.0971	29.80 - 30.40	431.3	30.28	59, 135, 176, 180, 264, 282
431.1522	30.60 - 31.00	431.1	30.70	59, 135, 176, 180, 264, 282
431.2427	39.50 - 40.10	431.3	39.96	59, 135, 176, 180, 264, 282
433.2278	32.00 - 32.40	433.3	32.00	59, 135, 176, 180, 264, 282
511.2835	37.50 - 37.90	511.3	37.86	59, 135, 176, 180, 264, 282
513.2993	39.00 - 39.50	513.3	39.36	59, 135, 176, 180, 264, 282

6.10 List of unknown metabolites found in urine exhibiting constant neutral losses common to glucoronide conjugates. None of these masses yielded any hits on the HMDB database.

Accurate *m/z* TOF	RT (min) TOF	*m/z* QTRAP	RT (min) QTRAP	Constant neutral losses (Da)
338.1013	22.90 - 23.40	338.1	24.02	176, 194
381.1872	26.20 - 26.70	381.2	26.61	175, 176, 194
400.1976	40.50 - 41.00	400.3	40.99	176, 193
435.1996	45.40 - 46.00	435.2	46.02	176, 194
454.2079	34.20 - 34.50	454.2	34.67	176, 194
461.1274	29.30 - 29.70	461.2	29.58	176
463.2323	43.60 - 44.10	463.3	44.06	176, 194
464.1921	34.50 - 35.10	464.2	35.05	176
473.2450	47.60 - 48.10	473.3	48.25	176
475.2472	35.60 - 36.10	475.4	36.14	176
478.2075	36.10 - 36.50	478.2	36.63	176, 194
483.25168	42.40 - 42.80	483.3	42.79	176
485.2676	43.40 - 43.70	485.3	43.84	176
499.3235	45.30 - 45.80	499.3	45.77	176, 194

557.3124	42.60 - 43.10	557.5	42.51	176, 194
575.3532	44.40 - 44.80	575.4	44.85	176